SYSTEM IDENTIFICATION OF LINEAR VIBRATING STRUCTURES

NOEL GERALD NALITOLELA

Doctor of Philosophy

THE UNIVERSITY OF ASTON IN BIRMINGHAM

January 1991

THE UNIVERSITY OF ASTON IN BIRMINGHAM

SYSTEM IDENTIFICATION OF LINEAR VIBRATING STRUCTURES

NOEL GERALD NALITOLELA

Doctor of Philosophy

January 1991

SUMMARY

Methods of dynamic modelling and analysis of structures, for example the finite element method, are well developed. However, it is generally agreed that accurate modelling of complex structures is difficult and for critical applications it is necessary to validate or update the theoretical models using data measured from actual structures. The techniques of identifying the parameters of linear dynamic models using Vibration test data have attracted considerable interest recently. However, no method has received a general acceptance due to a number of difficulties. These difficulties are mainly due to (i) Incomplete number of Vibration modes that can be excited and measured, (ii) Incomplete number of coordinates that can be measured, (iii) Inaccuracy in the experimental data (iv) Inaccuracy in the model structure.

This thesis reports on a new approach to update the parameters of a finite element model as well as a lumped parameter model with a diagonal mass matrix. The structure and its theoretical model are equally perturbed by adding mass or stiffness and the incomplete number of eigen-data is measured. The parameters are then identified by an iterative updating of the initial estimates, by sensitivity analysis, using eigenvalues or both eigenvalues and eigenvectors of the structure before and after perturbation. It is shown that with a suitable choice of the perturbing coordinates exact parameters can be identified if the data and the model structure are exact. The theoretical basis of the technique is presented. To cope with measurement errors and possible inaccuracies in the model structure, a well known Bayesian approach is used to minimize the least squares difference between the updated and the initial parameters. The eigen-data of the structure with added mass or stiffness is also determined using the frequency response data of the unmodified structure by a structural modification technique. Thus, mass or stiffness do not have to be added physically. The mass-stiffness addition technique is demonstrated by simulation examples and Laboratory experiments on beams and an H-frame.

KEY WORDS: System identification - parameter estimation - model updating
Vibration - structures.

ACKNOWLEDGEMENTS

I wish to express my sincere thanks to;

Dr JET Penny, my research Supervisor, for his guidance and constructive criticism through out the period of the research.

Mr MI Friswell, Lecturer in the department of Mechanical and Production engineering, for consultations and his invaluable comments during the course of the research.

Mr B Muddyman, a technician in the Vibration laboratory, for his assistance during the setting up of the Vibration tests.

The University of Dar-es-Salaam for granting a study leave.

The German Agency for Technical Coorperation (GTZ) for their generous financial assistance.

NG Nalitolela.

January 1991

LIST OF CONTENTS

LIST OF FIGURES

LIST OF TABLES

NOMENCLATURE

Matrices are denoted by bold symbols, vectors by plain symbols and scalars by italics.

M, K, D	Mass, stiffness and dynamic stiffness matrices.
H	Hysteretic damping matrix.
C	Viscous damping matrix.
$\mathbb{M}$, $\mathbb{K}$	Modal mass and modal stiffness matrices.
A, B	Mass and Stiffness matrices of a first order differential equation based on state variables.
R, S, T, L	Arbitrary matrices.
Δ**M**, Δ**K**	Mass and stiffness addition matrices.
δ**M**	Submatrix of the mass addition matrix spanning over those coordinates which are perturbed one in turn.
δ**K**	Submatrix of the stiffness addition matrix spanning over those coordinates which are perturbed one in turn.
V	Modal matrix
U	Mass normalized modal matrix
I	Identity matrix.
Ψ	Eigenvector matrix of a first order differential equation based on state variables.
Φ	Eigenvector matrix normalized w.r.t mass matrix of a first order equation based on state variables.
Θ	Matrix of complex mode shapes normalized w.r.t mass matrix of the first order state equation.
Λ	Eigenvalue matrix.
a	Diagonal matrix.

α	Receptance matrix.
β	Transfer function matrix.
G	Coefficient matrix.
Γ	Matrix of Lagrangian multipliers.
E	Error matrix.
J	Jacobian matrix.
W	Weighting matrix.
Z	Matrix from singular value decomposition.
N	Projector matrix.
I	identity matrix
μ	Arbitrary diagonal matrix
q	Displacement vector.
Q	Forcing vector.
y	State vector.
F	Forcing vector corresponding to the first order state space differential equation of motion.
V	Mode shape vector.
U	Mass normalized mode shape vector.
ψ	Eigenvector of a first order differential equation based on state variables.
Φ	Eigenvector normalized w.r.t mass matrix of a first order differential equation based on state variables.
Θ	Mode shape vector normalized w.r.t mass matrix of a first order differential equation based on state variables.
s	Vector of unknown model parameters.
b	Observation vector.
Δs	Vector of Difference between unknown model

	parameters and parameters of the analytical model.
ΔU	Vector of difference between measured modes and modes determined by the analytical model.
$\Delta\lambda$	Vector of difference between measured eigenvalues and eigenvalues of the analytical model.
P	Vector of principal coordinates.
E	Error vector.
j	Unit vector in the imaginary axis.
ω	Frequency in Rad/s.
λ	Eigenvalue.
m , k	Modal mass and modal stiffness.
η	Hysteretic damping factor.
ζ	Viscous damping factor.
N	Number of degrees-of-freedom.
n	Number of unknown parameters.
m	Mass.
k	Stiffness.
EI	Flexural rigidity.
A, B	Constants.
g	Constraint equation.
f	Function.
f	Frequency in Hz.
x	Variables.
e	An error variable.
t	Time.
$\dot{}$	First derivative with respect to time.
$\ddot{}$	Second derivative with respect to time.

^	Refer to the unmeasured modes.
l	Length.
α	Receptance.
K	Influence coefficient of the stiffness matrix.
M	Influence coefficient of the mass matrix.
r	Diagonal influence coefficient of the submatrix of **R**.
T	Influence coefficient of **T**.
R	Influence coefficient of **R**.
δ	Kronecker delta.
δm	Added mass
χ	Damping proportionality constant.
m	Scalar coefficient
d	Number of distinct eigenvalues.

Subscripts

a	Refer to the analytical model.
K	Refer to the stiffness matrix.
M	Refer to the mass matrix.
T	Refer to the **T** matrix.
C	Corrected matrix.
mm	Matrix/Vector corresponding to measured DOF.
oo	Matrix/Vector corresponding to unmeasured DOF.
mo, om	Matrix coupling measured and unmeasured coordinates.
x	Refer to an arbitrary model.
pc	Refer to the number of perturbed coordinates.

mc	Refer to the number of measurement coordinates.
km	Refer to the mass and stiffness parameters.
z	Refer to the maximum number of non-zero rows in mass and stiffness submatrices coupling the perturbed and unperturbed coordinates.
zd	Refer to the maximum number of non-zero coefficients above the main diagonals of the mass and stiffness submatrices corresponding to the perturbed coordinates.
R	Refer to a reduced order model.
r	Measured modes.
eff	Effective modes.
G	Reference to the **G** matrix.
INS	An instrumental variable matrix.
L	Lagrangian.
o	Objective
e	Experimental.
λ	Data based on eigenvalues.
U	Data based on mass normalized eigenvectors.
λ,U	Data based on eigenvalues and eigenvectors.
j	Reference to the j^{th} quantity.
i	Reference to the i^{th} quantity.
t	t^{th} quantity.
ij	Reference to a matrix element (or submatrix) in the i^{th} row and the j^{th} column.
u	Per unit length.
(2N)	Refer to a matrix of order $2N$
ca	Refer to the analytical model at current iteration.

Superscript

*	Complex conjugate.
p	Refer to the perturbed structure
I	Pseudo-inverse.
T	Matrix transpose.
'	Submatrix of a model reduced to the unperturbed coordinates.

CHAPTER 1

INTRODUCTION

1.1 Research background

The design of a mechanical system usually involves structures which are crucial for the overall performance of the system. For a dynamically loaded system, design criteria will involve factors which are important for the structural integrity, as well as factors necessary for an optimum dynamic behaviour. These design criteria will require, for example, optimization of the fatigue strength, minimization of vibration levels to within specified limits, avoidance of structural resonances or the reduction of structural borne noise. The optimization of the vibrational behaviour of a spindle and bearing system, for example, is an important criterion in machine tool design for the attainment of a high quality of machining, whereas automotive and aeroplane structures are required to withstand premature fatigue failures as well as to transmit very little vibrations to the passengers.

With increased competition, there is an increased demand for the optimization of the structural dynamics of systems operating under dynamic loading. Such an optimization requires a detailed dynamical analysis at the design stage. The dynamical analysis is performed by constructing mathematical models which are based on the materials properties data and the design drawings. With a mathematical model factors such as dynamic stresses, elastic deformations or natural frequencies, as well as the effects of structural design changes on the dynamic behaviour, can be predicted long before the system is manufactured.

Methods of dynamic modelling and analysis of structures are well developed. If a system can be adequately described by a very simplified conceptual model,

exact analytical techniques for dynamical analysis are available and well established. The majority of practical systems, however, are so complex that solution based on exact analysis is extremely difficult or impossible. The use of approximate methods in the dynamical analysis of practical structures has therefore been dominant. Among the approximate methods, the finite element method is currently the most advanced and widely used. Despite the sophistication of the finite element method, it is still difficult to produce accurate dynamic models of complex structures and for critical applications it is necessary to update the finite element model using test data measured on real structures. This procedure has the disadvantage in the sense that a prototype or an actual system needs to be constructed. However, it constitutes an important stage in the product design and development process.

The techniques of using experimental data in the dynamic modelling of structures were originally initiated by the demands in the aerospace industry, dating back to the 1960/1970's. Since then other branches of engineering, notably automotive industry, have become interested in the process, partly as a result of recent developments in digital electronics and signal processing capabilities and partly due to the availability of powerful microcomputers at competitive prices. Currently model updating and identification techniques constitute an active field of research in the general area of structural dynamics.

In spite of the tremendous strides made within the last decade or so, with numerous publications on the methods of dynamic modelling of structures using vibration test data, there is still no generally acceptable method of updating an analytical model of a practical structure. This is due to a number of difficulties that are mainly associated with the nature of the experimental data. The important ones are:

(i) Incomplete information about the dynamic behaviour of the structure from vibration test. This problem is caused by the fact that the number of vibration modes that can be excited or measured in the response spectra is usually much smaller than the number of degrees-of-freedom (DOF) of the corresponding analytical model, giving rise to an infinite number of solutions. This problem is commonly known as the problem of incomplete modes.

(ii) Mismatch between the number of DOF of the analytical model and the number of coordinates measured in a vibration test. This problem stems from the fact that a significant number of coordinates cannot be measured, for example coordinates corresponding to the rotational DOF cannot be measured because rotational transducers are not yet developed and some coordinates corresponding to the translational DOF cannot be measured because of inaccessibility. Furthermore, some otherwise accessible coordinates are not measured because it is a time consuming and expensive task to measure them all.

(iii) Measured data contains inevitable experimental errors.

The work reported in this thesis is concerned with the development of a technique to update dynamic models, with particular reference to the finite element models, by using vibration test data.

1.2 Problem identification

Practical structures have a continuous distribution of mass and elasticity and therefore an infinite number of degrees-of-freedom. Such structures can therefore only be exactly modelled by partial differential equations. The procedure is to write down the partial differential equations of motion by considering dynamical equilibrium of an infinitesimal element and solve the resulting equations using known boundary conditions of the problem. With complex geometry, typical of practical structures, exact solution to the partial differential equations is extremely difficult and in most cases not possible. Even for structures of simple forms boundary conditions and stiffness properties of joints cannot be determined accurately by theoretical analysis. Dynamical analysis of practical structures have, therefore, been carried out by approximate methods.

The approximate methods of dynamical analysis of practical structures are essentially methods of discretization in which a system with an infinite number of DOF is expressed by a finite number of DOF. Whilst the dynamic responses due to an arbitrary loading can be obtained directly from the differential equations of the discretized model using numerical methods, the solution of free vibration problem is of major importance in the dynamical analysis. The free vibration problem enables one to derive the modal model. The modal model contains necessary and sufficient information to uniquely characterize the dynamic behaviour of the system. Response due to any arbitrary loading can easily be computed by a linear combination of the vibration modes. Furthermore, the optimization of the dynamic behaviour can be performed more efficiently as the effects of changes in mass and stiffness on the dynamic characteristics can be predicted more efficiently using the modal model rather than by repeated numerical solution to the equations of motion.

Most efforts in the dynamic modelling of structures are therefore directed towards reducing a physical system to a mathematical model with a finite number of DOF and from which vibration modes, natural frequencies and damping coefficients can be determined. The finite element technique is currently the most advanced and most widely used method for dynamical modelling and analysis of practical structures. This technique uses a more rational discretization procedure and is extensively treated in the literature, see for example Burnett (1987), Rao (1989) and Zienkiewicz (1989).

Despite the advances made in finite element techniques the dynamic behaviour prediction by the finite element method is in general not in agreement with measurements made on real structures. Although measurements cannot be error-free, it is generally agreed that accurate modelling of complex structures is difficult. The discrepancy between analytical model predictions and measurements obtained from actual structures is mostly associated with inaccuracies in the analytical model. This discrepancy increases with the complexity of the structure. It is also not surprising to find discrepancy in the dynamic behaviour prediction between finite element packages prepared by different experts. Wang *et al* (1986) for example, reports deviations in natural frequency predictions, for a simple T-plate, of up to 20 percent between different FE packages.

There are two main sources of errors which gives rise to the discrepancy between experimental and FE analytical predictions of dynamic behaviour. The first is associated with the fundamental errors introduced by the 'expert' in the derivation of the FE basic equations due to some inevitable approximations. These approximations are not immediately apparent to the user of the FE package. The second is associated with assumptions and necessary approximations introduced by the user of the FE package in the

modelling, especially of complex structures. The two sources are explained as follow :

(i) The deformation shapes of structures are frequency dependent, are not known, are difficult to find and in general impractical to find them except for very simple structures such as a uniform beam. The finite element method, for simplicity, assumes static deflection shape functions within the elements which are a valid assumption at zero frequency only, and even these are also not very easy to find accurately. A closer approximation to static shape functions is achieved by assuming some trigonometrical or polynomial functions. The approximation to dynamic shape functions is better at low frequencies and does generally get better by increasing the number of elements.

(ii) Uncertainty in deciding the appropriate element type to use in modelling structures of complicated shapes. Often one has to make an intuitive judgement.

(iii) Stiffness properties of joints (Bolted joints, welded joints, composite construction) is difficult or impossible to evaluate accurately from the design drawings.

(iv) Damping in structures is complex involving a combination of different damping mechanisms (Internal material hysteresis, coulomb friction in joints and viscous damping from the air resistance and viscoelastic materials). It is not always possible to predetermine the dominant damping mechanism and even if this

is possible or an equivalent damping model assumed, it is difficult to find the damping coefficients accurately. The commonly established practice is to ignore damping in lightly damped structures. For most structures the discrepancy introduced by ignoring damping is not significant except for response levels around the resonance frequencies.

(v) Uncertainty in materials properties data affects mass and stiffness matrices.

Finally, it should be noted that analytical models of practical structures, following the discretization, will contain a finite number of degrees-of-freedom, N, whereas the actual structure has an infinite number of degrees-of-freedom. If an N degrees-of-freedom model is to reproduce exactly the first N modes of the structure, it will not be capable of reproducing the responses at higher frequencies since the contribution of the $(N+1)^{th}$ and higher modes which is present in the structure responses will be missing in the analytical model responses. In other words, it is not possible for a discretized N degrees-of-freedom analytical model to reproduce the *responses* of the structure up to the N^{th} mode frequency. Thus, a discretized analytical model can never be exact. For practical purposes, however, the concern is to attain agreement between analytical model predictions and actual structure behaviour over a relatively much larger frequency range of interest. When this is not the case the analytical model cannot be reliably used in the dynamical analysis. This is often the case with complex structures and important factors contributing to the disagreement have been identified.

1.3 Problem definition and the scope of the present work

The process of establishing a dynamic mathematical model of a system or structure falls under the general heading of system identification. This process essentially involves two main tasks.

(i) Estimation of system structure, that is the form of the differential equations or transfer functions that describes the systems input-output relationship is established.

(ii) Estimation of system parameters, that is the parameters in the established differential equations are established.

As far as the dynamic modelling of structures is concerned the differential equations are the differential equations of motion whose coefficients represents the mass, stiffness and damping distribution. When discretized to a finite number N of degrees-of-freedom, the differential equations becomes a matrix differential equation of motion. The estimation of the system structure will involve for example establishing the presence and type of damping mechanism, establishing the presence location and the type of non-linearities, establishing any coupling between the different coordinates within the inertial, damping and stiffness matrices, establishing any relation between the different submatrices within each of the matrices etc. A model based on the lumped mass matrix, for example, has a different structure from the model based on the finite element consistent mass matrix and therefore a system identification procedure should establish the appropriate structure of the mass matrix before parameters of the mass matrix are correctly estimated. The dynamic model in terms of the mass, stiffness and possibly damping matrices constitutes the spatial model. For a linear system the differential equation is a second order

linear differential equation with constant coefficient matrices.

The system transfer functions are the expressions for receptance, mobility or inertance. Its parameters are the natural frequencies, mode shape vectors and modal damping factors. These are the modal parameters. The last two modal parameters are usually associated with linear systems only. The dynamic model in terms of its modal parameters constitute a modal model.

The structure of the spatial model matrices in terms of the relationship, if any, between the different submatrices and the presence of coupling between the coordinates within the spatial matrices is usually established by the analytical technique used in the derivation of the equations of motion. A finite element linear model incorporating effects of shear deformation and rotatory inertia will have a different model structure from the model ignoring these effects. Likewise a linear model with proportional hysteretic damping will have a different model structure from a model employing a non-proportional viscous damping. When a system identification procedure is concerned with model updating, it is necessary that an appropriate model structure is established during the formulation of the initial analytical model. Thus, a system identification problem in the case of model updating becomes a problem of parameter estimation.

The work reported in this thesis is concerned with system identification of linear vibrating structures in which an initial analytical model is to be updated. Thus, the following main assumption are made:

(i) The physical system is adequately represented by a dynamic model with a finite number of DOF over a frequency range of interest, by a second order linear differential equation of

motion with constant coefficient matrices.

(ii) The structure of the spatial matrices in the analytical model is adequate to represent the physical distribution of the spatial parameters.

A general model updating procedure is aimed at but emphasis is on the updating of the finite element model. As damping is the least accurate to measure experimentally and difficult to estimate analytically, it has been ignored in the analytical modelling for majority of lightly damped structures. The priority in this work is therefore on the updating of undamped models although a generalized procedure for the treatment of damped systems when an appropriate initial damping model is available will be derived. The system identification problem in the context of this work is therefore a problem of parameter estimation.

A technique has been developed to update the structural parameters of a finite element model using modal data. It is based on sensitivity analysis of the eigen-data with respect to changes in the structural parameters and the generation of a sufficient number of linearized independent equations so that a meaningful solution can be obtained from an incomplete number of modes measured at an incomplete number of DOF. This is achieved by successive perturbation of both the actual structure and its analytical model, in order to change their eigen-data, by identical additions of lumped mass or grounded stiffness at a number of coordinates and using measured eigenvalues and eigenvectors or eigenvalues alone. Due to the presence of the experimental errors in the measured eigen-data, large changes in some parameters from their initial estimates is possible when the sensitivity of the eigen-data to the parameters in question is relatively low. To limit the changes in the parameters

due to the influence of the experimental errors, a minimum variance estimator based on the Bayesian approach is used. The technique is further improved by adopting a structural modification approach to find the eigen-data of the perturbed structure from measured frequency response data without physical mass or stiffness additions. Thus, large stiffness or mass addition is possible. The feasibility of the technique is verified by numerical examples and laboratory experiments.

1.4 Organization of the thesis

The thesis is organized into seven main chapters with the first chapter as an introduction. In Chapter 2, the literature of parameter estimation techniques relevant to structural dynamic modelling is reviewed. The review concludes by pointing out that most of the difficulties in model identification and adjustment methods and the limitations in the existing techniques originates from problems associated with an incomplete number of measured modes, inaccessibility of rotational and some translational DOF for measurement and inaccuracies in the experimental data.

These problems are tackled by a technique developed in this thesis. The technique is based on sensitivity analysis of the eigen-data before and after the structure and its analytical model are equally perturbed by adding mass or stiffness. It is shown that if the structure is perturbed by adding stiffness or mass in order to change its modal data, the incomplete modal data of the perturbed and the unperturbed structures may be sufficient to identify the correct parameters of the unperturbed structure. This is possible using eigenvalues and eigenvectors or using eigenvalues alone. Conditions for using eigenvalues and eigenvectors and for using eigenvalues alone are derived. The basic theoretical development and verification by numerical examples are

given in Chapter 3.

Chapter 4 discusses some practical aspects, in particular the effects of experimental errors in the measured data, the effects of fitting an undamped model using data from a lightly damped structure and the effects of fitting a model with a finite number of DOF using data from a continuous system.

Chapter 5 presents the results of the verification of the mass addition technique by laboratory experiments on a free beam and a cantilever beam.

The technique is further refined and improved in Chapter 6 by using measured frequency domain receptance data of the unperturbed structure to estimate analytically the unbiased modal data of the perturbed structure. Consequently mass or stiffness do not have to be physically added to the structure. Large structures for which physical mass addition is not practical can easily be updated in this manner. The feasibility of analytical stiffness addition is verified by numerical and laboratory experiments on lightly damped beams and an H-frame using undamped and proportionally damped models.

Finally, general discussion and conclusions are given in Chapter 7.

CHAPTER 2

LITERATURE REVIEW

2.1 General considerations

The process of linear dynamic modelling of structures, for example using the finite element technique, leads to a matrix differential equation of motion which may or may not involve a damping matrix. If a structure is adequately represented by a finite element model with hysteretic damping, the time domain differential equation of motion is given by (2.1).

$$\mathbf{M}\ddot{q}(t) + [\mathbf{K} + j\mathbf{H}]q(t) = Q(t) \tag{2.1}$$

For a harmonic forcing vector at a single frequency, ω, the response is also harmonic with the same frequency and its time dependence in the differential equation of motion is separable from its spatial dependence. Thus, using complex variables to account for the phase differences, (2.1) can be written as:

$$[-\omega^2 \mathbf{M} + \mathbf{K} + j\mathbf{H}]\, q = Q \tag{2.2}$$

Where q and Q are frequency dependent complex displacement and forcing vectors.

The vibration mode shapes and natural frequencies are found from the homogeneous solution of (2.2), which can be seen as an eigenvalue-eigenvector problem with a real mass matrix and a complex stiffness matrix. It can be shown that the mode shape vectors in the case of a hysteretic damped system are the same as the eigenvectors, which are generally complex and are orthogonal with respect to both the mass and the complex stiffness matrices.

The orthogonality relationships are of the form of (2.3) and (2.4) where δ_{ij} is a kronecker delta and m_j and k_j are complex constants referred to as the modal mass and modal stiffness.

$$\mathbf{V}_i^{\mathrm{T}} \mathbf{M} \mathbf{V}_j = \delta_{ij} m_j \tag{2.3}$$

$$\mathbf{V}_i^{\mathrm{T}} [\mathbf{K} + \mathrm{j}\mathbf{H}] \mathbf{V}_j = \delta_{ij} k_j \tag{2.4}$$

For N modes, (2.3) and (2.4) can also be written as:

$$\mathbf{V}^{\mathrm{T}} \mathbf{M} \mathbf{V} = \mathbb{M} \tag{2.5}$$

$$\mathbf{V}^{\mathrm{T}} [\mathbf{K} + \mathrm{j}\mathbf{H}] \mathbf{V} = \mathbb{K} \tag{2.6}$$

$\mathbb{M}$ and $\mathbb{K}$ are diagonal matrices of modal mass and modal stiffness respectively. The mode shape vectors contains arbitrary scaling. Often $\mathbf{V}_j$ is scaled so that the biggest term in each mode vector is unity. Alternatively the mode shape vectors can be conveniently scaled according to (2.7).

$$\mathbf{U}_j = \frac{\mathbf{V}_j}{\left(\mathbf{V}_j^{\mathrm{T}} \mathbf{M} \mathbf{V}_j \right)^{1/2}} \tag{2.7}$$

Mode shapes scaled using (2.7) are said to be mass normalized and satisfies the orthogonality relationships with respect to the mass and the complex stiffness matrices as given by (2.8) and (2.9):

$$\mathbf{U}^{\mathrm{T}} \mathbf{M} \mathbf{U} = \mathbf{I} \tag{2.8}$$

$$\mathbf{U}^{\mathrm{T}} [\mathbf{K} + \mathrm{j}\mathbf{H}] \mathbf{U} = \Lambda \tag{2.9}$$

Where **I** is an identity matrix and Λ is a diagonal matrix of complex eigenvalues.

It can also be shown that the eigenvalues are related to the natural frequencies and to the damping factors by (2.10):

$$\lambda_j = \omega_j^2 (1 + j\eta_j) \tag{2.10}$$

If the damping matrix is proportional to the mass and/or the stiffness matrix, the eigenvectors becomes real and the natural frequencies, ω_j, becomes the undamped natural frequencies.

The response-forcing relationship (2.2) can also be written as :

$$q = [\alpha(\omega)]Q \tag{2.11}$$

where

$$[\alpha(\omega)] = [\, -\omega^2 \mathbf{M} + \mathbf{K} + j\mathbf{H} \,]^{-1} = \mathbf{U} [\, -\omega^2 \mathbf{I} + \Lambda \,]^{-1} \mathbf{U}^T$$

$[\alpha(\omega)]$ defines the receptance matrix, where α_{ik} is the frequency domain displacement at coordinate i due to a unity forcing amplitude at coordinate k with the rest of the forces set to zero. From (2.11):

$$\alpha_{ik} = \sum_{j=1}^{N} \frac{U_{ij} U_{kj}}{\lambda_j - \omega^2} = \sum_{j=1}^{N} \frac{U_{ij} U_{kj}}{\omega_j^2 - \omega^2 + j\eta_j \omega_j^2} \tag{2.12}$$

In the case of a general viscous damping model the equation of motion is given by :

$$\mathbf{M}\ddot{q}(t) + \mathbf{C}\dot{q}(t) + \mathbf{K}q(t) = Q(t) \tag{2.13}$$

As in (2.1), the harmonic time dependence of the response is separable from its spatial dependence, and using complex variables, the time domain equation of motion is transformed into a frequency domain equation given by (2.14).

$$[-\omega^2 \mathbf{M} + j\omega \mathbf{C} + \mathbf{K}]q = Q \tag{2.14}$$

The mode shape vectors are found from the homogeneous solution of (2.14). However, as (2.14) is not amenable to standard eigensolution techniques due to the presence of the ω term in addition to the ω^2 term multiplied to the mass matrix, it is customary to convert it into a suitable form for eigenanalysis by the following transformations :

$$\mathbf{A} = \begin{bmatrix} \mathbf{C} & \mathbf{M} \\ \mathbf{M} & 0 \end{bmatrix} \qquad \mathbf{B} = \begin{bmatrix} \mathbf{K} & 0 \\ 0 & -\mathbf{M} \end{bmatrix}$$

$$y(t) = \begin{Bmatrix} q(t) \\ \dot{q}(t) \end{Bmatrix} \qquad F(t) = \begin{Bmatrix} Q(t) \\ 0 \end{Bmatrix}$$

Thus, (2.13) and (2.14) becomes:

$$\mathbf{A}\,\dot{y}(t) + \mathbf{B}\,y(t) = F(t) \tag{2.15}$$

$$j\omega \mathbf{A}\,y + \mathbf{B}\,y = F \tag{2.16}$$

There are $2N$ eigenvectors Ψ_j and $2N$ eigenvalues λ_j which are solutions of (2.16) when F is zero. The eigenvalues and eigenvectors for *underdamped* systems, which is usually the case for the majority of practical structures, occurs in complex conjugate pairs and are related to the mode shape vectors V_j, natural frequencies ω_j and viscous damping factors ζ_j by (2.17) and (2.18).

$$\lambda_j = \omega_j (-\zeta_j + (1 - \zeta_j^2)^{1/2}) \tag{2.17}$$

$$\Psi_j = \begin{Bmatrix} V_j \\ \lambda_j V_j \end{Bmatrix} \tag{2.18}$$

It can be shown that the eigenvectors of a general viscously damped model are orthogonal to the matrices **A** and **B** by (2.19) and (2.20),

$$\Psi^T \mathbf{A} \Psi = \mathbf{a} \tag{2.19}$$

$$\Psi^T \mathbf{B} \Psi = -\mathbf{a}\Lambda_{(2N)} \tag{2.20}$$

where **a** is a diagonal matrix and Ψ is a $2N$ x $2N$ eigenvector matrix with N pairs of complex conjugate vectors. The eigenvector matrix is given by:

$$\Psi = \begin{bmatrix} \mathbf{V} & \mathbf{V}^* \\ \mathbf{V}\Lambda & \mathbf{V}^*\Lambda^* \end{bmatrix} \tag{2.21}$$

The submatrix **V** contains the mode shape vectors. The eigenvectors (Ψ_j) and consequently the mode shape vectors (V_j) can be scaled according to:

$$\Phi_j = \frac{\Psi_j}{\left(\Psi_j^T \mathbf{A} \Psi_j\right)^{1/2}} \tag{2.22}$$

$$\Theta_j = \frac{V_j}{\left(\Psi_j^T \mathbf{A} \Psi_j\right)^{1/2}} \tag{2.23}$$

The orthogonality relations, (2.19) and (2.20), thus becomes:

$$\Phi^T \mathbf{A}\, \Phi = \mathbf{I} \tag{2.24}$$

$$\Phi^T \mathbf{B}\, \Phi = -\Lambda_{(2N)} \tag{2.25}$$

where

$$\Phi = \begin{bmatrix} \Theta & \Theta^* \\ \Theta\Lambda & \Theta^* \Lambda^* \end{bmatrix} \tag{2.26}$$

The forcing-response relationship, (2.16), can also be written as :

$$y = \beta\, F = [\, j\omega\, \mathbf{A} + \mathbf{B}\,]^{-1} F \tag{2.27}$$

where

$$\beta = [j\omega\, \mathbf{A} + \mathbf{B}]^{-1} = \Psi\, [j\omega\, \mathbf{a} - \mathbf{a}\Lambda_{(2N)}]^{-1}\, \Psi^T = \Phi\, [j\omega\, \mathbf{I} - \Lambda_{(2N)}]^{-1} \Phi^T$$

It can also be shown that the receptance α_{ik} measured at coordinate i due to a force input at coordinate k, for a general viscously damped system, is given by:

$$\alpha_{ik} = \sum_{j=1}^{2N} \frac{\Psi_{ij}\, \Psi_{kj}}{a_j (j\omega - \lambda_j)} = \sum_{j=1}^{N} \left(\frac{\Theta_{ij}\, \Theta_{kj}}{j\omega - \lambda_j} + \frac{\Theta_{ij}^* \Theta_{kj}^*}{j\omega - \lambda_j^*} \right) \tag{2.28}$$

If the viscous damping matrix is proportional to the mass and/or the stiffness matrix, (2.13) can be uncoupled by the real modal matrix of the undamped system. Real modes are known as normal-modes.

The process of dynamic modelling using vibration test data is the inverse mathematical process of finding parameters of the mass, stiffness and possibly damping matrices from measured vibration data. Such a process may involve updating the initial parameters when an initial model, which does not

accurately predict measured dynamic behaviour, is available from theoretical analysis. The initial model may have been developed by the finite element technique. Alternatively, the dynamic model may be identified directly from the experimental data without the use of a prior model. The vibration data can be the time domain forcing and response data, frequency domain forcing and response data or modal data.

Modelling by a time domain approach can be accomplished through the use of (2.1) for a hysteretic damped system or through the use of (2.13) or (2.15) for a viscously damped system. Frequency domain approach involves (2.2) or (2.16) as a basis for parameter estimation. Likewise, if modal data is used, one could start from the orthogonality relationships or from the frequency domain homogeneous equation of motion with frequency and displacement vector replaced by their measured modal data. The modal approach requires the use of mass normalized modes or modes normalized by the **A** matrix, in the case of a non-proportional viscously damped model, since the eigenvectors are otherwise arbitrarily scaled. The mass normalized modes are usually obtained by experimental modal analysis using either time domain or frequency domain curve fitting algorithms (Ewins 1985). It is also possible to find the mode shapes without curve fitting algorithms, by a *sine-dwell* test method. The modes obtained in this case, however, are arbitrarily scaled and therefore the determination of the modal mass becomes necessary. Thus, it may be seen that the basic equations relating model matrices to the experimental data, as given in the preceding paragraphs, could provide the base for solving for the model parameters once the experimental data is available. In all these equations the unknown model parameters appear linearly. Thus, the equations can easily be written as a set of simultaneous equations linear in the unknown parameters and can be put in the form of (2.29) where 's' is a vector of the unknown parameters.

$$\mathbf{G}\,\mathbf{s} = \mathbf{b} \tag{2.29}$$

The number of such simultaneous equations must be as large as, or may be larger than, the number of unknown parameters, for example by increasing the number of measured forcing and response samples in the time domain and frequency domain methods. In practice finding a solution using the equations in the preceding paragraphs as a base is not a straight forward problem due to the following reasons:

(i) The experimental data is often contaminated by measurement errors. Statistical techniques therefore need to be applied. However the coefficient matrix, **G**, is built up using this contaminated data. This introduces bias in the estimated parameters, which is often difficult to remove even with statistical techniques.

(ii) It is not possible in practice to have measurements at all coordinates of the structure corresponding to the degrees of freedom of the finite element model. In this case, the equations cannot be set up and solved without an estimate to be made of the responses of the unmeasured DOF. Such estimates are additional sources of errors. Alternatively the finite element model may be condensed to the measurement DOF but the condensation procedures which are commonly applied in the solutions of eigenvalue problems, results in non-linear equations which cannot be formulated as (2.29).

(iii) If modal data is used the above mentioned difficulties still exist and in addition there is a possibility of rank deficiency in

the coefficient matrix since the number of linearly independent equations is determined by the number of measured coordinates and the number of modes used in the formulation of the equations.

Thus, although the basic equations relating vibration data and spatial model parameters are simple, the inverse problem of finding parameters of the spatial model is an involved one. The following sections looks at the evolution of the spatial parameter estimation techniques and gives an overview of the current state of the art.

2.2 Parameter estimation based on the measured modal data

Although the need for the adjustment of dynamic models using measurements obtained from actual structures has been recognized for some time, most research on this subject has been done within the last two decades. A survey paper by Young and On (1969), noted only a few published references in structural parameter estimation prior to 1969. The earlier investigators recognized the fact that measured normal-modes failed to satisfy the orthogonality conditions with respect to the theoretical mass and stiffness matrices. The modes were measured by the sine-dwell test method as this was the only practical method of modal testing before the development of the more advanced curve fitting algorithms. Since such modes are arbitrarily scaled, it was necessary to find the modal mass matrix for the normalization of the modes. These earlier investigators had assumed the measured natural frequencies and the theoretical mass matrix to be accurately determined. The stiffness matrix, being more difficult to evaluate, was assumed to be less accurate. Thus, the loss of orthogonality was blamed on the experimental errors in the measured mode shape vectors and errors in the analytical stiffness

matrix.

Parameter estimation problem was therefore reduced to the problem of orthogonalizing the measured modes with respect to the theoretical mass matrix, and then using the corrected modes to identify the stiffness matrix. These early methods did not make effective use of statistics to account for errors in the measured modal data. The methods were mainly of the non-iterative type based of the orthogonality relationship. In later methods, assumptions of an error-free mass matrix and error-free natural frequencies are usually not made and statistical techniques are often utilized. The statistical techniques are useful when equations relating the unknown to the known quantities can be put in the form of (2.29). However, they are most effective when measurement errors are due to the quantities contained in the right hand side vector b rather than in the coefficient matrix **G**. As such equations are easily formulated by sensitivity analysis, truncated to first order, most of the more recent methods are iterative. Modal based methods for spatial parameter estimation can therefore be broadly categorized into non-iterative and iterative methods, with the later involving some sort of sensitivity analysis.

2.2.1 Non-iterative methods

It has been mentioned that earlier methods of spatial model parameter estimation assumed an exact mass matrix and error-free natural frequencies, and were mainly concerned with the orthogonalization of the normal-modes. The modes, measured by the sine-dwell method, were orthogonalized with respect to the mass matrix and corrected for the measurement errors. The corrected orthonormal modes were then used to determine the stiffness matrix. In these methods the stiffness matrix is found without the use of a prior analytical matrix. Gravitz (1958) was among the first to use this approach on

an undamped model. However, there is a practical limitation that the number of modes which can be excited and measured is much smaller than the number of degrees-of-freedom of the required analytical model. Real structures have an infinite number of DOF, and the analytical model needs to have a large number of DOF, if a complex structure is to be adequately modelled. The consequence of this limitation is that modal matrix is rectangular and matrix pseudo-inversion cannot be meaningfully used to solve for the stiffness matrix from (2.9).

For this reason, it is the flexibility matrix $\mathbf{K}^{-1}$ which has been evaluated, from:

$$\mathbf{K}^{-1} = \mathbf{V}\,\mathbb{K}^{-1}\,\mathbf{V}^T = \mathbf{V}\,[\Lambda\,\mathbb{M}\,]^{-1}\,\mathbf{V}^T = \mathbf{V}\,[\mathbf{V}^T\mathbf{M}_a\mathbf{V}]^{-1}\,\Lambda^{-1}\,\mathbf{V}^T \qquad (2.30)$$

Gravitz used measured normal-modes obtained by sine-dwell test and the analytical mass matrix to estimate the modal mass matrix. The modal mass matrix is then used with the measured modes and natural frequencies to compute the flexibility matrix. The modal mass matrix is supposed to be diagonal but it isn't due to measurement errors in the measured modal matrix. As a result, the flexibility matrix becomes non-symmetrical. Matching pairs of off-diagonal elements in the flexibility matrix are then averaged to obtain a symmetrical matrix. Finally, this flexibility matrix is substituted back in the free vibration equation to give a new set of 'corrected' orthonormal modes.

Rodden (1967), and later McGrew (1968), pointed out that the errors in the measured modes, which were obtained by sine-dwell testing, were due to the influence of low frequency modes, including rigid body modes in the case of free-free testing. Their proposal was to correct the modal matrix by use of a modal correction matrix, which takes into consideration rigid body and low frequency modes. The corrected modal matrix, after orthogonalization with

respect to the assumed error-free mass matrix, was then used to evaluate the flexibility matrix using inverse orthogonality equation.

A much better approach, but still based on the same assumption of error-free mass matrix and error-free measured natural frequencies, is given by Baruch and Bar-Itzhack (1978). The approach involves first finding a new set of corrected modes which are orthogonal with respect to the analytical mass matrix and are closest to the measured modes in a least squares sense. This was achieved by using the method of Lagrangian multipliers. The orthogonal modes are then used to find the stiffness matrix which is closest to the analytical stiffness matrix.

The method of Lagrangian multipliers is useful in the minimization or maximization of a function subject to several constraint equations. It is based on the theorem, the proof of which is given by Edwards (1973), that if f and g are differentiable functions in a given space, and if a set of points x satisfies the 'g' constraint equations :

$$g_1(x) = 0\,, \quad g_2(x) = 0 \;\ldots\; g_g(x) = 0$$

and the gradients

$$\frac{\partial g_1}{\partial x}\,,\ \frac{\partial g_2}{\partial x}\,,\ \ldots\ \frac{\partial g_g}{\partial x}$$

are linearly independent, then if the function f attains its minimum or maximum at $x = a$, there exist real numbers $\Gamma_1, \Gamma_2, \ldots \Gamma_t \ldots \Gamma_g$ called Lagrangian multipliers such that:

$$\frac{\partial f(a)}{\partial x} = \Gamma_1\frac{\partial g_1(a)}{\partial x} + \Gamma_2\frac{\partial g_2(a)}{\partial x} + \ldots + \Gamma_t\frac{\partial g_t(a)}{\partial x} + \ldots \Gamma_g\frac{\partial g_g(a)}{\partial x} \qquad (2.31)$$

Baruch and Bar-Itzhack uses the weighted Euclidean norm of the difference between the unknown orthonormal modes (corrected modes) and the measured modes (mass normalized with respect to the analytical mass matrix) as the function, *f*, to be minimized. The Orthogonality of the mode vectors with respect to the analytical mass matrix is taken as the 'g' constraint equations ($g=N_r^2$). The mode shape vectors are then corrected so as to have a minimum norm subject to the constraint condition. This is done by minimization of the following Lagrangian function,

$$f_L = \| \mathbf{M}_a^{1/2} [\mathbf{U}_c - \mathbf{U}] \| + \overline{\| \Gamma [\mathbf{U}_c^T \mathbf{M}_a \mathbf{U}_c - \mathbf{I}] \|} \tag{2.32}$$

where Γ is a matrix of Lagrangian multipliers and

$$\overline{\| \Gamma [\mathbf{U}_c^T \mathbf{M}_a \mathbf{U}_c - \mathbf{I}] \|} = \sum_{i=1}^{N_r} \sum_{j=1}^{N_r} \Gamma_{ij} \left(\sum_{t=1}^{N} \sum_{k=1}^{N} \left(U_{c,tj} M_{a,tk} U_{c,ki} - \delta_{ji} \right) \right)$$

The minimization of (2.32) is achieved by partial differentiation with respect to each of the unknown corrected modes and the result set to zero. This finally lead to a set of simultaneous equations, each of the form of (2.31), where

$$f = \| \mathbf{M}_a^{1/2} [\mathbf{U}_c - \mathbf{U}] \|, \quad g_t = \mathbf{U}_{c,j}^T \mathbf{M}_a \mathbf{U}_{c,i} - \delta_{ji} \quad \text{and} \quad \Gamma_t = \Gamma_{ij}$$

and yields a solution for the corrected modes in terms of the Lagrangian multipliers. The later are eliminated by substitution in the mass orthogonality constraint equation to yield the corrected modal matrix $\mathbf{U}_c$ in terms of the measured modes and the analytical mass matrix as:

$$\mathbf{U}_c = \mathbf{U} \left[\mathbf{U}^T \mathbf{M}_a \mathbf{U} \right]^{-1/2} \tag{2.33}$$

This expression was also obtained by Targoff (1976).

Having obtained the minimum norm corrected modes, Baruch and Bar-Itzhack proceed to the correction of the stiffness matrix by minimization of the weighted Euclidean norm of the difference between the analytical and the corrected stiffness matrices, using the equation of motion and symmetry of the stiffness matrix as constraint equations in the Lagrangian function.

Unlike the previous mentioned investigators, Baruch *et al* have utilized the prior knowledge of the analytical stiffness matrix to find a full rank stiffness matrix. However one of its major limitations, as with previous approaches, is the requirement of an error-free mass matrix. There has been a tendency to associate the accuracy of the mass matrix, which was obtained by lumping, with the accuracy obtained in the determination of the mass of the structural elements themselves by direct measurements. As it has been pointed out by Berman (1979), the assumption of an error-free mass matrix is for most applications unrealistic.

The work done from the early 1970s onwards shows a more rational change by dropping the assumption of an error-free analytical mass matrix and tuning both the analytical mass and stiffness matrices to match measured modes and natural frequencies.

Berman and Flannelly (**1971**), discuss the problem of identifying mass and stiffness matrices with due attention to the problem of *incomplete modes*. It has been shown in their theory of *incomplete models* that a stiffness matrix can be expressed as an algebraic sum of the terms representing contribution from each mode.

$$\mathbf{K} = \mathbf{U}^{-T}\Lambda\,\mathbf{U}^{-1} = \mathbf{M}\,\mathbf{U}\,\Lambda\,\mathbf{U}^{T}\mathbf{M} = \sum_{j=1}^{N} \frac{\lambda_j}{m_j}\mathbf{M}\,\mathbf{V}_j\,\mathbf{V}_j^{T}\mathbf{M} \qquad (2.34)$$

If the number of measured modes is smaller than the number of DOF, a situation which has been referred to as that of incomplete modes, the summation is carried over only the few measured modes. The resulting stiffness matrix, being of a rank less than its order, is defined as incomplete and is singular. This can be shown to be equally true in the case of mass matrix identification. The problem is worsened in the stiffness matrix identification, as compared to the mass matrix identification, due to the omission of the high frequency unmeasured modes which are supposed to be dominating the stiffness matrix since the frequency is entered as square in the summation. According to the theory of incomplete models, it is not possible therefore to find a *physically meaningful model from vibration tests alone.*

The procedure used by Berman and Flannelly is to first find a mass matrix which has parameters which are closest to the initial analytical estimates in a weighted least squares sense. This is achieved by using orthogonality equation of the mode shape vectors with respect to the unknown mass matrix. Additional equations are also generated using known features about the mass, for example the total mass obtained by direct measurement is equated to the sum of the diagonal elements of the lumped mass matrix. The equations, which are usually fewer than the number of unknown parameters, are then reassembled in the form of (2.29) and solved for the mass parameters using the pseudo-inverse technique. The resulting mass matrix is then used to find the incomplete stiffness matrix.

With a finite element model, it is possible, in some cases, to solve for the

unknown parameters without the problems of an incomplete number of measured modes. The use of submatrices for the element mass and stiffness matrices with a known linear relationship between the influence coefficients of an element submatrix means that only multipliers to the element submatrices are to be updated. This considerably reduces the total number of parameters in relation to the size of the model and an overdetermined equation in the form of (2.29) could be formulated.

Tlusty and Ismail (1980) proposes to use this approach, assuming prior knowledge about the structure of the mass and stiffness matrices, to reduce the number of unknown mass and stiffness parameters. An overdetermined matrix equation is then assembled from an incomplete number of measured modes, using the homogeneous equation of motion, mass orthogonality and stiffness orthogonality equations. The mass and stiffness parameters are then found by the pseudo-inverse technique. However, such an approach is liable to bias problems which cannot be easily dealt with by statistical techniques, as the coefficient matrix is formulated using measured mode shape and natural frequency data which is contaminated by experimental errors. In addition, the formulation of the equations requires mode shape displacement data for each coordinate. This is hardly possible as the number of coordinates is large and there are many coordinates which are not accessible for measurement. In practice the method therefore necessitate an estimation of the modal displacements of the missing DOF in the mode shape vectors.

Berman and Nagy (1983) extended the method of Lagrangian multipliers and updates both the mass and stiffness matrices. The mass matrix is updated by minimization of the weighted Euclidean norm of the difference between the updated and the analytical mass matrix, while satisfying the constraint of the orthogonality of the measured modes with respect to the updated mass matrix.

The stiffness matrix is then updated by minimization of the weighted Euclidean norm of the difference between the updated and the analytical stiffness matrix, subject to the constraint of the equation of motion, a technique similar to that used by Baruch *et al* (1978). The problem of unmeasured coordinates has been dealt with using an interpolation method given by Kidder (1973), to estimate modal displacements of the unmeasured coordinates. The interpolation involves partitioning the free vibration matrix equation of motion into submatrices corresponding to the measured and to unmeasured coordinates. The unmeasured part of the mode shape vector is expressed in terms of the mass and stiffness matrices and the measured subvector. As interpolation involves the knowledge of the mass and stiffness matrices, which are not known, the analytical mass and stiffness matrices are used instead. The estimated modal displacements contains, therefore, error contribution from the analytical model and from the experimental data.

Attempts to identify full rank mass and stiffness matrices directly from measured modal data without the use of an initial analytical model, have been reported by Ross (1971), Thoren (1972), and Richardson and Porter (1974). The practical usefulness of these direct methods is rather limited to small order problems, since they are based on the matrix inversion of the orthogonality equations with a complete modal matrix.

$$\mathbf{M} = \mathbf{U}^{-T}\mathbf{U}^{-1} \tag{2.35}$$

$$\mathbf{K} = \mathbf{U}^{-T}\Lambda\mathbf{U}^{-1} \tag{2.36}$$

Real structures however have an infinity number of DOF. Adequate modelling of complex structures for the frequency range of interest, covering the few lower modes, will usually require a model with a much higher number of DOF

than the measured modes.

Richardson and Porter have also suggested applying the inverse orthogonality equations to identify a large order model using an incomplete number of measured modes. The modal matrix and the eigenvalue matrix are completed by using arbitrary vectors and arbitrary frequencies which are much higher than the measured frequency range. Such a procedure, however, will lead to mass and stiffness matrices whose elements have no physical significance since there is an infinite number of arbitrary vectors that can be used to complete the modal model, each one giving different mass and stiffness matrices.

Most of the previous mentioned methods have not consider the identification or updating of the damping matrix, even though Vibration amplitude is very much dependent on damping levels. For many structures, however, damping levels are low and measured modes are of low complexity. The difficulties in accurate measurements of the damping factors and the difficulties in having a reasonable estimate of the damping matrix in the analytical model, did not seem to justify extra effort in the updating of the damping matrix using theoretical prior knowledge and experimental data. Measured real modes were therefore taken to be given by the moduli of the measured complex modes which had low complexity. There is also a significant number of structures for which mode complexity cannot be ignored.

Ibrahim (1983a), using simulated viscously damped model, show that highly complex modes are possible even at very low levels of non-proportional damping. The process of approximating measured complex modes to be normal-modes may introduce significant errors in the orthogonality equation.

Ibrahim used the approach of completing the modal model using high

frequency vectors in the identification of a viscously damped model from an incomplete number of measured complex modes. Rather than using arbitrary modes, as suggested by Richardson and Porter (1974), the high frequency modes of the analytical model are used to complete the measured modal model. As damping is difficult to estimate by theoretical analysis, it was assumed that the high frequency modes have damping factors which are the average of the damping factors of the measured modes. The approach involves identification of the mass modified stiffness matrix ($\mathbf{M}^{-1}\mathbf{K}$) and the mass modified damping matrix ($\mathbf{M}^{-1}\mathbf{C}$) from the homogeneous equation of motion.

$$\left[-\lambda_j^2\mathbf{M} + j\lambda_j\mathbf{C} + \mathbf{K}\right]\mathrm{V}_j = 0 \tag{2.37}$$

$$\left[\mathbf{M}^{-1}\mathbf{K} \quad \mathbf{M}^{-1}\mathbf{C}\right]\begin{Bmatrix}\mathrm{V}_j \\ j\lambda_j\mathrm{V}_j\end{Bmatrix} = \lambda_j^2\mathrm{V}_j \tag{2.38}$$

With a completed modal model ($j = 1{:}N$), each of the above equations represents N^2 complex equations or $2N^2$ real equations, from which the mass modified stiffness and damping matrices can be identified. The identified mass modified stiffness matrix, $\mathbf{M}^{-1}\mathbf{K}$, is used to compute the normal-modes. The computed normal-modes are mass normalized and used to identify the mass matrix using inverse orthogonality equation. However, as the modal masses are not known the modal masses of the analytical model are used in the normalization process. The stiffness and damping matrices are then found from the knowledge of $\mathbf{M}$, $\mathbf{M}^{-1}\mathbf{K}$ and $\mathbf{M}^{-1}\mathbf{C}$.

The method has been demonstrated, Ibrahim (1983b), using simulated data for a 10 DOF model with 4 measured modes. There is a convergence in natural frequency to the measured value for the 4 measured modes, whereas the high frequency unmeasured modes converges to the analytical modes. The

frequency response function shows good agreement with the correct model within the measured frequency range. Ibrahim, however, assumed that each coordinate is measured. The problem of unmeasured coordinates was not addressed.

More recently, Joeng *et al* (1989) proposed a method of identifying the mass, stiffness and damping matrices of a viscously damped system directly from measured complex mode shapes and frequencies without the use of an initial analytical model. The method is based on matrix inversion of complex orthogonality equations, (2.24) and (2.25), to identify the inverses of the transformed **A** and **B** matrices in terms of measured complex mode shapes and frequencies.

$$\mathbf{A}^{-1} = \Phi\Phi^{T} \tag{2.39}$$

$$\mathbf{B}^{-1} = -\Phi\Lambda_{(2N)}^{-1}\Phi^{T} \tag{2.40}$$

The inverses are also related to the spatial matrices by:

$$\mathbf{A}^{-1} = \begin{bmatrix} \mathbf{O} & \mathbf{M}^{-1} \\ \mathbf{M}^{-1} & -\mathbf{M}^{-1}\mathbf{C}\mathbf{M}^{-1} \end{bmatrix} \tag{2.41}$$

$$\mathbf{B}^{-1} = \begin{bmatrix} \mathbf{K}^{-1} & \mathbf{O} \\ \mathbf{O} & -\mathbf{M}^{-1} \end{bmatrix} \tag{2.42}$$

The mass, stiffness and damping matrices are then obtained by relating the submatrices in the inverse matrices in (2.41) and (2.42) to the corresponding submatrices in (2.39) and (2.40). The normalized complex mode shapes and frequencies in (2.39) and (2.40) are obtained by curve fitting a theoretical

expression to the measured frequency response function data. The method requires measurements at as many coordinates as the desired number of DOF in the corresponding analytical model, and in order to obtain *complete* matrices, measurement of as many modes as the number of DOF of the desired analytical model is also necessary. Since the number of measured modes in an actual structure is usually small, the model that could practically be identified by such a method is usually of a very low order. Furthermore, due to the unavoidable inaccuracies in the experimental data and also because modal data of a structure with a large number of DOF is forced to fit to a relatively low order model, the zero submatrices in (2.41) and (2.42) are not obtainable in the corresponding submatrices in (2.39) and (2.40). This introduces difficulties in relating the submatrices in (2.41) and (2.42) to the submatrices in (2.39) and (2.40). Joeng *et al* avoids this problem by introducing a constraint, $\text{Real}[\Theta\Theta^T] = 0$, which has to be satisfied during the identification of the modal data. However, as with other inverse orthogonality methods, for example those based on undamped and hysteretic damped models, the spatial matrices are fully populated. It is difficult to find a meaningful physical interpretation of the elements in the spatial matrices. Rotational DOF information, which may be important in a structural modification exercise, is lacking from the identified model and in general, it is difficult to relate the identified model to a finite element model.

2.2.2 Iterative methods

Iterative modal based methods are derived from non-linear relationships which express the eigen-data as a function of the spatial model parameters. They seek to find, iteratively, the adjustments to the parameters of the analytical model rather than finding whole matrices. They are based on sensitivities of the eigen-data to derive linearized relationships. The final

equations are in the form of (2.29) where the coefficient matrix is the Jacobian matrix of eigen-data sensitivities. The vectors s and b are replaced by a vector of parameter adjustments to the current analytical model and the vector of the difference between measured eigen-data and eigen-data of the current analytical model. Thus:

$$\begin{bmatrix} \mathbf{J}_\lambda \\ \mathbf{J}_U \end{bmatrix} \{\Delta s\} = \begin{Bmatrix} \Delta\lambda \\ \Delta U \end{Bmatrix} \tag{2.43}$$

Since the sensitivity relation is only exact for an infinitesimal parameter changes, the linear equations derived for finite parameter changes, based on first order approximations, are only approximate ones. Thus, an iterative process is involved. One feature of these methods, in general, is the requirement of an initial analytical model which is reasonably close to the true model, otherwise convergence problems are likely to occur. This requirement however is not of a major significance as in many cases a reasonable model can be found from theoretical considerations. As the sensitivity analysis is performed on the analytical model, the coefficient matrix is easily formulated without including experimental data that contains experimental errors. Statistical methods can therefore be utilized to advantage to deal with inaccuracies in the experimental data. However, in the case of a large complex structure with a large number of parameters to update, there is likely a difficulty in attaining a sufficient number of equations to facilitate a solution of (2.43).

Collins *et al* (1972) used sensitivities of the eigenvalues and eigenvectors and consider the case where the number of unknown parameters is larger than the number of equations. The underdetermined set of equations, in this case, is combined with an identity (2.44), to generate an overdetermined set of

equations which is solved by the pseudo-inverse technique.

$$[\mathbf{I}]\{\Delta s\} = \{0\} \tag{2.44}$$

The implication is that the updated parameters are determined which are close to the analytical model parameters and also reproduce measured eigen-data in a least squares sense. The analytical model parameters are treated as random quantities. Since the measured eigen-data and the analytical model parameters are of varying uncertainty, their variance estimates are taken as weighting factors in diagonal weighting matrices $\mathbf{W}_{\lambda,U}$ and $\mathbf{W}_{ca}$ respectively. Thus, the pseudo-inverse solution is given by:

$$\Delta s = \left[\begin{bmatrix}\mathbf{J}_\lambda \\ \mathbf{J}_U\end{bmatrix}^T \mathbf{W}_{\lambda,U} \begin{bmatrix}\mathbf{J}_\lambda \\ \mathbf{J}_U\end{bmatrix} + \mathbf{W}_{ca}\right]^{-1} \begin{bmatrix}\mathbf{J}_\lambda \\ \mathbf{J}_U\end{bmatrix}^T \mathbf{W}_{\lambda,U} \begin{Bmatrix}\Delta\lambda \\ \Delta U\end{Bmatrix} \tag{2.45}$$

However, (2.45) is a Bayesian estimate or minimum cost estimate for which the following cost function is minimum:

$$\{s - s_{ca}\}^T \mathbf{W}_{ca} \{s - s_{ca}\} + \begin{Bmatrix}\lambda_e - \lambda \\ U_e - U\end{Bmatrix}^T \mathbf{W}_{\lambda,U} \begin{Bmatrix}\lambda_e - \lambda \\ U_e - U\end{Bmatrix}$$

Expression (2.45) has been shown (Collins *et at* 1972) to be identical to (2.46).

$$\Delta s = \mathbf{W}_{ca} \begin{bmatrix}\mathbf{J}_\lambda \\ \mathbf{J}_U\end{bmatrix}^T \left[\begin{bmatrix}\mathbf{J}_\lambda \\ \mathbf{J}_U\end{bmatrix} \mathbf{W}_{ca} \begin{bmatrix}\mathbf{J}_\lambda \\ \mathbf{J}_U\end{bmatrix}^T + \mathbf{W}_{\lambda,U}\right]^{-1} \begin{Bmatrix}\Delta\lambda \\ \Delta U\end{Bmatrix} \tag{2.46}$$

Expression (2.46) was derived by Collins *et al* (1974) using a statistical approach, as a minimum variance estimate. If a set of parameter estimates of

the analytical model together with the measured eigen-data constitute a vector of random linearly independent entries, the Bayesian estimate becomes the minimum variance estimate. While this may be the case during the first iteration, subsequent parameter estimates are correlated with one another and also with measured eigen-data. Collins *et al* (1972) uses the diagonal of the computed covariance matrix of currently updated parameters, to update the weighting matrix, $\mathbf{W}_{ca}$, for the next iteration step. The off-diagonal terms in the computed covariance matrix are ignored. Collins *et al* (1974) uses the diagonal weighting matrix of the initial parameter estimate during the first iteration as a weighting matrix unchanged in subsequent iteration steps.

Iterative methods based on the Bayesian approach involving a constraint of minimum changes in the parameters of the analytical model have also been reported by Chen and Garba (1980), Natke and Cottin (1985), Heylen (1986), Thomas *et al* (1986), Zhang and Lallement (1989) and Friswell (1989a). In the case of a damped model, the real and imaginary parts on the left-hand-side of (2.43) can be equated to their corresponding real and imaginary parts on the right-hand-side of the equation, to obtain two sets of equations which are solved simultaneously. With non-proportional viscous damping, the eigen-vectors Θ are used instead of the mass normalized vectors U and the eigenvector sensitivity matrix becomes the sensitivity matrix with respect to Θ, $(\mathbf{J}_{\Theta})$.

Heylen suggested a combination of the linearized sensitivity equations with the linear equations, obtained by using the equations of motion and the orthogonality conditions. Zhang and Lallement particularly consider the difficulties of resolving modes with repeated frequencies. A selective structural modification technique is used to perturb the analytical model and the experimental data so as to achieve a frequency separation of modes with

repeated eigenvalues. Friswell discusses the correlation of the measurement vector to the updated parameters and derives a minimum variance estimator, which takes into account the correlation between the parameters and between the parameters and the measurement vector in each iteration step. It has been demonstrated that parameter convergence rate is slow if the correlation is ignored.

In all these methods a solution cannot be found with unconstrained optimization, even with very accurate data, if the number of measured modes is small such that the sensitivity equation is underdetermined, since there will be an infinite number of parameters that could exactly reproduce the measured data. The solution obtained with constrained optimization will therefore be strongly dependent on the parameters of the analytical model.

2.2.3 Localizing dominant modelling errors and expansion of the mode shape vectors.

Several investigators have addressed the question of localizing dominant modelling errors in the analytical model prior to the model updating process. It is expected that once zones of dominant modelling errors are identified, the number of parameters to be updated will be reduced. Furthermore, the effectiveness of the updating algorithm could be improved by concentrating on zones which requires adjustments and avoiding unnecessary adjustments to otherwise correctly modelled areas.

The error matrix method (Dobson 1984, Ewins and Sidhu 1984,1985) has been proposed for localizing dominant modelling errors in the stiffness matrix. The technique involves finding a matrix (an error matrix) which is a measure of the difference between the analytical stiffness matrix and the

stiffness distribution of the structure. The error matrix is then presented as a three dimensional plot with a base of grids defining nodes of the structure which are also coordinates of the analytical model. Zones which are sources of discrepancy between the analytical model and the experimental data are then revealed by bigger magnitudes of the error quantity at relevant nodal positions on the error matrix plot.

Since it is difficult to get a stiffness matrix which is a correct representative of the stiffness distribution of the structure from incomplete modes, Dobson uses the pseudo-flexibility matrix obtained from the stiffness orthogonality equation. This has two implications:

(i) An incomplete number of measured modes could yield a flexibility error matrix which resembles the flexibility error matrix obtained by using a complete number of modes.

(ii) The difference in the flexibility matrices is considered to reveal the difference in the stiffness matrices.

Since some coordinates cannot be measured, the modal matrix is partitioned into submatrices corresponding to the measured and unmeasured coordinates (subscripts mm and oo respectively) and submatrices corresponding to the measured and unmeasured modes. The eigenvalue matrix is also appropriately partitioned. The complete flexibility matrix is then given by:

$$\mathbf{K}^{-1} = \mathbf{U}\Lambda^{-1}\mathbf{U}^{T} = \begin{bmatrix} \mathbf{U}_{mm}\Lambda_{mm}^{-1}\mathbf{U}_{mm}^{T} + \mathbf{U}_{oo}\Lambda_{oo}^{-1}\mathbf{U}_{oo}^{T} & \mathbf{U}_{mm}\Lambda_{mm}^{-1}\widehat{\mathbf{U}}_{mm}^{T} + \mathbf{U}_{oo}\Lambda_{oo}^{-1}\widehat{\mathbf{U}}_{oo}^{T} \\ \widehat{\mathbf{U}}_{mm}\Lambda_{mm}^{-1}\mathbf{U}_{mm}^{T} + \widehat{\mathbf{U}}_{oo}\Lambda_{oo}^{-1}\mathbf{U}_{oo}^{T} & \widehat{\mathbf{U}}_{oo}\Lambda_{oo}^{-1}\widehat{\mathbf{U}}_{oo}^{T} \end{bmatrix} \quad (2.47)$$

The pseudo-flexibility matrix used by Dobson includes measured modal matrix at measurement DOF only, which is given by the first term in the top left hand corner of the complete flexibility matrix in (2.47). The contribution of the second term is ignored. With the flexibility matrix approach, it is difficult, however, to relate the error in the flexibility matrix to the error in the stiffness matrix. This is so because the elements of the inverted matrix usually involves a number of terms of the non-inverted matrix coupled together by the matrix inversion process. This is further complicated by the fact that a significant number of coordinates are not measured and the error in the pseudo-flexibility matrix defined through the use of a smaller number of coordinates has to be related to the overall structure.

Ewins and Sidhu (1984) attempts to derive an expression for the stiffness error matrix and thus avoiding the difficulties of correlating the flexibility error matrix to the actual zones of discrepancy in the stiffness matrix. The technique involves rewriting the stiffness matrix and hence the flexibility matrix in terms of the analytical stiffness matrix and the stiffness error matrix. After simplification using a truncated binomial expansion, an expression for the stiffness error matrix is obtained, which is approximately given by:

$$\mathbf{E}_k = \mathbf{K}_a[\mathbf{K}_a^{-1} - \mathbf{K}^{-1}]\mathbf{K}_a \qquad (2.48)$$

The Flexibility matrix, $\mathbf{K}^{-1}$, in (2.48) is obtained from the experimental data. However, because of practical limitations, an incomplete matrix generated using an incomplete number of modes measured at an incomplete number of coordinates is used together with a corresponding incomplete flexibility matrix of the analytical model. This is a significant improvement to the Dobson's method in the sense that a stiffness error matrix rather than the flexibility matrix is available. However, it is defined only at measurement

coordinates.

The main objections to the error matrix method in general, are the dependence of the error matrices on the modes used and the difficulties in extrapolating the error matrices defined at a small number of measurement coordinates to the full order stiffness matrix. The dependence of the pseudo-error matrices on the modes used has been demonstrated in a critical study by Gysin (1986) using simulated data. Gysin's study concluded by raising doubts on the general reliability of the technique in a practical situation of incomplete modes.

Ibrahim and Fissette (1988) use the equation of motion to define an error vector. The error vector is given by the residual force necessary to balance the equation of motion of the analytical model when frequency and displacement vector are substituted by their measured modal counterpart (force balance approach). With an error-free analytical model the equation should reproduce a zero forcing vector. However, with errors in the analytical model there is a residual force which, in the case of an undamped system, is given by:

$$E_j = [\mathbf{K}_a - \lambda_j \mathbf{M}_a] U_j \qquad (2.49)$$

It can be shown that the residual force in (2.49) is proportional to both the stiffness and the mass error matrices. This residual force is taken as an error vector which is an indicator of the coordinates associated with zones of dominant modelling errors. The absolute values of the error vectors are averaged over a number of measured modes and plotted against the coordinate number. Zones of significant modelling errors are identified by bigger magnitudes in the error plot at corresponding coordinate numbers. Numerical examples, given by Ibrahim *et al*, have shown the method to be capable in localizing modelling errors in the case of simulated error-free data. Unlike

the error matrix method, its capability is not affected by the number of modes used.

The use of the force balance method, however, requires "full length" mode shapes measured at each coordinate corresponding to the DOF of the analytical model. Since in practice some coordinates cannot be measured, the missing DOF have to be estimated by a suitable expansion process. Mode shape expansion can be achieved by :

(i) Geometrical interpolation by curve fitting a theoretical expression to the mode shape data, for example using spline functions.

(ii) Transformation of coordinates using modal matrix of the analytical model.

(iii) Dynamic expansion using a partitioned equation of motion.

The successful use of geometrical interpolation is limited to structures of simple forms and is difficult to apply to a three dimensional structure with complex changes in shape.

Mode shape expansion by the method of transformation of coordinates (O'Callahan *et al* 1984) is based on the expression of the structure's displacement vector as a linear combination of the eigenvectors of the analytical model. Thus:

$$\begin{Bmatrix} \mathbf{U}_{mm} \\ \mathbf{U}_{oo} \end{Bmatrix}_j = \begin{bmatrix} \mathbf{U}_{mm} \\ \mathbf{U}_{oo} \end{bmatrix}_a \mathrm{P}(j) \qquad (2.50)$$

The subscripts mm and oo refers to the subvectors/submatrices corresponding to the N_{mc} measured DOF and N - N_{mc} unmeasured DOF respectively. The process of mode shape expansion requires finding a vector P(j) of the coefficients of linear combination, for each measured mode j, and substitute it into (2.50). To find P(j), the measured part of the mode shape vector is equated to its corresponding partitioned part on the right-hand-side of the equation.

$$\{\mathrm{U}_{mm}\}_j = [\mathbf{U}_{mm}]_a \mathrm{P}(j) \tag{2.51}$$

If a complete number of analytical modes is used, (2.51) is underdetermined and there is an infinite number of solutions for P(j). However, if the structure's modal matrix was used as a transformation matrix, then it is fairly accurate to consider only N_{eff} lower modes ($N_{eff} < N$) which make an effective contribution to the response within the frequency range of interest. An assumption is therefore made that the analytical modal matrix can also be truncated to N_{eff} lower modes. This process obviously introduces an error which depends on how close is the analytical model to the correct model. Usually $N_{eff} < N_{mc} < N$. Thus a least squares solution for P(j) is found by pseudo-inverse. The expanded mode shape is then given by:

$$\mathrm{U}_j = \begin{bmatrix} \mathbf{U}_{mm} \\ \mathbf{U}_{oo} \end{bmatrix}_a [\mathbf{U}_{mm}]_a^{\mathbf{I}} \{\mathrm{U}_{mm}\}_j \tag{2.52}$$

This process involves modification of the already measured part of the mode shape vector since, in general, a rectangular matrix with more rows than columns, when post-multiplied by its pseudo-inverse, does not result in an identity matrix. It is possible, however, to retain the unsmoothed measured part of the modes in the expanded mode shapes. A similar formulation can be derived for a general viscously damped system, where the modes in (2.52) are

replaced by the system eigenvectors associated with the transformed first order differential equation of motion based on state variables. In either case, the missing DOF in the measured modes are estimated in terms of the measured DOF and eigenvectors of the analytical model. The accuracy of the expanded mode shapes is determined by the accuracy of the measured DOF and the validity of the analytical model.

Kidder's dynamic expansion method (1973), is based on the relationship of the unmeasured part of the mode shape vector with the measured part in terms of the spatial model submatrices. The relationship is obtained by partitioning the homogeneous equation of motion into submatrices and subvectors corresponding to the measured and unmeasured coordinates. This process retains the original measured part of the mode shape vector. As the correct model matrices are not known, analytical model matrices are used instead. The expanded mode shape is given by:

$$\mathbf{U}_j = \begin{bmatrix} \mathbf{I} \\ -\mathbf{D}_{oo}^{-1}\mathbf{D}_{om} \end{bmatrix}_a \{\mathbf{U}_{mm}\}_j \qquad (2.53)$$

Alternative ways of partitioning the equation of motion are possible. They result in slightly different expressions to that given by Kidder but, in all cases, the validity of the analytical model dictates the accuracy of the expanded mode shape and hence the reliability of the modelling error localization process.

Gysin (1990) has made some numerical studies on the capability to localize modelling errors using a force balance approach with expanded mode shape vectors. The modes were expanded by the method of transformation of coordinates and by dynamic expansion using a partitioned equation of motion. The main problem is that accurate expansion requires system matrices which

are not known and the analytical model matrices are used instead. Using a 9 DOF spring-mass chain model with different cases of modelling error, number of modes, and simulated measurement coordinates combination, Gysin found that localization capability is very sensitive to errors in the mode shape vectors and that no expansion method was satisfactory for all the cases that he investigated.

An alternative method based on the sensitivity analysis of the eigenvalues and measured part of the eigenvector is given by Zhang *et al* (1987). In this method the structure is further idealized into macro-elements or substructures and the analytical model is also divided into submatrices corresponding to the macro-elements. The unknown model matrices are assumed to be given by a linear combination of the submatrices of the analytical model and the coefficients of the linear combination of the submatrices are taken as the parameters to be found. The first step in the localization process is to find an initial vector, Δs, for the required parameter changes from their initial estimates in the analytical model. This is achieved by an unconstrained optimization using linearized equations which are developed by first order sensitivity analysis of the eigen-data and assembled in the form of (2.43). Relatively large absolute values in Δs implies that either there are large errors in the initial estimates or the eigen-data is simply insensitive to variations in the parameters of the corresponding macro-elements. To distinguish between the two cases each column in the coefficient matrix (Jacobian matrix) is multiplied by its corresponding value in the Δs vector to obtain a new vector 'E'. The vector E is supposed to indicate the contribution of a particular macro-element on the difference between measured and the analytical eigen-data. Then for each macro-element, i, a scalar indicator $e(i)$ is defined as:

$$e(i) = \frac{\| \mathrm{E}(i) \|}{\| \begin{Bmatrix} \Delta\lambda \\ \Delta\mathrm{U} \end{Bmatrix} \|} \tag{2.54}$$

According to Lallement *et al*, Macro-elements with dominant modelling errors are identified by large values in Δs and in $e(i)$. Only those macro-elements identified as having dominant modelling errors are retained in the updating process. The sensitivity approach to localize modelling errors can be utilized without the need for the estimation of the missing DOF in the mode shape vectors. Its success, however, relies on the ability to divide the structure into a smaller number of macro-elements so that the resulting sensitivity equations are not underdetermined.

2.3 Methods based on the frequency domain data

Parameter estimation methods based on the frequency domain data are derived from the frequency domain equation of motion (2.2), (2.14) or (2.16). These methods employ measured frequency domain forcing and response data directly without the need for an identification of the modal model. They can be divided into two main groups, the equation error and the output error methods.

Equation error methods utilize the linear relationship between the unknown model parameters and measured forcing data as depicted in the equation of motion. Parameters are then determined which best fits the frequency domain equation of motion, with measured response data, by reproducing a forcing vector which has a minimum deviation from the measured forcing vector in a least squares sense. Since the equation of motion is linear in the unknown parameters, it can easily be reformulated in the form of (2.29). The coefficient

matrix, **G**, is derived from measured response data and the right-hand-side vector b becomes a vector of measured excitation forces. Thus, by sweeping through the frequency range of interest at discrete frequency intervals, an overdetermined equation is obtained and is solved by a pseudo-inverse technique. A prior knowledge of the parameter values can also be utilized in a Bayesian framework. It is usual to employ the equation of motion with a single forcing coordinate and to normalize so that displacements are converted to receptances and the force to a unity.

Equation error methods based on the above mentioned principles have been reported by Natke *et al* (1985, 1986, 1988), Fritzen (1986), Mottershead and Stanway (1986), Mottershead (1988) and Friswell and Penny (1990). The equation error approach however presents two main difficulties.

The first difficulty is biased estimates, since the coefficient matrix is formulated using experimental data which is contaminated by measurement errors. With error-free data the least squares solution is a true solution and is given by:

$$s = [\mathbf{G}^T\mathbf{G}]^{-1}\mathbf{G}^T b \tag{2.55}$$

With errors in the response data, the coefficient matrix can be written as $\mathbf{G}+\mathbf{E}_G$, where $\mathbf{E}_G$ is an error matrix. The least squares solution, in this case, is given by:

$$s = [(\mathbf{G}+\mathbf{E}_G)^T(\mathbf{G}+\mathbf{E}_G)]^{-1}(\mathbf{G}+\mathbf{E}_G)^T b$$

$$= [\mathbf{G}^T\mathbf{G}+\mathbf{G}^T\mathbf{E}_G+\mathbf{E}_G^T\mathbf{G}+\mathbf{E}_G^T\mathbf{E}_G]^{-1}\{\mathbf{G}^T b+\mathbf{E}_G^T b\} \tag{2.56}$$

From (2.56), it is apparent that the expected value of the sum of terms inside the first bracket is different from that in (2.55) due to the presence of a quadratic error term which do no vanish and contributes to biased estimates.

Fritzen has addressed the bias problem by adopting an instrumental variable (IV) method. The IV method has been used in control engineering (Wong and Polak 1967, Young 1970) to identify parameters of a time discrete difference equation. The basis of the IV method, as presented by Fritzen, is to pre-multiply (2.29) by $\mathbf{G}^T_{INS}$ instead of $\mathbf{G}^T$. Thus, with errors in the response data, the unknown parameter vector is given by:

$$s = [\mathbf{G}^T_{INS}\mathbf{G} + \mathbf{G}^T_{INS}\mathbf{E}_G]^{-1}\{\mathbf{G}^T_{INS}b\} \qquad (2.57)$$

$\mathbf{G}_{INS}$ is an instrumental variable matrix. Its elements are selected such that the term inside the first bracket is invertible and the expected value of the error terms in (2.57) vanish. This implies the instrumental variable matrix is to be uncorrelated with measurement noise. The best formulation of the IV matrix is to use error-free response data since this is poorly correlated with measurement noise. However, since it is not possible to know the error-free responses, Fritzen formulates an auxiliary model using parameter estimates of the analytical model and subject it to the same excitation as the structure and compute is response data. The response data of the auxiliary model is then used to formulate an IV matrix. This process involves iteration, each time formulating an auxiliary model and hence an IV matrix using current parameter estimates. At the start of the iteration a non-IV least squares method is used to get starting parameters for the initial auxiliary model.

Numerical example as presented by Fritzen have shown the method to be effective in reducing bias to a small level, which was not achieved by a non-IV

least squares technique. The method however requires a large data sample, is time consuming and the computational efficiency of the equation error approach is lost.

The second difficulty with the equation error method is the requirement to have measurements at all coordinates corresponding to the DOF of the required model, since the equations cannot be formulated if response data of some coordinates is missing. This is particularly evident when a model compatible with a finite element model is required, since it usually involves some unmeasured translational and rotational coordinates. Fritzen assumed all coordinates are measured. Classical model reduction methods, which have been proposed for the economization of the eigenvalue problems (Guyan 1965, Irons 1965, Kidder 1973, Miller 1980, Paz 1984) are not suitable to solve this problem. They are based on the transformation of the 'full length' displacement vector to a reduced displacement vector. The transformation matrix is expressed in terms of the unknown model parameters using a partitioned equation of motion. The reduced order matrices obtained by the reduction process are non-linear in the parameters of the full order model. A possible solution to this problem is to construct the transformation matrix using parameters of the analytical model and iterate using the identified parameters. However, the reduction methods are only approximate with simplifying assumptions regarding the contributions of the inertial effects. The validity of the assumptions depends on the selection of the coordinates to be retained in the reduced equation of motion. While this may not pose a major limitation in the eigensolution of the analytical model, vibration testing has its limitation on the coordinates which can practically be measured. It has been demonstrated (O'Callahan *et al* 1989a) that incorrect selection of the coordinates to be retained in the reduced equation of motion, results in significant errors in the eigenvalues of the reduced order model.

Model reduction methods particularly suited for parameter identification have been reported by Natke (1988), O'Callahan *et al* (1989b), Friswell (1989b) Friswell and Penny (1990). They are based on the transformation of coordinates using an incomplete modal matrix of the analytical model, following similar principles to the mode shape expansion method which has been discussed in section 2.2.3. Thus, if $\mathbf{U_a}$ is an N x N_R analytical modal matrix the displacement vector is assumed to be given by :

$$q(\omega) = \mathbf{U}_a P(\omega) \tag{2.58}$$

The higher order displacement vector in the differential equation of motion is written in terms of the analytical modes and a lower order vector using (2.58). The differential equation of motion is then pre-multiplied by the transposed incomplete analytical modal matrix to obtain a reduced equation of motion which, in the case of a hysteretic damped system, is given by:

$$[-\omega^2 \mathbf{U}_a^T \mathbf{M} \mathbf{U}_a + \mathbf{U}_a^T [\mathbf{K} + j\mathbf{H}] \mathbf{U}_a] P(\omega) = \mathbf{U}_a^T \mathbf{Q} \tag{2.59}$$

The reduced equation retains the linear relation of the unknown model parameters of the full order model. The process of finding model parameters, therefore, requires the computation of the reduced vector $P(\omega)$ and its corresponding forcing vector. The reduced equation can then be rewritten in the form of (2.29). By using data from a sufficient number of discrete frequencies in the measurement frequency range, an overdetermined equation is obtained and solved by least squares method, usually following a Bayesian framework.

To obtain $P(\omega)$, (2.58) is partitioned into subvectors and submatrices corresponding to the measured and unmeasured DOF and equating the

measured part of the displacement vector to its corresponding partitioned part on the other side of the equation. To reduce modal truncation errors, the order N_R of the reduced equation is selected to be not less than the number N_r of excited modes in the measurement frequency range. Usually $N_{mc} > N_R > N_r$, thus :

$$P(\omega) = \left([U_{mm}]_a^T [U_{mm}]_a \right)^{-1} [U_{mm}]_a^T q(\omega) \qquad (2.60)$$

Natke (1988) and Friswell and Penny (1990) have applied this approach to a viscously damped model. In this case, a transformed first order differential equation (2.16) is used and the displacement vector is replaced by the state vector. Since the analytical modes are used in (2.50) instead of the true modes of the structure, the reduction process is liable to errors. Friswell and Penny used an iterative approach where the updated parameters are used to compute a new set of improved analytical modes which are used in the next iteration step. The process, however, does not eliminate bias due to measurement errors in the frequency response data. Furthermore, with measurement errors there is no guarantee of the best convergence of the frequency response data to the measured one since the approach minimize the equation error rather than the difference between measured and model's frequency response data.

The output error method (Natke and Cottin 1985, Natke 1988, Fritzen and Zhu 1989) seeks to minimize, in a least squares sense, the objective function which is a weighted difference between measured displacement vector and model displacement vector. i.e minimize f_o by setting:

$$\frac{\partial f_o}{\partial s_i} = 0 \qquad (2.61)$$
$$(i = 1 \ldots p)$$

where

$$f_o = \{ [-\omega^2 \mathbf{M} + \mathbf{K} + j\mathbf{H}]^{-1} Q_e - q_e \}^T \mathbf{W} \{ [-\omega^2 \mathbf{M} + \mathbf{K} + j\mathbf{H}]^{-1} Q_e - q_e \}$$

The displacement and forcing vectors (for a given excitation coordinate) are usually normalized so that the displacement vector can be substituted by a receptance vector and the forcing vector replaced with a unit amplitude at the excitation coordinate. Since the relation between the unknown model parameters and measured displacement vector is non-linear, the objective function is also non-linear in the unknown parameters. For each excitation frequency, (2.61) consists of N simultaneous equations non-linear in the unknown parameters. The output error method, therefore, involves a non-linear optimization which require an initial estimate of the parameters so as to linearize and reduce (2.61) into a linear form. This is achieved by a first order Taylor's expansion of the objective function about the current parameter estimates and then employing (2.61). By data sampling at discrete frequency intervals in the measured frequency range, an overdetermined equation is obtained which can be solved by pseudo-inverse technique.

Natke and Cottin (1985) have applied an output error method on a numerical example by assuming a single excitation coordinate and response measurement at all coordinates. Fritzen and Zhu (1989) have applied a Bayesian output error method using a second order Taylor's expansion of f_o to a practical plane frame. A single coordinate was measured and an excitation was applied in one of the translational coordinates at each node of the finite elements connectivity points.

2.4 Methods based on time domain data

Although proposals to use time domain data in the identification of the spatial

matrices of a dynamic system have been reported as far back as 1969 (Young and On 1969), there is relatively fewer references on time domain methods as compared to those based on the modal data. Time domain methods are mainly derived from the matrix equation of motion rewritten with the coefficients as signal matrices which are constructed from measured data. The data is sampled at discrete time intervals and model matrices are the unknown quantities. Time domain methods have been proposed for the identification of the spatial matrices directly from the experimental data and they normally perform well with numerical simulation of error-free data (Young and On 1969, Ronald and Xu 1986). In a practical situation a number of coordinates cannot be measured and measurement noise give rise to an equation error which is correlated with the unknown parameters. Time domain methods therefore suffer the problems of missing DOF in the experimental data and biased estimates as with frequency domain equation error methods. The applicability of time domain methods is currently limited to low order models condensed to the measurement DOF.

Young and On discuss a response time history product and averaging technique which was intended for the identification of the mass, stiffness and damping matrices without the use of an initial analytical model. The technique requires simultaneous measurement of the excitation force and responses at all coordinates of the desired mathematical model. From (2.1), each of the N equations involves a maximum of $3N$ unknown model parameters and $3N$ known variables which are measured displacements, velocities and accelerations. Each of the N equations is then multiplied by each of the $3N$ variables to generate a set of $3N$ equations in $3N$ unknowns. By data sampling at discrete time intervals, each set of the equations is averaged out and solved for the unknown parameters. This procedure, as presented by Young and On, assumes that all influence coefficients in the model matrices are to be identified

as independent unknowns. This however is not necessary. With a finite element model the matrices are usually symmetrical and some influence coefficients in the matrices are known to be zero. The total number of parameters to be identified could therefore be reduced by imposing a condition of symmetry and forcing some parameters to be zero. However, since it is usually practical to measure only some translational DOF the identified model is a condensed one, usually fully populated, and the elements of its matrices cannot be easily related to the parameters of the full order finite element model.

Xu and Ronald have suggested a technique which uses free vibration data to identify the mass modified stiffness matrix ($\mathbf{M}^{-1}\mathbf{K}$) and mass modified damping matrix ($\mathbf{M}^{-1}\mathbf{C}$) directly from the equation of motion which is written as:

$$\mathbf{M}^{-1}\mathbf{C}\dot{\mathbf{q}}(t) + \mathbf{M}^{-1}\mathbf{K}\mathbf{q}(t) = -\ddot{\mathbf{q}}(t) \tag{2.62}$$

By successive data sampling, the measurement vectors in the above equation are transformed into matrices and by transposing the equation the mass modified matrices are obtained from (2.63):

$$\left[\left[\dot{\mathbf{q}}(t)\right]^{T} \quad \left[\mathbf{q}(t)\right]^{T} \right] \begin{bmatrix} \left[\mathbf{M}^{-1}\mathbf{C}\right]^{T} \\ \left[\mathbf{M}^{-1}\mathbf{K}\right]^{T} \end{bmatrix} = - \left[\ddot{\mathbf{q}}(t)\right]^{T} \tag{2.63}$$

Since the responses can be written as a linear combination of the mode shape vectors, the rank of the coefficient matrix in (2.63) is limited by the effective number of excited modes. This number is usually small since some modes are not excited or only weakly excited. For a large number of measurement coordinates, it should theoretically be difficult to solve for the spacial matrices as the coefficient matrix in (2.63) becomes rank deficient. However, due to the

measurement errors, the coefficient matrix is usually full rank and invertible. The effects of errors, therefore, is to introduce some *false modes* in the response data. The identified matrices will contain true modes which correspond to the effectively excited modes and some false modes which are due to the measurement errors. The identified model is therefore not reliable in the prediction of, for example, the natural frequencies of the system.

Badenhauser (1986) suggest a technique of removing the false modes from the measured data. It involves first establishing the number of effective modes in the measured data by singular value decomposition of the transposed matrices of measured acceleration, velocity and displacement. The rank detection number is computed by arranging the singular values of each data matrix in a descending order and starting from the first singular value (i = 1), the value of i for which the ratio of the $i+1^{th}$ to the i^{th} singular value deviates sharply from the previous ratios is determined by inspection, say i_b. The number of effective modes is then taken as $N_{eff}=i_b$ The false modes are then removed by post-multiplying the transpose of the measured displacement, velocity and acceleration matrices by a square projector matrix, **N**, of rank N_{eff} and order N. In this way substitute data matrices of rank equal to the number of effective modes are obtained. The projector matrix is given by:

$$\mathbf{N} = \mathbf{Z}\mathbf{Z}^{T} \tag{2.64}$$

Z is an N x N_{eff} matrix formed by assembling vectors of length N and which correspond to the i_b highest singular values obtained from the singular value decomposition of the transposed acceleration data matrix.

Using forced vibration, Badenhauser rewrites the equation of motion with data matrices simply replaced by substitute data matrices of rank N_{eff}, as:

$$[\ddot{q}(t)]^T ZZ^T + [\dot{q}(t)]^T ZZ^T [M^{-1}C]^T + [q(t)]^T ZZ^T [M^{-1}K]^T = [F(t)]^T M^{-T} \qquad (2.65)$$

By post-multiplying (2.65) by **Z**, a reduced equation is obtained from which Badenhauser defines the reduced mass modified stiffness and damping matrices as:

$$[M^{-1}K]_R = Z^T [M^{-1}K] Z, \qquad [M^{-1}C]_R = Z^T [M^{-1}C] Z$$

In this approach, the reduced order model has as many DOF as the number of effective modes. Attempt to expand the reduced order model is only possible up to the measurement DOF only. Correlation with a finite element model is difficult. Badenhauser's approach could be effective in removing noise related modes in the measured time domain data and therefore avoid predicting incorrect natural frequencies. However, the prediction of the frequency response functions will be degraded by the fact that high frequency residues are not accounted for. To get better results more modes have to be effectively excited and this naturally involves extra precautions and consideration on the method to be used to excite the structure. In general, the process is cumbersome with no major advantages.

2.5 Summary

2.5.1 Modal based methods

Modal based methods can be divided into the iterative and the non-iterative groups. The non-iterative methods can further be divided into three subgroups as follows:

(i) Methods which attempts to find model matrices without using prior knowledge of the system matrices. In these methods, whole matrices rather than individual parameters are identified, usually using inverse orthogonality equations. Examples include Ross (1971),Thoren (1972) and Joeng *et al* (1989).

(ii) Methods which assumes prior knowledge about the system in the form of analytical model matrices and attempts to derive formula for the updated model matrices which are closer to the analytical model matrices subject to some constraint conditions. Examples: Baruch *et al* (1978), Berman and Nagy (1983).

(iii) Methods which assumes only the structure of the model matrices rather than individual parameters. The unknown parameters are obtained from a set of algebraic equations derived from the homogeneous equation of motion and/or the orthogonality equations. Example: Tlusty and Ismail (1980).

The first subgroup represent the simplest of the modal based methods. Its capability depends on the availability of a complete modal model with as many measured modes and measurement coordinates as the number of DOF. This is

not practical. When these methods are applied, the number of measurement coordinates has to be restricted to the number of identified modes. The identified model is then fully populated, of a very low order and cannot be related to a finite element model.

In the second subgroup, equations for the full order model matrices are derived. Among an infinite number of models that can reproduce the incomplete number of measured modal data or a set of corrected modes, only that model whose matrices have a minimum norm difference from the analytical model is selected as an optimum solution. The use of the method requires "full length" mode shapes. Since the method attempts to identify whole matrices rather than the individual parameters, the structure of the matrices is liable to be distorted, bearing in mind the incompleteness of the data and experimental errors in the measured modal data.

The third subgroup retains both the order of the analytical model and also the structure of the matrices since the individual parameters rather than whole matrices are determined. The identification of the parameters is performed from the algebraic equations derived from the homogeneous equation of motion and/or the orthogonality equations and written in the form of (2.29). This requires "full length" mode shapes. While the missing DOF in the measured mode shapes can be estimated, the process introduces additional errors due to the approximate mode shape expansion process.

The iterative methods are based on eigen-data sensitivity to derive a set of linearized equations from which parameter changes to the current analytical model are found iteratively. Prior knowledge of both the structure of the model matrices and its parameters is used. Thus, the updated model retains the order and the structure of the matrices of the analytical model and therefore it

could be compatible with a finite element model. The updated model may be unique only if the number of linearly independent equations is not less than the number of unknown parameters. With a large number of parameters to update and a smaller number of measured coordinates and measured modes, a situation of an infinite number of solution for the parameters can arise. Usually the experimental data is dominated by the mode shape data rather than the natural frequency data, and the measurement of the mode shapes is generally less accurate than the natural frequencies.

2.5.2 Frequency domain methods

The advantage of parameter estimation directly from frequency domain data as opposed to the modal data is the avoidance of the modal identification routine and therefore uncertainties associated with modal identification are avoided. Frequency domain methods are mainly based on the equation error and the output error approaches. The advantage of the equation error approach over the output error approach is the linear appearance of the parameters in the equation of motion.

The equation error approach has its limitations. First the response of the unmeasured coordinates have to be estimated or the equations have to be reduced to the measurement DOF. Both processes only can be performed approximately by relying on the approximation of the analytical mode shapes as the correct mode shapes of the structure. While this limitation could be minimized by an iterative process, iteration is time consuming and an important advantage of the equation error approach is lost. Secondly the estimated parameters are biased because measured response data, which is contaminated with measurement noise, is used in the formulation of the coefficient matrix. This results in an equation error which is correlated with

the unknown parameters. Thirdly the method does not guarantee best convergence of the frequency response function to the measured one since it minimize the difference between the forcing vectors rather than the response vectors.

The above limitations of the equation error approach seems to have been overcome by the output error method which minimize the difference in the response vectors between the structure and the updated model. The output error method does not require response data for each coordinate as the formulation of the equation allows for a selective approach by using only those rows corresponding to the measurement coordinates. This is achieved at an extra computational cost using a non-linear optimization. While, in principle, the output error method has all the best qualities of unbiased estimates and no need for model reduction, its main limitations is the complication of the equations and considerable computational effort.

2.5.6 Time domain methods

Time domain methods have attracted least interest. They are mainly based on the equation error approach using a time domain equation of motion, usually with or without an assumption of the structure of the model matrices. Consequently, time domain methods encounters most of the difficulties experienced by the frequency domain equation error methods. Problem specific to the use of time domain data is the effect of the contribution of the measurement errors. Measurement errors has an effect of additional modes (false modes) which shows up when an eigensolution of the identified model is performed. Noise related modes can only be removed by restricting the number of DOF of the model to the number of effective modes in the measurement data. The resulting model is then not compatible with the finite element model.

2.6 Conclusion

Whilst the relationship between vibration data and model matrices can be formulated using modal data, frequency response data and time domain data, the most promising methods of updating a finite element model are based on modal data and frequency response data. The modal based methods are either non-iterative ones using the homogeneous equation of motion and/or the orthogonality equations to derive an algebraic set of equations and the iterative ones using sensitivity analysis of the eigen-data. Methods using frequency response data are based on the equation of motion either to derive an algebraic set of equations and find an updated model which minimize the equation error or to minimize the differences between measured and model's frequency response functions by a non-linear optimization technique. These methods have their limitations and as such there is no method which has received a general acceptance. From the literature review the following can be concluded:

(i) The identification of a model which is compatible with a finite element model directly from vibration test data alone is not possible due to the incomplete number of measured coordinates and measured modes.

(ii) The use of an incomplete number of modes to update whole matrices, rather than individual parameters, without utilizing prior knowledge of the structure of the model matrices results in model matrices whose structure is not compatible with the analytical model.

(iii) Parameters updated using the homogeneous equation of motion

and orthogonality equations are liable to bias problems due to the inaccuracies in the measured modal data.

(iv) In some cases, it is not necessary to have response data from every coordinate if an iterative method based on linearized eigen-data sensitivity equations or frequency domain output error is used.

(v) It is possible to find a unique solution for the model parameters using an iterative method based on the eigen-data sensitivities. However, appropriate conditions cannot be guaranteed due to the limit on the number of linearly independent equations that can be generated as a result of the limitations on the number of measured modes and measured coordinates.

(vi) Difficulties in using experimental data to update a dynamic model are mainly due to, inability to excite or measure the high frequency modes with natural frequencies outside the measurement frequency range, inability to measure some coordinates and inaccuracies in the measured data.

(vii) No parametric updating method can rectify a fundamental conceptual error in the finite element model.

From the findings of this literature review, it is considered that a model updating method which is based on the minimization of the output quantities (eigenvalues, eigenvectors or response data) is the most attractive for further research. Such a method avoids the difficulties of biased estimates associated with a correlated error vector as is the case with methods based on the equation

error approach. In addition, the output quantities are usually the ones which are taken as a basis of agreement or disagreement between the analytical model and the actual mass and stiffness distribution. Thus, direct minimization of the output quantities is more attractive than minimization of an equation error which may not necessarily lead to the agreement in the dynamic behaviour.

Most attempts in this direction have been on the use of the eigenvalues and eigenvectors by sensitivity approach. Since the eigenvalues are usually measured with more certainty than the eigenvectors, the present research will attempt to find a method of using eigenvalues alone as well as using both eigenvalues and eigenvectors. With previous methods, the use of eigenvalues alone certainly results in infinity solutions. The use of both eigenvalues and eigenvectors may result in a unique solution if a sufficient number of coordinates have been measured such that the sensitivity equation is not underdetermined. Since the case of an infinite number of solutions for a given set of measured eigen-data will develop, if the number of parameters is larger than the number of independent equations, an attempt will be made to generate extra eigen-data by perturbing the structure. Perturbation will be performed by adding mass or stiffness to a structure so as to change its eigen-data, and use the eigen-data of the structure before and after perturbation in parameter estimation. However, the problem is not simply of the number of measurement coordinates. The structure of the mass and stiffness matrices as well as the choice of the measurement coordinates all could have an influence. This problem seems not to have been fully analysed. In the present research the question of the uniqueness of the parameters, in both cases, will be looked at. Investigation will be performed on the suitable choice of the perturbing coordinates so that a given set of measured eigenvalues alone could be used in a more rational updating algorithm.

CHAPTER 3

MODEL UPDATING BY ADDING MASS OR STIFFNESS TO THE SYSTEM

3.1 Introduction

It is apparent that one of the main difficulties experienced by model parameter updating or identification methods is the incomplete modal information from vibration tests. This difficulty is manifest by an insufficient number of linearly independent equations to solve for the desired parameters. Previous investigators have dealt with this difficulty by various approaches. The most popular ones are:

(i) Using overdetermined eigen-data sensitivity equations based on first order approximation.

(ii) Using reduced order equation of motion and orthogonality equations linearized by coordinate transformation method.

In both cases a number of parameters with physical interpretations are updated, rather than treating all matrix influence coefficients as independent parameters. The identification of a unique solution, however, depends very much on the availability of mode shape data measured at a sufficiently large number of coordinates. This is so because the number of measured modes is usually small and mode shape measurement at many coordinates is necessary to increase the data sample. It is also generally agreed that the mode shapes are usually measured with more uncertainty than the natural frequencies. The more accurate natural frequencies, however, cannot be used alone to estimate

the parameters as there will be an infinity of solutions.

In this Chapter a technique which makes possible to use the eigenvalue data alone is proposed. It is based on generating at least as many eigenvalues as the number of parameters to update by perturbing the structure by adding mass or stiffness. The parameters are then determined iteratively by updating the parameters of the initial analytical model using the well known sensitivity analysis method. Thus if $\mathbf{J}_\lambda$ is the Jacobian matrix of eigenvalue sensitivities with respect to the parameters of the current analytical model, parameter update Δs are determined by a least squares solution of:

$$[\mathbf{J}_\lambda]\Delta s = \{\Delta\lambda\} \tag{3.1}$$

It is assumed that the FE parameters to update are the structural parameters which are coefficients of the element matrices, whereas the lumped parameter model has a diagonal mass matrix and the parameters to update are the lumped masses and stiffnesses. By perturbing the structure and its analytical model by identical perturbations, the eigen-data sensitivity analysis is performed only with respect to the parameters of the unperturbed system. This simplifies the updating algorithm. The updating algorithm is given in fig B1.1 in appendix B. It will be shown that with mass or stiffness addition method, a unique solution for the model parameters may be identified. The conditions for the identification of the exact mass and stiffness parameters based on error-free data and exact structure of the model matrices will be investigated. A statistical approach, which considers the fact that measured data is not exact and the model structure may possibly be inexact, will then be introduced in Chapter 4. The mass or stiffness addition technique can alternatively be used with both eigenvalues and eigenvectors.

3.2 Updating an undamped model using eigenvalues alone

The eigenvalues are solutions of the determinant equation:

$$\left| \mathbf{K} - \lambda \mathbf{M} \right| = 0 \tag{3.2}$$

Let **R** and **S** be arbitrary but non-singular matrices of the same order as the mass and stiffness matrices. Then (3.2) can be pre and post-multiplied by the determinants of the arbitrary matrices and results in (3.3).

$$\left| \mathbf{RKS} - \lambda \mathbf{RMS} \right| = 0 \tag{3.3}$$

It follows therefore, there are arbitrary matrices $\mathbf{K}_x$ and $\mathbf{M}_x$ given by (3.4) which have the same eigenvalues as the true system matrices **K** and **M**.

$$\mathbf{K}_x = \mathbf{RKS}, \qquad \mathbf{M}_x = \mathbf{RMS} \tag{3.4}$$

The implication of (3.4) is that there are infinite mass and stiffness matrices which can reproduce the measured eigenvalues. The principle behind mass or stiffness addition is to impose constraints on **R** and **S** so that the number of solutions for $\mathbf{K}_x$ and $\mathbf{M}_x$ is finite. A unique solution is preferred but, generally, with a finite number of solutions it is usually the case that if a reasonable estimate of the initial parameters is made, the updated parameters converge to the correct mass and stiffness parameters. The other solutions, if any, are usually not feasible solutions and are not identified by the iterative updating process. By adding a known mass to the system at a known coordinate the eigenvalues of the perturbed system are solutions of:

$$\left| \mathbf{R} \left[\mathbf{K} - \lambda \left(\mathbf{M} + \Delta \mathbf{M} \right) \right] \mathbf{S} \right| = 0 \tag{3.5}$$

Since $\mathbf{M}_x$ and $\mathbf{K}_x$ are the mass and stiffness matrices that reproduce the eigenvalues of the system, **R** and **S** must satisfy the following constraint:

$$\mathbf{R}\,\Delta\mathbf{M}\,\mathbf{S} = \Delta\mathbf{M} \tag{3.6}$$

It is possible to explore the form of **R** and **S** with different mass addition coordinates.

3.2.1 Updating by adding mass or stiffness at each coordinate

From the form of (3.5) and (3.6), adding a grounded stiffness at a given coordinate has the same constraining effects on **R** and **S** as adding a mass to the same coordinate. Thus, to consider the effect of stiffness addition on the existence of a unique or a finite number of solutions, it is sufficient to consider only the effect of mass addition. While different combinations of added mass and stiffness are possible, only simple cases of adding lumped masses or lumped grounded stiffeners are considered due to their simplicity. The masses or stiffeners are added one in turn at a coordinate and determine the eigen-data. Then repeat at as many coordinates as necessary. The aim is to generate extra eigen-data so that at least as many data as the number of parameters to update are generated. For practical reasons adding mass or stiffness at each coordinate is difficult. This chapter investigates the necessary requirements, with respect to the choice of the perturbed coordinates, so that the Jacobian matrix of eigen-data sensitivities in (3.1) is not rank deficient. However, before the more realistic cases of adding mass or stiffness at an incomplete number of coordinates is considered, the case of mass addition at each coordinate is first analysed to establish some important concepts.

Consider the perturbation of the mass matrix by a mass δm_i at coordinate i. Then **R** and **S** can be partitioned as follow:

$$\mathbf{R}=\begin{bmatrix} \mathbf{R}_{11} & \mathbf{R}_{12} & \mathbf{R}_{13} \\ \mathbf{R}_{21} & \mathbf{R}_{ii} & \mathbf{R}_{23} \\ \mathbf{R}_{31} & \mathbf{R}_{32} & \mathbf{R}_{33} \end{bmatrix}, \quad \mathbf{S}=\begin{bmatrix} \mathbf{S}_{11} & \mathbf{S}_{12} & \mathbf{S}_{13} \\ \mathbf{S}_{21} & \mathbf{S}_{ii} & \mathbf{S}_{23} \\ \mathbf{S}_{31} & \mathbf{S}_{32} & \mathbf{S}_{33} \end{bmatrix}, \quad \Delta\mathbf{M}=\begin{bmatrix} 0 & 0 & 0 \\ 0 & \delta m_i & 0 \\ 0 & 0 & 0 \end{bmatrix} \qquad (3.7)$$

$\mathbf{R}_{ii}$ and $\mathbf{S}_{ii}$ are 1x1 coefficients corresponding to the mass added coordinate. Since **R** and **S** satisfies (3.6), then some terms in **R** and **S** are not arbitrary. By using (3.7) in (3.6) it can be shown (Appendix A1) that:

$$\mathbf{S}_{ii}=\mathbf{R}_{ii}^{-1}, \quad \mathbf{R}_{12}=\mathbf{R}_{32}=0, \quad \mathbf{S}_{21}=\mathbf{S}_{23}=0.$$

Therefore, if mass is added at a single coordinate i, **R** and **S** are given by:

$$\mathbf{R}=\begin{bmatrix} \mathbf{R}_{11} & 0 & \mathbf{R}_{13} \\ \mathbf{R}_{21} & \mathbf{R}_{ii} & \mathbf{R}_{23} \\ \mathbf{R}_{31} & 0 & \mathbf{R}_{33} \end{bmatrix}, \qquad \mathbf{S}=\begin{bmatrix} \mathbf{S}_{11} & \mathbf{S}_{12} & \mathbf{S}_{13} \\ 0 & \mathbf{R}_{ii}^{-1} & 0 \\ \mathbf{S}_{31} & \mathbf{S}_{32} & \mathbf{S}_{33} \end{bmatrix} \qquad (3.8)$$

It follows, therefore, if mass is to be added in turn at each coordinate, all the columns of **R** and all the rows of **S** should have zero terms except the ones corresponding to the main diagonals. That is **R** and **S** are diagonal matrices and they are related as follow:

$$\mathbf{S}=\mathbf{R}^{-1} = \text{diagonal matrix.}$$

Therefore, the expressions for $\mathbf{K}_x$ and $\mathbf{M}_x$ becomes:

$$\mathbf{K}_x = \begin{bmatrix} K_{11} & K_{12}\frac{R_{11}}{R_{22}} & K_{13}\frac{R_{11}}{R_{33}} & \cdots\cdots & K_{1N}\frac{R_{11}}{R_{NN}} \\ K_{21}\frac{R_{22}}{R_{11}} & K_{22} & K_{23}\frac{R_{22}}{R_{33}} & \cdots\cdots & K_{2N}\frac{R_{22}}{R_{NN}} \\ \cdots\cdots & \cdots\cdots & \cdots\cdots & \cdots\cdots & \cdots\cdots \\ K_{N1}\frac{R_{NN}}{R_{11}} & K_{N2}\frac{R_{NN}}{R_{22}} & K_{N3}\frac{R_{NN}}{R_{33}} & \cdots\cdots & K_{NN} \end{bmatrix} \tag{3.9}$$

$$\mathbf{M}_x = \begin{bmatrix} M_{11} & M_{12}\frac{R_{11}}{R_{22}} & M_{13}\frac{R_{11}}{R_{33}} & \cdots\cdots & M_{1N}\frac{R_{11}}{R_{NN}} \\ M_{21}\frac{R_{22}}{R_{11}} & M_{22} & M_{23}\frac{R_{22}}{R_{33}} & \cdots\cdots & M_{2N}\frac{R_{22}}{R_{NN}} \\ \cdots\cdots & \cdots\cdots & \cdots\cdots & \cdots\cdots & \cdots\cdots \\ M_{N1}\frac{R_{NN}}{R_{11}} & M_{N2}\frac{R_{NN}}{R_{22}} & M_{N3}\frac{R_{NN}}{R_{33}} & \cdots\cdots & M_{NN} \end{bmatrix} \tag{3.10}$$

Thus, all the diagonal influence coefficients in the mass and stiffness matrices are uniquely defined. The mass and stiffness matrices are usually symmetrical and this is a useful prior knowledge. Imposing a constraint of symmetry on $\mathbf{K}_x$ and $\mathbf{M}_x$ by equating the corresponding off-diagonal terms in (3.9) and in (3.10) the following is obtained:

$$K_{ij}\frac{R_{ii}}{R_{jj}} = K_{ji}\frac{R_{jj}}{R_{ii}}$$

$$M_{ij}\frac{R_{ii}}{R_{jj}} = M_{ji}\frac{R_{jj}}{R_{ii}}$$

$$(i, j = 1 \ldots . N \quad)$$

But **K** and **M** are also symmetrical. Therefore:

$$\frac{R_{ii}}{R_{jj}} = \frac{R_{jj}}{R_{ii}}$$

$$R_{ii}^2 = R_{jj}^2$$

$$\frac{R_{ii}}{R_{jj}} = +(-)1 \qquad (3.11)$$

Thus, the off-diagonal mass and stiffness influence coefficients have values of + or - their correct values. Since there is a finite number (>1) of solutions for the off-diagonal influence coefficients, the uniqueness of the non-diagonal stiffness or mass matrix depends on the relationship of the off-diagonal and the diagonal influence coefficients.

In the case of a finite element model, the parameters to be determined are the coefficients of the element matrices. The relationship between the off-diagonal and the diagonal influence coefficients of the finite element mass and stiffness matrices is in many cases adequate to determine, uniquely, the parameters if mass or stiffness is added at each coordinate.

With a lumped parameter model the relationship between the diagonal and the off-diagonal influence coefficients may not yield unique lumped parameters when the diagonal influence coefficients are known. Depending on the complexity and form of the mass-stiffness network, it is possible to have cases with more than one solutions for the lumped parameters even if mass is added at each coordinate. However, the correct parameters are usually identified if reasonable initial estimates are made.

EXAMPLE 3.1

Consider a 3 DOF lumped parameter model of a spring mass chain with both ends fixed. The true mass and stiffness matrices are given as:

$$\mathbf{M} = \text{diagonal}\,[m_1 \;\; m_2 \;\; m_3]$$

$$\mathbf{K} = \begin{bmatrix} k_1+k_2 & -k_2 & 0 \\ -k_2 & k_2+k_3 & -k_3 \\ 0 & -k_3 & k_3+k_4 \end{bmatrix}$$

From (3.9) and (3.11), the off-diagonal coefficients in $\mathbf{K}_x$ are given by +(-) their corresponding terms in **K**. That is:

$$K_{12,x} = +(-)k_2$$
$$K_{23,x} = +(-)k_3$$

The possible values of $K_{12,x}$ and $K_{23,x}$ are therefore $+(-)k_2$ and $+(-)k_3$ respectively. With these values there are four possibilities for the value of $K_{22,x}$. These are:

$$-k_2 - k_3\,,\;\; -k_2 + k_3\,,\;\; k_2 - k_3 \;\text{ and }\; k_2 + k_3.$$

However $K_{22,x}$ is a diagonal coefficient and is uniquely defined as K_{22} of the true model. Therefore only one of the possible values of $K_{12,x}$ and $K_{23,x}$ is identified and this corresponds to:

$$K_{12,x} = k_2$$
$$K_{23,x} = k_3$$

The stiffness matrix is therefore completely identified. The mass matrix is also identified since it is diagonal and from (3.10), the diagonal influence coefficients are identified if mass is added at least to each coordinate.

EXAMPLE 3.2

Consider a 5 DOF spring mass system of fig 3.1.

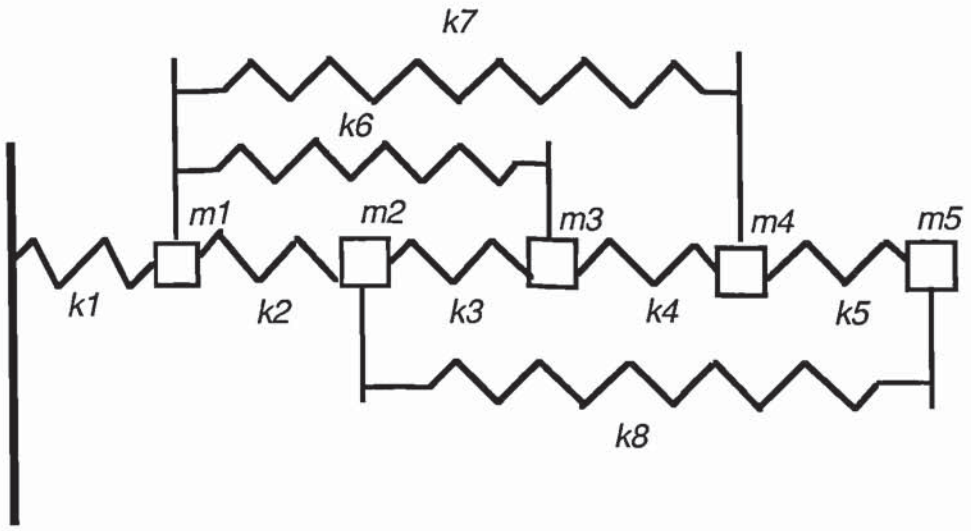

Fig 3.1 Spring-mass system (5 DOF).

The stiffness matrix is given by:

$$\mathbf{K} = \begin{bmatrix} k_1+k_2+k_6+k_7 & -k_2 & -k_6 & -k_7 & 0 \\ -k_2 & k_2+k_3+k_8 & -k_3 & 0 & -k_8 \\ -k_6 & -k_3 & k_3+k_4+k_6 & -k_4 & 0 \\ -k_7 & 0 & -k_4 & k_4+k_5+k_7 & -k_5 \\ 0 & -k_8 & 0 & -k_5 & k_5+k_8 \end{bmatrix}$$

If mass is added at each coordinate, all the masses and the diagonal stiffness

influence coefficients are uniquely defined. Thus:

$$K_{11,x} = k_{1x} + k_{2x} + k_{6x} + k_{7x} = K_{11}$$
$$K_{22,x} = k_{2x} + k_{3x} + k_{8x} = K_{22}$$
$$K_{33,x} = k_{3x} + k_{4x} + k_{6x} = K_{33}$$
$$K_{44,x} = k_{4x} + k_{5x} + k_{7x} = K_{44}$$
$$K_{55,x} = k_{5x} + k_{8x} = K_{55}$$

The off-diagonal coefficients are +(-) their correct values: Therefore,

$$k_{5x} = +(-)k_5 \quad \text{and} \quad k_{8x} = +(-)k_8$$

which implies four possible values for $K_{55,x}$ which are:

$$k_5 + k_8,\ k_5 - k_8,\ -k_5 + k_8,\ -k_5 - k_8\ .$$

But $K_{55,x}$ is unique by virtue of being a diagonal influence coefficient and mass is added at each coordinate. Thus of the four possible values only one is actually valid and this corresponds to:

$$k_{5x} = k_5 \quad \text{and} \quad k_{8x} = k_8.$$

The stiffeners k_5 and k_8 are therefore uniquely defined. Similarly the off-diagonal terms k_{4x} and k_{7x} which are contained in $K_{44,x}$ are given by +(-) their correct values. But $K_{44,x}$ is unique and is given by:

$$K_{44,x} = k_{4x} + k_{5x} + k_{7x} = K_{44} = k_4 + k_5 + k_7$$

Since k_{5x} is uniquely defined, the sum $k_{4x} + k_{7x}$ is also unique. But k_{4x} and k_{7x} can take values of +(-) their correct values. Therefore, since the sum $k_{4x} + k_{7x}$ is unique, of the possible values of k_{4x} and k_{7x}, the valid ones must correspond to:

$$k_{4x} = k_4 \quad \text{and} \quad k_{7x} = k_7.$$

Thus k_4 and k_7 are unique. If k_4 is uniquely defined then by the same arguments k_3 and k_6 which are off-diagonal coefficients and are also contained in $K_{33,x}$ are also uniquely identified. If k_3 and k_8 are uniquely defined then k_2 is also identified from the identification of the diagonal coefficient K_{22} . If k_2 , k_6 and k_7 are identified then k_1 is also identified following the identification of the diagonal coefficient K_{11}.

Thus all the stiffness parameters k_1 . . k_8 and all masses are uniquely defined.

EXAMPLE 3.3

This example considers a numerical simulation of the 5 DOF system of example 3.2. Let the system have the following mass (kg) and stiffness (N/m) data.

$$m_1 \ldots\ldots m_5 = 10$$
$$k_1 = k_2 = k_5 = k_7 = k_8 = 1000, \quad k_3 = k_4 = k_6 = 500$$

Consider an initial analytical model with the following mass and stiffness data:

k_{1a}=1200	k_{2a}=1100	k_{3a}=400	k_{4a}=450	k_{5a}=900
k_{6a}=600	k_{7a}=1100	k_{8a}=1200		
m_{1a}=11	m_{2a}=12	m_{3a}=8	m_{4a}=9	m_{5a}=9

The system and the initial model were both perturbed by adding masses of 0.25 kg and 0.5 kg in turn at each coordinate. The eigenvalues of the system and the initial model before and after mass addition were determined, where only the first two modes were considered to have been measured. The eigenvalues of the system and the initial model are given in table 3.1. With this data an iterative least squares solution of (3.1) was performed. All the parameters converged to their correct values. Table 3.2 shows the results at each iteration step:

Added mass (kg)	Coordinate	System eigenvalues		Eigenvalues of the initial model	
		Mode 1 λ	Mode 2 λ	Mode 1 λ	Mode 2 λ
0	-	14.375	153.182	16.895	178.968
0.25	1	14.339	152.729	16.855	178.281
	2	14.306	152.604	16.809	177.924
	3	14.300	152.564	16.800	178.757
	4	14.293	153.070	16.791	178.423
	5	14.280	151.135	16.779	176.954
0.5	1	14.303	152.268	16.816	177.578
	2	14.238	152.016	16.725	176.876
	3	14.226	151.942	16.706	178.535
	4	14.211	152.955	16.688	177.869
	5	14.186	149.153	16.663	174.967

TABLE 3.1 Eigenvalues (Rad^2/s^2) of the simulated 5 DOF lumped spring-mass system and its initial model.

	Iteration steps				
	0	1	2	3	4
k_1	1200	1002.0	999.9	1000.0	1000.0
k_2	1100	1126.8	1061.4	993.0	1000.0
k_3	400	331.5	475.1	504.1	500.0
k_4	450	498.9	475.6	501.2	500.0
k_5	900	1134.0	1044.5	992.6	1000.0
k_6	600	548.8	536.0	496.4	500.0
k_7	1100	798.1	937.5	1003.4	1000.0
k_8	1200	932.8	969.8	1005.6	1000.0
m_1	11	10.3	9.9	10.0	10.0
m_2	12	12.0	10.7	9.9	10.0
m_3	8	7.6	9.8	10.1	10.0
m_4	9	9.9	9.5	10.0	10.0
m_5	9	10.0	10.1	10.0	10.0

TABLE 3.2 Convergence of the lumped mass (kg) and stiffness (N/m) parameters of the 5 DOF spring-mass system.

EXAMPLE 3.4

Consider a 4 DOF system shown in fig 3.2.

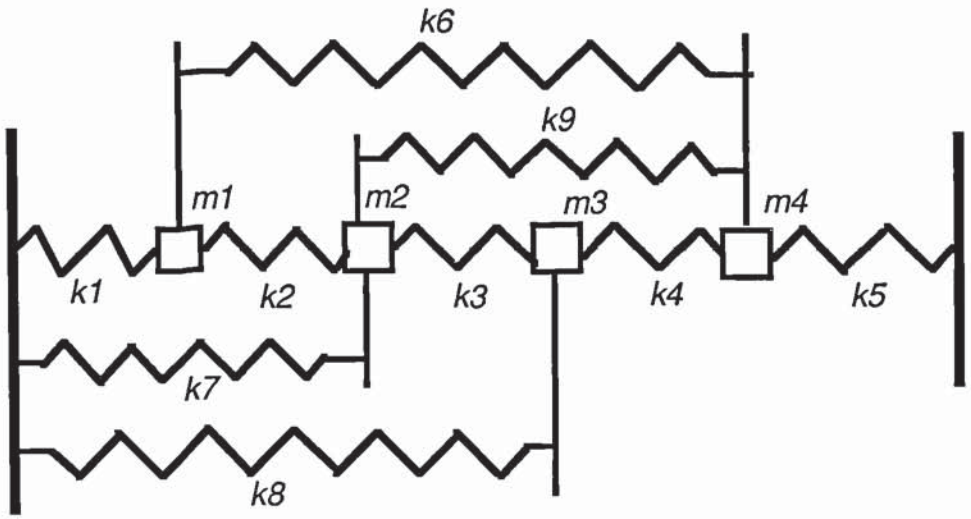

Fig 3.2 Spring-mass system with fixed ends (4 DOF).

The stiffness matrix is given by:

$$\mathbf{K} = \begin{bmatrix} k_1+k_2+k_6 & -k_2 & 0 & -k_6 \\ -k_2 & k_2+k_3+k_7+k_9 & -k_3 & -k_9 \\ 0 & -k_3 & k_3+k_4+k_8 & -k_4 \\ -k_6 & -k_9 & -k_4 & k_4+k_5+k_6+k_9 \end{bmatrix}$$

With mass addition at each coordinate, all mass parameters are unique and the diagonal influence coefficients of the stiffness matrix are also unique. Thus:

$$K_{11,x} = k_{1x} + k_{2x} + k_{6x} = K_{11}$$
$$K_{22,x} = k_{2x} + k_{3x} + k_{7x} + k_{9x} = K_{22}$$
$$K_{33,x} = k_{3x} + k_{4x} + k_{8x} = K_{33}$$

$$K_{44,x} = k_{4x} + k_{5x} + k_{6x} + k_{9x} = K_{44}$$

While each of the lumped stiffness corresponding to the off-diagonal stiffness influence coefficients (k_{2x} , k_{3x} , k_{4x} , k_{6x} , k_{9x}) can attain a value of +(-) its correct value, each of the preceding four equations contain an arbitrary grounded stiffness (k_{1x} , k_{7x} , k_{8x} , k_{5x}). The four equations cannot be solved for a unique solution. Each of the possible combinations for the signs of the off-diagonal stiffness influence coefficients will result in a different solution for the stiffness parameters. The number of possible solutions, however, is not infinite. Thus, starting with reasonable initial estimates the parameters of the system of fig 3.2 can be identified using eigenvalues if mass or stiffness is added at each coordinate.

Lets consider a numerical simulation with the following system and initial model parameters:

System: $k_1 = k_2 = k_3 = k_4 = k_5 = 1000$ N/m
$k_6 = k_7 = k_8 = k_9 = 500$ N/m
$m_1 = m_2 = m_3 = m_4 = 10$ kg

Initial model $k_{1a} = k_{2a} = k_{3a} = k_{4a} = 1100$ N/m
$k_{5a} = 9500$ N/m, $k_{6a} = 550$ N/m, $k_{7a} = 450$ N/m
$k_{8a} = 550$ N/m, $k_{8a} = 450$ N/m
$m_{1a} = m_{2a} = m_{3a} = m_{4a} = 9.5$ kg.

Masses of 0.25 kg and 0.5 kg were added in turn at each coordinate of the simulated system and the initial model. The eigenvalues of the first two modes of the system before and after each mass addition were taken to simulate

measured data. The simulated and the initial model eigenvalues are shown in table 3.3. The parameters were then updated using this eigenvalue data. It was possible to achieve convergence to the correct mass and stiffness parameters as shown in table 3.4.

It should be noted that there is a finite number of solutions for the parameters of the system of fig 3.2 that will reproduce the eigenvalues of the simulated system before and after mass additions. The number of such solutions depends on the number of possible combinations for the signs of the off-diagonal stiffness influence coefficients. Only the correct parameters are identified because the other solutions are not in the neighbourhood of the initial estimates.

Added mass (kg)	Coordinate	System eigenvalues		Eigenvalues of the initial model	
		Mode 1 λ	Mode 2 λ	Mode 1 λ	Mode 2 λ
0	-	72.40	242.56	77.30	277.88
0.25	1	72.06	238.99	76.93	273.75
	2	71.88	242.41	76.70	277.56
	3	71.83	240.53	76.68	275.58
	4	72.02	242.31	76.85	277.35
0.5	1	71.72	235.53	76.56	269.72
	2	71.36	242.25	76.11	277.22
	3	71.26	238.53	76.06	273.31
	4	71.63	242.04	76.41	276.78

TABLE 3.3 Eigenvalues (Rad^2/s^2) of the simulated 4 DOF lumped spring-mass system and its initial model.

	Iteration steps				
	0	1	2	3	4
k_1	1100	994.1	999.5	1000.0	1000.0
k_2	1100	997.3	997.7	999.9	1000.0
k_3	1100	1004.0	1000.0	1000.0	1000.0
k_4	1100	994.7	999.0	999.9	1000.0
k_5	950	984.9	997.3	999.9	1000.0
k_6	550	501.6	502.1	500.1	500.0
k_7	450	510.1	502.6	500.1	500.0
k_8	550	497.4	500.1	500.0	500.0
k_9	450	446.3	487.5	499.6	10.00
m_1	9.5	9.89	9.99	10.00	10.00
m_2	9.5	10.00	10.00	10.00	10.00
m_3	9.5	9.92	9.99	10.00	10.00
m_4	9.5	9.94	9.99	9.99	10.00

TABLE 3.4 Convergence of the lumped mass (kg) and stiffness (N/m) parameters of the 4 DOF spring-mass system.

3.2.2 Mass or stiffness addition at a smaller number of coordinates

3.2.2.1 General considerations

Let **R** and **S** be partitioned into submatrices corresponding to the perturbed and unperturbed coordinates. Let the matrices be rearranged such that the perturbed coordinates are the first N_{pc} ($N_{pc}<N$) coordinates along the main diagonal. Thus,

$$\Delta\mathbf{M} = \begin{bmatrix} [\delta\mathbf{M}] & 0 \\ 0 & 0 \end{bmatrix}$$

where $[\delta\mathbf{M}]$ is a N_{pc}xN_{pc} submatrix with zero elements except the ith diagonal element which is given by δm_i and corresponds to the current mass addition at coordinate i.

From (3.8), **R** and **S** are also partitioned and takes the form of (3.12).

$$\mathbf{R} = \begin{bmatrix} \mathbf{R}_{11} & \mathbf{R}_{12} \\ 0 & \mathbf{R}_{22} \end{bmatrix}, \qquad \mathbf{S} = \begin{bmatrix} \mathbf{R}_{11}^{-1} & 0 \\ \mathbf{S}_{21} & \mathbf{S}_{22} \end{bmatrix} \tag{3.12}$$

The mass and stiffness matrices are then given by:

$$\mathbf{M}_x = \begin{bmatrix} \mathbf{R}_{11} & \mathbf{R}_{12} \\ 0 & \mathbf{R}_{22} \end{bmatrix} [\mathbf{M}] \begin{bmatrix} \mathbf{R}_{11}^{-1} & 0 \\ \mathbf{S}_{21} & \mathbf{S}_{22} \end{bmatrix} \tag{3.13}$$

$$\mathbf{K}_x = \begin{bmatrix} \mathbf{R}_{11} & \mathbf{R}_{12} \\ 0 & \mathbf{R}_{22} \end{bmatrix} [\mathbf{K}] \begin{bmatrix} \mathbf{R}_{11}^{-1} & 0 \\ \mathbf{S}_{21} & \mathbf{S}_{22} \end{bmatrix} \tag{3.14}$$

But $\mathbf{R}_{11}$ is a diagonal matrix which can be written as:

$$\mathbf{R}_{11} = \begin{bmatrix} r_1 & 0 & 0 & 0 \ldots 0 \\ 0 & r_2 & 0 & 0 \ldots 0 \\ 0 & 0 & r_3 & 0 \ldots 0 \\ \ldots & \ldots & \ldots & \ldots \\ 0 & 0 & 0 & \ldots r_t \end{bmatrix}$$

It is possible to factor out one term from $\mathbf{R}_{11}$ and a corresponding term from the **S** matrix. Since $\mathbf{S}_{11} = \mathbf{R}_{11}^{-1}$, the factored terms cancel. Let r_1 and $1/r_1$ be factored out from $\mathbf{R}_{11}$ and $\mathbf{S}_{11}$ respectively. The mass and stiffness matrices can be written as:

$$\mathbf{M}_x = \begin{bmatrix} \mathbf{T}_{11} & \mathbf{T}_{12} \\ 0 & \mathbf{T}_{22} \end{bmatrix} [\mathbf{M}] \begin{bmatrix} \mathbf{T}_{11}^{-1} & 0 \\ \mathbf{L}_{21} & \mathbf{L}_{22} \end{bmatrix} \tag{3.15}$$

$$\mathbf{K}_x = \begin{bmatrix} \mathbf{T}_{11} & \mathbf{T}_{12} \\ 0 & \mathbf{T}_{22} \end{bmatrix} [\mathbf{K}] \begin{bmatrix} \mathbf{T}_{11}^{-1} & 0 \\ \mathbf{L}_{21} & \mathbf{L}_{22} \end{bmatrix} \tag{3.16}$$

where $\mathbf{T}_{11}$ is a diagonal submatrix with at least one of its diagonal elements as unity and

$$\mathbf{T}_{12} = \frac{1}{r_1}\mathbf{R}_{12}, \qquad \mathbf{T}_{22} = \frac{1}{r_1}\mathbf{R}_{22},$$

$$\mathbf{L}_{21} = r_1\mathbf{S}_{21}, \qquad \mathbf{L}_{22} = r_1\mathbf{S}_{22}.$$

It can be shown (Appendix A2) that:

$$\mathbf{L} = \mathbf{T}^{\mathrm{T}}, \qquad \mathbf{T}_{11}^2 = \mathbf{I} \tag{3.17}$$

where

$$\mathbf{T} = \begin{bmatrix} \mathbf{T}_{11} & \mathbf{T}_{12} \\ 0 & \mathbf{T}_{22} \end{bmatrix} \tag{3.18}$$

Therefore, to show the existence of unique mass and stiffness matrices, it is sufficient to show that

$$\mathbf{K}_x = \mathbf{T}\mathbf{K}\mathbf{T}^T \qquad \text{and} \qquad \mathbf{M}_x = \mathbf{T}\mathbf{M}\mathbf{T}^T \tag{3.19}$$

are unique. If $\mathbf{K}_x$ and $\mathbf{M}_x$ have a finite number (>1) of solutions and if initial estimates of the mass and stiffness parameters are made close to one of the solutions, the Jacobian matrix of eigen-data sensitivities will generally become non-singular and the updated parameters converge to a solution in the neighbourhood of the initial estimates.

3.2.2.2 Identifying the parameters in the mass and stiffness matrices

Let the mass and stiffness matrices be partitioned into submatrices corresponding to the perturbed (subscript 11) and unperturbed coordinates (subscript 22). Thus,

$$\mathbf{K}_x = \begin{bmatrix} \mathbf{K}_{11,x} & \mathbf{K}_{12,x} \\ \mathbf{K}_{21,x} & \mathbf{K}_{22,x} \end{bmatrix} \qquad \mathbf{M}_x = \begin{bmatrix} \mathbf{M}_{11,x} & \mathbf{M}_{12,x} \\ \mathbf{M}_{21,x} & \mathbf{M}_{22,x} \end{bmatrix} \tag{3.20}$$

$$\mathbf{K} = \begin{bmatrix} \mathbf{K}_{11} & \mathbf{K}_{12} \\ \mathbf{K}_{21} & \mathbf{K}_{22} \end{bmatrix} \qquad \mathbf{M} = \begin{bmatrix} \mathbf{M}_{11} & \mathbf{M}_{12} \\ \mathbf{M}_{21} & \mathbf{M}_{22} \end{bmatrix} \tag{3.21}$$

The submatrices in $\mathbf{K}_x$ and $\mathbf{M}_x$ can be written in terms of the submatrices in $\mathbf{K}$, $\mathbf{M}$ and $\mathbf{T}$ using (3.19) as:

$$\mathbf{K}_{11,x} = \mathbf{T}_{11}\mathbf{K}_{11}\mathbf{T}_{11}^T + \mathbf{T}_{12}\mathbf{K}_{21}\mathbf{T}_{11}^T + \mathbf{T}_{11}\mathbf{K}_{12}\mathbf{T}_{12}^T + \mathbf{T}_{12}\mathbf{K}_{22}\mathbf{T}_{12}^T \tag{3.22}$$

$$\mathbf{K}_{12,x} = \mathbf{T}_{11}\mathbf{K}_{12}\mathbf{T}_{22}^{T} + \mathbf{T}_{12}\mathbf{K}_{22}\mathbf{T}_{22}^{T} \tag{3.23}$$

$$\mathbf{K}_{22,x} = \mathbf{T}_{22}\mathbf{K}_{22}\mathbf{T}_{22}^{T} \tag{3.24}$$

$$\mathbf{M}_{11,x} = \mathbf{T}_{11}\mathbf{M}_{11}\mathbf{T}_{11}^{T} + \mathbf{T}_{12}\mathbf{M}_{21}\mathbf{T}_{11}^{T} + \mathbf{T}_{11}\mathbf{M}_{12}\mathbf{T}_{12}^{T} + \mathbf{T}_{12}\mathbf{M}_{22}\mathbf{T}_{12}^{T} \tag{3.25}$$

$$\mathbf{M}_{12,x} = \mathbf{T}_{11}\mathbf{M}_{12}\mathbf{T}_{22}^{T} + \mathbf{T}_{12}\mathbf{M}_{22}\mathbf{T}_{22}^{T} \tag{3.26}$$

$$\mathbf{M}_{22,x} = \mathbf{T}_{22}\mathbf{M}_{22}\mathbf{T}_{22}^{T} \tag{3.27}$$

With a diagonal mass matrix, $\mathbf{M}_{12,x} = \mathbf{M}_{12} = 0$. Since $\mathbf{T}_{22}$ and $\mathbf{M}_{22}$ are non zero (3.26) results in $\mathbf{T}_{12} = 0$. The same result is obtained if the stiffness matrix is diagonal. Thus, with a diagonal mass matrix (3.22), (3.23) and (3.25) simplifies to:

$$\mathbf{K}_{11,x} = \mathbf{T}_{11}\mathbf{K}_{11}\mathbf{T}_{11}^{T} \tag{3.28}$$

$$\mathbf{K}_{12,x} = \mathbf{T}_{11}\mathbf{K}_{12}\mathbf{T}_{22}^{T} \tag{3.29}$$

$$\mathbf{M}_{11,x} = \mathbf{T}_{11}\mathbf{M}_{11}\mathbf{T}_{11}^{T} \tag{3.30}$$

Let N_{pc} be the number of perturbed coordinates. Then $\mathbf{K}_{22}$, $\mathbf{M}_{22}$ and $\mathbf{T}_{22}$ are matrices of order $N - N_{pc}$. Since $\mathbf{T}_{11}$ is a diagonal submatrix with at least one of the diagonal elements as unity, there is a maximum of N_{pc}-1 elements in $\mathbf{T}_{11}$ which are either +1 or -1. The number of possible combinations for the signs of these elements indicates the minimum number of possible solutions. $\mathbf{T}_{22}$ and $\mathbf{T}_{12}$ have $(N - N_{pc})^2$ and $N_{pc}\text{x}(N - N_{pc})$ unknowns respectively. Equations (3.22) to (3.27) consists of a maximum of number of unknowns given by,

$$\text{No of unknowns} = (N - N_{pc})^2 + N_{pc}x(N - N_{pc}) + n_{km} \quad (3.31)$$

where n_{km} is the total number of unknown mass and stiffness parameters. With a diagonal mass or stiffness matrix, $\mathbf{T}_{12}$ is zero. The total number of unknowns is reduced to

$$\text{No of unknowns} = (N - N_{pc})^2 + n_{km} \quad (3.32)$$
(Diagonal **M** or **K**)

Let N_z be the total number of non-zero rows in $\mathbf{K}_{12,x}$ and $\mathbf{M}_{12,x}$. The maximum number of equations in (3.22) to (3.27) is:

$$\text{No of equations} = (N - N_{pc})^2 + (N - N_{pc}) + N_z x(N - N_{pc}) + N_{pc}^2 + N_{pc} \quad (3.33)$$

The first two terms in (3.33) represents the number of equations in (3.24) and (3.27). The last two terms represents the number of equations in (3.22) and (3.25). The intermediate term is the number of equations in (3.23) and (3.26). With the diagonal mass or stiffness matrix, $\mathbf{M}_{11,x}$ and $\mathbf{K}_{11,x}$ are given by (3.28) and (3.30). Since $\mathbf{T}_{11}$ is diagonal, the number of equations associated with $\mathbf{K}_{11,x}$ and $\mathbf{M}_{11,x}$ is simply equal to the total number of non-zero influence coefficients above the main diagonals of $\mathbf{K}_{11,x}$ and $\mathbf{M}_{11,x}$ plus the number of diagonal influence coefficients in $\mathbf{K}_{11,x}$ and $\mathbf{M}_{11,x}$. Thus, let N_{zd} be the total number of non-zero influence coefficients above the main diagonals of $\mathbf{K}_{11,x}$ and $\mathbf{M}_{11,x}$. The last two terms in (3.33) are modified for a diagonal mass or stiffness matrix and the number of equations in (3.22) to (3.27) becomes

$$\text{No of equations} = (N - N_{pc})^2 + (N - N_{pc}) + N_z x(N - N_{pc}) + 2xN_{pc} + N_{zd} \quad (3.34)$$
(Diagonal **M** or **K**)

The existence of a unique set of mass and stiffness parameters which reproduce exactly the eigenvalues of the system before and after adding mass (or stiffness) is possible if the total number of equations in (3.22) to (3.27) is equal to or greater than the number of unknowns.

The above represents the minimum requirement with respect to the choice of the perturbing coordinates. The existence of a unique solution following the satisfaction of this requirement is not so obvious because the equations are non-linear, involving products of the parameters of **T**. For a system with a small number of DOF it is feasible to expand (3.22) to (3.27) and assess the existence of a unique solution. With an increase in the model order this becomes impractical. However, it can be shown that if the number of equations is not less than the number of unknowns, the equations have a finite number of solutions. It follows, therefore, starting with a reasonable estimate of the initial parameters, the Jacobian matrix of eigenvalue sensitivities will generally become non-singular. Consider the following argument. Equations (3.22) to (3.27) can be linearized by a first order Taylor's expansion and expressed as follow,

$$\begin{bmatrix} \mathbf{G}_{K,T} & 0 & \mathbf{G}_K \\ \mathbf{G}_{M,T} & \mathbf{G}_M & 0 \end{bmatrix} \begin{Bmatrix} \Delta T \\ s \end{Bmatrix} = \{b_1\} \tag{3.35}$$

where $\mathbf{G}_{K,T}$ and $\mathbf{G}_{M,T}$ are coefficient matrices of the linearized part of the equations with respect to the stiffness and mass matrices respectively, and $\mathbf{G}_M$, $\mathbf{G}_K$ are coefficient matrices corresponding to the unknown mass and stiffness parameters. Equation (3.35) can be solved if the following matrix is non-singular.

$$\begin{bmatrix} \mathbf{G}_{K,T}^T & \mathbf{G}_{M,T}^T \\ 0 & \mathbf{G}_M^T \\ \mathbf{G}_K^T & 0 \end{bmatrix} \begin{bmatrix} \mathbf{G}_{K,T} & 0 & \mathbf{G}_K \\ \mathbf{G}_{M,T} & \mathbf{G}_M & 0 \end{bmatrix}$$

$$= \begin{bmatrix} \mathbf{G}_{K,T}^T\mathbf{G}_{K,T} + \mathbf{G}_{M,T}^T\mathbf{G}_{M,T} & \mathbf{G}_{M,T}^T\mathbf{G}_M & \mathbf{G}_{K,T}^T\mathbf{G}_K \\ \mathbf{G}_M^T\mathbf{G}_{M,T} & \mathbf{G}_M^T\mathbf{G}_M & 0 \\ \mathbf{G}_K^T\mathbf{G}_{K,T} & 0 & \mathbf{G}_K^T\mathbf{G}_K \end{bmatrix} \quad (3.36)$$

If $\mathbf{TKT}^T = \mathbf{K}$ and $\mathbf{TMT}^T = \mathbf{M}$ equation (3.35) is reduced to (3.37)

$$\begin{bmatrix} \mathbf{G}_{K,T} \\ \mathbf{G}_{M,T} \end{bmatrix} \{\Delta T\} = \{b_2\} \quad (3.37)$$

and (3.37) can be solved if the following matrix is non-singular:

$$\left[\mathbf{G}_{K,T}^T\mathbf{G}_{K,T} + \mathbf{G}_{M,T}^T\mathbf{G}_{M,T}\right]$$

But the equations $\mathbf{TKT}^T = \mathbf{K}$ and $\mathbf{TMT}^T = \mathbf{M}$ where $\mathbf{T}$ is of the form of (3.18) have a unique solution for the parameters of $\mathbf{T}$, given by $\mathbf{T} = \mathbf{I}$ (Appendix A3). Hence

$$\left[\mathbf{G}_{K,T}^T\mathbf{G}_{K,T} + \mathbf{G}_{M,T}^T\mathbf{G}_{M,T}\right]$$

is non-singular.

Similarly, $\mathbf{G}^T{}_M\mathbf{G}_M$ and $\mathbf{G}^T{}_K\mathbf{G}_K$ are usually non-singular because the equations $\mathbf{K}_x = \mathbf{K}$ and $\mathbf{M}_x = \mathbf{M}$, usually, have a unique solution for the parameters. Thus (3.36) is non-singular. Therefore with reasonable initial estimates, $\mathbf{J}_\lambda$ will generally become non-singular if the preceding requirement have been

satisfied and the updated parameters will converge to a solution closest to the initial estimates. The equations, however, may have more than one solution because they are non-linear, but it is not feasible to determine the exact number of solutions. Simulation tests shows that when the preceding requirement is satisfied, then starting with a reasonable estimate of the initial parameters, the updated parameters usually converge to the correct mass and stiffness parameters. Other solutions, if there are any, are usually not feasible solutions in the neighbourhood of reasonable initial estimates and are not identified. The satisfaction of the preceding requirement, therefore, can serve as a useful test for the adequacy of the perturbing coordinates for parameter updating using eigenvalues. Some examples are now considered.

EXAMPLE 3.5

Fig 3.3 show a 2 DOF spring mass chain with fixed ends. Let coordinate 1 be perturbed by mass addition. $\mathbf{T}$ becomes a 2x2 diagonal matrix and $\mathbf{T}_{11} = T_{11} = 1$ and $\mathbf{T}_{22} = T_{22}$ are scalars.

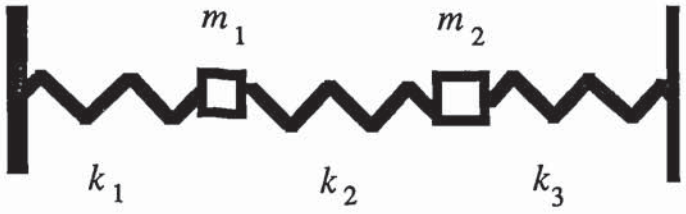

Fig 3.3 Spring-mass chain (2 DOF) with fixed ends.

Therefore from (3.22) to (3.27),

$$\mathbf{K}_{11,x} = \mathbf{T}_{11}\mathbf{K}_{11}\mathbf{T}_{11}^{T} = k_1 + k_2 = k_{1x} + k_{2x}$$

$$\mathbf{K}_{12,x} = \mathbf{T}_{11}\mathbf{K}_{12}\mathbf{T}_{22}^{T} = -k_2 T_{22} = -k_{2x}$$
$$\mathbf{K}_{22,x} = \mathbf{T}_{22}\mathbf{K}_{22}\mathbf{T}_{22}^{T} = (k_2 + k_3)T_{22}^{2} = k_{2x} + k_{3x}$$
$$\mathbf{M}_{11,x} = \mathbf{T}_{11}\mathbf{M}_{11}\mathbf{T}_{11}^{T} = m_1 = m_{1x}$$
$$\mathbf{M}_{22,x} = \mathbf{T}_{22}\mathbf{M}_{22}\mathbf{T}_{22}^{T} = m_2 T_{22}^{2} = m_{2x}.$$

Thus (3.22) to (3.27) as applied to this example results in 5 equations in 6 unknowns (k_{1x}, k_{2x} , k_{3x} ,m_{1x}, m_{2x} and T_{22}). The total number of unknowns is greater than the number of equations. Alternatively we can use the formula:

No of equations = $(N - N_{pc})^2 + (N - N_{pc}) + N_z x(N - N_{pc}) + 2xN_{pc} + N_{zd}$
(Diagonal **M** or **K**)

$$= (2-1)^2 + (2-1) + 1x(2-1) + 2x1 + 0 = 5$$

No of unknowns = $(N - N_{pc})^2 + n_{km} = (2-1)^2 + 5 = 6.$
(Diagonal **M** or **K**)

The mass and stiffness parameters of the system in this example cannot, therefore, be identified using eigenvalues by adding mass or stiffness at a single coordinate.

EXAMPLE 3.6

A two elements 2 DOF FE model of a beam in flexure with both ends fixed is shown in fig 3.4. The stiffness matrix is of the following form,

$$\mathbf{K} = \begin{bmatrix} A_{11}EI_1 + B_{11}EI_2 & A_{12}EI_1 + B_{12}EI_2 \\ A_{21}EI_1 + B_{21}EI_2 & A_{22}EI_1 + B_{22}EI_2 \end{bmatrix}$$

where A_{ij} and B_{ij} are known constants. The mass matrix is of the same format with mass parameters m_{u1} and m_{u2} instead.

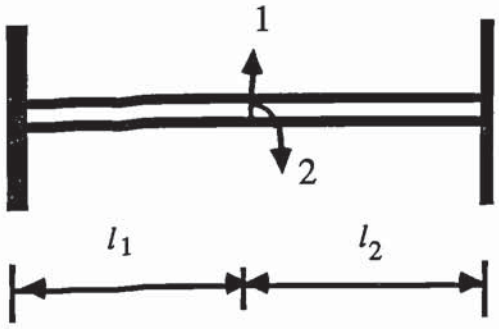

Fig 3.4 A 2 DOF fixed-fixed beam in flexure.

Let coordinate 1 only be perturbed by adding mass, $\mathbf{T}_{11} = T_{11} = 1$. Using formula, the total numbers of equations and unknowns in (3.22) to (3.27) are given by (3.33) and (3.31) respectively

$$\text{No of equations} = (N - N_{pc})^2 + (N - N_{pc}) + N_z x(N - N_{pc}) + N_{pc}^2 + N_{pc}$$
$$= (2-1)^2 + (2-1) + 2x(2-1) + 1^2 + 1 = 6$$

$$\text{No of unknowns} = (N - N_{pc})^2 + N_{pc} x(N - N_{pc}) + n_{km}$$
$$= (2-1)^2 + 1x(2-1) + 4 = 6$$

The mass and stiffness parameters of the 2 elements beam of fig 3.4 can therefore be identified using eigenvalues by mass or stiffness addition at coordinate 1. Consider a numerical simulation with the following data:

System: $EI_1 = EI_2 = 5000\ \text{Nm}^2$

$m_{u1} = m_{u2} = 3.5\ \text{kg/m}$

$l_1 = 0.4\ \text{m}, \quad l_2 = 0.6\ \text{m}.$

Initial model: $EI_{1,a} = 5100\ \text{Nm}^2$, $EI_{2,a} = 4800\ \text{Nm}^2$

$m_{u1,a} = m_{u2,a} = 3.3\ \text{kg/m}$.

The system and its initial model were perturbed by adding a single mass of 0.25 kg at coordinate 1. The natural frequencies for the two modes before and after mass addition are shown in table 3.5. A total of 4 simulated eigenvalues were generated. The simulated eigenvalues were used to update the 4 parameters by sensitivity analysis using (3.1). It was possible to achieve convergence in the mass and stiffness parameters to their correct values. Table 3.6 show the updated parameters at each iteration step.

Added mass (kg)	Simulated natural frequencies (Hz)		Natural frequencies of the initial model (Hz)	
	Mode 1	Mode 2	Mode 1	Mode 2
0	138.66	528.86	141.60	545.32
0.25	128.07	519.21	130.27	534.60

TABLE 3.5 Natural frequencies of the simulated and the initial model of the 2 DOF fixed-fixed beam with and without added mass.

	Iteration steps			
	0	1	2	3
EI_1 (Nm^2)	5100	4996.5	4999.9	5000.0
EI_2 (Nm^2)	4800	4975.3	4999.8	5000.0
m_{u1}(kg/m)	3.30	3.481	3.499	3.500
m_{u2}(kg/m)	3.30	3.483	3.499	3.500

TABLE 3.6 Convergence of the mass and stiffness parameters of the fixed-fixed beam.

EXAMPLE 3.7

Fig 3.5 show a 4 DOF spring-mass chain with fixed ends. Let coordinates 1 and 3 be perturbed. Then $\mathbf{T}_{11}$ and $\mathbf{T}_{22}$ are 2x2 submatrices given by:

$$\mathbf{T}_{11}=\begin{bmatrix}1 & 0\\ 0 & +(-)1\end{bmatrix}, \qquad \mathbf{T}_{22}=\begin{bmatrix}T_{22} & T_{24}\\ T_{42} & T_{44}\end{bmatrix}$$

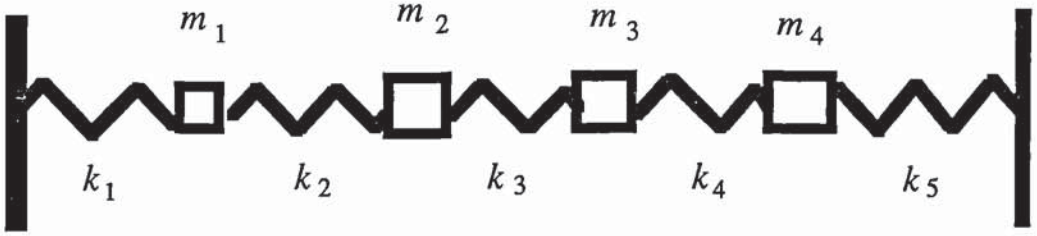

Fig 3.5 A 4 DOF spring-mass chain with fixed ends

The stiffness and mass matrices are given by:

$$\mathbf{K}=\begin{bmatrix} k_1+k_2 & -k_2 & 0 & 0 \\ -k_2 & k_2+k_3 & -k_3 & 0 \\ 0 & -k_3 & k_3+k_4 & -k_4 \\ 0 & 0 & -k_4 & k_4+k_5 \end{bmatrix}, \qquad \mathbf{M}=\begin{bmatrix} m_1 & 0 & 0 & 0 \\ 0 & m_2 & 0 & 0 \\ 0 & 0 & m_3 & 0 \\ 0 & 0 & 0 & m_4 \end{bmatrix}$$

The stiffness and mass matrices are also partitioned into submatrices corresponding to the perturbed and unperturbed coordinates resulting in

$$\mathbf{K}_{11}=\begin{bmatrix} k_1+k_2 & 0 \\ 0 & k_3+k_4 \end{bmatrix}, \quad \mathbf{K}_{12}=\begin{bmatrix} -k_2 & 0 \\ -k_3 & -k_4 \end{bmatrix}, \quad \mathbf{K}_{22}=\begin{bmatrix} k_2+k_3 & 0 \\ 0 & k_4+k_5 \end{bmatrix}$$

$$\mathbf{M}_{11}=\begin{bmatrix} m_1 & 0 \\ 0 & m_3 \end{bmatrix}, \qquad \mathbf{M}_{22}=\begin{bmatrix} m_2 & 0 \\ 0 & m_4 \end{bmatrix}$$

and

$$\mathbf{K}_{11,x}=\begin{bmatrix} k_{1x}+k_{2x} & 0 \\ 0 & k_{3x}+k_{4x} \end{bmatrix}, \quad \mathbf{K}_{12,x}=\begin{bmatrix} -k_{2x} & 0 \\ -k_{3x} & -k_{4x} \end{bmatrix}, \quad \mathbf{K}_{22,x}=\begin{bmatrix} k_{2x}+k_{3x} & 0 \\ 0 & k_{4x}+k_{5x} \end{bmatrix}$$

$$\mathbf{M}_{11,x}=\begin{bmatrix} m_{1x} & 0 \\ 0 & m_{3x} \end{bmatrix}, \qquad \mathbf{M}_{22,x}=\begin{bmatrix} m_{2x} & 0 \\ 0 & m_{4x} \end{bmatrix}$$

Applying (3.22) to (3.27) to the above submatrices ($\mathbf{T}_{12} = 0$) results in a total of 13 unknowns which are k_{1x}, k_{2x}, k_{3x}, k_{4x}, k_{5x}, m_{1x}, m_{2x}, m_{3x}, m_{4x},T_{22}, T_{24}, T_{42}, and T_{44}. This number of unknowns can also be arrived at by computation using (3.32). The number of equations is 14 and can be arrived at by computation using (3.34). As the number of unknowns is less than the number of equations, the mass and stiffness parameters may be identified by

perturbing coordinates 1 and 3 and using eigenvalues alone. Consider a numerical simulation with the following parameters:

System: $k_1 = 10000$ N/m, $k_2 = 12000$ N/m
$k_3 = 16000$ N/m, $k_4 = 8000$ N/m
$k_5 = 10000$ N/m
$m_1 = m_2 = m_3 = m_4 = 2$ kg

Initial model: $k_{1a} = k_{2a} = 11000$ N/m, $k_{3a} = 18000$ N/m
$k_{4a} = k_{5a} = 9000$ N/m
$m_{1a} = m_{2a} = m_{3a} = m_{4a} = 1.8$ kg

The system and its initial model were perturbed by adding a grounded stiffness of 5000 N/m in turn at coordinates 1 and 3. The first three eigenvalues of the system before and after stiffness addition at the two coordinates were used in the updating process. A total of 9 eigenvalues were used to update the 9 parameters. The natural frequencies are shown in table 3.7. Table 3.8 shows the updated parameters which converged to the exact parameters in 3 iterations.

Added stiffness (N/m)	Stiffness added coordinate	Simulated natural frequencies (Hz)			Natural frequencies of the initial model (Hz)		
		Mode 1	Mode 2	Mode 3	Mode 1	Mode 2	Mode 3
0	-	6.929	14.188	18.078	7.324	15.155	19.235
5000	1	7.477	14.736	18.893	7.801	15.751	20.202
	3	8.301	14.275	18.540	8.793	15.200	19.616

TABLE 3.7 Natural frequencies of the fixed-fixed 4 DOF spring-mass model.

	Iteration steps			
	0	1	2	3
k_1	11000	9933	10012	10000
k_2	11000	11991	12009	12000
k_3	18000	15596	15997	16000
k_4	9000	7914	7797	8000
k_5	9000	10112	9969	10000
m_1	1.8	1.959	2.005	2.000
m_2	1.8	1.983	2.000	2.000
m_3	1.8	2.050	1.999	2.000
m_4	1.8	1.966	1.995	2.000

TABLE 3.8 Convergence of the mass (kg) and stiffness (N/m) parameters.

EXAMPLE 3.8

Fig 3.6 show a free beam modelled by a 5 elements 12 DOF model. The beam was simulated using the following parameters,

Simulated: $EI = 5000\ \text{Nm}^2$, $m_u = 3.5$ kg/m (all elements)

which resulted in the following natural frequencies for the first three elastic modes.

$$f_1 = 86.18\ \text{Hz}, f_2 = 238.19\ \text{Hz}, f_3 = 469.96\ \text{Hz}.$$

The beam was then modelled using the following initial parameters.

$$\text{Initial model } EI_a = 5200 \text{ Nm}^2, \quad m_{ua} = 3.3 \text{ kg/m (all elements)}$$
$$f_{1a} = 90.51 \text{ Hz}, f_{2a} = 250.16 \text{ Hz}, f_{3a} = 493.57 \text{ Hz}.$$

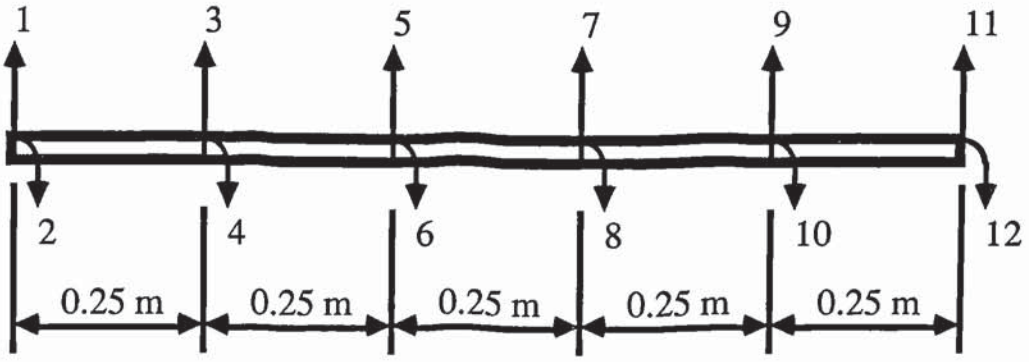

Fig 3.6 Free beam, 12 DOF model.

Let the initial model be updated by perturbing coordinates 3 and 7. The number of equations and unknowns in (3.22) to (3.27) are:

$$\text{Number of equations} = (N - N_{pc})^2 + (N - N_{pc}) + N_z x(N - N_{pc}) + N_{pc}^2 + N_{pc}$$
$$= (12-2)^2 + (12-2) + 4x(12-2) + 2^2 + 2 = 156$$

$$\text{Number of unknowns} = (N - N_{pc})^2 + N_{pc} x(N - N_{pc}) + n_{km}$$
$$= (12-2)^2 + 2x(12-2) + 10 = 130$$

The number of equations is greater than the number of unknowns and therefore the parameters may be identified using eigenvalues and perturbing coordinates 3 and 7. The initial parameters were updated by adding masses of 0.35 kg and 0.45 kg in turn at coordinates 3 and 7. Eigenvalues of the first

three elastic modes before and after each mass addition were used in the updating process. Table 3.9 shows the simulated and the analytical natural frequencies. The parameters converged to the exact mass and stiffness parameters (table 3.10).

Added mass (kg)	Mass added coordinate	Simulated natural frequencies (Hz)			Analytical natural frequencies (Hz)		
		Mode 1	Mode 2	Mode 3	Mode 1	MOde 2	Mode 3
0	-	86.18	238.19	469.96	90.51	250.16	493.57
0.35	3	86.06	232.88	444.52	90.38	244.29	465.62
	7	82.90	230.79	462.87	86.88	242.00	485.77
0.45	3	86.04	231.61	439.25	90.35	242.90	459.93
	7	82.11	229.14	461.29	86.01	240.21	484.04

TABLE 3.9 Simulated and analytical natural frequencies of the 12 DOF beam.

	Iteration steps			
	0	1	2	3
EI_1	5200	4920	5004	5000
EI_2	5200	4981	4998	5000
EI_3	5200	4861	4996	5000
EI_4	5200	5046	5001	5000
EI_5	5200	5014	5001	5000
m_{u1}	3.3	3.457	3.499	3.500
m_{u2}	3.3	3.493	3.499	3.500
m_{u3}	3.3	3.410	3.498	3.500
m_{u4}	3.3	3.530	3.500	3.500
m_{u5}	3.3	3.423	3.499	3.500

TABLE 3.10 Convergence of the mass (kg/m) and stiffness (Nm^2) parameters of the 12 DOF free beam (element numbers start from the left of the beam in fig 3.9)

EXAMPLE 3.9

Fig 3.7 show a 10 DOF plane frame modelled by 2 dimensional beam elements. Only degrees of freedom in the plane of the frame were considered in the modelling and the longitudinal flexibility of the elements ignored.

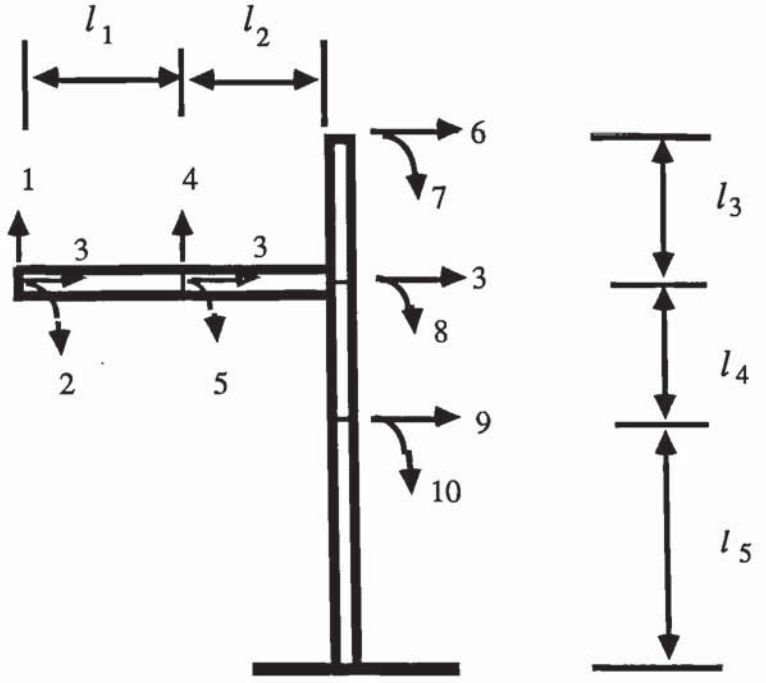

Fig 3.7 A 10 DOF plane frame

The simulated frame and the initial model had the following set of parameters:

Simulated: $EI_1 = EI_2 = EI_3 = EI_4 = EI_5 = 5000\ \text{Nm}^2$

$m_{u1} = m_{u2} = m_{u3} = m_{u4} = m_{u5} = 3.5\ \text{kg/m}$

$l_1 = l_2 = l_3 = l_4 = 0.25\ \text{m},\ l_5 = 0.5\ \text{m}$

$f_1 = 14.31\ \text{Hz}, f_2 = 56.09\ \text{Hz}, f_3 = 183.69\ \text{Hz}$

Initial model $EI_{1a} = 5200\ \text{Nm}^2,\ EI_{2a} = 5100\ \text{Nm}^2$

$$EI_{3a} = EI_{4a} = EI_{5a} = 4800 \text{ Nm}^2$$

$$m_{u1,a} = m_{u2,a} = m_{u3,a} = m_{u4,a} = m_{u5,a} = 3.3 \text{ kg/m}$$

l_1, l_2, l_3, l_4 and l_5 same as the simulated system.

$f_{1a} = 14.48$ Hz, $f_{2a} = 57.17$ Hz, $f_{3a} = 187.98$ Hz

Let coordinates 4 and 9 be perturbed by mass addition and the parameters updated using eigenvalues. There is a total of 10 parameters to update. The submatrices $\mathbf{K}_{22,x}$ and $\mathbf{M}_{22,x}$ are of order 8. The number of equations in (3.22) to (3.27) is given by (3.33) as

$$\begin{aligned}\text{No of equations} &= (N - N_{pc})^2 + (N - N_{pc}) + N_z x(N - N_{pc}) + N_{pc}^2 + N_{pc} \\ &= (10\text{-}2)^2 + (10\text{-}2) + 4x(10\text{-}2) + 2^2 + 2 = 110\end{aligned}$$

The number of unknowns is given by (3.31) as

$$\begin{aligned}\text{No of unknowns} &= (N - N_{pc})^2 + N_{pc} x(N - N_{pc}) + n_{km} \\ &= (10\text{-}2)^2 + 2x(10\text{-}2) + 10 = 90\end{aligned}$$

The number of equations is greater than the number of unknowns and therefore the mass and stiffness parameters may be identified using eigenvalues by perturbing coordinate 4 and 9.

The parameters were updated by adding in turn masses of 0.35 kg and 0.45 kg at coordinates 4 and 9. It was not possible to achieve any parameter convergence using the first three modes of the frame before and after each mass addition. The first two modes are dominated by the local modes of the vertical beam which has lower natural frequencies. The motion of the horizontal beam is close to that of a rigid body with the flexure of the beam playing an

insignificant role. This problem was overcome by using the higher elastic modes. Thus, by omitting the first two modes and use modes 3 to 5, the parameters converged to their correct values. The simulated and the analytical natural frequencies for modes 3 to 5 are shown in table 3.11. The updated parameters converged to their correct values and are shown in table 3.12.

Added mass (kg)	Mass added coordinate	Simulated natural frequencies (Hz)			Analytical natural frequencies (Hz)		
		Mode 3	Mode 4	Mode 5	Mode 3	MOde 4	Mode 5
0	-	183.69	335.71	496.76	187.98	339.29	515.03
0.35	4	183.64	333.87	434.02	187.95	337.62	447.23
	9	171.38	328.13	496.72	174.73	331.48	514.99
0.45	4	183.62	333.21	422.20	187.94	337.03	434.62
	9	168.45	326.28	496.71	171.61	329.91	514.98

TABLE 3.11 Simulated and analytical natural frequencies of the plane frame.

	Iteration steps				
	0	1	2	3	4
EI_1	5200	5093	5003	5000	5000
EI_2	5100	4901	4996	5000	5000
EI_3	4800	4855	4985	4999	5000
EI_4	4800	4838	4982	4999	5000
EI_5	4800	5041	5000	5000	5000
m_{u1}	3.3	3.466	3.500	3.500	3.500
m_{u2}	3.3	3.470	3.498	3.499	3.500
m_{u3}	3.3	3.406	3.493	3.499	3.500
m_{u4}	3.3	3.486	3.503	3.500	3.500
m_{u5}	3.3	3.491	3.498	3.499	3.500

TABLE 3.12 Convergence of the stiffness (Nm^2) and mass (kg/m) parameters of the 10 DOF plane frame.

EXAMPLE 3.10

This example analyses the systems simulated in examples 3.2 and 3.3 (figs 3.1 and 3.2 respectively) using the formula for the numbers of equations and unknowns in (3.22) to (3.27) when the systems are perturbed at each coordinate. The numbers of equations and unknowns are given as:

No of equations = $(N - N_{pc})^2 + (N - N_{pc}) + N_z x(N - N_{pc}) + 2xN_{pc} + N_{zd}$
(Diagonal **M** or **K**)

No of unknowns = $(N - N_{pc})^2 + n_{km}$
(Diagonal **M** or **K**)

N_{zd} (the total number of non-zero influence coefficients above the main diagonals of the mass and stiffness matrices) for the systems of figs 3.1 and 3.2 are obtained from the structure of the stiffness and mass matrices in examples 3.2 and 3.3. They are 7 and 5 respectively. In each case $N_{pc} = N$. Thus the formula for the numbers of unknowns and equations are simplified to:

For fig 3.1: No of equations = $2xN_{pc} + N_{zd} = 2x5 + 7 = 17$
No of unknowns = $n_{km} = 13$

For fig 3.2: No of equations = $2xN_{pc} + N_{zd} = 2x4 + 5 = 15$
No of unknowns = $n_{km} = 13$

Thus, the parameters of the system of figs 3.1 and 3.2 can be identified using eigenvalues by perturbing each coordinate. This is consistent with the findings in examples 3.2 and 3.3.

3.3 Updating using eigenvalues and eigenvectors

The eigenvalues and the mass-normalized eigenvectors are solutions of the homogeneous equation of motion and orthogonality equations.

$$[\,\mathbf{K} - \lambda_j \mathbf{M}\,]\,U_j = 0 \tag{3.38}$$

$$U_j^T \mathbf{K} U_j = \lambda_j \tag{3.39}$$

$$U_j^T \mathbf{M} U_j = 1 \tag{3.40}$$

For any j^{th} mode, (3.38) to (3.40) represents a system of simultaneous equations linear in the mass and stiffness parameters. It can be noted that (3.39) is automatically derived from (3.38) and (3.40). Similarly (3.40) can be derived from (3.38) and (3.39). Thus, the coefficient matrix of the simultaneous equations derived from (3.38) to (3.40) is of rank N+1, where N is the order of the mass and stiffness matrices. It follows therefore, the Jacobian matrix of eigenvalue and eigenvector sensitivities is of rank N+1. The process of parameter identification involves formulating the eigenvalue and eigenvector sensitivity matrix for all measured modes. The analytical model parameters are then updated by solving (3.41) iteratively.

$$\begin{bmatrix} \mathbf{J}_\lambda \\ \mathbf{J}_U \end{bmatrix} \Delta s = \begin{Bmatrix} \Delta\lambda \\ \Delta U \end{Bmatrix} \tag{3.41}$$

If the number of measured modes is such that (3.41) is not underdetermined, then in principle the updated parameters should converge to the correct model parameters. Thus, among other factors, the identification of the mass and stiffness parameters depends on the availability of a sufficient number of mode

shape data so that $\mathbf{J}^T\mathbf{J}$, is not rank deficient.

In practice mode shape measurement at each coordinate is not possible. The eigenvectors in (3.38) to (3.40) are therefore incomplete. This section analyses the conditions for the identification of the correct mass and stiffness parameters of a model with the same measured mode shapes and eigenvalues as a given system before and after perturbation by mass or stiffness. It is assumed that the structure of the mass and stiffness matrices is exact and the modal data is error-free. The mode shapes are incomplete in number and are measured at an incomplete number of coordinates.

The incompleteness of the mode shapes creates difficulties in the formulation of (3.38) to (3.40) since some mode shape data is missing. Arbitrary replacement of the missing data may result in arbitrary parameters. However it can be noted that the formulation of (3.41) for the coordinates which have been measured, do not depend on the availability of the mode shape data at the unmeasured coordinates. So can we simply ignore the unmeasured coordinates and solve (3.41) using the measured coordinates ? The answer is not obvious.

Let N_{mc} be the number of measured coordinates. The mass and stiffness matrices can be partitioned into submatrices corresponding to the measured and unmeasured coordinates. Let $\mathbf{K}_R$ and $\mathbf{M}_R$ be the mass and stiffness matrices of a reduced order model defined at the measured coordinates. For any given eigenvalue λ_j of the system:

$$[\,\mathbf{K}_R - \lambda_j\mathbf{M}_R\,]\,U_j = 0 \tag{3.42}$$

$$U_j^T\mathbf{K}_R U_j = \lambda_j \tag{3.43}$$

$$U_j^T \mathbf{M}_R U_j = 1 \tag{3.44}$$

If a suitable choice of parameters to update can be made so that they are linear in the reduced order model, then (3.42) to (3.44) represents a system of simultaneous equations linear in the parameters. The coefficient matrix is of rank $N_{mc}+1$. In this case we can formulate the Jacobian matrix of eigenvalue and eigenvector sensitivities of rank $N_{mc}+1$. For a total of n_p parameters at least r modes, ($(N_{mc}+1)r > n_p$), are needed in order to identify the parameters.

Our choice of parameters however, is such that they are linear in the full order model but non-linear in the reduced order model. Thus $(N_{mc}+1)r>n_p$, does not necessarily means that the sensitivity matrix is non-singular. A unique reduced order model may be identified if a suitable choice of parameters is made. Thus, it is reasonable to suppose that the conditions which ensure the existence of a unique set of parameters of a full order model for a unique reduced order model will ensure the identification of the full order mass and stiffness matrices.

It has been shown in section **3.2** that there exist an arbitrary model of mass and stiffness matrices $\mathbf{M}_x$ and $\mathbf{K}_x$ given by **RMS** and **RKS** respectively that has the same eigenvalues as the given system of mass and stiffness matrices **M** and **K**. Let **K**, **M** and the dynamic stiffness matrix **D**, be partitioned into submatrices corresponding to the measured and unmeasured coordinates (subscript mm and oo respectively). Thus:

$$\mathbf{K}_x = \mathbf{R}\begin{bmatrix} \mathbf{K}_{mm} & \mathbf{K}_{mo} \\ \mathbf{K}_{om} & \mathbf{K}_{oo} \end{bmatrix}\mathbf{S} \tag{3.45}$$

$$\mathbf{M}_x = \mathbf{R}\begin{bmatrix}\mathbf{M}_{mm} & \mathbf{M}_{mo}\\ \mathbf{M}_{om} & \mathbf{M}_{oo}\end{bmatrix}\mathbf{S} \tag{3.46}$$

$$\mathbf{D}_x = \mathbf{R}\begin{bmatrix}\mathbf{D}_{mm} & \mathbf{D}_{mo}\\ \mathbf{D}_{om} & \mathbf{D}_{oo}\end{bmatrix}\mathbf{S} \tag{3.47}$$

The reduced dynamic stiffness matrix of the system and of the arbitrary model with the same eigenvalues as the system are given by:

$$\mathbf{D}_R = \mathbf{D}_{mm} - \mathbf{D}_{mo}\mathbf{D}_{oo}^{-1}\mathbf{D}_{om} \tag{3.48}$$

$$\mathbf{D}_{R,x} = \mathbf{D}_{mm,x} - \mathbf{D}_{mo,x}\mathbf{D}_{oo,x}^{-1}\mathbf{D}_{om,x} \tag{3.49}$$

It has been shown that with mass or stiffness addition $\mathbf{S} = \mathbf{R}^T = \mathbf{T}^T$. If $\mathbf{D}_{R,x} = \mathbf{D}_R$ is unique then by inspection of (3.48) and (3.49), $\mathbf{D}_{mm,x}$, $\mathbf{D}_{mo,x}$ and $\mathbf{D}_{oo,x}$ should be of the following forms:

$$\mathbf{D}_{mm,x} = \mathbf{D}_{mm} \tag{3.50}$$

$$\mathbf{D}_{mo,x} = \mathbf{D}_{mo}\mathbf{T}_{oo}^T \tag{3.51}$$

$$\mathbf{D}_{oo,x} = \mathbf{T}_{oo}\mathbf{D}_{oo}\mathbf{T}_{oo}^T \tag{3.52}$$

$\mathbf{T}$ is consequently given by,

$$\mathbf{T} = \begin{bmatrix} +(-)\mathbf{I} & 0\\ 0 & \mathbf{T}_{oo}\end{bmatrix} \tag{3.53}$$

where $\mathbf{T}_{oo}$ is an arbitrary submatrix corresponding to the unmeasured DOF. Parameters of the full order model will be identified using (3.41) only if $\mathbf{K}_x$ and $\mathbf{M}_x$ given by

$$\mathbf{K}_x = \mathbf{T}\mathbf{K}\mathbf{T}^T \quad \text{and} \quad \mathbf{M}_x = \mathbf{T}\mathbf{M}\mathbf{T}^T$$

do not have an infinite number of solutions. Infinity solutions for $\mathbf{K}_x$ and $\mathbf{M}_x$ means infinity set of parameters of the full order model that can reconstruct unique reduced order mass and stiffness matrices.

Equations (3.50) to (3.52) have been derived by inspection. The form of **T** is in (3.53) is very similar to its form when eigenvalues alone were used with mass/stiffness addition. The difference is the replacement of the submatrix corresponding to the perturbed coordinates, by an identity submatrix corresponding to the measurement coordinates. Similar procedures are therefore used to establish the adequacy of the measurement coordinates for the identification of the correct mass and stiffness parameters. The **T** matrix, however, has to be modified to account for the constraining due to the perturbing coordinates as well as the measurement coordinates. The number of equations in (3.22) to (3.27) is then compared to the number of unknowns. A solution is possible only if the number of equations is equal or larger than the number of unknowns. In this case, the eigen-data sensitivity matrix will become non-singular. Some examples will now be considered.

EXAMPLE 3.11

A cantilever beam is simulated by an 8 DOF FE model (fig 3.8).

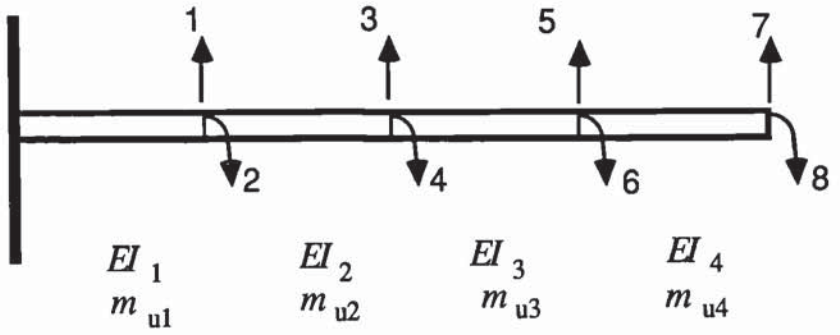

Fig 3.8 An 8 DOF cantilever beam.

Let the beam be perturbed by stiffness addition at coordinate 5 and the mode shape displacements measured at coordinate 1 only. We analyse the adequacy of the measurement and the perturbing coordinates in order to identify the correct parameters using eigenvalues and eigenvectors. In this case the measurement and the perturbing coordinates are different. **T** is an 8x8 matrix of the following form,

$$\mathbf{T} = \begin{bmatrix} \mathbf{T}_{AA} & \mathbf{T}_{AB} & \mathbf{T}_{AC} \\ \mathbf{T}_{BA} & \mathbf{T}_{BB} & \mathbf{T}_{BC} \\ \mathbf{T}_{CA} & \mathbf{T}_{CB} & \mathbf{T}_{CC} \end{bmatrix}$$

where $\mathbf{T}_{AA} = +(-)1$, $\mathbf{T}_{AB} = \mathbf{T}_{AC} = \mathbf{T}_{BA} = \mathbf{T}_{CA} = 0$ and accounts for the constraining due to measurement at coordinate 1.

$\mathbf{T}_{BB} = 1$, $\mathbf{T}_{CB} = 0$ and accounts for the constraining due stiffness addition at coordinate 5.

The unknowns in **T** are therefore due to $\mathbf{T}_{BC}$ (a 1x6 submatrix) and $\mathbf{T}_{CC}$ (a 6x6 submatrix) giving 42 unknowns. The total number of unknowns in (3.22) to (3.27) is therefore 42 + 8 mass and stiffness parameters = 50.

The number of equations is $N^2 + N = 72$ which is greater than the number of unknowns. The measurement and perturbing coordinates are therefore adequate to identify the parameters. Consider a numerical simulation with the following data.

System: $EI_1 = EI_2 = EI_3 = EI_4 = 5000\ \text{Nm}^2$

$m_{u1} = m_{u2} = m_{u3} = m_{u4} = 3.5\ \text{kg/m}$

Initial model: $EI_{1,a} = EI_{2,a} = 5100\ \text{Nm}^2, EI_{3,a} = EI_{4,a} = 4800\ \text{Nm}^2$

$m_{u1,a} = m_{u2,a} = m_{u3,a} = m_{u4,a} = 3.3\ \text{kg/m}$

The system and the initial model were perturbed by adding, in turn, stiffness of $1.0\text{x}10^6$ N/m and $2.0\text{x}10^6$ N/m at coordinate 5. The first two eigenvalues and mode shapes of the simulated beam before and after stiffness addition were taken as the measured data. The mode shape data used is for coordinate 1 only. Table 3.13 shows the eigen-data of the simulated beam and the initial model (in brackets), before and after perturbation. This data was used to update the 8 mass and stiffness parameters of the beam elements. The parameters converged to their correct values as shown in table 3.14.

Added stiffness (N/m)	Mass-normalized mode shape data at coord. 1		Natural frequencies (Hz)	
	Mode 1	Mode 2	Mode 1	Mode 2
0	-0.1040 (-0.1068)	-0.4471 (-0.4532)	21.15 (21.96)	132.70 (136.16)
1.0×10^6	-0.0004 (-0.0032)	-0.4828 (-0.4912)	105.02 (107.66)	137.29 (141.33)
2.0×10^6	-0.2588 (-0.2574)	-0.4374 (-0.4499)	123.89 (126.60)	155.14 (160.02)

TABLE 3.13 Eigen-data of the 8 DOF cantilever beam (Data in brackets is for the initial model)

	Ieration steps			
	0	1	2	3
EI_1	5100	5097	5002	5000
EI_2	5100	4788	4983	5000
EI_3	4800	4898	4997	5000
EI_4	4800	4548	4939	4999
m_{u1}	3.30	5.15	3.49	3.50
m_{u2}	3.30	3.02	4.48	3.50
m_{u3}	3.30	3.76	3.52	3.50
m_{u4}	3.30	3.42	3.49	3.50

TABLE 3.14 Convergence of the mass (kg/m) and stiffness (Nm^2) parameters of the cantilever beam.

EXAMPLE 3.12

The 2 DOF spring-mass system of example 3.5 (fig 3.3) is perturbed at coordinate 1 and the mode shape measured at coordinate 1 only. Lets analyse the adequacy of perturbing and measuring coordinate 1 only in order to identify the parameters. Since coordinate 1 only is measured the effect of measuring this coordinate on **T** is to constrain it so that it becomes diagonal with one diagonal element, corresponding to the measured coordinate, as +(-)1 and the other diagonal element as arbitrary. The effect of perturbing this coordinate is to constrain **T** so that it becomes diagonal with the element corresponding to coordinate 1 becoming unique and equal to 1. Thus, the combined effect is **T** having the same form as when coordinate 1 was perturbed and eigenvalues alone used

$$\mathbf{T} = \begin{bmatrix} 1 & 0 \\ 0 & \mathbf{T}_{BB} \end{bmatrix}$$

where $\mathbf{T}_{BB}$ becomes an arbitrary scalar. The number of unknowns in (3.22) to (3.27) is 5 mass and stiffness parameters plus 1 due to $\mathbf{T}_{BB}$ = 6. The number of equations is 3 for the stiffness matrix + 2 for the diagonal mass matrix = 5. The number of equations is less than the number of unknowns and therefore the parameters cannot be identified by measuring and perturbing coordinate 1 only.

If coordinate 2 is measured instead of coordinate 1 but mass is still added at coordinate 1 only, then $\mathbf{T}_{BB}$ becomes a scalar given by +(-)1. Thus, the number of unknowns is reduced by 1. The system parameters can now be identified by perturbing coordinate 1 and measure the mode shape at coordinate 2. It can be noted that there are two solutions for the parameters each corresponding to

a different sign of $\mathbf{T}_{BB}$ ($\mathbf{T}_{BB}$ = scalar = +(-)1).

Consider a numerical simulation with the following data

System: $k_1 = k_2 = k_3 = 1.0\text{x}10^6$ N/m

$m_1 = 10$ kg, $m_2 = 5$ kg.

Initial model: $k_{1a} = 1.05\text{x}10^6$ N/m, $k_{2a} = k_{3a} = 0.96\text{x}10^6$ N/m

$m_{1a} = 11$ kg, $m_{2a} = 5.5$ kg.

Coordinate 1 was perturbed by mass of 0.5 kg and 0.75 kg. The eigenvalues and mode shape data for the two modes before and after mass addition were used in the updating process. The mode shape data used was for coordinate 2 only. Table 3.15 shows the simulated and the analytical natural frequencies and mode shape data. The updated parameters converged to their correct values and are shown in table 3.16 .

It can be noted that this system has two sets of solutions which have the same natural frequency and mode shape data as the one simulated in table 3.15. One solution is the correct solution corresponds to $\mathbf{T}_{BB} = 1$. The other solution corresponds to $\mathbf{T}_{BB} = -1$ with the following parameters:

$k_1 = 3\text{x}10^6$ N/m, $k_2 = -10^6$ N/m, $k_3 = 3\text{x}10^6$ N/m,

$m_1 = 10$ Kg, $m_2 = 5$ kg.

This second solution is not identified, however, because the initial estimates are not close to it.

Added mass (kg) at coord. 1	Simulated natural frequencies and mass-normalized modes at coordinate 2. (Mode shape data is given in brackets)		Analytical natural frequencies and mass-normalized modes at coordinate 2. (Mode shape data is given in brackets)	
	Mode 1	Mode 2	Mode 1	Mode 2
0	56.67 Hz (0.2056)	109.48 Hz (0.3975)	54.46 Hz (0.2003)	102.50 Hz (0.3765)
0.5	55.58 Hz (0.1988)	108.94 Hz (0.4006)	53.51 Hz (0.1941)	102.01 Hz (0.3796)
0.75	55.06 Hz (0.1957)	108.69 Hz (0.4021)	53.06 Hz (0.1913)	101.79 Hz (0.3811)

TABLE 3.15 Natural frequencies and mode shape data of the simulated and analytical 2 DOF spring-mass system.

	Iteration steps			
	0	1	2	3
k_1	1.05×10^6	1.01×10^6	0.99×10^6	1.00×10^6
k_2	0.96×10^6	0.98×10^6	1.00×10^6	1.00×10^6
k_3	0.96×10^6	0.97×10^6	1.00×10^6	1.00×10^6
m_1	11	9.96	10.00	10.00
m_2	5.5	4.67	4.99	5.00

TABLE 3.16 Convergence of the stiffness (N/m) and mass (kg) parameters of the 2 DOF spring-mass system using eigenvalues and eigenvectors.

EXAMPLE 3.13

A 4 DOF lumped parameter branched system is shown in fig 3.9. Let coordinates 1 and 2 be measured and perturbed.

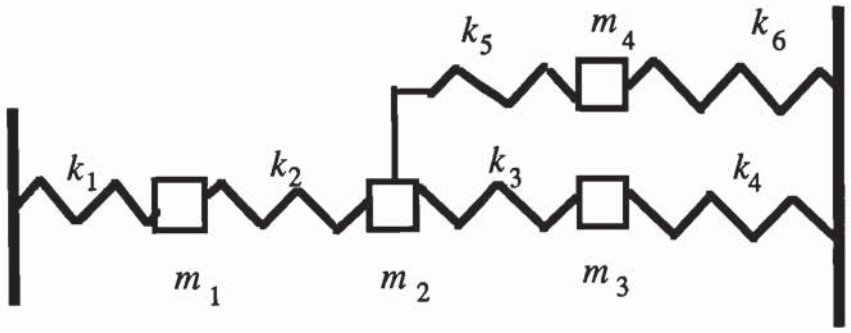

Fig 3.9 A branched 4 DOF spring=mass system.

The stiffness submatrices are:

$$\mathbf{K}_{mm,x}=\begin{bmatrix} k_{1x}+k_{2x} & -k_{2x} \\ -k_{2x} & k_{2x}+k_{3x}+k_{5x} \end{bmatrix}$$

$$\mathbf{K}_{mo,x}=\begin{bmatrix} 0 & 0 \\ -k_{3x} & -k_{5x} \end{bmatrix}, \quad \mathbf{K}_{oo,x}=\begin{bmatrix} k_{3x}+k_{4x} & 0 \\ 0 & k_{5x}+k_{6x} \end{bmatrix}$$

A submatrix of **T** which corresponds to the measured coordinates (which are also perturbed) is a 2x2 diagonal of the same form as the matrix **T** in the previous example. The number of unknowns in **T** are due to the 2x2 submatrix which corresponds to the unmeasured (which are also unperturbed) coordinates. Thus, the total number of unknowns in (3.22) to (3.27) is 4 (due to **T**) plus 10 mass and stiffness parameters = 14. The number of equations is 3 (due to $\mathbf{K}_{oo,x}$) plus 2 (due to $\mathbf{K}_{mo,x}$) plus 3 (due to $\mathbf{K}_{mm,x}$) plus 3 (due to $\mathbf{M}_{oo,x}$)

plus 2 (due to $\mathbf{M}_{mm,x}$) = 13. The number of equations is less than the number of unknowns. The parameters of this system cannot, therefore, be identified using eigenvalues and eigenvectors by perturbing and measuring coordinates 1 and 2.

Consider a numerical simulation with the following mass and stiffness data:

System: $k_1 = k_2 = k_3 = k_4 = k_5 = 1.0\text{x}10^6$ N/m
$k_6 = 0.5\text{x}10^6$ N/m
$m_1 = m_2 = 10$ kg, $m_3 = m_4 = 5$ kg
Natural frequencies(Hz): 42.86, 76.33, 94.29, 117.66

Initial model: $k_{1a} = k_{2a} = 1.02\text{x}10^6$ N/m
$k_{3a} = k_{4a} = k_{5a} = 0.98\text{x}10^6$ N/m
$k_{6a} = 0.51\text{x}10^6$ N/m,
$m_{1a} = 10.25$ kg, $m_{2a} = 9.8$ kg
$m_{3a} = m_{4a} = 5.1$ kg
Natural frequencies(Hz): 42.93, 76.09, 92.84, 116.73

Coordinates 1 and 2 were perturbed by stiffness of $1.0\text{x}10^6$ N/m. All four eigenvalues and all four mode shapes at coordinates 1 and 2 before and after stiffness addition were taken to have been measured. The eigen-data is given in tables 3.17 to 3.19. The Jacobian matrix contained 10 columns for the 10 parameters and a total of 36 rows for the eigenvector and eigenvalue data. It was not possible to solve for any meaningful parameters. The Jacobian matrix was rank deficient. The buildup of the rank of the Jacobian matrix is shown in table 3.20:

Stiffness added coordinate	Simulated natural frequencies (Hz)				Analytical natural frequencies (Hz)			
	Mode 1	Mode 2	Mode 3	Mode 4	Mode 1	Mode 2	Mode 3	Mode 4
-	42.86	76.33	94.29	117.66	42.93	76.09	92.84	116.73
1	48.11	87.17	95.12	118.18	48.24	86.44	93.74	117.32
2	53.15	77.40	95.04	122.80	53.11	77.09	93.53	122.28

TABLE 3.17 Simulated and analytical natural frequencies of the 4 DOF branched spring-mass system with and without added stiffness.

Stiffness added coordinate	Measurement coordinate	Mass-normalized mode shape data of the simulated system			
		Mode 1	Mode 2	Mode 3	Mode 4
-	1	0.1677	-0.2565	0.0501	-0.0596
	2	0.2130	0.0770	-0.0757	0.2065
1	1	0.1100	-0.2582	0.1204	-0.0821
	2	0.2295	0.0000	-0.0689	0.2064
2	1	0.2036	-0.2297	0.0473	-0.0593
	2	0.1802	0.0839	-0.0740	0.2346

TABLE 3.18 Mode shape data of the simulated 4 DOF branched spring-mass system with and without added stiffness.

Stiffness added coordinate	Measurement coordinate	Mass-normalized mode shape data of the initial analytical model			
		Mode 1	Mode 2	Mode 3	Mode 4
-	1	0.1680	-0.2506	0.0507	-0.0629
	2	0.2131	0.0745	-0.0719	0.2145
1	1	0.1112	-0.2489	0.1257	-0.0862
	2	0.2287	0.0040	-0.0636	0.2137
2	1	0.2029	-0.2244	0.0475	-0.0616
	2	0.1788	0.0803	-0.0698	0.2420

TABLE 3.19 Mode shape data of the initial model of the 4 DOF branched spring-mass system with and without added stiffness.

Total number of modes	1	2	3	4	5	6	7	8	9	10	11	12
Rank of $\mathbf{J}^T\mathbf{J}$	3	6	8	9	9	9	9	9	9	9	9	9

TABLE 3.20 Rank of the eigenvalue and eigenvector sensitivity matrix as a function of the number of modes

If coordinates 1, 2 and 3 are measured, the stiffness submatrices becomes,

$$\mathbf{K}_{mm,x}=\begin{bmatrix} k_{1x}+k_{2x} & -k_{2x} & 0 \\ -k_{2x} & k_{2x}+k_{3x}+k_{5x} & -k_{3x} \\ 0 & -k_{3x} & k_{3x}+k_{4x} \end{bmatrix}, \qquad \mathbf{K}_{mo,x}=\begin{bmatrix} 0 \\ -k_{5x} \\ 0 \end{bmatrix}$$

$$\mathbf{K}_{oo,x}=\begin{bmatrix} k_{5x}+k_{6x} \end{bmatrix}$$

the number of unknowns in **T** is reduced from 4 to 1 since $\mathbf{T}_{mm}$ becomes a 3x3 diagonal matrix with the diagonal elements as 1 or -1. The unknowns in **T** are

only due to $\mathbf{T}_{oo}$ which is now a 1x1 arbitrary scalar. Consequently, the total number of unknowns in (3.22) to (3.27) is reduced to 11. The number of equations is also reduced to 11 (7 from the stiffness matrix and 4 from the mass matrix). Thus, measuring coordinates 1 to 3 and perturbing coordinates 1 to 2 is adequate to identify the parameters of this system.

It can be noted that measuring coordinates 1,2 and 3 constrains the matrix **T** to the extent that the contribution of the constraining due to the perturbation at coordinates 1 and 2 is not needed in order for the number of unknowns to be equal to or less than the number of equations. Thus, in this case it is possible to identify the parameters even without mass or stiffness addition provided the number of modes is such that (3.41) is not underdetermined. As an example consider a numerical simulation of the same system but with different initial parameters which are not as close to the true system parameters as before. Thus let:

$$k_{1a} = k_{2a} = 1.05\text{x}10^6 \text{ N/m}, \quad k_{3a} = k_{4a} = k_{5a} = 0.95\text{x}10^6 \text{ N/m}$$
$$k_{6a} = 0.55\text{x}10^6 \text{ N/m},$$
$$m_{1a} = m_{2a} = 10.5 \text{ kg}, \qquad m_{3a} = m_{4a} = 4.8 \text{ kg}.$$

The first three modes (measured at 1 , 2 and 3) and their eigenvalues were used in the updating process without mass or stiffness addition. The natural frequencies and mass-normalized modes are given in table 3.21. The Jacobian matrix had 12 rows and 10 columns with 10 parameters to update. It was possible to achieve parameter convergence to their correct values (Table 3.22).

Measurement coordinate	Simulated natural frequencies and mass-normalized mode shapes			Analytical natural frequencies and mass-normalized mode shapes		
	Mode 1 f_1 (Hz) = 42.86	Mode 2 f_2 (Hz) = 76.33	Mode 3 f_3 (Hz) = 94.29	Mode 1 f_{1a} (Hz) = 42.86	Mode 2 f_{2a} (Hz) = 77.02	Mode 3 f_{3a} (Hz) = 94.67
1	0.1677	-0.2565	0.0501	0.1671	-0.2489	0.0427
2	0.2130	0.0770	-0.0757	0.2131	0.0850	-0.0657
3	-0.1306	0.0905	-0.3086	-0.1304	0.1041	-0.3093

TABLE 3.21 Simulated and analytical modal data for the second case.

	Iteration steps		
	0	1	2
k_1	$1.05\text{x}10^6$	$0.998\text{x}10^6$	$1.000\text{x}10^6$
k_2	$1.05\text{x}10^6$	$0.999\text{x}10^6$	$1.000\text{x}10^6$
k_3	$0.95\text{x}10^6$	$0.999\text{x}10^6$	$1.000\text{x}10^6$
k_4	$0.95\text{x}10^6$	$1.007\text{x}10^6$	$1.000\text{x}10^6$
k_5	$0.95\text{x}10^6$	$0.997\text{x}10^6$	$1.000\text{x}10^6$
k_6	$0.55\text{x}10^6$	$0.502\text{x}10^6$	$0.500\text{x}10^6$
m_1	10.5	9.99	10.00
m_2	10.5	10.04	10.00
m_3	4.8	4.99	5.00
m_4	4.8	5.02	5.00

TABLE 3.22 Convergence of the stiffness (N/m) and mass (kg) parameters of the 4 DOF branched spring-mass system.

3.4 Summary

A technique of updating the parameters of a finite element model and a lumped parameter model with a diagonal mass or stiffness matrix has been presented. It is based on perturbation of the system by adding mass or stiffness so as to increase the amount and content of useful information about the dynamic characteristics of the system. This extra information comes from the eigenvalues or both eigenvalues and eigenvectors of an incomplete number of modes of the perturbed system. Parameters are then determined using the well known sensitivity analysis approach, where the analytical model is iteratively updated so as to reproduce the eigen-data of the system. If eigenvectors are also used then the mode shape does not have to be measured at each coordinate.

It has been established that the choice of the perturbing coordinates as well as the choice of the mode shape measurement coordinates is important. A simple test has been proposed to assess the adequacy of the perturbing and the measurement coordinates with respect to meaningful identification of the parameters. In general, this test involves comparison of the number of unknowns and the number of equations in a system of simultaneous non-linear equations derived from $\mathbf{K}_x = \mathbf{T}\mathbf{K}\mathbf{T}^T$ and $\mathbf{M}_x = \mathbf{T}\mathbf{M}\mathbf{T}^T$, where $\mathbf{T}$ is an arbitrary matrix which has been constrained by the perturbation process. It has also been shown that if the number of such equations is less than the number of unknowns there is an infinity of solutions for the parameters that can reproduce the eigen-data of the structure. The eigen-data sensitivity matrix becomes singular. In order to identify the parameters the number of unknowns must be less or equal to the number of equations. In this case it is possible to have more than one solution. With a reasonable estimate of the initial parameters, close to the correct mass and stiffness parameters, a correct

solution is usually identified as the other solutions, if any, are usually not feasible.

The work in this chapter has considered the addition of a lumped mass or lumped stiffness, one at a time. This is considered to be the relatively simplest form of perturbation to perform practically. In theory, any type of mass and stiffness combinations is possible. However, these may have a different constraining effect on the **R** and **S** matrices in (3.6), and may result in a slightly different conclusions on the choice of the perturbing coordinates. These are outside the scope of this work as their practical implementation is doubtful.

The verification of the theoretical developments in this chapter have been based of error-free data and a correct conceptual model. In a practical situation the experimental data is corrupted by measurement inaccuracies and the analytical model may be corrupted by conceptual modelling inaccuracies. These factors will have an effect on the quality of the results. The method of parameter identification as presented in this chapter cannot correct fundamental modelling errors in the analytical model. This problem is further addressed in Chapter 4. The technique presented overcomes the difficulties of identifying the parameters using incomplete eigen-data.

The practicality of adding the simulated masses or stiffnesses has not been considered. This problem is treated in Chapter 6 where a method of numerical simulation using the measured FRF to predict the eigen-data of the perturbed structure is presented.

CHAPTER 4

NUMERICAL SIMULATION OF SOME PRACTICAL UPDATING PROBLEMS

4.1 Introduction

The theory of the mass or stiffness addition technique for updating model parameters using eigenvalues or both eigenvalues and eigenvectors has been developed in Chapter 3. From this theory, it is evident that the choice of the mass addition and measurement coordinates, in the case of a lumped parameter model, needs careful consideration. With a finite element model, where the parameters to update are the coefficients of the element mass and stiffness matrices, the number of parameters in comparison to the number of DOF is small. The choice of the mass addition and measurement coordinates is therefore not so crucial, although adding mass to a single coordinate has to be avoided as it tends to result in poor conditioning of the sensitivity matrix. So far, it has been assumed that the structure of the mathematical model is exact. The numerical simulations presented have assumed error-free measured data. The technique developed in Chapter 3 overcomes the problems of parameter estimation due to the incompleteness of the measured data, with respect to the number of measured or excited modes and with respect to the number of measurement coordinates. In a practical situation, there are other factors which may affect the estimation of reasonable model parameters and could result in parameters losing their physical meaning. These factors are:

(i) Incompatibility in the number of DOF between the idealized model and the system.

(ii) Inaccuracy in the structure of the model matrices.

(iii) Incompatibility between the undamped FE model and data from a system with some degree of non-proportional damping.

(iv) Experimental errors in the measured data

In this Chapter, numerical simulation studies will be performed to investigate the effects of these factors on the accuracy of the updated parameters. The use of statistics in parameter estimation of "real structures" will be explored. The studies will first be performed by parameter estimation using an unconstrained least squares and weighted least squares optimization. It will be shown that the identification of parameters which retain their physical meaning, using an unconstrained optimization, is practically difficult due to the presence of the preceding factors. A minimum cost Bayesian approach, which includes a constraint of minimum changes of the parameters from their initial estimates, will then be introduced so as to maintain the physical interpretation of the parameters. The minimum cost Bayesian approach treats parameters of the initial analytical model and measured eigen-data as independent and having random errors with an expected mean of zero. With a low degree of incompatibility between the idealized model structure and the system, the minimum cost estimator gives acceptable results, with parameter changes from their initial estimates comparable to the uncertainty specified on these estimates. As the mismatch between the structure of the model matrices and measured data becomes larger, the minimum cost estimator cannot prevent large parameter changes from their initial estimates although the eigen-data used in the updating could be reasonably reproduced.

4.2 Incompatibility in the number of DOF.

Real structures have an infinite number of DOF whereas analytical models, FE models for example, are usually discretized to a finite number of DOF. Even if exact mass and stiffness parameters are known, the analytical model's natural frequencies will deviate from the natural frequencies of a system with an infinite number of DOF. This discrepancy, which is caused by the discretization error, increases with frequency. The frequency range over which this discrepancy is not significant can be increased by increasing the degree of discretization. That is, the higher the number of elements, the larger the frequency range over which the discrepancy becomes negligible. In parameter estimation literature, the larger the measurement frequency range the better, since more modes are measured. However, measuring over a larger frequency range may be a source of problems if the degree of discretization of the FE model is not compatible with the data from the higher end of the measured frequency spectrum. With the mass or stiffness addition technique, the measurement frequency range can be limited because extra modes are generated by perturbation. Some examples will now be considered:

EXAMPLE 4.1

A uniform beam of length 1.0 m and structural parameters EI = 5000 Nm^2 and m_u= 3.5 kg/m was modelled by a 16 elements FE model, ignoring axial flexibility. The beam was free and the FE model had 34 DOF. The first two elastic modes had natural frequencies of f_1 = 134.587 Hz and f_2 = 371.007 Hz. Whilst the beam could be modelled "exactly" from the Euler-Bernoulli equation we will imagine this to be a more complex structure and have chosen to model using the FE method. Thus, the eigen-data of the 16 elements beam was taken to simulate measured data.

The beam was then modelled by a 4 elements FE model with 10 DOF. Each element was 0.25 m long. This model was taken to represent the analytical model whose parameters were inaccurate and were to be updated. To simulate a system with many parameters, parameters of the 4 elements were treated as independent unknowns. Thus, there were 8 parameters to update. Parameter estimates and natural frequencies are:

$EI_{1a} = 4600\ \text{Nm}^2$ $\quad$ $EI_{2a} = 4600\ \text{Nm}^2$

$EI_{3a} = 5300\ \text{Nm}^2$ $\quad$ $EI_{4a} = 4800\ \text{Nm}^2$

$m_{u1,a} = m_{u2,a} = 3.3\ \text{kg/m}$ $\quad$ $m_{u3,a} = m_{u4,a} = 3.7\ \text{kg/m}$

$f_{1a} = 133.568\ \text{Hz}$ $\quad$ $f_{2a} = 368.141\ \text{Hz}$

The analytical model was to be updated by mass addition using eigenvalues of the first two elastic modes of the system with and without additional masses. Masses of 0.25 kg and 0.35 kg were added in turn at each of coordinates 9 and 17 of the simulated system (16 elements model, fig 4.1). A total of 10 natural frequencies, which simulated measured natural frequencies, were generated.

The masses were also added at corresponding coordinates of the analytical model, coordinates 3 and 5 in fig 4.2.

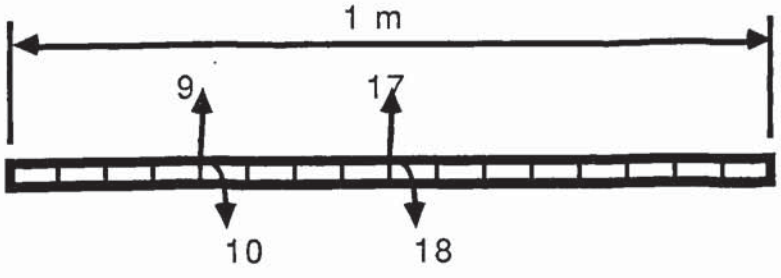

Fig 4.1 34 DOF free beam (Simulated system)

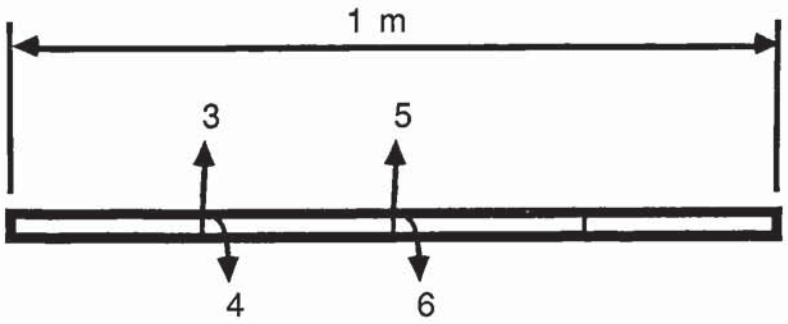

Fig 4.2 10 DOF free beam (Analytical model)

Table 4.1 shows the natural frequencies of the simulated system and the analytical model before and after mass addition.

Added mass (kg)	Coord (Fig 4.1)	Natural frequency (Hz) of the Simulated system		Natural frequency (Hz) of the analytical model	
		Mode 1	Mode 2	Mode 1	Mode 2
0		134.587	371.007	133.568	368.141
0.25	9	134.416	355.363	133.413	351.418
0.25	17	128.379	371.007	127.403	368.114
0.35	9	134.357	350.274	133.359	346.061
0.35	17	126.313	371.007	125.352	368.105

TABLE 4.1 Simulated and analytical natural frequencies of the free beam.

Parameters of the analytical model were then updated iteratively using the method of sensitivity of the eigenvalues with respect to parameter changes. The 10 eigenvalues of the simulated system, before and after mass addition, generated 10 sensitivity equations in 8 unknown parameters. The equations were solved by an ordinary least squares method without any constraints on the parameters. Table 4.2 show the convergence of the mass and stiffness

parameters in 5 iteration steps. Table 4.3 gives natural frequency predictions of the updated model before and after mass addition.

	Iteration steps					
	0	1	2	3	4	5
EI_1	4600	5062	4862	4842	4829	4822
EI_2	4600	5433	5640	5663	5665	5666
EI_3	5300	4412	4550	4537	4535	4534
EI_4	4800	4787	4621	4665	4681	4688
m_{u1}	3.30	3.66	3.69	3.69	3.69	3.69
m_{u2}	3.30	3.55	3.59	3.61	3.62	3.62
m_{u3}	3.70	3.46	3.41	3.40	3.39	3.39
m_{u4}	3.70	3.32	3.38	3.37	3.37	3.37

TABLE 4.2 Convergence of the mass and stiffness parameters of the beam.

Added mass (kg)	Coord (Fig 4.2)	Frequency prediction (Hz)	
		Mode 1	Mode 2
0		134.587	371.007
0.25	3	134.416	355.363
0.25	5	128.379	371.007
0.35	3	134.357	350.274
0.35	5	126.313	371.007

TABLE 4.3 Frequency prediction of the updated model of the free beam.

Examination of tables 4.3 and 4.1 shows that the updated model reproduces accurately the simulated natural frequencies of the system with and without additional masses (accurate to 3 decimal places). However, the updated parameters, table 4.2, are not very close to the correct parameters and natural frequency prediction of modes not used in the updating process is not good. For example, natural frequencies of modes 3 and 4 are predicted as:

Updated model:	$f_3 = 722.5$ Hz	$f_4 = 1326.5$ Hz.
Simulated system:	$f_3 = 727.4$ Hz	$f_4 = 1202.7$ Hz.
Initial FE model:	$f_{3a} = 718.8$ Hz	$f_{4a} = 1317.8$ Hz.

While the beam is uniform, there is a substantial difference in parameters of the updated model. In this example, discretization by a 4 elements 10 DOF model is not sufficiently accurate to fit the parameters using data from a 34 DOF system. It is also apparent that the existence of a deficiency in the structure of the model matrices cannot necessarily be detected by the failure of the eigen-data of the updated model to converge to the measured eigen-data. This example suggest that such a deficiency may be revealed by unexpectedly large deviation of the parameters from their initial estimates, rather than by comparing eigen-data prediction of the updated model to the measured ones. If the number of DOF is increased, a more reasonable result can be expected. It should also be noted that the parameters were obtained by solving an overdetermined set of equations using an ordinary least squares method without any constraints on the parameters. The parameters will converge to the same values irrespective of the values of the initial estimates, provided the initial parameters are not so unreasonable as to cause the solution process to diverge.

EXAMPLE 4.2

The 10 DOF analytical model of example 4.1 was improved to an 18 DOF model by dividing each of the four elements into two elements. Parameters of any such two elements were constrained, in the updating process, to be identical. Thus, there were 8 finite elements but 4 sets of independent mass and stiffness parameters to update. These are the mass and stiffness parameters corresponding to the four elements of the 10 DOF model of fig 4.2. Parameter estimation was performed using the same mass additions, simulated measured eigenvalues and initial parameters as in example 4.1. The only difference was in the degree of discretization of the finite element model. Thus:

$$EI_{1a} = EI_{2a} = 4600 \text{ Nm}^2 \qquad EI_{3a} = EI_{4a} = 4600 \text{ Nm}^2$$
$$EI_{5a} = EI_{6a} = 5300 \text{ Nm}^2 \qquad EI_{7a} = EI_{8a} = 4800 \text{ Nm}^2$$
$$m_{u1,a} = m_{u2,a} = 3.3 \text{ kg/m} \qquad m_{u3,a} = m_{u4,a} = 3.3 \text{ kg/m}$$
$$m_{u5,a} = m_{u6,a} = 3.7 \text{ kg/m} \qquad m_{u7,a} = m_{u8,a} = 3.7 \text{ kg/m}.$$

Table 4.4 shows the convergence of the mass and stiffness parameters in three iterations.

Clearly, with the same data and the same parameters to update, increasing the number of elements had improved the updated parameters. In this case, an 8 elements model is sufficiently discretized such that the effect of the discretization on natural frequency prediction is not significant for the first two modes. Attempts to increase the frequency range of interest will result in the degradation of the updated parameters if there is no accompanying refinement in discretization.

	Initial estimate	Iteration steps		
		1	2	3
$EI_1 = EI_2$	4600	5127	5041	5015
$EI_3 = EI_4$	4600	4932	5037	5037
$EI_5 = EI_6$	5300	5025	4966	4967
$EI_7 = EI_8$	4800	4870	4924	4950
$m_{u1} = m_{u2}$	3.30	3.49	3.52	3.51
$m_{u3} = m_{u4}$	3.30	3.44	3.49	3.50
$m_{u5} = m_{u6}$	3.70	3.56	3.51	3.50
$m_{u7} = m_{u8}$	3.70	3.48	3.49	3.49

TABLE 4.4 Parameter convergence of an 8 elements model.

For example, if the first five modes are now used with mass addition of 0.35 kg at the same points (coordinates corresponding to 9 and 17 of the 16 elements model), more eigenvalues are generated. However, after 5 iterations, parameters converged to:

$$EI_1 = EI_2 = 4414 \text{ Nm}^2 \qquad EI_3 = EI_4 = 5661 \text{ Nm}^2$$
$$EI_5 = EI_6 = 4210 \text{ Nm}^2 \qquad EI_7 = EI_8 = 4524 \text{ Nm}^2$$
$$m_{u1} = m_{u2} = 3.32 \text{ kg/m} \qquad m_{u3} = m_{u4} = 3.70 \text{ kg/m}$$
$$m_{u5} = m_{u6} = 3.65 \text{ kg/m} \qquad m_{u7} = m_{u8} = 2.75 \text{ kg/m}$$

The parameters, when 5 modes are used, are less accurate than when 2 modes were used. This illustrates how the updated parameters can be degraded by an attempt to use more modes by measuring a larger frequency range, while the degree of discretization is such that the model is not compatible with the eigen-

data measured on the higher end of the spectrum.

4.3 Inaccuracy in the structure of the model matrices.

While incompatibility between the number of model DOF and measured data can be viewed as a form of inaccuracy in the structure of the model matrices, this section deals with difficulties in idealization of some parts of the system. An example is the idealization of a clamped-clamped beam as a simply supported beam. In practical situations, difficulties are often encountered in the correct idealization of the boundary conditions and joints. A cantilever beam may be modelled as rigidly clamped, while in actual fact there may be some degree of flexibility at the clamped end. A bolted joint may be modelled as a rigid, point joint while there may exist some flexibility and the joint occupies a space. Incorrect choice of element type for some parts of the system could also have an undesirable effect on the updated parameters. The effects of incorrect model structure on parameter updating by mass or stiffness addition is investigated by the following numerical examples of an H-frame.

EXAMPLE 4.3

An H frame is made by bolting together three beam members. It is assumed that the joints are not infinitely rigid and they can be idealized by lumped rotational and translational stiffness. Also the axial flexibility of the beam members, denoted as B1, B2 and B3, will be ignored. The frame with a total of 8 FE beams and 23 DOF is shown in fig 4.3, where only motion in the plane of the frame is considered.

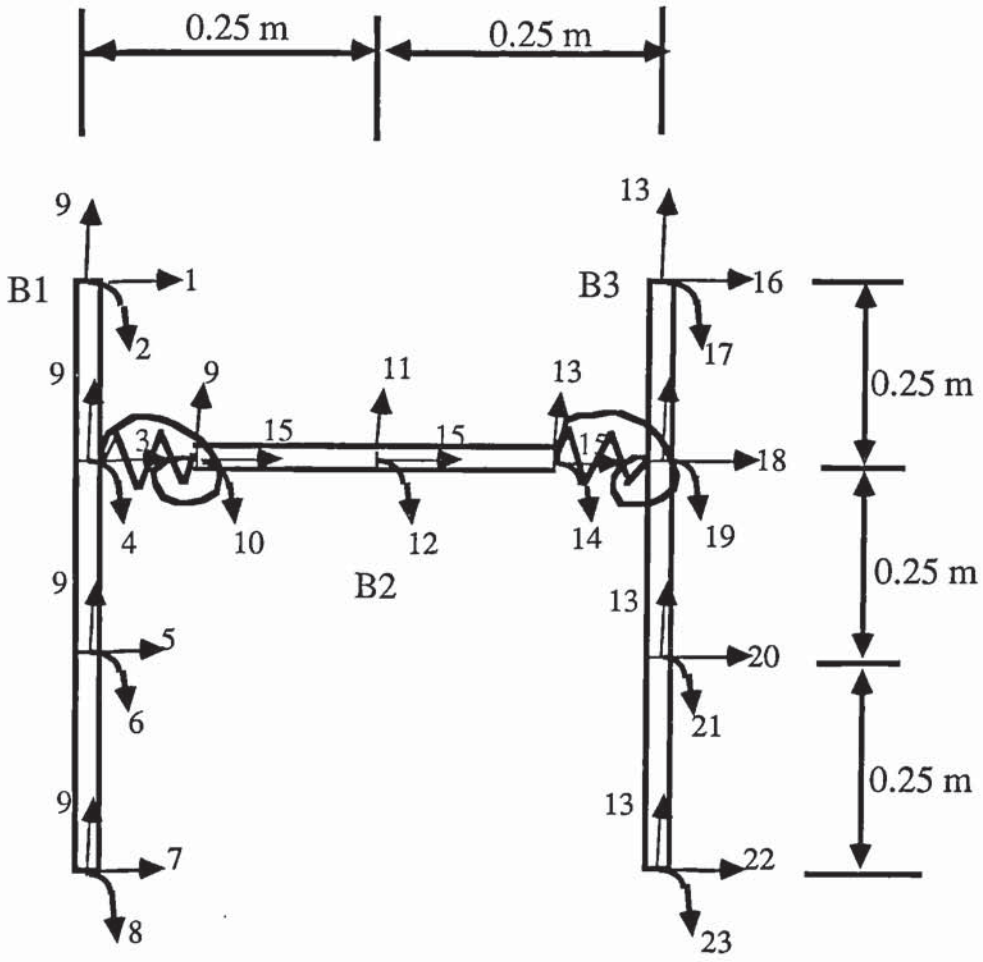

Fig 4.3 H-Frame : Simulated system.

The 23 DOF frame model with non-rigid joints is used to simulate a system with the following parameters:

FE parameters:

$EI_{B1} = 5000\ \text{Nm}^2$ $\quad EI_{B2} = 4000\ \text{Nm}^2$

$EI_{B3} = 6000\ \text{Nm}^2$ $\quad m_{uB1} = 3.5\ \text{kg/m}$

$m_{u,B2} = 3.0\ \text{kg/m}$ $\quad m_{u,B3} = 4.0\ \text{kg/m}$

Translational stiffness between:

Coordinate 3 and 15	$k_{T,3\text{-}15} = 10^7$ N/m
Coordinate 15 and 18	$k_{T,15\text{-}18} = 10^7$ N/m

Rotational stiffness between:

Coordinate 4 and 10	$k_{T,4\text{-}10} = 10^6$ Nm/rad
Coordinate 14 and 19	$k_{T,14\text{-}19} = 10^6$ Nm/rad.

Natural frequencies computed from the 23 DOF frame model (first three elastic modes) are:

$$f_1 = 41.71 \text{ Hz} \quad f_2 = 89.74 \text{ Hz} \quad f_3 = 193.46 \text{ Hz}.$$

The frame is now idealized by an analytical model with perfectly rigid joints. Two updating cases are considered.

CASE 1:

In the first case, the elements subdivision is similar to that of the simulated system. Each beam member is treated as uniform. Parameters for the elements of the same beam member are constrained to be identical. Thus, the analytical model has 19 DOF with 6 independent parameters to update, fig 4.4. Consider the following analytical model parameters.

$EI_{B1,a} = 5400$ Nm^2	$EI_{B2,a} = 4200$ Nm^2
$EI_{B3,a} = 5800$ Nm^2	$m_{u,B1,a} = 3.3$ kg/m
$m_{u,B2,a} = 3.1$ kg/m	$m_{u,B3,a} = 4.2$ kg/m

Natural frequencies (Hz): $f_{1a} = 43.09$ $f_{2a} = 92.84$ $f_{3a} = 208.19$.

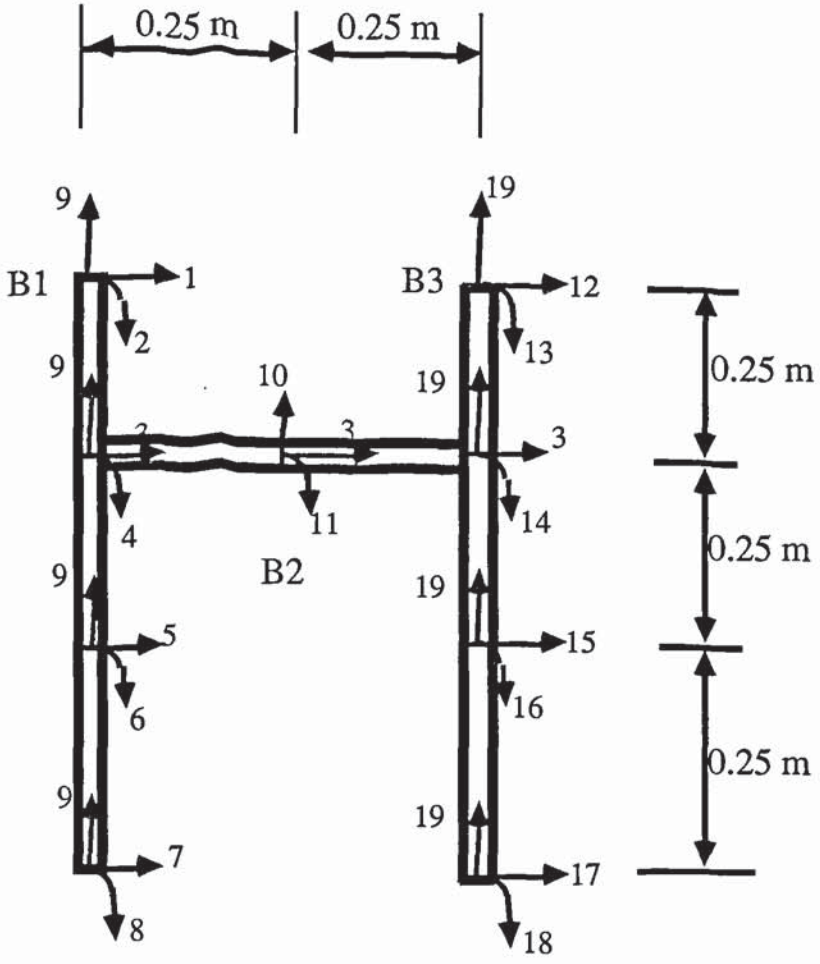

Fig 4.4 Analytical model of the H-frame (Case 1).

The analytical model parameters are now updated using eigenvalues, by adding mass of 0.25 kg and 0.35 kg, in turn, at coordinates 5 and 22 of the simulated system and the corresponding coordinates of the analytical model (Coordinates 5 and 17 of fig 4.4). Natural frequencies of the first three elastic modes before mass addition and their new natural frequencies after mass addition are used in the updating process. The natural frequencies are shown in table 4.5.

Added mass (kg)	Mass addition coordinate (fig 4.3)	Simulated natural frequencies (Hz)			Analytical natural frequencies (Hz)		
		Mode 1	Mode 2	Mode 3	Mode 1	Mode 2	Mode 3
0	-	41.71	89.74	193.46	43.09	92.84	208.19
0.25	5	40.82	89.45	193.46	42.12	92.45	208.16
	22	38.56	85.92	189.85	39.88	89.14	201.06
0.35	5	40.49	89.34	193.46	41.77	92.32	208.14
	22	37.57	84.93	188.84	38.88	88.17	199.15

TABLE 4.5 Natural frequencies of the simulated H-frame and the initial analytical model (Case 1).

The parameters are updated by an ordinary least squares solution method, using the error-free data of the simulated system. Table 4.6 shows the convergence of the parameters in 5 iteration steps.

	Iteration steps					
	0	1	2	3	4	5
EI_{B1}	5400	7413	8522	8640	11118	8939
EI_{B2}	4200	5290	6622	6678	7220	7395
EI_{B3}	5800	7052	6048	5607	6717	2341
$m_{u,B1}$	3.30	4.92	6.68	6.94	8.28	7.29
$m_{u,B2}$	3.10	8.27	2.17	0.15	5.98	-14.18
$m_{u,B3}$	4.20	4.92	5.56	5.45	5.64	5.62

TABLE 4.6 Convergence of the parameters of the H-frame with rigid joints (Case 1, fig 4.4).

It can be seen that there are large changes in the parameters from their initial

estimates. The changes in the parameters are so great that the fifth iteration result in a negative mass for the cross-beam member ($m_{u,B2}$). At the end of the 4th iteration, the natural frequencies of the updated model had converged towards the measured (simulated) natural frequencies. For example, the first three modes of the updated model, after 4 iterations, had natural frequencies which compare favourably with the simulated system. The parameters, however, are very far from reflecting the actual mass and stiffness distribution of the frame.

System:	$f_1 = 41.71$ Hz,	$f_2 = 89.74$ Hz,	$f_3 = 193.46$ Hz.
Updated:	$f_1 = 41.2$ Hz,	$f_2 = 86.9$ Hz,	$f_3 = 193.7$ Hz.
Initial model:	$f_{1a} = 43.09$ Hz	$f_{2a} = 92.84$ Hz	$f_{3a} = 208.19$ Hz.

After the fifth iteration, further iteration is not possible because the mass matrix with negative diagonal terms is meaningless and it results in negative eigenvalues. This case illustrate the difficulties that may be experienced when the structure of the model matrices is not correct.

CASE 2:

The second analytical model use a different element subdivision, fig 4.5, resulting in 29 DOF. For each beam member, elements next to the joint(s) are treated as having identical parameters which are different from the elements away from the joints. Thus each beam has two mass and two stiffness parameters to update. These are defined as follow:

EI_{1a}, m_{u1a}: Stiffness and mass of elements away from the joint for beam B1.
EI_{2a}, m_{u2a}: Stiffness and mass of elements next to the joint for beam B1.
EI_{3a}, m_{u3a}: Stiffness and mass of elements next to the joints for beam B2.

EI_{4a}, m_{u4a}: Stiffness and mass of element away from the joints for beam B2.

EI_{5a}, m_{u5a}: Stiffness and mass of elements away from the joint for beam B3.

EI_{6a}, m_{u6a}: Stiffness and mass of elements next to the joint for beam B3.

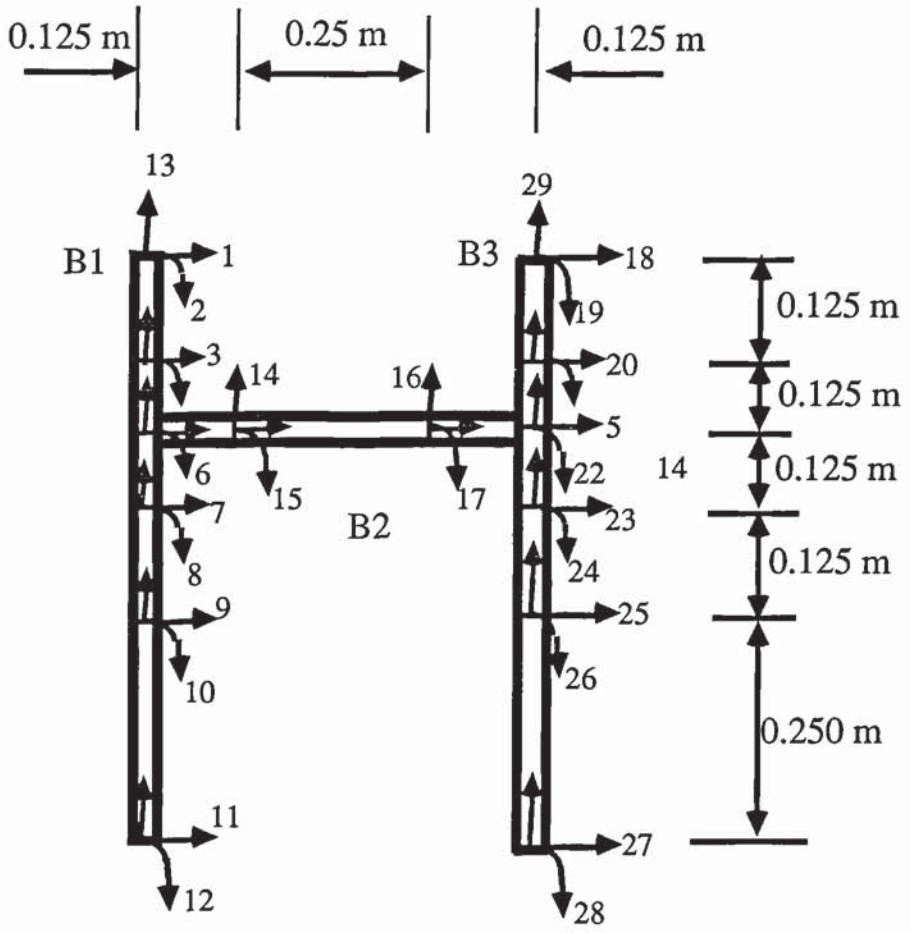

Fig 4.5 Analytical model of the H-frame (Case 2).

The analytical model has the same mass and flexural rigidity for the three beam members as in Case 1. Model parameters were updated using error-free simulated data of the system of fig 4.3, with the same mass additions as in Case 1 (mass addition at coordinates 9 and 27 of the analytical model, fig 4.5). The simulated and analytical natural frequencies are shown in table 4.7. The analytical natural frequencies are slightly different from the previous case due

to the difference in the number of DOF and the elements division. Dividing the beams into elements according to fig 4.5 is considered to be much closer to what one will naturally attempt to do in order to model the joints than it is in the first case (fig 4.4).

Added mass (kg)	Mass addition coordinate (fig 4.3)	Simulated natural frequencies (Hz)			Analytical natural frequencies (Hz)		
		Mode 1	Mode 2	Mode 3	Mode 1	Mode 2	Mode 3
0	-	41.71	89.74	193.46	43.09	92.83	207.88
0.25	5	40.82	89.45	193.46	42.12	92.44	207.84
	22	38.56	85.92	189.85	39.88	89.13	200.76
0.35	5	40.49	89.34	193.46	41.77	92.31	207.89
	22	37.57	84.93	188.84	38.88	88.17	198.86

TABLE 4.7 Simulated and analytical natural frequencies of the H-frame (Case2).

The updated parameters after one iteration were:

$EI_1 = 6191$ Nm^2 $\quad$ $EI_2 = 3083$ Nm^2

$EI_3 = 4631$ Nm^2 $\quad$ $EI_4 = 3809$ Nm^2

$EI_5 = 6406$ Nm^2 $\quad$ $EI_6 = 4069$ Nm^2

$m_{u1} = 3.54$ kg/m $\quad$ $m_{u2} = 3.52$ kg/m

$m_{u3} = 2.81$ kg/m $\quad$ $m_{u4} = -0.025$ kg/m

$m_{u5} = 4.11$ kg/m $\quad$ $m_{u6} = 5.38$ kg/m.

The mass parameter of the central element in the cross-beam (m_{u4}) is negative. Further iteration was useless as more parameters and eigenvalues became negative. Incorrect structure of the model matrices results in difficulties in obtaining parameters without losing their physical meaning.

4.4 Damping.

The use of experimental data to update a finite element model may encounter some difficulties if damping is ignored. Real structures always contain some degree of damping. It is difficult to include damping in analytically derived models since the determination of reasonable damping coefficients, by theoretical considerations alone, is difficult. In many cases, damping is ignored in analytical modelling. This may be justified for lightly damped structures. The updating of an undamped model, however, requires data for the undamped system. As real structures are always damped, the determination of an undamped modal model from data which involves damping is becoming an area of increasing importance in system identification. However, there is no reliable method which will accurately extract an undamped modal model directly from eigen-data measured on a system with non-proportional damping. A simple approach is to assume damping in structures is essentially proportional. If expressions of measured eigenvalues and eigenvectors are given by:

$$\lambda_{j,Measured} = \omega_j^2(1 + j\eta_j) \tag{4.1}$$

or

$$\lambda_{j,Measured} = \omega_j^2\left(-\xi_j + j\sqrt{1 - \xi_j^2}\right) \tag{4.2}$$

and

$$U_{j,Measured} = U_{j,Real} + jU_{j,Imag} \tag{4.3}$$

The eigenvalues and eigenvectors of the undamped system are approximated by (4.4), where the elements in U_j are taken to be of the same signs as the elements in $U_{j,Real}$.

$$\lambda_j = \omega_j^2, \qquad U_j = \sqrt{U_{j,Real}^2 + U_{j,Imag}^2} \tag{4.4}$$

Approximation (4.4) becomes exact if damping is "proportional". If damping is highly non-proportional, a significant error may result using the above approximation. In that case a damped model has to be identified. The discussion of damped models is covered in Chapter 6. This section investigates by numerical examples, the validity of approximation (4.4) in parameter estimation using the mass addition method. The investigation is based on a beam model with hysteretic damping.

EXAMPLE 4.4

A 10 DOF free beam of fig 4.2 was used to simulate a system with non-proportional damping. The system and its analytical model had the same number of DOF and therefore, only the effect of damping is investigated. Element damping proportional to the element stiffness matrix was assumed. The damping non-proportionality was simulated by using different proportionality constants for different elements. Thus, the following system parameters were assumed:

$$EI_1 = 5000(1 + j0.001)\ \text{Nm}^2 \qquad EI_2 = 5000(1 + j0.01)\ \text{Nm}^2$$
$$EI_3 = 5000(1 + j0.001)\ \text{Nm}^2 \qquad EI_4 = 5000(1 + j0.01)\ \text{Nm}^2$$
$$m_{u1} = m_{u2} = m_{u3} = m_{u4} = 3.5\ \text{kg/m}.$$

The eigenvalues and eigenvectors (translational coordinates only) for the first two elastic modes are:

$$\lambda_1 = 134.73^2(1 + j0.0055) \qquad \lambda_2 = 373.31^2(1 + j0.0055)$$

U_1	U_2
-1.0714 + j0.0006	-1.0811 - j0.0025
0.1063 - j0.0004	0.6345 + j0.0006
0.6512 - j0.0000	0.0000 + j0.0003
0.1053 + j0.0004	-0.6345 + j0.0006
-1.0714 - j0.0006	1.0811 - j0.0025

An undamped analytical model was assumed with parameters similar to the analytical model in example 4.1. That is:

$$EI_{1a} = EI_{2a} = 4600 \text{ Nm}^2, \quad EI_{3a} = 5300 \text{ Nm}^2, \quad EI_{4a} = 4800 \text{ Nm}^2,$$
$$m_{u1,a} = m_{u2,a} = 3.3 \text{ kg/m}, \quad m_{u3a} = m_{u4,a} = 3.7 \text{ kg/m}.$$
$$f_{1a} = 133.57 \text{ Hz}, \quad f_{2a} = 368.14 \text{ Hz}.$$

The analytical model parameters were updated using the simulated data for the damped system. Two updating studies were performed, using eigenvalues alone and using both eigenvalues and eigenvectors.

UPDATING USING EIGENVALUES.

In this study, masses of 0.25 kg and 0.35 kg were added in turn at coordinates 3 and 5. The eigenvalues of the first two elastic modes with each mass addition, together with the first two eigenvalues of the unperturbed beam, were used to simulate measured data. The damping factors of the perturbed beam varied between 0.0053 and 0.0055. The real parts of the simulated eigenvalues were taken to represent the estimated undamped eigenvalues. Table 4.8 shows the simulated natural frequencies and damping factors and the natural frequencies of the initial analytical model.

Added mass (kg)	Mass addition coordinate (fig 4.2)	Simulated natural frequencies (Hz) and damping factors (in brackets)		Analytical natural frequencies (Hz)	
		Mode 1	Mode 2	Mode 1	Mode 2
0	-	134.734 (0.0055)	373.305 (0.0055)	133.568	368.141
0.25	3	134.562 (0.0055)	357.170 (0.0053)	133.413	351.418
	5	128.496 (0.0055)	373.305 (0.0055)	127.403	368.114
0.35	3	134.502 (0.0055)	351.954 (0.0053)	133.359	346.061
	5	126.421 (0.0055)	373.305 (0.0055)	125.352	368.105

TABLE 4.8 Simulated natural frequencies and damping factors and the analytical natural frequencies.

The updated parameters, determined in 4 iterations using an unconstrained least squares optimization, are very close to the correct parameters as can be seen below:

Updated parameters:

$EI_1 = 5014\ \text{Nm}^2$ $EI_2 = 4999\ \text{Nm}^2$ $EI_3 = 5001\ \text{Nm}^2$

$EI_4 = 4986\ \text{Nm}^2$ $m_{u1} = 3.50\ \text{kg/m}$ $m_{u2} = 3.49\ \text{kg/m}$

$m_{u3} = 3.51\ \text{kg/m}$ $m_{u4} = 3.50\ \text{kg/m}$.

UPDATING USING EIGENVALUES AND EIGENVECTORS

A single mass of 0.35 kg was added at coordinates 3 and 5 in turn. Eigenvalues and eigenvectors of the first two elastic modes of the perturbed and unperturbed system were used in the updating process. The eigenvectors were

simulated to have been measured at coordinates 3 and 5 only. The real modes of the undamped system were estimated to be equal to the amplitudes of the complex eigenvectors of the simulated system. Table 4.9 shows the phase angles of the complex eigenvectors, the estimated mass-normalized real modes and mass-normalized modes of the undamped initial analytical model. The undamped eigenvalues of the simulated system were estimated by the real parts of the complex eigenvalues. The estimated undamped natural frequencies are therefore a subset of the natural frequencies given in table 4.8.

Parameter estimation was performed by an unconstrained least squares solution method without any weighting. It was found that parameters diverge to unacceptable values with some becoming negative after the first iteration. In this case, the problem was traced to the poor conditioning of the sensitivity matrix. The order of magnitude of the elements in the eigenvector sensitivity matrix is considerably smaller than that of eigenvalue sensitivity. As a result a square matrix $[\mathbf{J}^T\mathbf{J}]$, which has to be inverted in a least squares solution and

Mass addition coordinate (added mass 0.35 kg)	Measurement coordinate	Mass normalized eigenvector of the simulated system				Mass normalized eigenvector of the analytical model	
		Amplitude		Phase (degrees)			
		Mode 1	Mode 2	Mode 1	Mode 2	Mode 1	Mode 2
-	3	0.1063	0.6345	-0.23	0.06	0.1016	0.6525
	5	0.6512	0.0003	0.00	89.70	0.6501	0.0260
3	3	0.0925	-0.5289	-0.23	-179.95	0.0879	-0.5400
	5	0.6402	0.0984	0.00	-0.17	0.6394	0.0793
5	3	0.0405	0.6345	-0.56	0.05	0.0339	0.6480
	5	0.5590	0.0002	0.00	89.68	0.5581	0.0210

TABLE 4.9 Mass normalized eigenvectors of the simulated system and the analytical model.

which is given by the sum of $[\mathbf{J}_\lambda{}^T\mathbf{J}_\lambda]$ and $[\mathbf{J}_U{}^T\mathbf{J}_U]$, is dominated by the eigenvalue sensitivity data. As the total number of eigenvalues is smaller than the number of unknowns, the sensitivity matrix becomes poorly conditioned. Small errors in the measured data, for example those due to the estimation of the undamped modal model from a damped modal model, results in large unreasonable parameter changes.

This problem can be solved by scaling the sensitivity equations. Any form of scaling which result in the order of magnitude of the matrices $[\mathbf{J}_\lambda{}^T\mathbf{J}_\lambda]$ and $[\mathbf{J}_U{}^T\mathbf{J}_U]$ not to differ considerably should work. In this example, the sensitivity equations were scaled in a form consistent with the weighted least squares method, by assuming diagonal weighting matrices whose inverses consists of the variances of the eigenvalues and eigenvectors. This is equivalent to scaling each equation by the standard deviation of the eigen-data concerned. It was assumed that the estimated real modes and the undamped natural frequencies were accurate with confidence expressed by standard deviations of 0.01 and 1 Hz respectively. The values of the standard deviations were chosen to be as close as possible to some realistic orders of magnitude. Parameters updated using the scaled equations are very accurate. The result after 4 iterations is:

$EI_1 = 5009$ Nm^2	$EI_3 = 4966$ Nm^2	$EI_3 = 5037$ Nm^2
$EI_4 = 4991$ Nm^2	$m_{u1} = 3.49$ kg/m	$m_{u2} = 3.49$ kg/m
$m_{u3} = 3.51$ kg/m	$m_{u4} = 3.51$ kg/m	
$f_1 = 134.73$ Hz	$f_2 = 373.31$ Hz.	

EXAMPLE 4.5

The same beam of example 4.4 was analysed with an increased damping level. Thus, the following were used to simulate the complex stiffness (Nm^2) and

mass (kg/m) parameters with increased non-proportional damping,

$EI_1 = 5000(1 + j0.005)$ $EI_2 = 5000(1 + j0.2)$

$EI_3 = 5000(1 + j0.005)$ $EI_4 = 5000(1 + j0.1)$

$m_{u1} = m_{u2} = m_{u3} = m_{u4} = 3.5$

and result in (first two elastic modes):

$\lambda_1 = 135.36^2(1 + j0.096)$ $\lambda_2 = 374.09^2(1 + j0.085)$

U_1 (translational DOF)	U_2 (translational DOF)
-1.0699+j0.0156	-1.0842-j0.0469
0.1051-j0.0105	0.6340+j0.0062
0.6512-j0.0013	0.0033+j0.0173
0.1081+j0.0131	-0.6352+j0.0033
-1.0746-j0.0206	1.0791-j0.0334

Two updating studies were performed. Using eigenvalues alone, and using both eigenvalues and eigenvectors. The added mass, initial parameters and the measurement and perturbing coordinates in both cases were the same as in example 4.4. Table 4.10 shows the natural frequencies and damping factors of the simulated system. The natural frequencies were taken to represent the undamped natural frequencies of the system and were used to update the undamped analytical model. The analytical model's natural frequencies are the same as the ones given in table 4.8.

Added mass (kg)	Mass addition coordinate	Natural frequencies (Hz) and damping factors of the simulated system			
		Natural frequency		Damping factor η	
		Mode 1	Mode 2	Mode 1	Mode 2
0	-	135.37	374.09	0.096	0.085
0.25	3	135.20	357.97	0.097	0.083
	5	129.10	374.10	0.096	0.085
0.35	3	135.14	352.76	0.097	0.082
	5	127.01	374.10	0.097	0.085

TABLE 4.10 Natural frequencies and damping factors of the system simulated with a higher damping level.

The updated parameters, using eigenvalues alone, after 4 iterations, are:

$EI_1 = 5203$ Nm^2 $EI_2 = 5045$ Nm^2 $EI_3 = 5067$ Nm^2

$EI_4 = 4697$ Nm^2 $m_{u1} = 3.50$ kg/m $m_{u2} = 3.40$ kg/m

$m_{u3} = 3.59$ kg/m $m_{u4} = 3.51$ kg/m

$f_1 = 135.34$ Hz $f_2 = 373.94$ Hz.

When both eigenvalues and eigenvectors were used in the updating process, one mass of 0.35 kg was added at coordinates 3 and 5. The eigenvalues, in this case, are a subset of the eigenvalues shown in table 4.10. The mass-normalized eigenvectors of the simulated system are given in table 4.11. The corresponding eigenvectors of the undamped initial analytical model are the same as in example 4.4 and are given in table 4.9.

Mass addition coordinate (added mass 0.35 kg)	Measurement coordinate	Mass-normalized eigenvectors of the simulated system			
		Amplitude		Phase (degrees)	
		Mode 1	Mode 2	Mode 1	Mode 2
-	3	0.1057	0.6340	-5.72	0.56
	5	0.6512	0.0176	-0.11	79.07
3	3	0.0919	-0.5285	-5.67	-179.52
	5	0.6403	0.0965	0.00	-10.36
5	3	0.0406	0.6334	-13.52	0.30
	5	0.5589	0.0148	-0.09	79.10

TABLE 4.11 Mass-normalized eigenvectors (amplitude and phase) of the system simulated with a higher level of damping.

The updated parameters using eigenvalues and eigenvectors are less accurate as can be seen from tables 4.12 and 4.13.

	Iteration steps					
	0	1	2	3	4	5
EI_1	4600	5226	4834	4919	4919	4919
EI_2	4600	3479	3810	3810	3811	3811
EI_3	5300	7182	7739	7742	7744	7744
EI_4	4800	4345	4268	4279	4281	4281

TABLE 4.12 Convergence of the stiffness parameters.

	Iteration steps					
	0	1	2	3	4	5
m_{u1}	3.30	3.017	3.047	3.046	3.046	3.046
m_{u2}	3.30	3.238	3.262	3.259	3.259	3.259
m_{u3}	3.70	3.770	3.698	3.703	3.703	3.703
m_{u4}	3.70	4.163	4.202	4.189	4.192	4.192

TABLE 4.13 Convergence of the mass parameters.

The poor results in this case are due to the errors in the estimation of the real modes. From table 4.11 it can be seen that the mode shape displacement for the second mode at coordinate 5 is highly complex, with a phase angle of up to 79°. While the modal displacement of this coordinate was also complex in example 4.4 (table 4.9) with a phase angle of up to 89°, the amplitude in the former example was negligible. As coordinate 5 is close to the node of the second elastic mode of the undamped system, the error in the approximation of the real mode to be given by the amplitude of the complex mode (which is very small in example 4.4) is also negligible. In example 4.5 coordinate 5 has an amplitude which is not negligible, as a result the approximation of the real mode by the amplitude of the complex mode shape displacement introduces errors. Table 4.14 shows the errors in the estimation of the undamped natural frequencies for example 4.5. The errors in the estimation of the real modes are given in table 4.15. It can be seen that the errors in the real modes are very small except coordinate 5 which has relatively large errors.

Added mass (kg)	Mass addition coordinate	Estimated undamped natural frequency (Hz)		Error in the estimated natural frequency f_{est}-f_{exact}(Hz)	
		Mode 1	Mode 2	Mode 1	Mode 2
-	-	135.37	374.09	0.64	0.78
0.25	3	135.20	357.97	0.64	0.80
	5	129.10	374.10	0.61	0.79
0.35	3	135.14	352.76	0.64	0.81
	5	127.01	374.10	0.60	0.80

TABLE 4.14 Errors in the estimated undamped natural frequencies of the simulated beam

Mass added (0.35 kg) coordinate	Measurement coordinate	Estimated real modes (Mass-normalized)		Error in the estimated real modes U_{est}- U_{exact}	
		Mode 1	Mode 2	Mode 1	Mode 2
0	3	0.1057	0.6340	-0.0007	-0.0005
	5	0.6512	0.0176	-0.0001	0.0176
3	3	0.0910	-0.5285	-0.0006	0.0004
	5	0.6403	0.0965	0.0001	-0.0019
5	3	0.0406	0.6334	0.0001	-0.0011
	5	0.5589	0.0148	0.0000	0.0148

TABLE 4.15 Errors in the estimated real modes of the simulated beam.

4.5 Experimental errors in the measured data.

Measured data is inevitably contaminated by measurement errors. In order to reliably estimate parameters of a mathematical model using measured data, it is logical that experimental errors should be accounted for, using a statistically based parameter estimation algorithm. The simplest method of dealing with

errors is the use of a weighted least squares solution method. If an estimate of the variance of errors in the experimental data is made, a weighting matrix **W** can be defined as an inverse of a diagonal variance matrix. The weighted least squares solution for the parameter changes on the current analytical model is given by:

$$\Delta s = \left[\mathbf{J}_\lambda^T \mathbf{W}_\lambda \mathbf{J}_\lambda\right]^{-1} \mathbf{J}_\lambda^T \mathbf{W}_\lambda \{\Delta\lambda\} \tag{4.5}$$

or

$$\Delta s = \left[\begin{bmatrix}\mathbf{J}_\lambda \\ \mathbf{J}_U\end{bmatrix}^T \mathbf{W}_{\lambda,U} \begin{bmatrix}\mathbf{J}_\lambda \\ \mathbf{J}_U\end{bmatrix}\right]^{-1} \begin{bmatrix}\mathbf{J}_\lambda \\ \mathbf{J}_U\end{bmatrix}^T \mathbf{W}_{\lambda,U} \begin{Bmatrix}\Delta\lambda \\ \Delta U\end{Bmatrix} \tag{4.6}$$

The choice of (4.5) or (4.6) depends on whether eigenvalues alone or both eigenvalues and eigenvectors are used in the updating process.

If errors in the measured eigen-data are random quantities with an expected mean of zero, the weighted least squares solution yields statistically unbiased parameter estimates. In practice, systematic biased errors may be present in addition to the random errors, for example due to changes in the sensitivity of the accelerometer. It is rather difficult both to estimate the contribution of the systematic errors in the measured eigen-data and to remove its effect in the parameter estimation process. Most published literature uses statistical methods on the assumption that the error in each measured data is a random quantity with a mean of zero. This assumption will be used in this work.

It should be noted that the weighted least squares solution is statistically unbiased. This implies, the result obtained approaches the correct solution as the data sample approaches infinity. In practice, measured data is finite and the estimated solution will therefore deviate from the correct solution by an amount which depends on the data sample used. Inspection of (4.5) and (4.6)

suggests that the deviation of the estimated parameters from the correct solution is also influenced by the conditioning of one of the following matrices, depending on whether eigenvalues alone or both eigenvalues and eigenvectors are used:

$$\left[\mathbf{J}_\lambda{}^T \mathbf{W}_\lambda \mathbf{J}_\lambda\right] \quad \text{and} \quad \left[\begin{bmatrix}\mathbf{J}_\lambda \\ \mathbf{J}_U\end{bmatrix}^T \mathbf{W}_{\lambda,U} \begin{bmatrix}\mathbf{J}_\lambda \\ \mathbf{J}_U\end{bmatrix}\right]$$

Thus, while the above matrices may not be rank deficient and a correct solution could be identified using error-free data, large deviation in the parameters is possible if contaminated data is used. Such a case is most likely to occur if the eigen-data used is relatively insensitive to changes in some parameters as compared to others. This fact is illustrated by the following examples:

EXAMPLE 4.6

A FE model of an 8 elements cantilever beam with 16 DOF, fig 4.6, was updated using eigenvalues and eigenvectors contaminated with measurement errors. The beam is 1m long and the elements are 0.125 m each. The following parameters were used to simulate the system, where element number one is at the fixed end.

$EI_1 = \ldots\ldots = EI_8 = 6666\ \text{Nm}^2$

$m_{u1} = \ldots\ldots = m_{u8} = 7.85\ \text{kg/m}.$

$f_1 = 16.31\ \text{Hz}$ $\qquad f_2 = 102.20\ \text{Hz}$ $\qquad f_3 = 286.32\ \text{Hz}.$

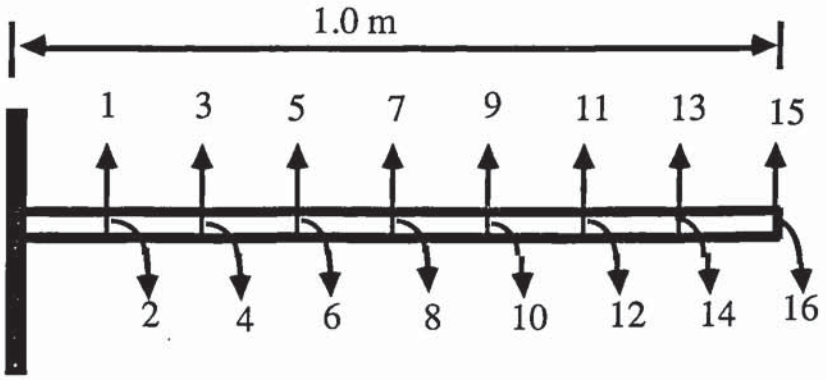

Fig 4.6 Cantilever beam

The initial analytical model was assumed with the following parameters:

$EI_{1a} = \ldots\ldots = EI_{8a} = 7300\ \text{Nm}^2$

$m_{u1,a} = \ldots\ldots = m_{u8,a} = 7.0\ \text{kg/m}$

$f_{1a} = 18.07\ \text{Hz}$ $\quad f_{2a} = 113.26\ \text{Hz}$ $\quad f_{3a} = 317.29\ \text{Hz}.$

The analytical model was updated by adding a single mass of 0.5 kg at three coordinates and using both eigenvalues and eigenvectors of the first three modes in the updating process. The eigenvectors were simulated to have been measured at 6 translational coordinates. These are:

Measurement coordinates:	1, 3, 5, 7, 9, 11.
Mass addition coordinates:	3, 7, 11.

The natural frequencies of the simulated beam and the analytical model, before and after mass addition, are shown in table 4.16. The eigenvectors are not shown for brevity. To simulate the contaminated measured data, random errors with expected means of zero and standard deviations of 0.25 Hz and 0.01 were generated and added to the natural frequencies and the mass-normalized eigenvectors respectively.

Added mass (kg)	Mass addition coordinate	Error-free natural frequencies of the beam (Hz)			Analytical natural frequencies (Hz)		
		Mode 1	Mode 2	Mode 3	Mode 1	Mode 2	Mode 3
-	-	16.31	102.20	286.32	18.07	113.26	317.29
0.5	3	16.29	99.96	269.05	18.05	110.48	296.10
0.5	7	16.07	96.29	286.30	17.78	106.01	317.28
0.5	11	15.46	101.99	275.49	17.05	112.99	304.05

TABLE 4.16 Simulated and analytical natural frequencies of the 8 elements beam with and without mass addition.

The parameters were updated using the weighted least squares solution method. Standard deviations of 0.25 Hz and 0.01 were also used for the natural frequencies and eigenvectors respectively, in the computation of the variances and the eigen-data weighting matrix, $\mathbf{W}_{\lambda,U}$. With error-free data, the updated parameters converged to correct values. However, using the contaminated data, the first iteration result in a negative mass and stiffness parameters for elements 1 and 8 respectively, table 4.17. Further iteration with negative mass is meaningless as the eigenvalues becomes negative.

	Element number (Number 1 at fixed end)							
	1	2	3	4	5	6	7	8
EI	6507	7161	6884	6549	7961	4513	11924	-89708
m_u	-17.1	8.8	9.8	3.7	14.1	1.1	11.9	6.5

TABLE 4.17 Mass (kg/m) and Stiffness (Nm^2) parameters of the 8 elements cantilever beam after the first iteration.

The same analytical model is now updated by stiffness addition. With stiffness addition large natural frequency changes are possible, and this has an effect of improving the conditioning of the sensitivity matrix. There is no guarantee, however, that the improvements will be adequate to facilitate a reasonable solution using the weighted least squares method. Consider a stiffness of 10^6 N/m added at the same coordinates as with mass addition. The error-free natural frequencies of the simulated beam and the analytical model are shown in table 4.18.

Consider the updating using eigenvectors and eigenvalues, where the eigenvectors are measured at the same coordinates as in the mass addition case. Random errors with expected means of zero and standard deviations of 0.25 Hz and 0.01 are added to the natural frequencies and eigenvectors respectively, to simulate the measured data. The same standard deviations are used to formulate the weighting matrices. With error-free data, the weighted least squares solution converged to correct parameters. With the contaminated data, the first iteration result in parameters with a negative mass, table 4.19.

Added stiffness (N/m)	Stiffness addition coordinate	Error-free natural frequencies of the simulated beam (Hz)			Analytical natural frequencies (Hz)		
		Mode 1	Mode 2	Mode 3	Mode 1	Mode 2	Mode 3
-	-	16.31	102.20	286.32	18.07	113.26	317.29
10^6	3	18.91	111.65	297.92	20.78	122.94	329.06
10^6	7	33.55	132.06	286.33	36.45	143.71	317.30
10^6	11	72.38	104.25	294.18	77.28	115.21	325.23

TABLE 4.18 Simulated and analytical natural frequencies of the 8 elements beam with and without added stiffness.

	Element number (Number 1 at fixed end)							
	1	2	3	4	5	6	7	8
EI	6647	6636	7214	5917	7691	5837	7520	-12536
m_u	-29.2	13.9	6.14	7.0	9.6	5.7	9.0	7.4

TABLE 4.19 Mass (kg/m) and Stiffness (Nm^2) parameters of the cantilever beam after the first iteration (updated by stiffness addition).

This example has demonstrated the difficulties in using the weighted least squares solution method, with data contaminated with measurement errors. In this example the beam element at the free end undergoes, relatively, little flexure and the element at the fixed end undergoes little displacements for the modes used in the updating. The eigen-data is less sensitive to the stiffness changes of elements undergoing little flexure and to the mass parameter of elements with little displacements. With measurement errors, such parameters are liable to unexpectedly large deviations from their initial estimates although error-free data could result in correct parameters. The use of large stiffness additions results in large perturbations in the eigen-data as can be seen by comparing table 4.16 with table 4.18. This is useful in improving the conditioning of the sensitivity matrix but does not guarantee a meaningful parameter convergence.

If the beam is to be tested in a free-free configuration, better results should be expected as most elements undergoes flexure and displacements comparable to other elements. The stiffness parameter of elements at the free ends, however, have less flexure and are expected to be identified less accurately than other parameters. This is illustrated by the following example.

EXAMPLE 4.7

The beam of example 4.6 (fig 4.6) is now to be simulated in a free-free configuration and updated by mass addition. The parameters of the simulated beam and its initial analytical model are the same as in example 4.6 and result in the following natural frequencies (Hz) for the first three elastic modes:

Correct system:	$f_1 = 103.77$	$f_2 = 286.20$	$f_3 = 561.92$
Initial model:	$f_{1a} = 115.00$	$f_{2a} = 317.16$	$f_{3a} = 622.71$

The perturbing mass, perturbing points and measurement points are the same as in example 4.6. Using the same standard deviations for the simulated errors in the natural frequencies and eigenvectors as in example 4.6 (0.25 Hz and 0.01 respectively) and the same weighting matrices, the parameters converged to physically meaningful values (table 4.20). However, stiffness parameters of the elements at the free ends are the least accurate. The updated model has reproduced, with an acceptable accuracy, the following natural frequencies (Hz) of the first three elastic modes:

Updated model:	$f_1 = 103.94$	$f_2 = 286.36$	$f_3 = 561.91$

	Element number (Number 1 at the LHS)							
	1	2	3	4	5	6	7	8
EI	4842	6962	6114	6811	6585	7456	6759	3494
m_u	7.63	8.02	7.51	8.11	7.21	8.41	6.30	8.45

TABLE 4.20 The updated mass (kg/m) and stiffness (Nm^2) parameters of the free beam after 6 iterations.

4.6 The need for updating by optimization with constraints on the parameters

While an exact solution for the mass and stiffness parameters can easily be identified, using error-free eigen-data, if the structure of the model matrices is exact, practical parameter updating faces a number of difficulties. These difficulties arise from one or a combination of the following factors.

(i) Incompatibility in the number of DOF between the idealized model and the system.

(ii) Inaccuracy in the structure of the mathematical model.

(iii) Incompatibility between the undamped FE model and data from a system with some degree of non-proportional damping.

(iv) Experimental errors in the measured data.

This Chapter has demonstrated the vulnerability of the ordinary least squares and the weighted least squares to estimate parameters in practical conditions, where the preceding factors are usually present.

Generally, the difficulties due to the incompatibility in the number of DOF between the model and a real system, with an infinite number of DOF, can practically be avoided by increasing the degree of discretization of the FE model with respect to the highest frequency used in the updating process.

The problem of updating an undamped FE model using data from a system with some degree of non-proportional damping is usually not so important if

damping has a relatively low level of non-proportionality. With phase angles of within 10^o of 0^o or 180^o, the undamped natural frequencies and real modes can be approximated using (4.4) because the errors involved in the approximation are small and can be ignored.

If the structure of the model matrices is not correct, unexpectedly large changes in the parameters are likely to occur. This is also the case when the data is contaminated with measurement noise. The deviation of a parameter from its correct value is influenced by the sensitivity of the data to changes in such a parameter. As a result, stiffness parameters of elements undergoing relatively little flexure and mass parameters of elements with relatively little displacements tend to have poor convergence. In some simple cases, it is possible to select a test configuration where there is no parameter of which the eigen-data is relatively insensitive to. In many cases this may not be possible and unrealistic parameters are likely to result if an unconstrained least squares solution method is used. Generally, the weighted least squares method is not a suitable solution method as there is no control on the changes in the parameters. For realistic parameter estimates, it is important to introduce a constraint which inhibits unrealistic parameter estimates. Since in many cases, parameters of an initial analytical model are reasonably good initial estimates, a minimum cost Bayesian approach will be used, incorporating confidence on the initial estimates in a diagonal weighting matrix.

4.7 Parameter updating using a minimum cost Bayesian approach.

4.7.1 Theoretical derivation.

Consider a matrix equation $\mathbf{G}x = b$, where b is an observation vector contaminated by random errors and a solution for the vector x is sought. We can use

the weighted least squares solution method to find an estimate x_{est} such that when x_{est} is substituted for x, the sum of squares of the weighted difference between the elements in the resulting vector and the corresponding elements in vector b is the least. That is, find x such that (4.7) is minimized.

$$\{\mathbf{G}x - b\}^T\mathbf{W}\{\mathbf{G}x - b\} \tag{4.7}$$

Minimization of (4.7) is achieved by differentiation with respect to the unknown, x, and set the result to zero.

$$\frac{\partial}{\partial x}\left(\{\mathbf{G}x - b\}^T\mathbf{W}\{\mathbf{G}x - b\}\right) = 0 \tag{4.8}$$

This results in x_{est} as a solution of (4.8) and is given by:

$$x_{est} = \left[\mathbf{G}^T\mathbf{W}\mathbf{G}\right]^{-1}\mathbf{G}^T\mathbf{W}b \tag{4.9}$$

In our case of parameter estimation by eigenvalue and eigenvector sensitivity analysis, x, b, **W** and **G** are given by:

$$x = s - s_{ca} = \Delta s, \qquad \mathbf{W} = \mathbf{W}_{\lambda,U}$$

$$b = \begin{Bmatrix} \Delta\lambda \\ \Delta U \end{Bmatrix}$$

$$\mathbf{G} = \begin{bmatrix} \mathbf{J}_\lambda \\ \mathbf{J}_U \end{bmatrix}$$

Parameter updates on the current analytical model is therefore given by:

$$\Delta s = \left[\begin{bmatrix} J_\lambda \\ J_U \end{bmatrix}^T W_{\lambda,U} \begin{bmatrix} J_\lambda \\ J_U \end{bmatrix} \right]^{-1} \begin{bmatrix} J_\lambda \\ J_U \end{bmatrix}^T W_{\lambda,U} \begin{Bmatrix} \Delta\lambda \\ \Delta U \end{Bmatrix} \tag{4.10}$$

Equation (4.10) is an expression for the weighted least squares solution of parameter changes on the current parameter vector, s_{ca}. We now introduce a constraint that the updated parameter estimates, s_{est} should be close to the analytical estimates, s_a, of the initial analytical model in a weighted least squares sense. The initial parameter estimates are treated as independent quantities with random errors with zero mean. That is:

$$\text{Expected value of } \{s - s_a\} = 0 \tag{4.11}$$

As a result of (4.11), equation (4.12) is introduced and simultaneously solved with the equation $\mathbf{G}x = b$.

$$[\mathbf{I}]\{s - s_a\} = \{0\} \tag{4.12}$$

But $x = s - s_{ca} = \Delta s$. Therefore $\{s - s_a\} = \{s_{ca} + \Delta s - s_a\}$

Equation (4.12) can therefore be written as:

$$[\mathbf{I}]\{s_{ca} + \Delta s - s_a\} = \{0\}$$
$$[\mathbf{I}]\{\Delta s\} = \{s_a - s_{ca}\} \tag{4.13}$$

The combined matrix equation which is to be solved by a least squares method becomes:

$$\left[\mathbf{I} \quad [J_\lambda]^T \quad [J_U]^T \right]^T \{\Delta s\} = \begin{Bmatrix} s_a - s_{ca} \\ \Delta\lambda \\ \Delta U \end{Bmatrix} \tag{4.14}$$

If $\mathbf{W}_a$ and $\mathbf{W}_{\lambda,U}$ are the weighting matrices on the initial parameter estimates, s_a, and measured eigen-data respectively, the weighted least squares solution of (4.14) is given by:

$$\Delta s = \left(\begin{bmatrix} \mathbf{J}_\lambda \\ \mathbf{J}_U \end{bmatrix}^T \mathbf{W}_{\lambda,U} \begin{bmatrix} \mathbf{J}_\lambda \\ \mathbf{J}_U \end{bmatrix} + [\mathbf{I}]^T \mathbf{W}_a [\mathbf{I}] \right)^{-1} \left\{ \begin{bmatrix} \mathbf{J}_\lambda \\ \mathbf{J}_U \end{bmatrix}^T \mathbf{W}_{\lambda,U} \begin{Bmatrix} \Delta\lambda \\ \Delta U \end{Bmatrix} + [\mathbf{I}]^T \mathbf{W}_a \{ s_a - s_{ca} \} \right\}$$

$$\Delta s = \left(\begin{bmatrix} \mathbf{J}_\lambda \\ \mathbf{J}_U \end{bmatrix}^T \mathbf{W}_{\lambda,U} \begin{bmatrix} \mathbf{J}_\lambda \\ \mathbf{J}_U \end{bmatrix} + \mathbf{W}_a \right)^{-1} \left\{ \begin{bmatrix} \mathbf{J}_\lambda \\ \mathbf{J}_U \end{bmatrix}^T \mathbf{W}_{\lambda,U} \begin{Bmatrix} \Delta\lambda \\ \Delta U \end{Bmatrix} + \mathbf{W}_a \{ s_a - s_{ca} \} \right\} \qquad (4.15)$$

If $\mathbf{W}_a$ and $\mathbf{W}_{\lambda,U}$ are diagonal matrices and the errors on the right-hand-side vector of (4.14), which consist of the errors in s_a, λ and U, are not correlated, (4.15) is an unbiased estimator. Equation (4.15) is also an expression of the minimum cost estimator of which the cost function (4.16) is minimum for all possible s:

$$\{ s - s_a \}^T \mathbf{W}_a \{ s - s_a \} + \begin{Bmatrix} \lambda_e - \lambda \\ U_e - U \end{Bmatrix}^T \mathbf{W}_{\lambda,U} \begin{Bmatrix} \lambda_e - \lambda \\ U_e - U \end{Bmatrix} \qquad (4.16)$$

The derivation of (4.15) is similar to that used by Collins *et al* (1972) to derive a minimum cost Bayesian estimator which includes a constraint of minimum changes on the parameters of the current analytical model. The main difference is, in this work a constraint of minimum changes on the parameters of the initial analytical model is used rather than on the parameters of the current analytical model. This has been preferred so as to ensure an unbiased estimator since the errors in the parameters after the first iteration are correlated with the errors in the measured λ and U. Hence the final equation, (4.15), is slightly different from that given by Collins *et al*. The algorithm for parameter updating has been implemented in a computer program, written in

MATLAB language, and its listing is given in appendix B.

4.7.2 Numerical examples

EXAMPLE 4.8

The 8 elements cantilever beam of example 4.6 (fig 4.6) was to be updated in the presence of experimental errors using the minimum cost estimator. Updating was performed by stiffness addition and using both eigenvalues and eigenvectors where the first three modes were taken to have been measured. Simulated parameters, initial model parameters, added stiffness measurement and stiffness addition coordinates were the same as in example 4.6.

To simulate the experimental errors, random errors with zero mean and standard deviations of 0.25 Hz and 0.01 were added to the natural frequencies and the mode shape data respectively. These standard deviations were also used in the computation of a diagonal weighting matrix, $\mathbf{W}_{\lambda,U}$, and are the same as in example 4.6.

The initial parameters were treated as independent quantities with random errors and their confidence was expressed by estimates of their standard deviations. The parameters and their standard deviations, for all elements, are:

$$EI_a = 7300 \text{ Nm}^2, \quad \text{STD} = 800 \text{ Nm}^2$$
$$m_{ua} = 7.0 \text{ kg/m}, \quad \text{STD} = 1 \text{ kg/m}.$$

Table 4.21 shows the updated parameters after 4 iterations. The convergence of the parameters as percentage changes from their initial estimates is shown in figs 4.7 to 4.10. This example is essentially similar to example 4.6 with the

exception that the Bayesian approach is now used. The minimum cost Bayesian estimator has resulted in physically more meaningful parameters. The first three natural frequencies have been accurately reproduced:

Simulated (error-free): $f_1 = 16.31$ Hz $f_2 = 102.20$ Hz $f_3 = 286.32$ Hz

Analytical model: $f_{1a} = 18.07$ Hz $f_{2a} = 113.26$ Hz $f_{3a} = 317.29$ Hz

Updated model: $f_1 = 16.31$ Hz $f_2 = 102.25$ Hz $f_3 = 286.52$ Hz

	Element number (Number 1 at fixed end)							
	1	2	3	4	5	6	7	8
EI	6646	6480	7254	6587	6618	7031	6782	7228
m_u	7.11	7.99	8.28	7.39	7.81	8.54	7.11	8.17

TABLE 4.21 Mass (kg/m) and stiffness (Nm^2) parameters of the 8 elements cantilever beam using the minimum cost estimator after 4 iterations.

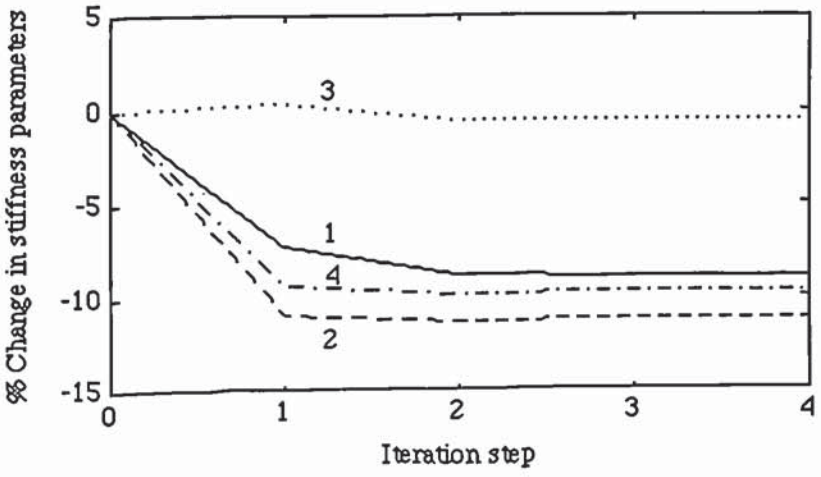

Fig 4.7 Convergence of the stiffness parameters of elements 1 to 4 of the cantilever beam.

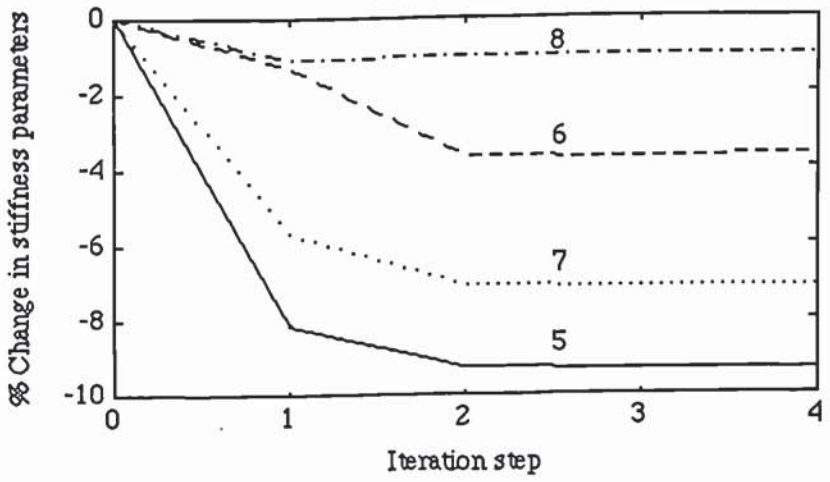

Fig 4.8 Convergence of the stiffness parameters of elements 5 to 8 of the cantilever beam.

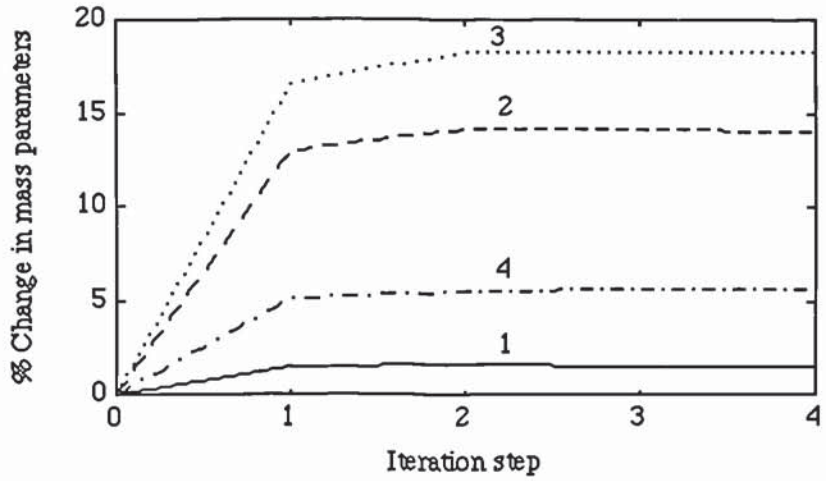

Fig 4.9 Convergence of the mass parameters of elements 1 to 4 of the cantilever beam.

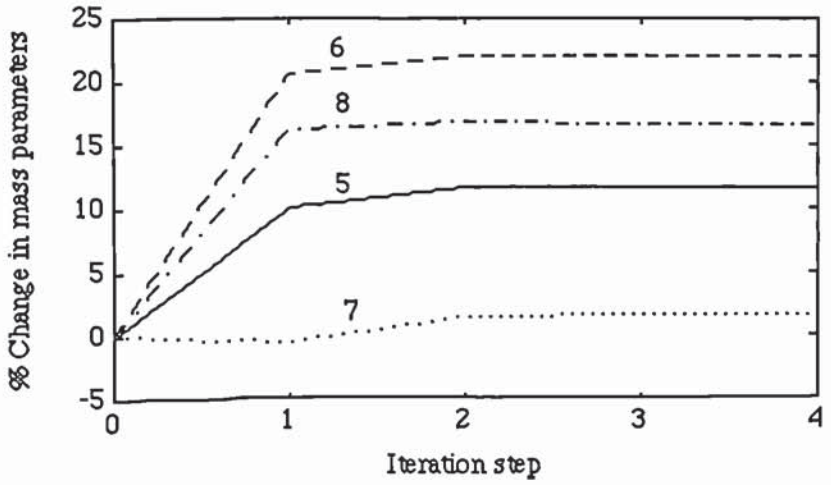

Fig 4.10 Convergence of the mass parameters of elements 5 to 8 of the cantilever beam.

EXAMPLE 4.9

A plane frame, fig 4.11, is made of 6 beam members denoted by B1 . . B6. The frame was modelled by a 22 DOF FE model in a free-free configuration as shown. Only motion in the plane of the frame was considered. The frame was simulated using the following data:

Parameter	Beam member					
	B1	B2	B3	B4	B5	B6
EI (Nm^2)	21333	9000	21333	5208	5208	14292
EA (N)	$1.6x10^8$	$1.2x10^8$	$1.6x10^8$	$1.0x10^8$	$1.0x10^8$	$1.4x10^8$
m_u (kg/m)	6.28	4.71	6.28	3.93	3.93	5.5

TABLE 4.22 Parameters of the simulated frame.

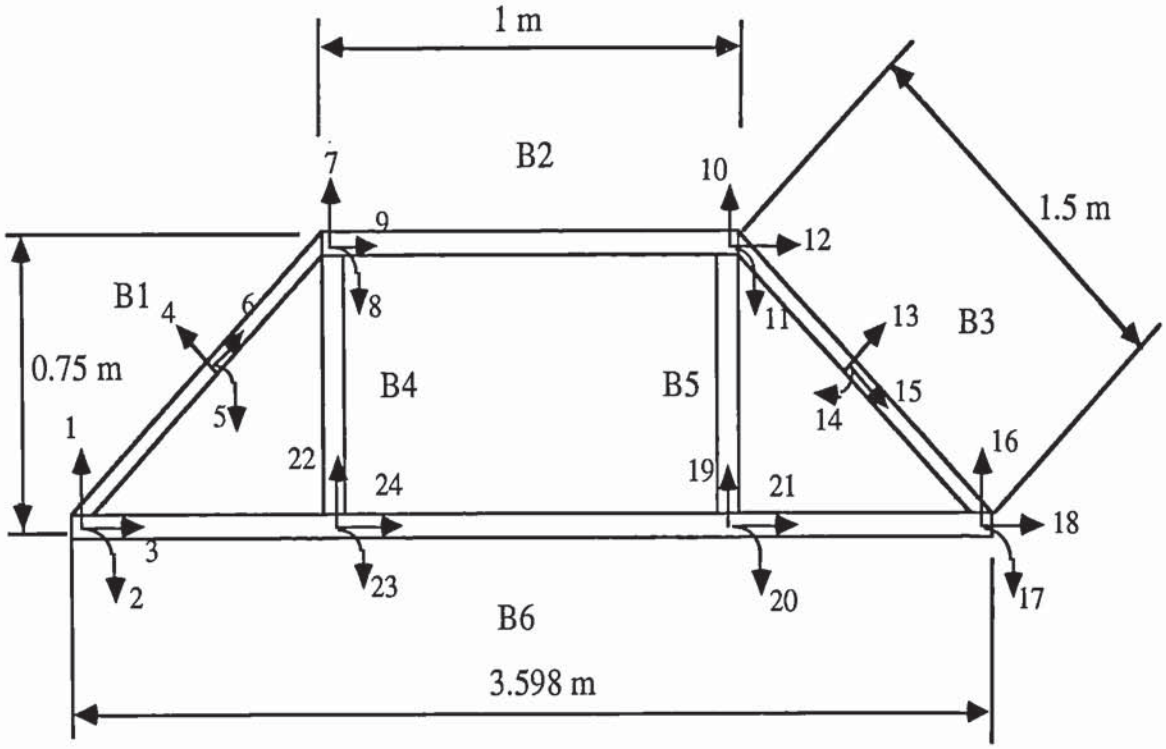

Fig 4.11 Plane frame example: Free-free configuration.

The simulated frame (22 DOF) had the following natural frequencies for the first three elastic modes:

$$\text{System } f \text{ (Hz)}: \quad f_1 = 34.98 \qquad f_2 = 62.24 \qquad f_3 = 83.56.$$

The initial analytical model had the same number of DOF as the simulated frame and was constructed using the parameters shown in table 4.23 which result in the following natural frequencies:

$$\text{Analytical } f_a \text{ (Hz)}: f_{1a} = 36.36 \quad f_{2a} = 66.16 \qquad f_{3a} = 88.26$$

The flexural rigidity and mass per unit length of all beam members of the analytical model were set to be different from their correct values whereas axial flexibility, which has very little influence on the dynamic characteristics

of the first three modes, was unchanged and not updated.

Parameter	Beam member					
	B1	B2	B3	B4	B5	B6
EI_a(Nm^2)	25000	10000	19000	4800	4900	18000
EA_a (N)	1.6x10^8	1.2x10^8	1.6x10^8	1.0x10^8	1.0x10^8	1.4x10^8
$m_{u,a}$(kg/m)	6.0	4.0	5.5	4.5	4.5	6.0

TABLE 4.23 Parameters of the initial analytical model (FE model).

The analytical model of the frame was updated by mass addition using eigenvalues alone and using both eigenvalues and eigenvectors. The updating was performed using the minimum cost estimator. In both cases the following standard deviations for the weighting matrix $\mathbf{W}_a$ of the initial estimates were assumed.

	Beam member					
	B1	B2	B3	B4	B5	B6
STDEI_a(Nm^2)	5000	2500	5000	500	500	2500
STD$m_{u\,a}$(kg/m)	0.5	0.5	0.5	0.5	0.5	0.5

TABLE 4.24 Assumed standard deviations of the initial parameter estimates.

Masses of 0.35 kg and 0.5 kg were simulated to be added at coordinates 4, 13, 19 and 22 of the free-free frame, fig 4.11. Each mass addition involved adding a single mass to a single coordinate, compute the eigenvalues and remove the mass. In each case, only the first three elastic modes were taken to have been measured. The perturbations were also performed on the analytical model and result in a total of 27 eigenvalue sensitivity equations with 12 parameters to update. Table 4.25 shows the natural frequencies of the simulated frame and the analytical model.

Added mass (kg)	Mass addition coordinate	Natural frequencies (Hz) of the simulated frame			Natural frequencies (Hz) of the analytical model		
		Mode 1	Mode 2	Mode 3	Mode 1	Mode 2	Mode 3
0	-	34.98	62.24	83.56	36.36	66.16	88.26
0.35	4	34.92	61.32	82.34	36.31	65.27	86.75
	13	34.92	61.32	82.34	36.29	64.85	86.90
	19	34.83	62.17	83.37	36.22	66.06	88.09
	22	34.83	62.17	83.37	36.22	66.10	88.03
0.5	4	34.89	60.92	81.88	36.28	64.89	86.18
	13	34.89	60.92	81.88	36.26	64.30	86.41
	19	34.77	62.14	83.28	36.16	66.02	88.03
	22	34.77	62.14	83.28	36.16	66.07	87.94

TABLE 4.25 Simulated and analytical natural frequencies of the plane frame.

To simulate the contaminated measured data, random errors with zero mean and standard deviation of 0.5 Hz were added to the natural frequencies. The same standard deviation was used in the computation of the weighting matrix $\mathbf{W}_\lambda$. The parameters were updated using the minimum cost Bayesian estimator using the contaminated eigenvalues. The result, after 4 iterations, is given in

table 4.26. The convergence of the stiffness and mass parameters is shown in figs 4.12 and 4.13 respectively. The updated model has natural frequencies, which are close to the natural frequencies of the simulated system.

System f (Hz):	$f_1 = 34.98$	$f_2 = 62.24$	$f_3 = 83.56.$
Analytical f_a(Hz):	$f_{1a} = 36.36$	$f_{2a} = 66.16$	$f_{3a} = 88.26$
Updated f (Hz):	$f_1 = 34.89$	$f_2 = 62.62$	$f_3 = 83.37$

Updated Parameter	Beam member					
	B1	B2	B3	B4	B5	B6
EI (Nm^2)	22127	9463	18242	4270	4777	16641
m_u (kg/m)	6.30	4.13	5.84	4.54	4.49	6.03

TABLE 4.26 The updated parameters of the Plane frame using eigenvalues.

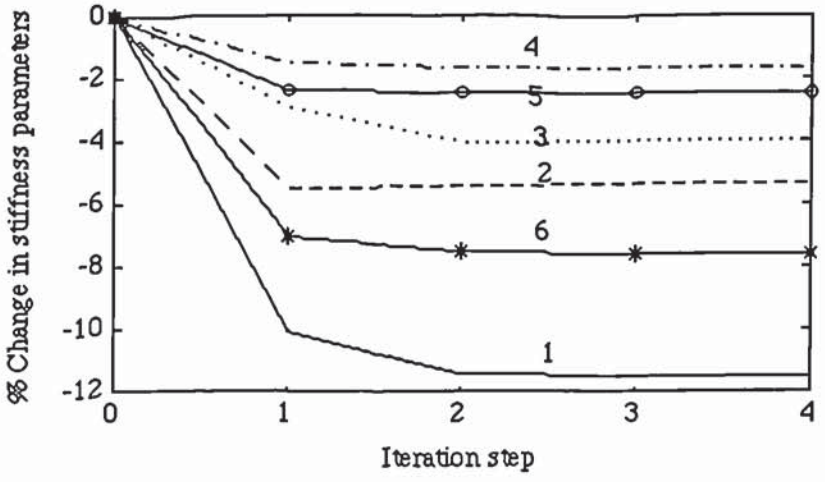

Fig 4.12 Convergence of the stiffness parameters of the plane frame.

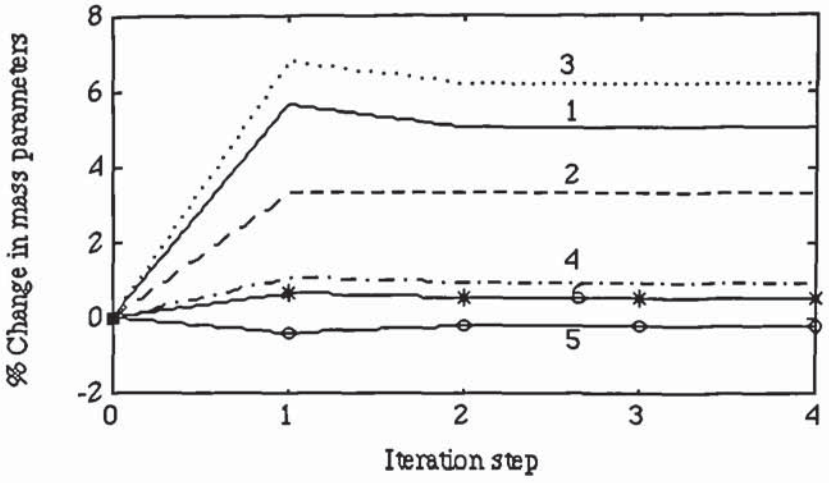

Fig 4.13 Convergence of the mass parameters of the plane frame.

UPDATING USING BOTH EIGENVALUES AND EIGENVECTORS.

Masses of 0.35 kg and 0.5 kg were simulated to be added in turn at each of coordinates 4 and 13 of the free frame. The first three elastic mode shapes and natural frequencies of the frame with and without added mass were taken to have been measured. The same masses were also added to the analytical model. A total of 15 mode shapes, measured at 4 coordinates, and 15 natural frequencies were obtained. For brevity, only the mode shape data of the unperturbed frame is shown, table 4.27. The natural frequencies are a subset of the natural frequencies shown in table 4.25. To simulate the contaminated measured data, random errors with zero mean and standard deviations of 0.5 Hz and 0.02 were added to the natural frequencies and the mode shape data respectively. The same standard deviations were used in the formulation of the weighting matrix $\mathbf{W}_{\lambda,U}$. The parameters were updated using the minimum cost Bayesian estimator, using both eigenvalues and eigenvectors. The updated parameters, in 3 iterations, are shown in table 4.28. Figs 4.14 and 4.15 shows the convergence of the parameters in the 3 iterations.

	Mass-normalized modes of the simulated frame			Mass-normalized modes of the analytical model		
Coordinate	Mode 1	Mode 2	Mode 3	Mode 1	Mode 2	Mode 3
4	0.0962	0.2914	0.3041	0.0939	0.2738	0.3251
13	-0.0962	0.2914	-0.3041	-0.1069	0.3367	-0.3148
19	-0.1550	-0.0837	0.1177	-0.1504	-0.0929	0.1033
22	0.1550	-0.0837	-0.1177	0.1519	-0.0724	-0.1221

TABLE 4.27 Mass-normalized mode shapes of the simulated frame and the analytical model at the measurement coordinates.

System f (Hz): $f_1 = 34.98$ $f_2 = 62.24$ $f_3 = 83.56$.
Analytical f_a (Hz): $f_{1a} = 36.36$ $f_{2a} = 66.16$ $f_{3a} = 88.26$
Updated f (Hz): $f_1 = 34.86$ $f_2 = 62.52$ $f_3 = 83.25$

Updated Parameter	Beam member					
	B1	B2	B3	B4	B5	B6
EI (Nm^2)	19586	10721	19613	4712	5060	14974
m_u (kg/m)	6.22	3.67	6.05	4.03	4.50	6.16

TABLE 4.28 The updated parameters using eigenvalues and eigenvectors.

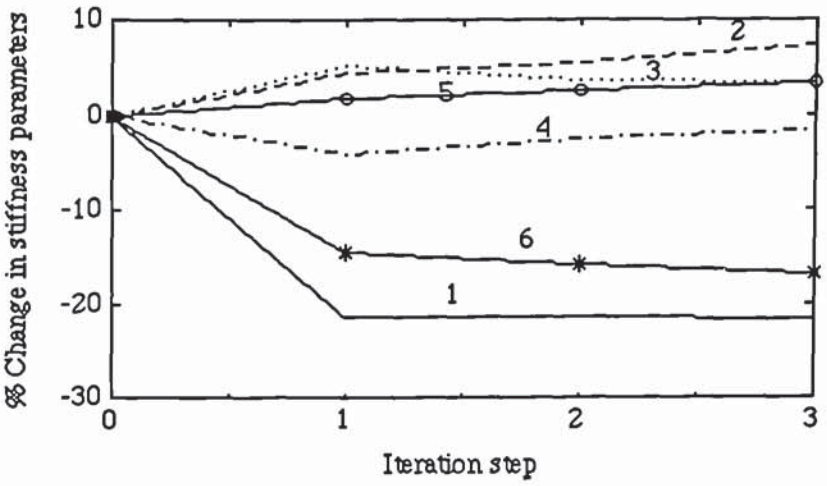

Fig 4.14 Convergence of the stiffness parameters of the plane frame in the 3 iterations, using eigenvalues and eigenvectors.

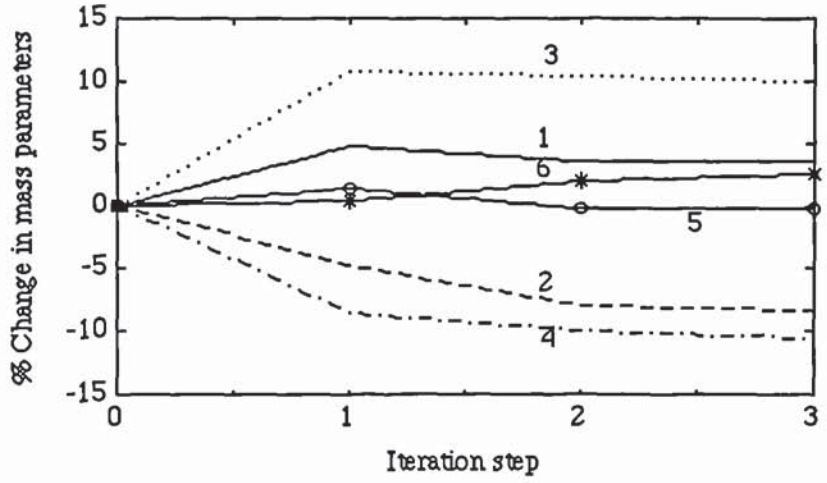

Fig 4.15 Convergence of the mass parameters of the plane plane frame in the 3 iterations, using eigenvalues and eigenvectors.

COMPARING RECEPTANCE PREDICTION.

The updated models using eigenvalues and using both eigenvalues and eigenvectors are each tested for the prediction of the FRF of the unmeasured coordinates in an untested configuration. The test is performed by comparing receptance prediction of a fixed-fixed frame between the simulated system, initial model and updated model. The fixed-fixed configuration is shown in fig 4.16.

Coordinate 13 of the fixed-fixed frame is assumed to be excited. Rotational and translational receptances at coordinates 5 and 4 are compared in figs 4.17 and 4.18 respectively for the updating case using eigenvalues alone. Figs 4.19 and 4.20 compares the receptances for the updating case using both eigenvalues and eigenvectors. The receptances are given in deciBels where 0 dB represents 1 m/N (reference receptance 1 m/N). The results shows the capability of the updated models to predict the dynamic behaviour in the untested configuration and unmeasured coordinates over a larger frequency range than the one used in the updating process, if the structure of the model matrices is correct.

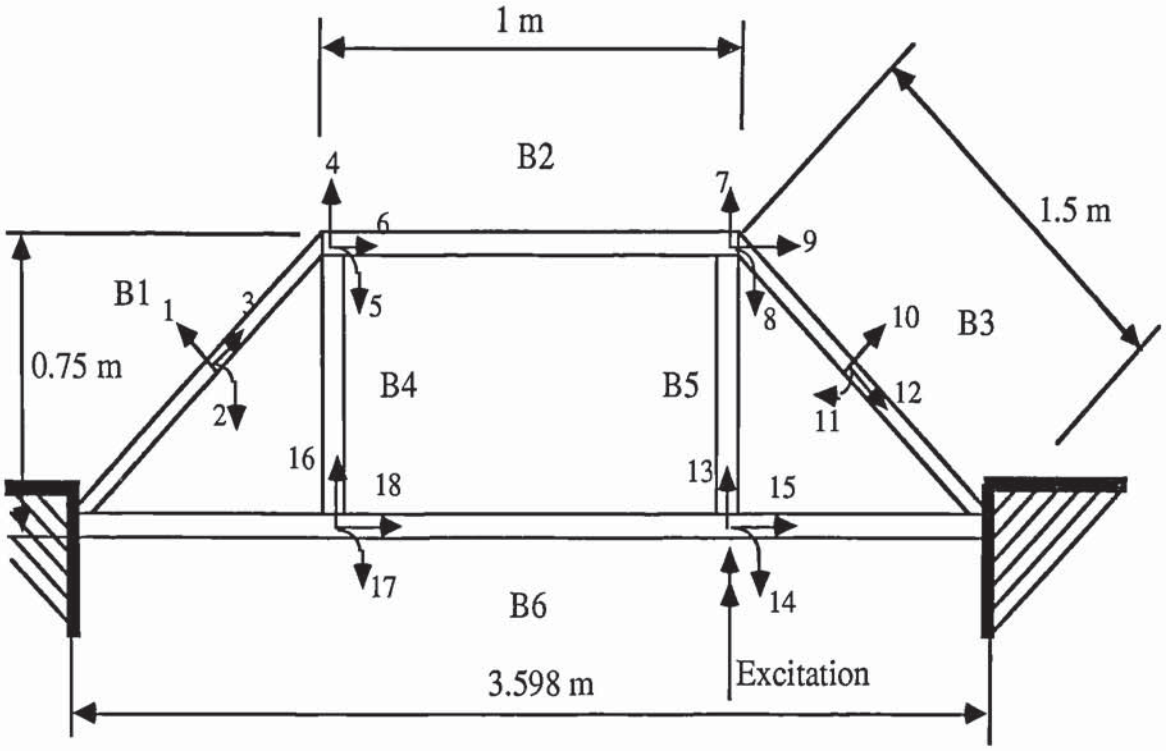

Fig 4.16 Plane frame example: Fixed-fixed configuration.

Correct model ____ , Initial model - - - , Updated model (using eigenvalues alone) ****

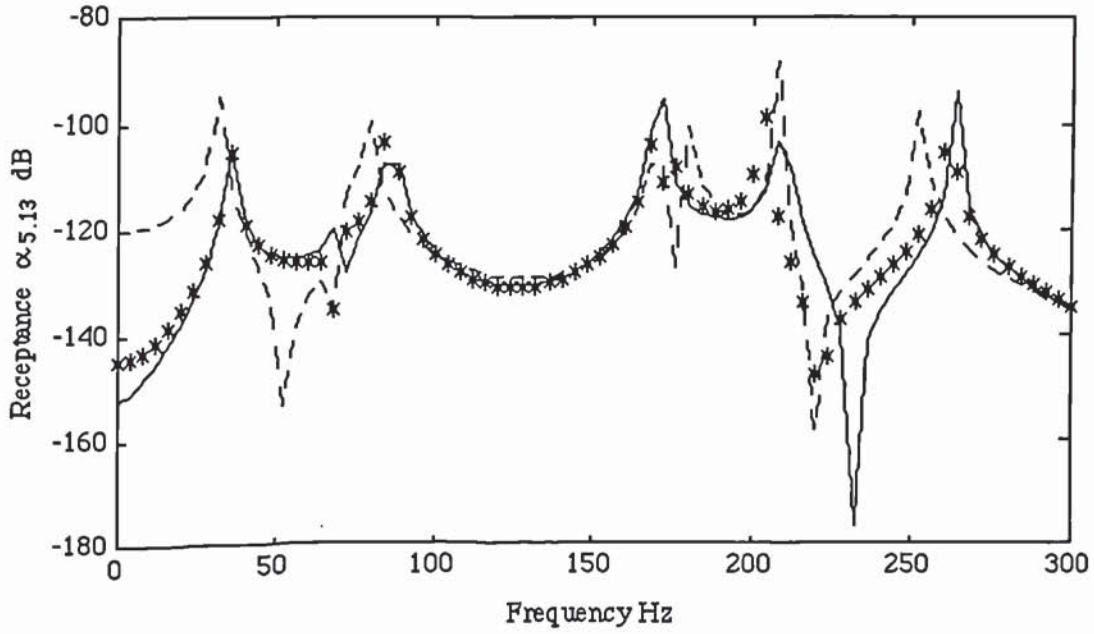

Fig 4.17 Receptance prediction at coordinate 5 of the fixed frame.

Correct model ____ , Initial model - - - , Updated model (using eigenvalues alone) ****

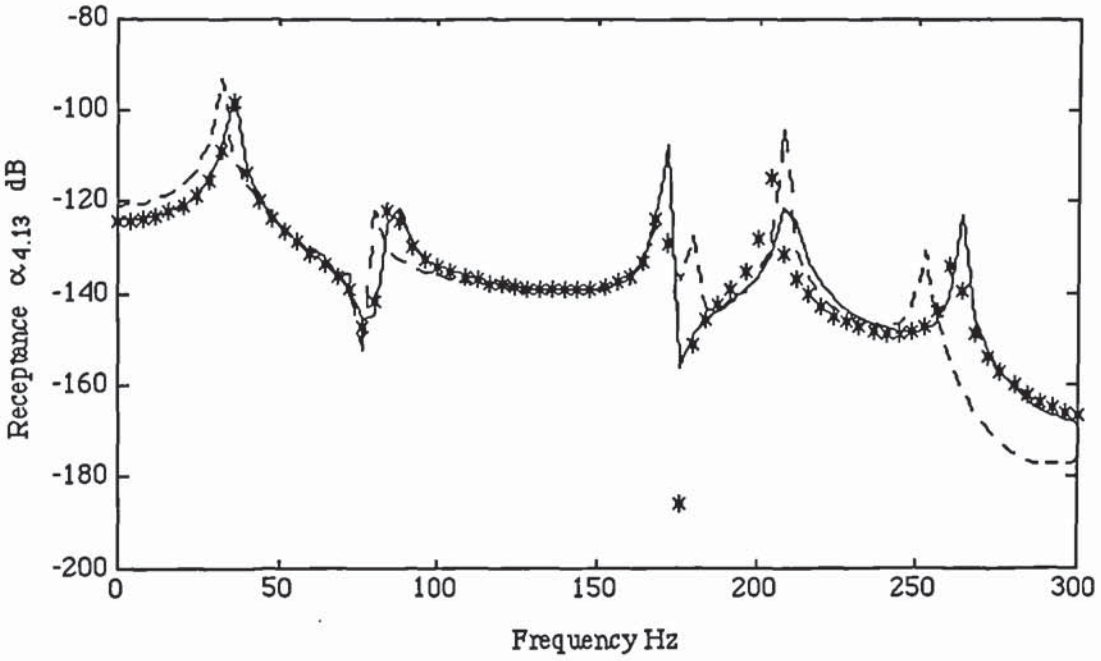

Fig 4.18 Receptance prediction at coordinate 4 of the fixed frame.

Correct model ___ , Initial model - - - , Updated model (eigenvalues and eigenvectors) ***

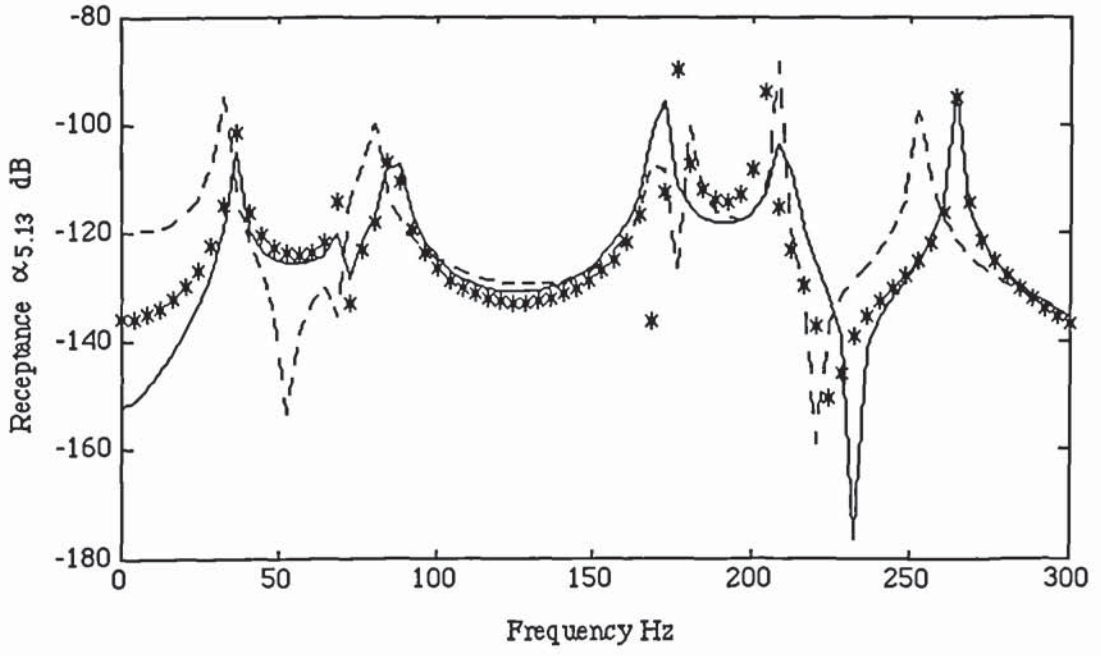

Fig 4.19 Receptance prediction at coordinate 5 of the fixed frame.

Correct model ___ , Initial model - - - , Updated model (eigenvalues and eigenvectors) ***

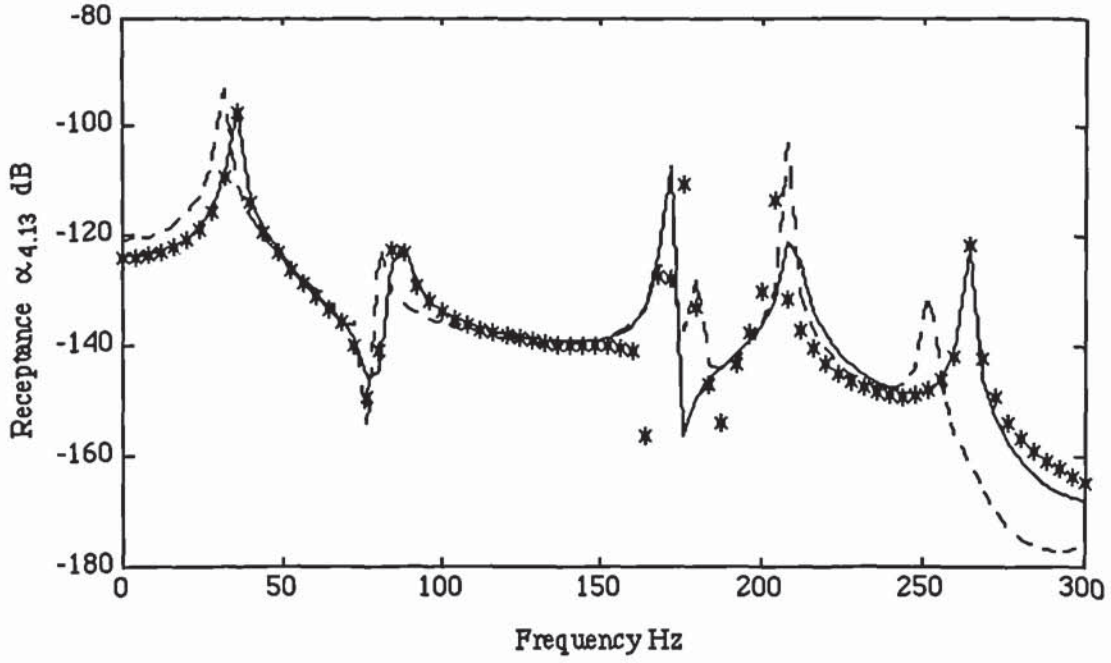

Fig 4.20 Receptance prediction at coordinate 4 of the fixed frame.

In the plane frame example, unrealistic large changes in the parameters from their initial estimates due to the presence of measurement errors, have been avoided by the use of the minimum cost Bayesian estimator. The updated parameters retain their physical significance although there are variations from the correct mass and stiffness parameters. Some parameters are more accurate than their initial estimates whereas some are less accurate, with variations comparable to the level of the uncertainty expressed in the initial parameters. The dynamic behaviour of the updated model, however, is more accurate than the initial model. The updated model could reasonably reproduce the FRFs of the unmeasured coordinates in a configuration different from the test (simulated) configuration. The frequency range of agreement between the updated model and the simulated system is much larger than the frequency range used in the updating process.

The plane frame example has dealt with the case where the structure of the model matrices is correct. In practice the structure of the model matrices may not be exact due to, for example, difficulties in the modelling of joints or errors involved in discretizing a system with an infinite number of DOF. While small discrepancies in the model structure could be tolerated, large discrepancies will introduce unexpectedly large changes in the updated parameters from their initial estimates. The minimum cost Bayesian estimator, which has proved useful in minimizing parameter changes due to measurement errors, may also be helpful in minimizing parameter changes due to possible inaccuracies in the model structure. The following examples explores this possibility using a simulated damped beam and the H-frame of example 4.3.

EXAMPLE 4.10

The 16 elements, 34 DOF free beam of example 4.1 (fig 4.1), was then simulated with damping. The undamped mass and stiffness matrices had identical data to the one simulated in example 4.1. Damping was simulated by a hysteretic damping matrix which formed the imaginary part of the complex stiffness matrix. The complex stiffness matrix was simulated by assuming the stiffness parameters of elements 5, 6, 9,10, 15 and 16, where element numbers starts from the left-hand-side of the beam, to be complex and given by:

$$EI = 5000(1 + j0.1)\ \mathrm{Nm}^2$$

The rest of the element parameters were real. With these simulated parameters, the eigenvalues for the first and second elastic modes are as follow:

$$\lambda_1 = 134.75^2(1 + j0.045) \qquad \lambda_2 = 371.44^2(1 + j0.034)$$

The phase angles of the translational coordinates are given in table 4.29. It can be seen that the phase angles are very close to the in-phase or out-of-phase condition with the exception of the second mode at coordinate 17. This coordinate is at the node of the undamped system and its mode shape amplitude, for the second mode, is very small. From the phase angle information, the complex mode shapes are very close to real modes. Thus, the natural frequencies of the simulated system can be treated as the undamped natural frequencies and can be used to update an undamped model.

The undamped analytical model of the beam was formulated using 8 FE with a total of 18 DOF. It was assumed that the beam was made of 4 sections which may be of different structural characteristics. Each section was 0.25 m long and consists of 2 elements of identical mass and stiffness parameters, fig 4.21.

Coordinate	Phase angle (degrees)	
	Mode 1	Mode 2
1	-0.06	0.09
3	-0.09	-0.04
5	-0.13	-1.54
7	-0.11	179.93
9	179.15	179.34
11	179.49	179.14
13	179.84	179.80
15	-179.97	-178.63
17	179.89	-93.79
19	179.79	-2.34
21	-179.95	-0.59
23	-179.39	0.41
25	-177.77	0.98
27	-1.00	1.58
29	-0.02	176.09
31	0.20	-179.68
33	0.28	-179.59

TABLE 4.29 Phase angles of the simulated 16 elements beam of fig 4.1.

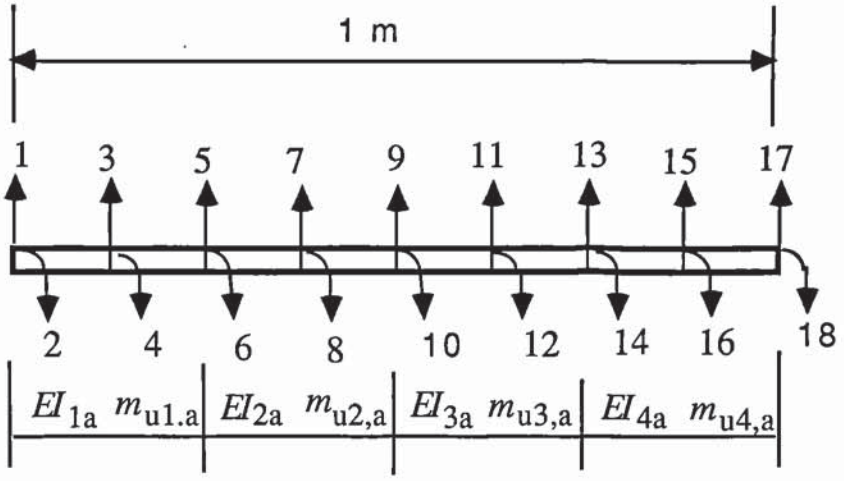

Fig 4.21 An 8 elements analytical model.

The following parameters were assumed for the initial analytical model. The analytical natural frequencies of the first two elastic modes are also given.

$EI_{1a} = 4800\ \text{Nm}^2$ $EI_{2a} = 4800\ \text{Nm}^2$

$EI_{3a} = 5200\ \text{Nm}^2$ $EI_{4a} = 5100\ \text{Nm}^2$

$m_{u1,a} = m_{u2,a} = m_{u3,a} = m_{u4,a} = 3.4\ \text{kg/m}.$

$f_{1a} = 136.38\ \text{Hz}$ $f_{2a} = 375.92\ \text{Hz}.$

The confidence in the analytical model parameters was expressed by the following estimates of their standard deviations:

$\text{STD}\ EI_a = 150\ \text{Nm}^2,\ \text{STD}\ m_{ua} = 0.15\ \text{kg/m}$ for all elements.

The analytical model was updated using eigenvalues of the first two elastic modes, by adding masses of 0.25 kg and 0.35 kg to the system, fig 4.1, in turn at coordinates 9 and 17. The analytical model was also perturbed at the corresponding coordinates (coordinates 5 and 9, fig 4.21). A total of 10 eigenvalue sensitivity equations were generated. Table 4.30 shows the

damping factors and error-free natural frequencies of the simulated and the analytical models with added mass.

		Simulated system				Analytical model	
Added mass (kg)	Coordinate (fig 4.1)	Natural frequency (Hz) f_1	f_2	Damping factor (x0.01) η_1	η_2	Natural frequency (Hz) f_{1a}	f_{2a}
0.25	9	134.58	355.79	4.55	3.58	136.18	359.30
0.25	17	128.54	371.45	4.57	3.40	129.94	375.90
0.35	9	134.52	350.69	4.55	3.63	136.11	353.94
0.35	17	126.47	371.45	4.58	3.40	127.80	375.90

TABLE 4.30 Natural frequencies and damping factors of the simulated beam and the analytical model (undamped) with added mass.

To simulate measured natural frequencies with measurement errors, random errors each with an expected mean of zero and standard deviation of 0.5 Hz were added to the natural frequencies of the simulated beam with and without added mass. The contaminated natural frequencies of the damped 16 elements simulated beam were treated as measured natural frequencies and were used to update the 8 elements undamped analytical model. The updating was performed using the minimum cost Bayesian estimator which, after 4 iterations, resulted in the following parameter:

$EI_1 = 4730$ Nm2 $\quad EI_2 = 4761$ Nm2

$EI_3 = 5154$ Nm2 $\quad EI_4 = 5061$ Nm2

$m_{u1} = 3.46$ kg/m $\quad m_{u2} = 3.40$ kg/m

$m_{u3} = 3.47$ kg/m $\quad m_{u4} = 3.44$ kg/m

$f_1 = 134.9$ Hz $\quad f_2 = 371.8$ Hz.

Figs 4.22 and 4.23 shows the convergence of the stiffness and mass parameters as percentage changes from their initial estimates.

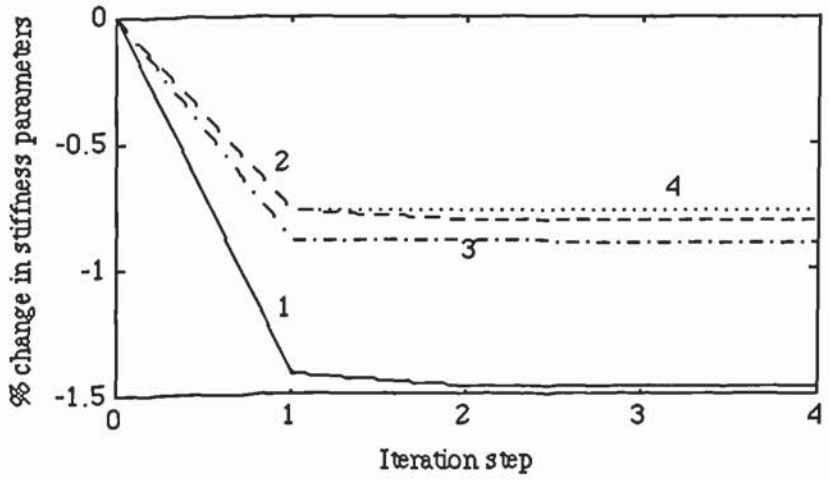

Fig 4.22 Convergence of the stiffness parameters.

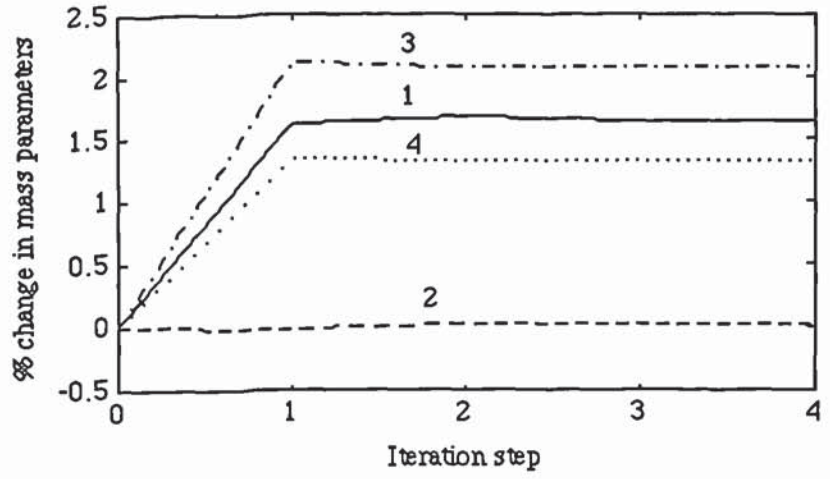

Fig 4.23 Convergence of the mass parameters.

The updated model could reproduce accurately the FRF of the undamped system, but may not be able to reproduce the FRF of the damped system since the damping matrix has not been identified, and the level of damping is not so low to be neglected. The updated model could only reproduce the FRF of the

damped system if damping was of low magnitude. For example, lets compare the point receptance between the updated model (18 DOF) and the simulated damped system (34 DOF) at coordinate 5 of the updated model. The comparison is shown in fig 4.24.

Damped system (34DOF) __ , Initial model(18DOF) - - -, Updated model (18DOF) __ . __ .

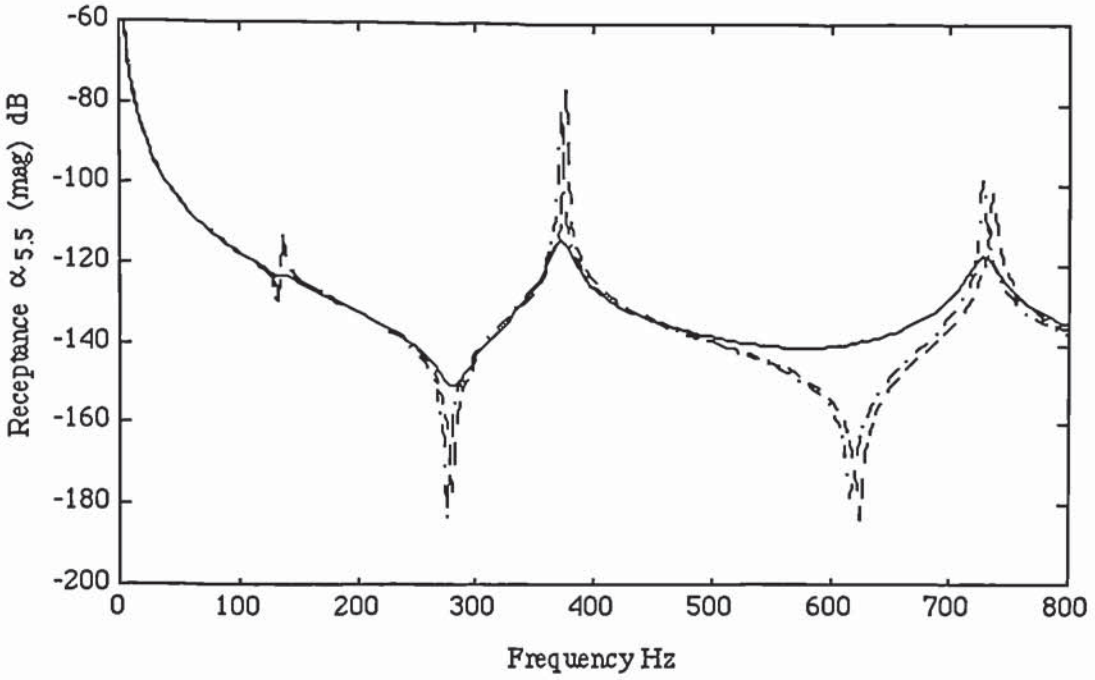

Fig 4.24 Comparing the FRF of the updated undamped 18 DOF model to that of the damped 34 DOF system.

Now compare the FRF of the updated model with that of a system with light damping (of the order of $\eta = 0.01$). The lightly damped model, in this case, is obtained by reducing the simulated damping matrix by a factor of 3 and result in the following damping factors.

$$\eta_1 = 0.0152 \qquad \eta_2 = 0.0114 \qquad \eta_3 = 0.0086 \qquad \eta_4 = 0.0097.$$

Figs 4.25 show the point receptance at coordinate 5 of the updated model, as

compared to the lightly damped 16 elements system (34 DOF).

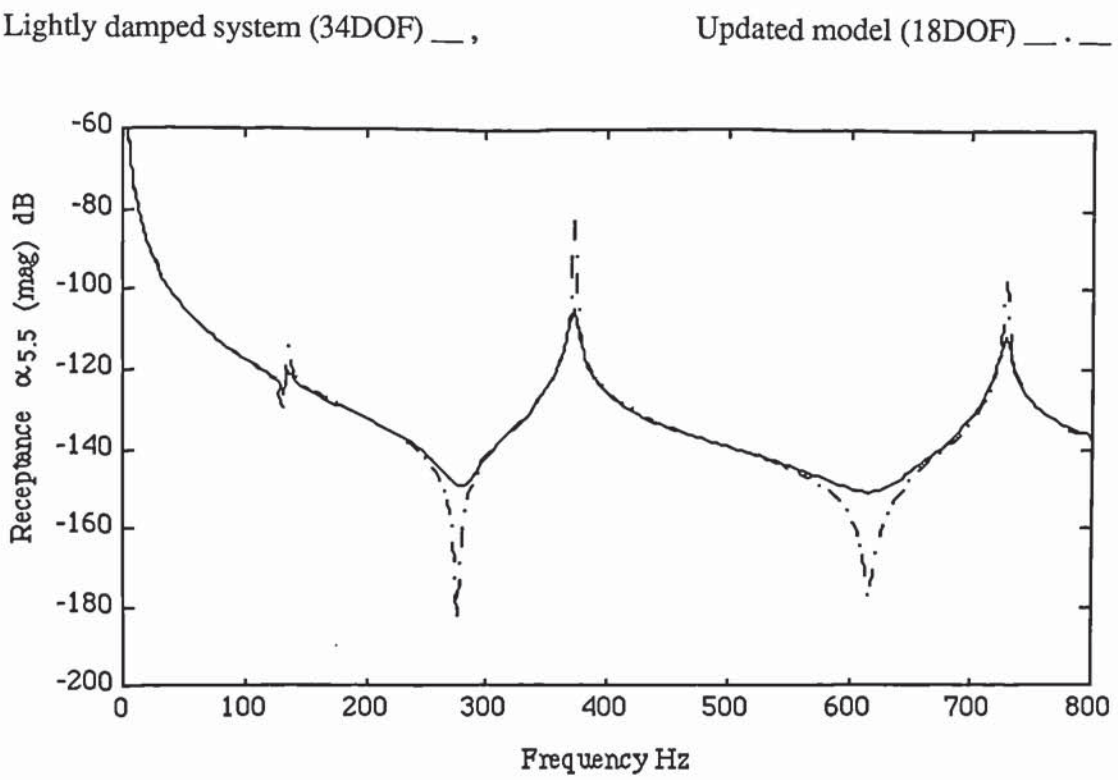

Fig 4.25 Comparing the FRF of the updated undamped 18 DOF model to that of a lightly damped 34 DOF system.

Example 4.10 has demonstrated the application of the minimum cost Bayesian estimator in parameter estimation of an undamped model using data from a damped system. The simulated data was contaminated by measurement errors and the model structure was not exact. The minimum cost Bayesian estimator has prevented large unrealistic parameter changes from their initial estimates. The simulated natural frequencies of the beam have been reproduced with good accuracy. However, the FRF of the simulated system was not accurately reproduced because the damping level was high and the damping model was not identified. The updated model only reproduced accurately the FRF of a lightly damped system. In this example, although the model structure was not exact, the degree of discretization for the frequency range of interest was

sufficiently high. Thus, the slight incompatibility between the analytical model structure and the simulated system was tolerable and the changes in the parameters from their initial estimates were comparable to the order of uncertainty specified in the initial estimates.

EXAMPLE 4.11

The H-frame simulated with non-perfectly rigid joints in example 4.3 (fig 4.3), is idealized by a FE model with rigid joints and whose elements division is shown in fig 4.5. The flexibility of the joints is due to the simulated translational and rotational lumped stiffness shown. The frame parameters and natural frequencies are the same as in example 4.3. The initial analytical model is identical to the one used in Case 2 of example 4.3. The analytical model is now updated using the minimum cost estimator, using eigenvalues alone, by adding masses of 0.25 kg and 0.35 kg in turn at coordinates 5 and 22 of the simulated frame (fig 4.3). The analytical model is also perturbed at its corresponding coordinates (coordinates 9 and 27 in fig 4.5). Only error-free eigenvalues of the first three elastic modes are considered to have been measured in each perturbation. Parameter updating in this example is similar to Case 2 of example 4.3, with the exception that the minimum cost estimator is now used. The natural frequencies of the simulated frame and the analytical model are the same as in example 4.3 and are shown in table 4.7. The confidence in the initial parameter estimates is given by the following assumed standard deviations.

$$\text{STD } EI_{1a} = \text{STD } EI_{2a} = 300 \text{ Nm}^2$$
$$\text{STD } EI_{3a} = \text{STD } EI_{4a} = 200 \text{ Nm}^2$$
$$\text{STD } EI_{5a} = \text{STD } EI_{6a} = 150 \text{ Nm}^2$$
$$\text{STD } m_{u1,a} = \text{STD } m_{u2,a} = 0.2 \text{ kg/m}$$

$$\text{STD } m_{u3,a} = \text{STD } m_{u,4a} = 0.05 \text{ kg/m}$$
$$\text{STD m}_{u5,a} = \text{STD } m_{u6,a} = 0.15 \text{ kg/m.}$$

Measurement errors are not simulated and therefore the eigenvalues are accurate. However, they are treated as measured data which may be contaminated by measurement errors. Their confidence is expressed by a standard deviation of 0.5 Hz in the natural frequencies. The parameters updated in 5 iterations are:

$EI_1 = 5123 \text{ Nm}^2$	$EI_2 = 4413 \text{ Nm}^2$
$EI_3 = 4629 \text{ Nm}^2$	$EI_4 = 4422 \text{ Nm}^2$
$EI_5 = 5827 \text{ Nm}^2$	$EI_6 = 5826 \text{ Nm}^2$
$m_{u1} = 3.920$ kg/m	$m_{u2} = 3.344$ kg/m
$m_{u3} = 3.097$ kg/m	$m_{u4} = 3.106$ kg/m
$m_{u5} = 4.264$ kg/m	$m_{u6} = 4.180$ kg/m

Natural frequencies of the first three elastic modes are shown below:

System f (Hz):	$f_1 = 41.71$	$f_2 = 89.74$	$f_3 = 193.46$
Initial model f_a (Hz):	$f_{1a} = 43.09$	$f_{2a} = 92.84$	$f_{3a} = 208.19$
Updated model f (Hz):	$f_1 = 41.51$	$f_2 = 89.61$	$f_3 = 194.00$

Figs 4.26 and 4.27 shows the convergence of the stiffness and mass parameters as percentage changes from their initial estimates at each iteration step. It can be seen that the large changes in the parameters in example 4.3 have now been prevented by the minimum cost estimator. However, the relative magnitudes of the parameters of different elements is different from their actual mass and stiffness distribution. Furthermore, unlike in example 4.10, the changes in some parameters are much larger than the specified uncertainty of the initial

estimates. This is due to the large mismatch between the structure of the idealized model and the simulated system.

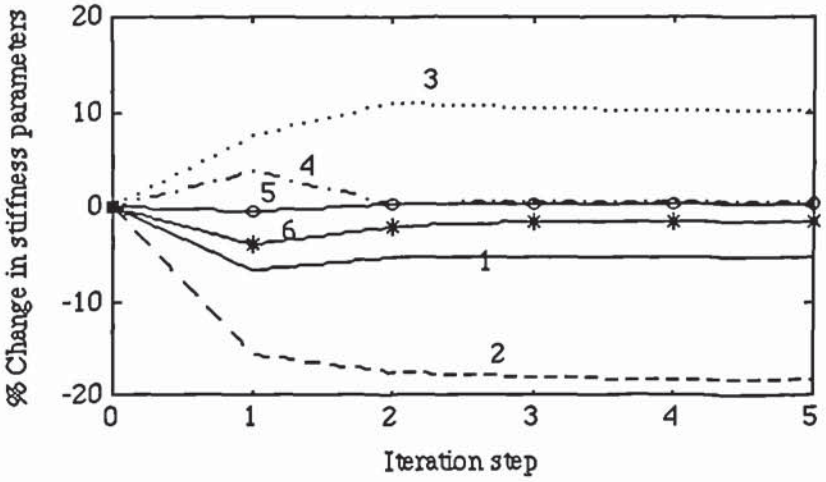

Fig 4.26 Convergence of the stiffness parameters of the H-frame updated using the minimum cost estimator.

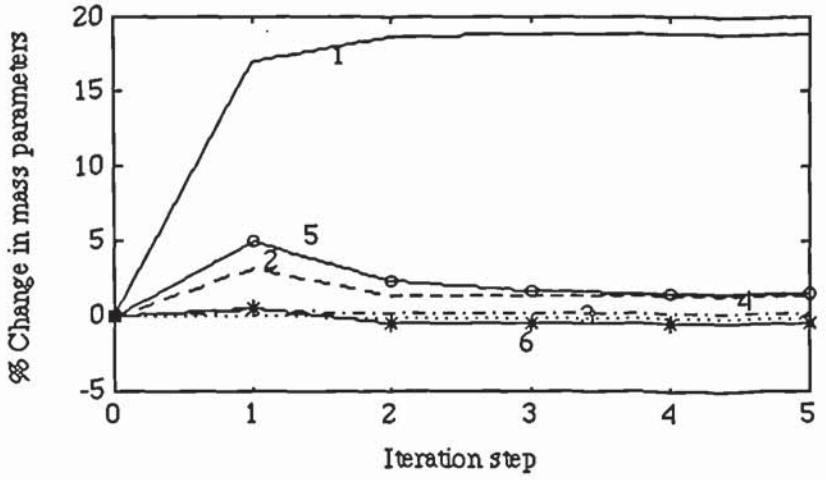

Fig 4.27 Convergence of the mass parameters of the H-frame updated using the minimum cost estimator.

The FRF predictions of the updated model as compared to the simulated system and the initial model are shown in figs 4.28 and 4.29. The first graph shows the point receptance at coordinate 5 of the system (corresponds to

coordinate 9 of the idealized model, fig 4.5). This is one of the coordinates where masses were added. The second graph shows the receptance at coordinate 20 of the system (corresponds to coordinate 25 of the idealized model, fig 4.5) for an excitation at coordinate 5. There is a good agreement with the correct FRF at the perturbed coordinate. Coordinates which were not perturbed show a gross departure, with an abrupt transition, from the correct FRF from the third mode frequency. Certainly the good match in the natural frequency prediction for the first three elastic modes does not reveal the disagreements seen in fig 4.29.

Simulated system (with joint flexibility) __ , initial model - - , Updated model * * *

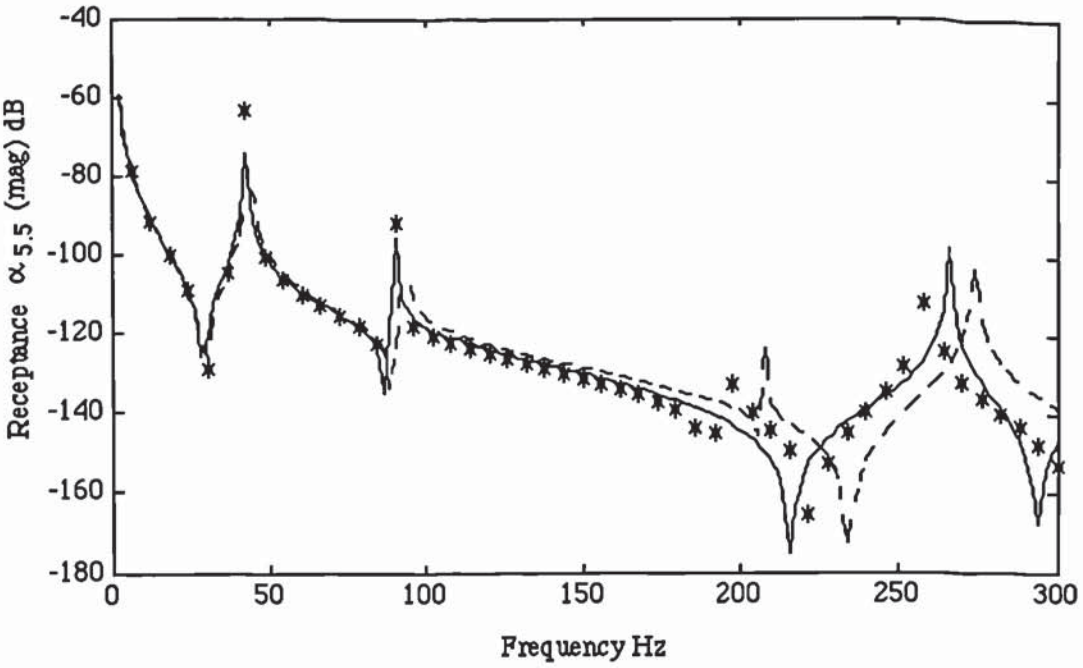

Fig 4.28 Point receptance prediction for the free H-frame at coord. 5 of fig 4.3

Simulated system (with joint flexibility) __ , initial model - - , Updated model * * *

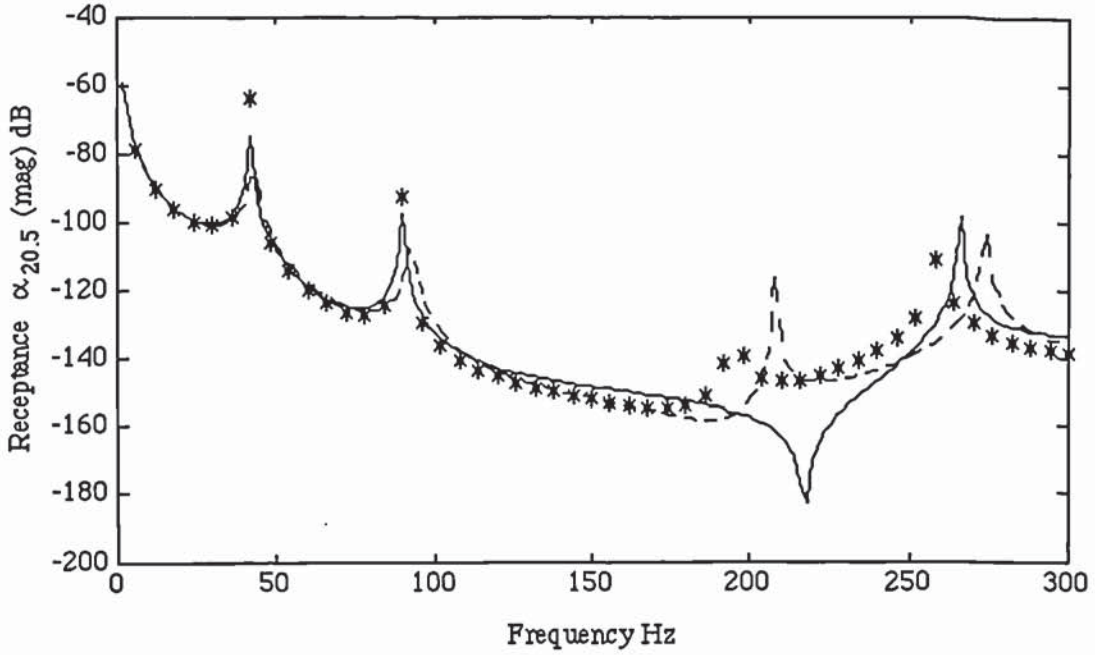

Fig 4.29 Receptance prediction for the free H-frame at coord. 20 of fig 4.3.

When random errors with zero mean and standard deviation of 0.5 Hz were added to the natural frequencies, the parameters converged to the following values:

$EI_1 = 5063$ Nm^2	$EI_2 = 4318$ Nm2
$EI_3 = 4623$ Nm^2	$EI_4 = 4288$ Nm^2
$EI_5 = 5814$ Nm2	$EI_6 = 5723$ Nm^2
$m_{u1} = 3.953$ kg/m	$m_{u2} = 3.354$ kg/m
$m_{u3} = 3.098$ kg/m	$m_{u4} = 3.107$ kg/m
$m_{u5} = 4.169$ kg/m	$m_{u6} = 4.186$ kg/m

System f (Hz):	$f_1 = 41.71$	$f_2 = 89.74$	$f_3 = 193.46$
Initial model f_a (Hz):	$f_{1a} = 43.09$	$f_{2a} = 92.84$	$f_{3a} = 208.19$
Updated model f (Hz):	$f_1 = 41.71$	$f_2 = 89.61$	$f_3 = 193.66$

The accuracy of the updated parameters has changed very little when measurement errors were simulated. The effective errors due to the model structure are more dominant and, in this case, had strong influence on the accuracy of the parameters.

The same frame model is now updated by stiffness addition at the same perturbing coordinates. With stiffness addition, large changes in the eigenvalues are possible and consequently the eigenvalue sensitivity matrix becomes relatively better conditioned than with mass addition. The added stiffness are $2x10^6$ N/m and $4x10^6$ N/m. The simulated and the analytical natural frequencies are shown in table 4.31. The parameters are updated using the Bayesian approach with the same confidence in the initial parameters as in the previous case. Measurement errors are not added to the data but, as in the previous case, the natural frequencies are considered to have been measured with confidence expressed by a standard deviation of 0.5 Hz.

Added stiffness (N/m)	Stiffness addition coordinate (fig 4.3)	Simulated natural frequencies (Hz)			Analytical natural frequencies (Hz)		
		Mode 1	Mode 2	Mode 3	Mode 1	Mode 2	Mode 3
0	-	41.71	89.74	193.46	43.09	92.83	207.88
$2x10^6$	5	84.78	130.37	193.47	86.65	136.63	208.08
	22	75.94	170.68	223.25	79.00	171.56	246.01
$4x10^6$	5	85.80	159.91	193.47	87.87	169.42	208.40
	22	76.37	175.39	231.08	79.50	177.66	252.07

TABLE 4.31 Simulated and analytical natural frequencies of the H-frame with and without added stiffness.

The parameters, in this case, converged to the following:

$EI_1 = 5484$ Nm^2 $EI_2 = 3809$ Nm^2

$EI_3 = 4555$ Nm^2 $EI_4 = 4175$ Nm^2

$EI_5 = 6098$ Nm^2 $EI_6 = 5351$ Nm^2

$m_{u1} = 3.666$ Kg/m $m_{u2} = 3.479$ Kg/m

$m_{u3} = 3.099$ Kg/m $m_{u4} = 3.108$ Kg/m

$m_{u5} = 4.029$ Kg/m $m_{u6} = 4.135$ Kg/m

$f_1 = 42.19$ Hz $f_2 = 89.74$ Hz $f_3 = 193.15$ Hz.

The convergence of the parameters is shown in figs 4.30 and 4.31. Although the data is error-free, there is some changes in the parameters from the case of mass addition. Changes are inevitable because the model structure is not exact and the frequencies used are different. Therefore, the effective errors as a result of an incorrect model structure in the two cases are obviously different. The parameters, however, shows a similar trend of changes from their initial estimates as in the mass addition case. The masses can be considered to have been updated satisfactorily as their accuracy is of the same order as the specified uncertainty (standard deviation) in the initial estimates. The fact that the mismatch between the simulated system and the structure of the analytical model is mainly in the stiffness matrix and that large perturbations in the eigenvalues (by stiffness addition) were made, accounts for the good result in the mass parameters.

The prediction of the FRF at coordinates 5 (point receptance) and 20 for an excitation at coordinate 5 are shown in figs 4.32 and 4.33. The departure from the correct FRF at the unmeasured coordinate (fig 4.33) is as severe as in the previous case (fig 4.29).

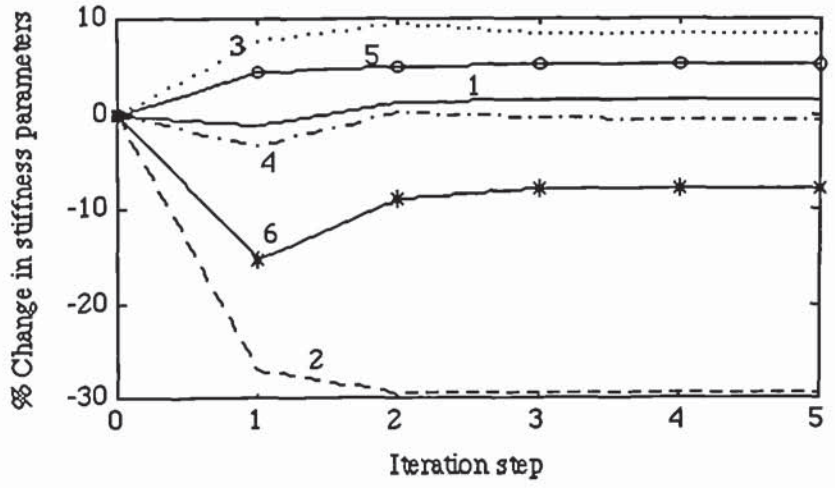

Fig 4.30 Convergence of the stiffness parameters of the H-frame updated by stiffness addition using the minimum cost estimator.

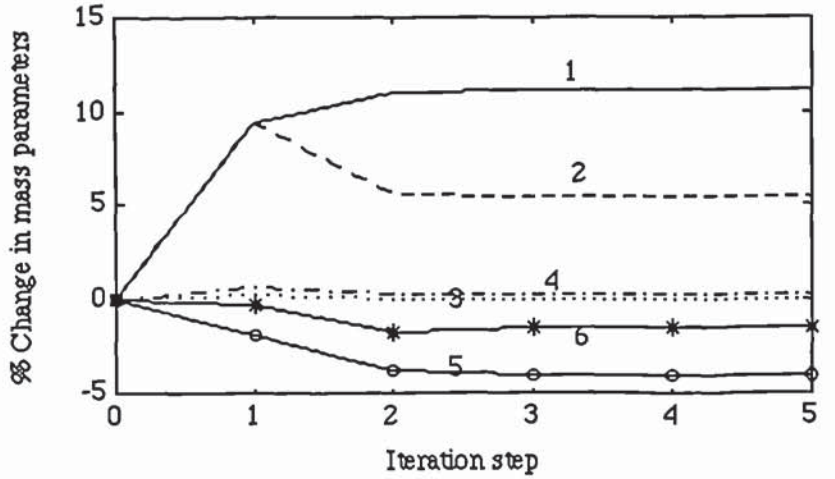

Fig 4.31 Convergence of the mass parameters of the H-frame updated by stiffness addition using the minimum cost estimator

Simulated system (with joint flexibility) __ , initial model - - , Updated model * * *

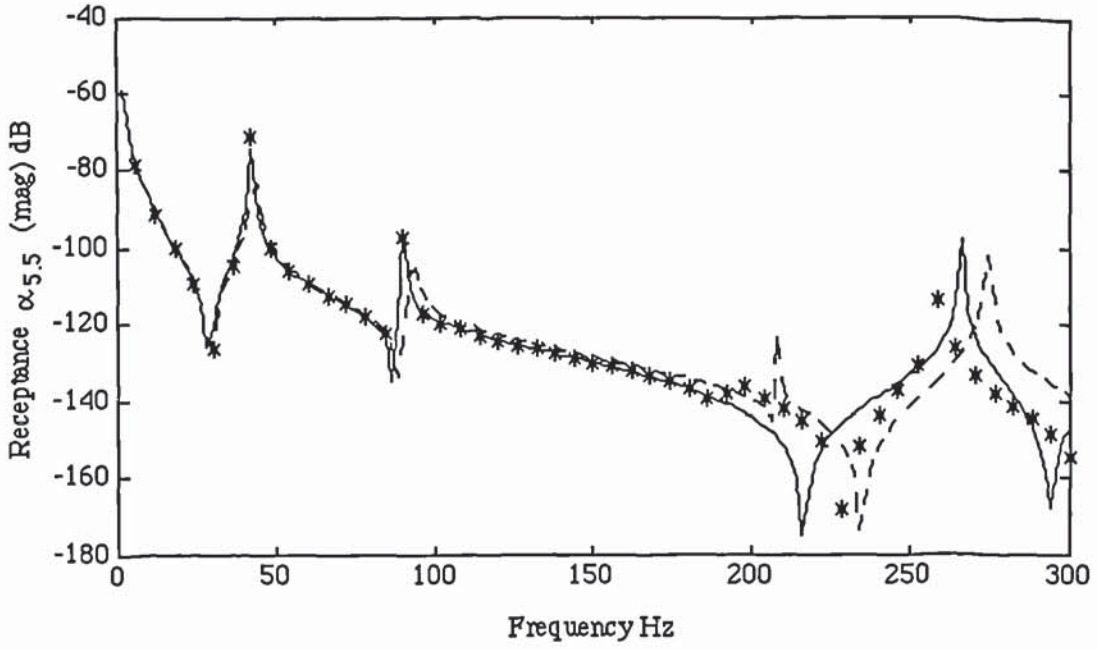

Fig 4.32 Point receptance prediction at coordinate 5 of the H-frame (fig 4.3) (updated by stiffness addition).

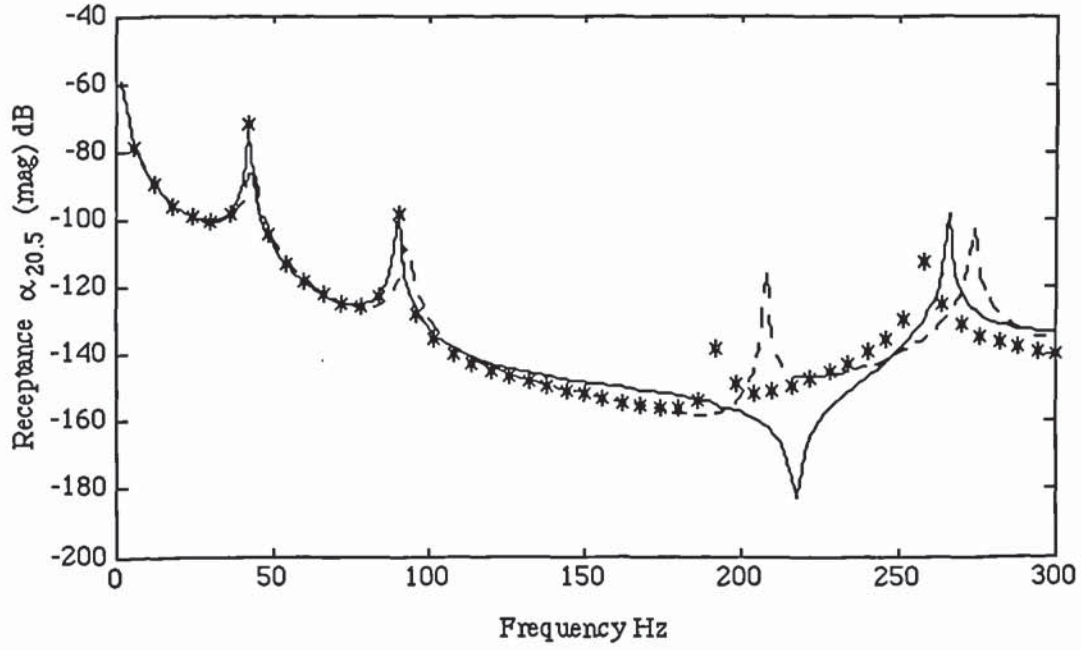

Fig 4.33 Receptance prediction at coordinate 20 of the H-frame (fig 4.3) for an excitation at coordinate 5 (updated by stiffness addition).

4.8 Summary

The identification of exact mass and stiffness parameters of a FE model which reproduce exactly a given incomplete number of eigenvalues before and after the system is perturbed requires error-free data and exact structure of the mass and stiffness matrices. In a practical situation a number of problems are encountered. Measured data is not error-free and the structure of the model matrices may not be exact. This chapter has looked, by numerical examples, at practical problems in parameter estimation using the mass addition technique developed in Chapter 3. In particular, the following problems have been looked at:

(i) Incompatibility in the number of DOF between the idealized model and the system.

(ii) Inaccuracy in the structure of the model matrices.

(iii) Incompatibility between the undamped FE model and data from a system with some degree of non-proportional damping.

(iv) Experimental errors in the measured data

It has been found that, with an unconstrained least squares solution method, all these factors affect the accuracy of the updated mass and stiffness parameters to the extent that parameters easily lose their physical interpretation. The degradation in the accuracy of the parameters, due to the incompatibility in the number of DOF between the model and the system can be practically reduced by increasing the degree of discretization. The degradation in accuracy due to the errors in the estimation of real modes and undamped natural frequencies is

negligible if the complex modes are very close to real modes. For many structures, damping levels are low and measured modes are close to real modes. Since it is practically feasible to discretize the system such that the effects of discretization error on the few eigen-data in the frequency range of interest is negligible, the first and the third factors are, for many structures, not so crucial. Measurement errors and inaccuracies in the model structure cannot be easily avoided. Practical parameter updating, therefore, certainly requires optimization with constraints on the parameters. The minimum cost estimator has proved useful in avoiding large parameter changes to unrealistic values. With the Bayesian estimator the changes in the parameters from their initial estimates have been found to be comparable to the uncertainty specified on the initial estimates. However, with a large mismatch between the structure of the model matrices and the system, the minimum cost estimator does not prevent parameter changes orders of magnitude larger than the uncertainty on the initial estimates. This may also happen if the initial estimates or the weighting matrices are not realistic. In many cases, the initial parameters are a good approximation and the eigenvalues are measured with a good estimate of their uncertainty. The gross mismatch in the model structure does not necessarily lead to a failure of the natural frequencies of the updated model to converge to the measured natural frequencies. However, Large unrealistic parameter changes from their initial estimates can serve as a useful warning of the existence of a gross mismatch in the model structure.

CHAPTER 5

EXPERIMENTAL VERIFICATION OF THE MASS ADDITION TECHNIQUE

5.1 Introduction

The technique of updating parameters of structural dynamic models by adding mass or stiffness to the system has been developed in Chapter 3. It is based on perturbation of the system by adding lumped mass or grounded stiffness at a number of coordinates and measurement of the eigen-data of the unperturbed and the perturbed structure. The perturbations involve adding a single mass or stiffness at a single coordinate, measure the eigen-data, remove the mass (or stiffness), and continue with another perturbations at the same or different coordinates. The mass and stiffness parameters are then found by iterative updating of the initial parameters by eigen-data sensitivity analysis, using the eigen-data of the structure before and after perturbation.

It has been shown, in Chapter 3, that with a suitable choice of the perturbing coordinates, and if the eigen-data is error-free and the model structure exact, exact parameters of a FE model or a lumped parameter model with a diagonal mass matrix could be identified. It is essential to perturb both the structure and its analytical model by identical perturbations so that sensitivity analysis is performed with respect to the parameters of the unperturbed structure. The technique, as presented in Chapter 3, overcomes parameter estimation difficulties associated with the incompleteness of the measured data, in terms of the number of measured or excited modes and the number of measurement coordinates.

The feasibility of the mass or stiffness addition technique in a practical

situation of non-error-free measurements and some degree of inaccuracy in the structure of the mass and stiffness matrices has been investigated in Chapter 4. The study in Chapter 4 has found the technique to be feasible. This Chapter is devoted to the experimental verification of the mass addition technique as applied to a FE model of a simple but real structure. The test structure was an aluminium beam of size 25x50x800mm long, in free-free and clamped-free configurations.

5.2 Experimental set up.

5.2.1 Clamped-free configuration.

The beam was firmly clamped horizontally at one of its ends, leaving a free overhang length of 710mm. The wider side of the beam cross-section was set horizontal. The clamping was done at a steel support block, which was itself clamped on a massive cast iron bed. The clamping was intended to approximate, as far as practical, the ideal case of a fixed boundary condition. An electro-dynamic shaker (Derritron type VP 4B) was used to excite the beam in the vertical direction normal to the undeformed neutral plane. The shaker was connected to the beam by a force transducer and an extension push rod, which passed through a hole drilled in the beam, 400mm from the clamped end. The push rod was fixed to the beam by two locking nuts, one on the top side and one on the under side of the beam. The diameter of the push rod was 6mm. The static mass of the force transducer, push rod and the lock nuts was 93g. The clamped-free configuration is shown in fig 5.1.

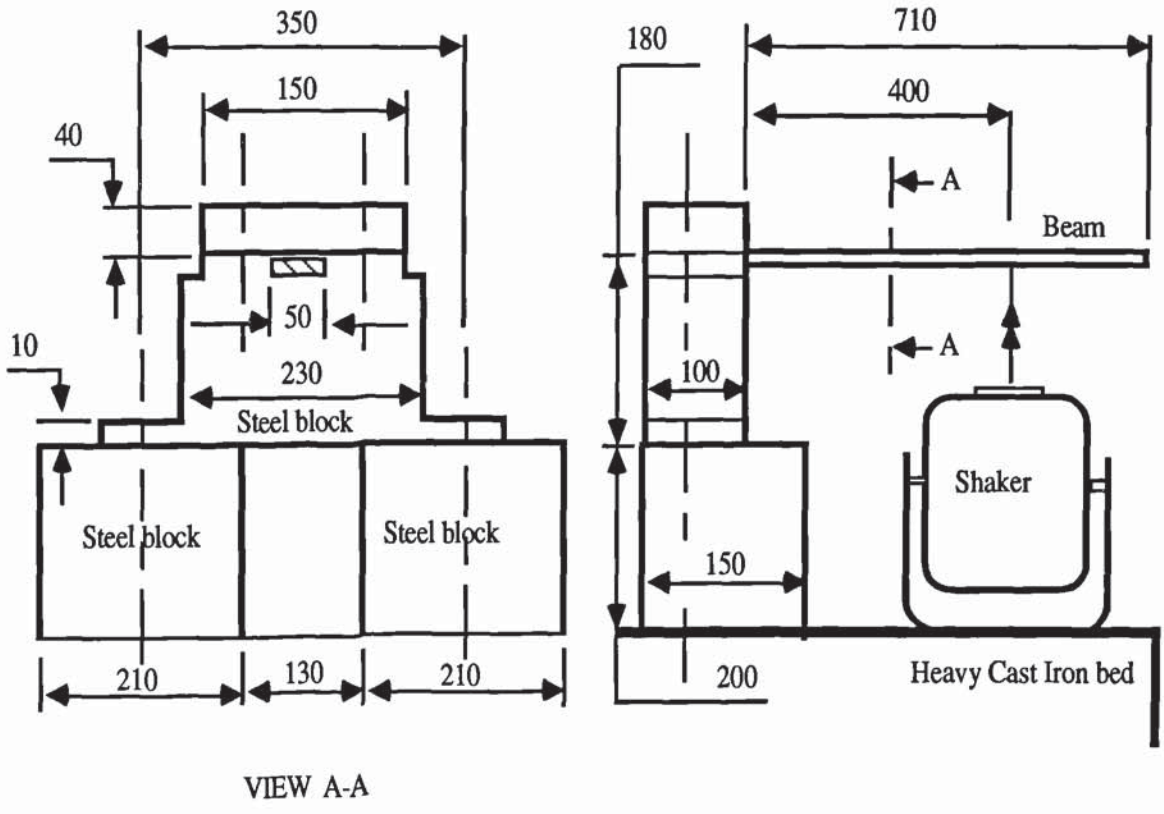

Fig 5.1 Clamped-free test configuration (dimension in mm).

5.2.2 Free-free configuration.

The beam was supported horizontally by two sets of relatively light suspension springs to simulate a free-free boundary condition. The supports were situated at 90mm and 112mm from the ends of the beam. The beam was set with the wider side of the cross-section horizontal. An electro-dynamic shaker, which was used in the clamped-free configuration (section 5.2.1), was used to excite the beam 490mm from one end. The force transducer, push rod, lock nuts and the form of the beam-shaker connection was essentially similar to that used in the clamped-free configuration. The configuration for the free-free test is shown in fig 5.2.

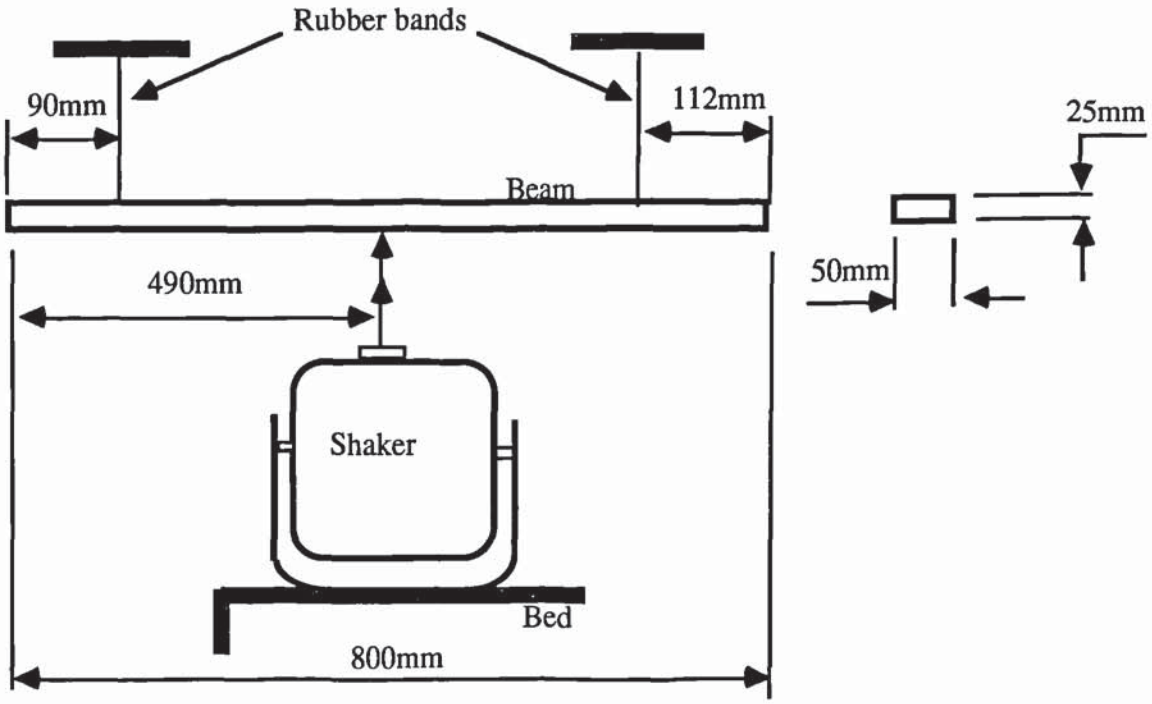

Fig 5.2 Free-free test configuration

5.2.3 Instrumentation.

A signal analyser (Bruel & Kjaer, type 2034) was used to generate a random excitation signal. The excitation signal was amplified by a separate power amplifier and then connected to the shaker. An accelerometer and a force transducer were used to measure vibrations of the beam and the excitation force. Signals from these transducers were passed through signal conditioning amplifiers and then to the analyser for processing to generate spectral data. The spectral data was then transmitted to an IBM-AT computer for further processing, using a commercial signal processing and modal analysis package, SPIDERS, produced by PAFEC Ltd. The instrumentation used in the free-free and in the clamped-free test configurations was the same. Fig 5.3 shows the instrumentation layout.

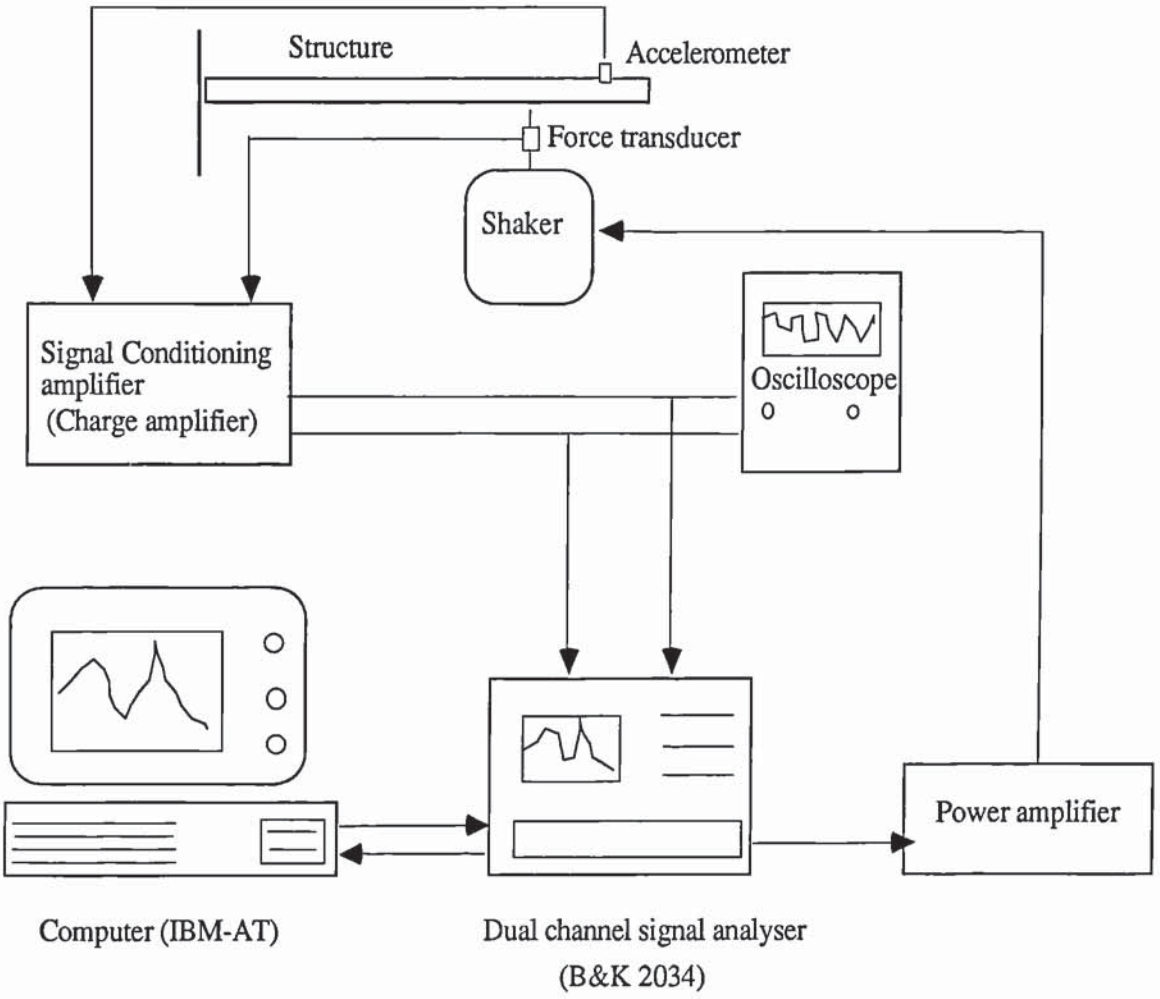

Fig 5.3 Instrumentation layout

5.2.4 Signal analysis.

Signal analysis involved the computation of the frequency response function for each measured coordinate, and extraction of the modal data. The frequency response function is given as a complex ratio of the sinusoidal displacement (response) to the sinusoidal excitation (a single forcing coordinate) for each discrete frequency in the measured spectrum. As the forcing and response data captured is time domain random, computation of the frequency response functions involves resolution into auto and cross spectral densities. The frequency response function (receptance α_{ij}) is then given by

(Ewins 1985),

$$S_{ji}(\omega) = \alpha_{ij}(\omega)S_{jj}(\omega) \quad \text{or} \quad S_{ii}(\omega) = \alpha_{ij}(\omega)S_{ij}(\omega) \tag{5.1}$$

where $S_{ii}(\omega)$ and $S_{jj}(\omega)$ are the auto spectra of the response and forcing signals, and $S_{ji}(\omega)$ is the cross spectrum.

Modal data was extracted from the frequency response data using Dobson's modal analysis algorithm (Dobson 1987), which is implemented in SPIDERS.

5.3 Updating a FE model of the clamped-free beam.

The cantilever beam of Section 5.2.1 was modelled by a 7 elements undamped FE model with 14 DOF, assuming a perfectly rigid clamping. The first six elements from the clamped end have length of 100mm each. The seventh element has a length of 110mm. A Youngs modulus of 70 KN/mm^2 was used for aluminium. With this data and from the dimensions and mass of the beam, the structural parameters used in the FE model and their confidence, expressed by their standard deviations are:

$EI_a = 4557$ Nm^2 STD = 150 Nm^2 all elements.

$m_{u,a} = 3.4$ kg/m STD = 0.1 kg/m all elements.

Natural frequencies and mode shapes for the first three modes were determined from measured receptance data. The measurement frequency range was from 0 to 800 Hz with a resolution of 1 Hz. The mode shape displacements were measured at all translational coordinates (nodes 1 to 7 in fig 5.4).

Measured and analytical natural frequencies and mass-normalized mode shape data of the first three modes are given below:

Analyt. f_a (Hz):	f_{1a}= 40.6	f_{2a} = 254.7	f_{3a} = 713.9
Measured f (Hz):	f_1 = 38.7	f_2 = 238.0	f_3 = 670.7
Measured η :	η_1 = 0.0028	η_2 = 0.008	η_3 = 0.0042

	Measured mode shape data (values in bracket are phase angles in degrees)			Analytical mode shape data		
Measurement point (See fig 5.4)	Mode 1	Mode 2	Mode 3	Mode 1	Mode 2	Mode 3
1	0.0904 (0.06)	0.2495 (-0.01)	0.5136 (0.89)	0.0420	0.2184	0.5012
2	0.2165 (0.03)	0.6045 (0.01)	0.7810 (0.79)	0.1564	0.6281	0.9750
3	0.3184 (-0.09)	0.8170 (0.01)	0.3949 (-0.31)	0.3261	0.9050	0.5514
4	0.4712 (-0.03)	0.7156 (-0.01)	-0.3630 (177.99)	0.5348	0.8410	-0.4067
5	0.7482 (-0.06)	0.3085 (-0.01)	-0.6713 (178.72)	0.7678	0.3897	-0.8454
6	0.9508 (-0.03)	-0.3633 (-3.14)	-0.1205 (-178.72)	1.0131	-0.3467	-0.1891
7	1.2047 (-0.02)	-1.1435 (3.13)	0.9249 (-0.18)	1.2873	-1.2877	1.2902

TABLE 5.1 Measured mass-normalized modes (Amplitude and phase) and analytical mass-normalized modes.

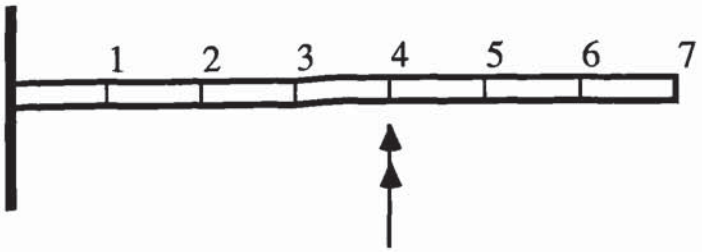

Fig 5.4 Measurement points

Measurements of the mode shape displacements in all the translational coordinates involved repeated measurements of the natural frequencies. The natural frequencies and damping factors given are the average values. Their actual variations are:

$f_{1,max} = 39.19$ Hz $\quad f_{1,min} = 38.59$ Hz

$f_{2,max} = 238.2$ Hz $\quad f_{2,min} = 237.4$ Hz

$f_{3,max} = 671.2$ Hz $\quad f_{3,min} = 669.2$ Hz

$\eta_{1,max} = 0.0042$ $\quad \eta_{1,min} = 0.0022$

$\eta_{2,max} = 0.0089$ $\quad \eta_{2,min} = 0.0075$

$\eta_{3,max} = 0.0047$ $\quad \eta_{3,min} = 0.0039$

From measured and analytical data it is apparent that the analytical model prediction is not in agreement with measured dynamic characteristics, implying that the model required updating. It is also evident that an undamped model can be assumed due to the low damping factors and almost real measured mode shapes. Thus, measured natural frequencies were taken as the undamped natural frequencies and moduli of the mode shape displacements were taken as real modes. However further examination of the frequency data suggest that the beam is not behaving as a rigidly clamped cantilever. For a rigidly clamped Euler-Bernoulli cantilever beam the frequency ratio for

modes 2 to 1 and 3 to 1 should, in theory, be:

$$f_{2a}:f_{1a} = 6.267 \quad \text{and} \quad f_{3a}:f_{1a} = 17.548$$

The frequency ratios using measured data are:

$$f_2:f_1 = 6.149, \quad \text{and} \quad f_3:f_1 = 17.33$$

It was felt that this behaviour may be due to the flexibility of the clamped boundary condition as it is difficult to ensure the rigidity of the clamped end, as well as the mass loading of the shaker interface. It was therefore decided to improve the structure of the mathematical model by including flexibility at the clamped end and extra mass for the loading caused by the shaker. The flexibility of the clamped end was idealized by a lumped translational stiffness (k_T) and a lumped rotational stiffness (k_R). Mass loading of the shaker was idealized by a lumped mass (m_L) at the excitation coordinate. Thus, the model had 16 DOF and 3 additional parameters to update. The beam is uniform, so there will only be 2 mass and stiffness parameters giving rise to a total of 5 parameters to update. However, to simulate a large system with many parameters to update, parameters for each element have also been treated as independent.

The following values are the initial estimates for the lumped translational and rotational stiffness at the clamped end and mass loading of the shaker, with their confidence expressed by standard deviations in bracket.

$k_T = 8.0\text{x}10^7$ N/m	(STD = $2.0\text{x}10^7$ N/m)
$k_R = 4.0\text{x}10^5$ Nm/Rad	(STD = $1.0\text{x}10^5$ Nm/Rad)
$m_L = 0$ kg	(STD = 0.1 kg)

With these parameters, the analytical model has natural frequencies given by:

$$f_{1a} = 39.4 \text{ Hz} \quad f_{2a} = 245.6 \text{ Hz} \quad f_{3a} = 680.6 \text{ Hz}$$

The initial estimates for k_T and k_R were determined by guessing some values and then adjusting by trial and error so that the analytical natural frequencies are improved. The analytical model incorporating mass loading of the shaker and flexibility of the clamped end, fig 5.5, was taken as an initial analytical model, which has to be updated by mass addition. Two mass addition studies have been performed using eigenvalues alone (Cases 1 to 3) and using eigenvalues and eigenvectors (Cases 4 and 5).

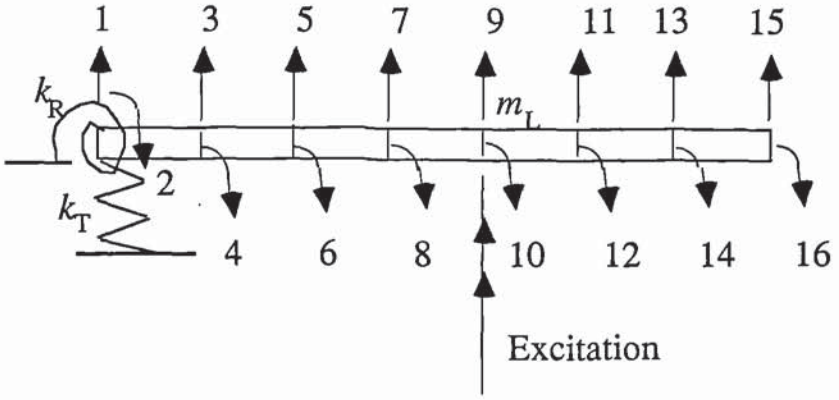

Fig 5.5 FE model including support flexibility and mass loading of shaker.

5.3.1 Updating a FE model of the cantilever beam using eigenvalues.

CASE 1

The FE model of the uniform cantilever beam, fig 5.5, was updated by mass addition, using eigenvalues alone. Masses of 0.199 kg and 0.355 kg were added one in turn and removed to each of coordinates 5, 7, 11 and 13 of the beam and

its analytical model. Natural frequencies of the first two modes, for each mass addition, were measured. These, together with the first two natural frequencies of the unperturbed beam, generate 18 eigenvalue sensitivity equations with 5 parameters to update. The natural frequencies are given in table 5.2. From the experimental data, standard deviations in natural frequencies for modes 1 and 2 were estimated as 0.1 Hz and 0.2 Hz respectively.

Added mass (kg)	Mass addition coordinate (See fig 5.5)	Measured natural frequencies (Hz)		Analytical natural frequencies (Hz)	
		Mode 1	Mode 2	Mode 1	Mode 2
-	-	38.7	238.0	39.4	245.6
0.199	5	38.6	227.1	39.3	235.4
	7	38.2	219.1	38.9	227.9
	11	36.3	234.6	37.2	242.7
	13	34.9	234.0	35.9	243.0
0.355	5	38.5	219.5	39.2	228.0
	7	37.9	210.4	38.6	216.8
	11	35.0	232.5	35.8	240.8
	13	33.0	231.2	33.7	241.6

TABLE 5.2 Measured and analytical (Case 1) natural frequencies.

Parameters were updated using the minimum cost Bayesian estimator. The result after 5 iterations is:

$EI = 4272\ \text{Nm}^2$ $\quad m_u = 3.16\ \text{kg/m}$

$k_T = 5.23\text{x}10^7\ \text{N/m}$ $\quad k_R = 2.86\text{x}10^5\ \text{Nm/Rad}$

$m_L = 0.09\ \text{kg.}$

$f_1 = 38.6\ \text{Hz}$ $\quad f_2 = 236.8\ \text{Hz}$ $\quad f_3 = 666.7\ \text{Hz.}$

Fig 5.6 show the convergence of the mass (m_u) and stiffness (EI) parameters of the uniform beam. Figs 5.7-5.9 compares receptance prediction between the

updated model, initial model and experimental data at coordinates 3, 9 and 15. The receptances are given in deciBels where 0 dB represent 1 m/N. It can be seen that there is a considerable improvement in receptance prediction after updating the model, except for the low frequency (<30Hz) prediction at coordinate 3. The experimental data show a large receptance amplitude, which resemble a rigid body mode, at coordinate 3. Since the beam is clamped, there are no rigid body modes. The large discrepancy between the experimental data and the analytical model in the low frequency range (<30Hz) at coordinate 3, is likely due to the measurement noise. Coordinate 3 is near the clamped end where the acceleration level is low and the noise to signal ratio relatively high. The acceleration measured at coordinate 3 (inertance plot is shown in fig 5.10) is also likely to be most influenced by the vibration of the clamping system due to its proximity, than is the case with other measured coordinates. The extreme case can be imagined as the measurement of coordinate 1. Both the effects of the vibration of the clamping system and the low acceleration level towards the clamped end of the beam are possible contributors to the discrepancy in the FRF at coordinate 3. The discrepancy was also apparent in the low frequency range at coordinate 5 (see Case 2), but became negligible as the measurement point was moved towards the end of the beam.

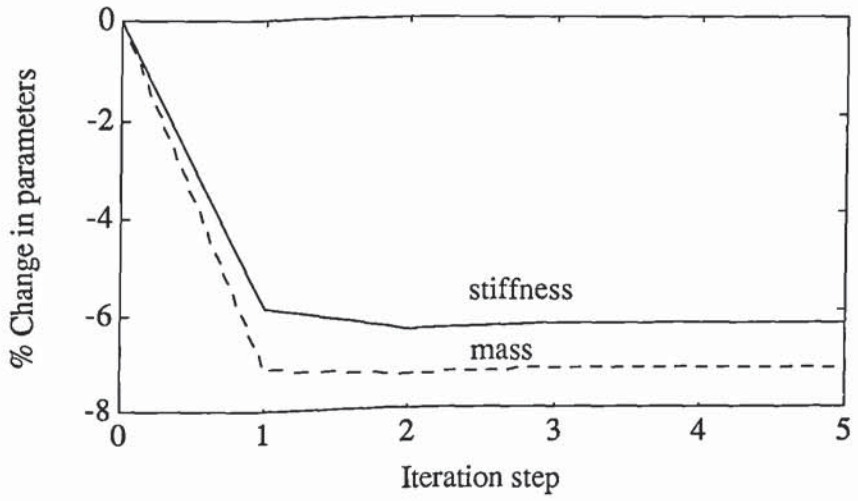

Fig 5.6 Convergence of the parameters of the uniform cantilever beam.

Experimental data ___ , Initial model - - -, Updated model (Using eigenvalues alone) ***

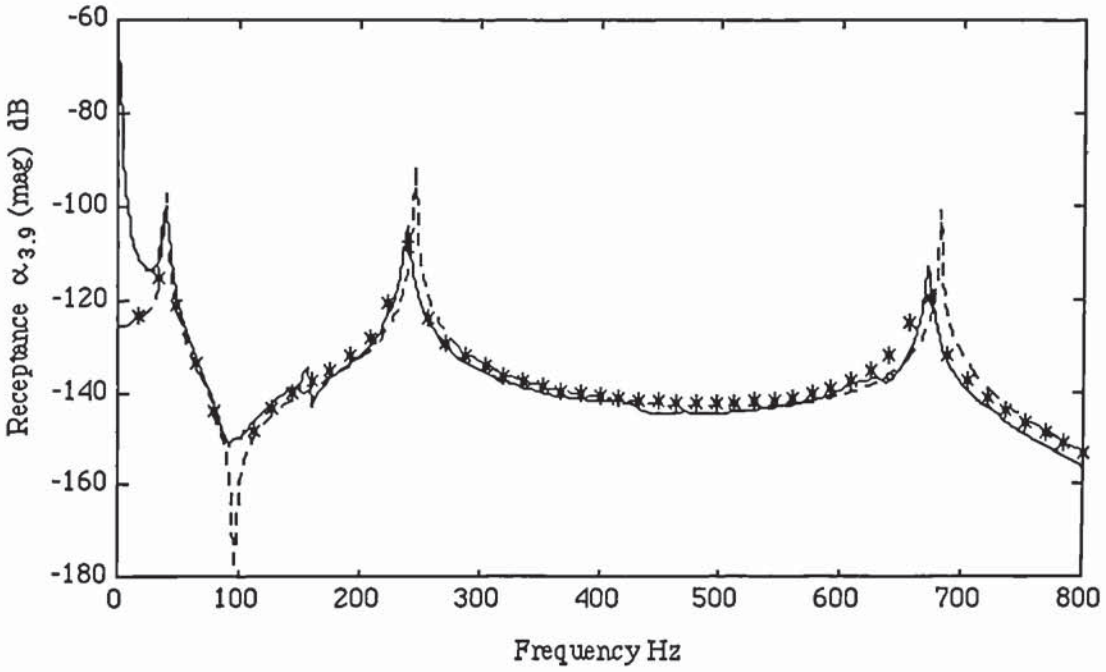

Fig 5.7 Receptance prediction at coordinate 3 of the beam for Case 1.

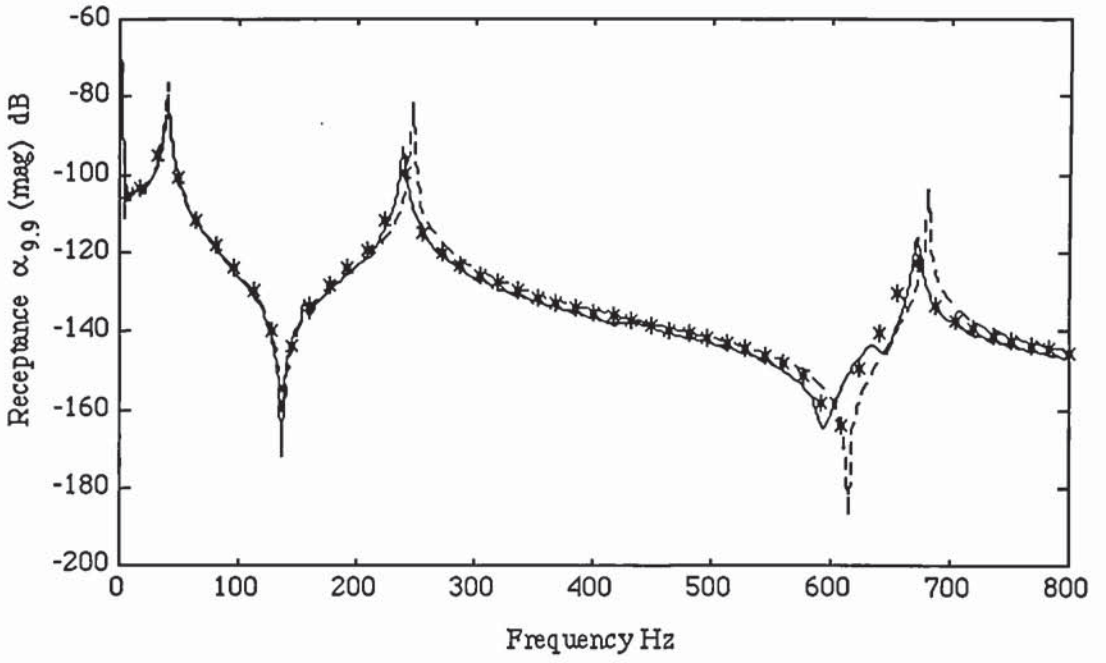

Fig 5.8 Receptance prediction at coordinate 9 of the beam for Case 1.

Experimental data ___ , Initial model - - -, Updated model (Using eigenvalues alone) ***

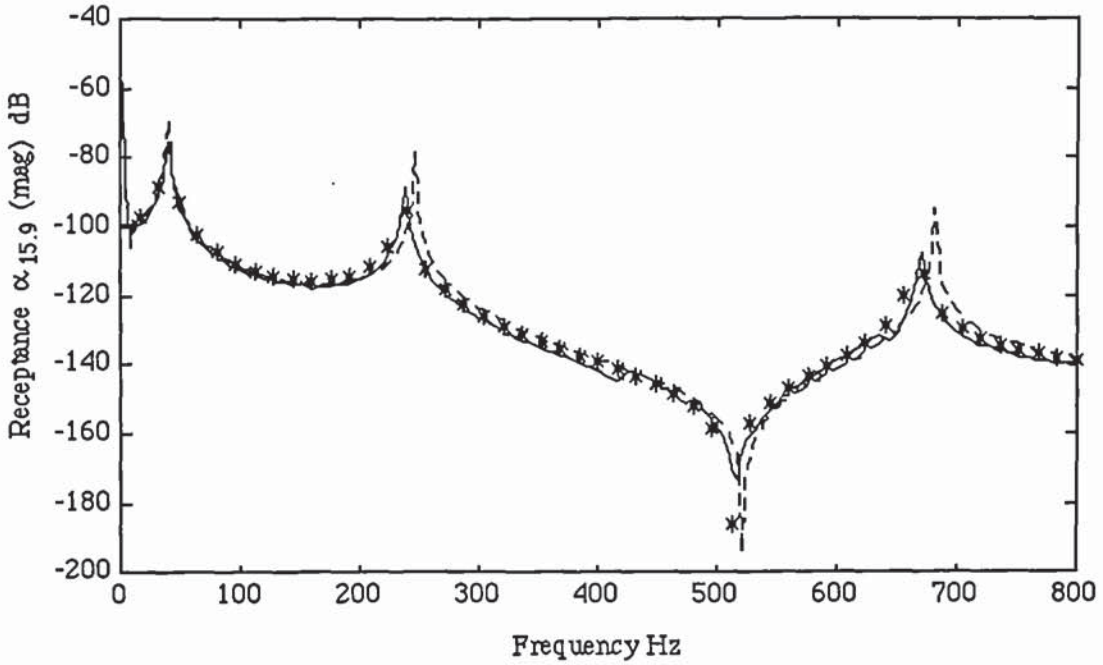

Fig 5.9 Receptance prediction at coordinate 15 of the beam for Case1

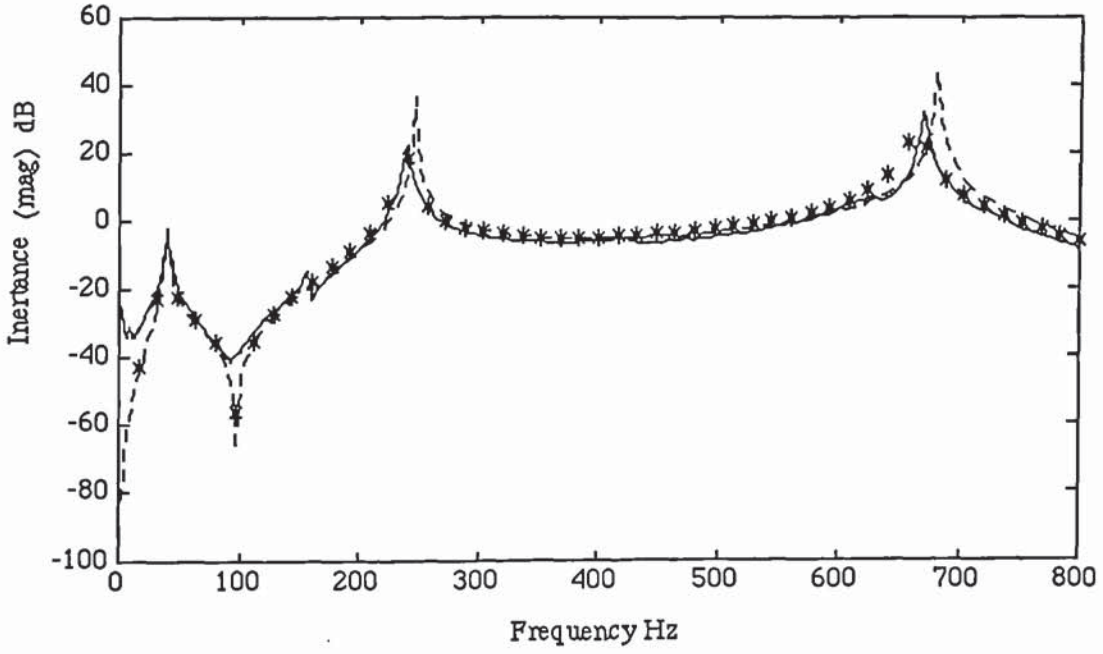

Fig 5.10 Inertance prediction at coordinate 3 of the beam for Case 1 (0 dB represent 1 m/Ns^2).

CASE 2

This case simulates a large system with many parameters to update, by treating the parameters for each element as independent. Thus, there are 17 parameters to update in Case 2. Parameter updating was performed by mass addition with the same masses and the same mass addition coordinates as in Case 1. Eigenvalues of the first two modes of the perturbed and unperturbed beam, for each added mass (table 5.2), were used in the updating process.

The updated parameters, after 4 iterations are (element numbers start from the clamped end):

$EI_1 = 4550$ Nm^2 $\quad$ $EI_2 = 4561$ Nm^2

$EI_3 = 4524$ Nm^2 $\quad$ $EI_4 = 4384$ Nm^2

$EI_5 = 4292$ Nm^2 $\quad$ $EI_6 = 4473$ Nm^2

$EI_7 = 4561$ Nm^2

$m_{u1} = 3.398$ kg/m $\quad$ $m_{u2} = 3.385$ kg/m

$m_{u3} = 3.379$ kg/m $\quad$ $m_{u4} = 3.395$ kg/m

$m_{u5} = 3.394$ kg/m $\quad$ $m_{u6} = 3.333$ kg/m

$m_{u7} = 3.202$ kg/m.

$k_T = 8.02\text{x}10^7$ N/m $\quad$ $k_R = 2.06\text{x}10^5$ Nm/Rad

$m_L = 0.028$ kg

$f_1 = 38.6$ Hz $\quad$ $f_2 = 236.7$ Hz $\quad$ $f_3 = 663.2$ Hz

Figs 5.11 and 5.12 shows the convergence of the mass and stiffness parameters of the first 4 elements of the beam. The convergence rate is shown as a

percentage of parameter changes from the initial estimates. Figs 5.13-5.16 compare receptance prediction between the initial model, updated model and experimental data measured at coordinates 3, 5, 9 and 15 of the unperturbed beam.

element 1 ___1, element 2 - - -2, element 3 -.-.-.3, element 4 4

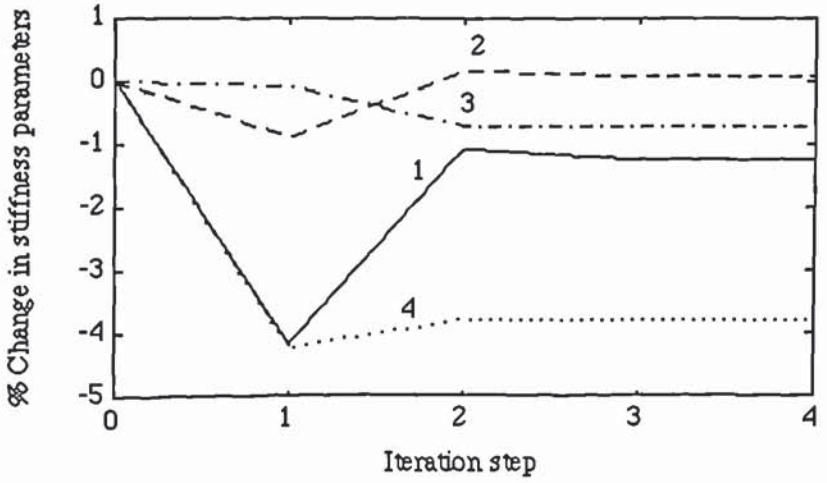

Fig 5.11 Convergence of the stiffness parameters of the cantilever beam for Case 2.

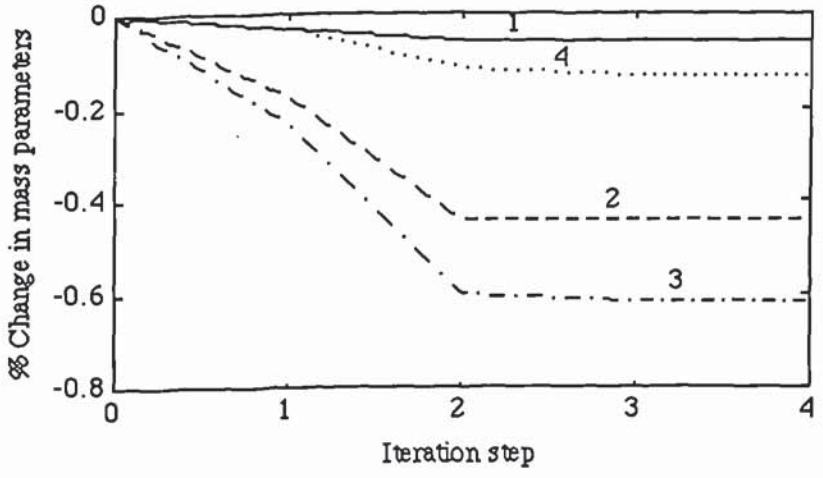

Fig 5.12 Convergence of the mass parameters of the cantilever beam for Case 2.

Experimental data ___ , Initial model - - -, Updated model (Using eigenvalues alone) ***

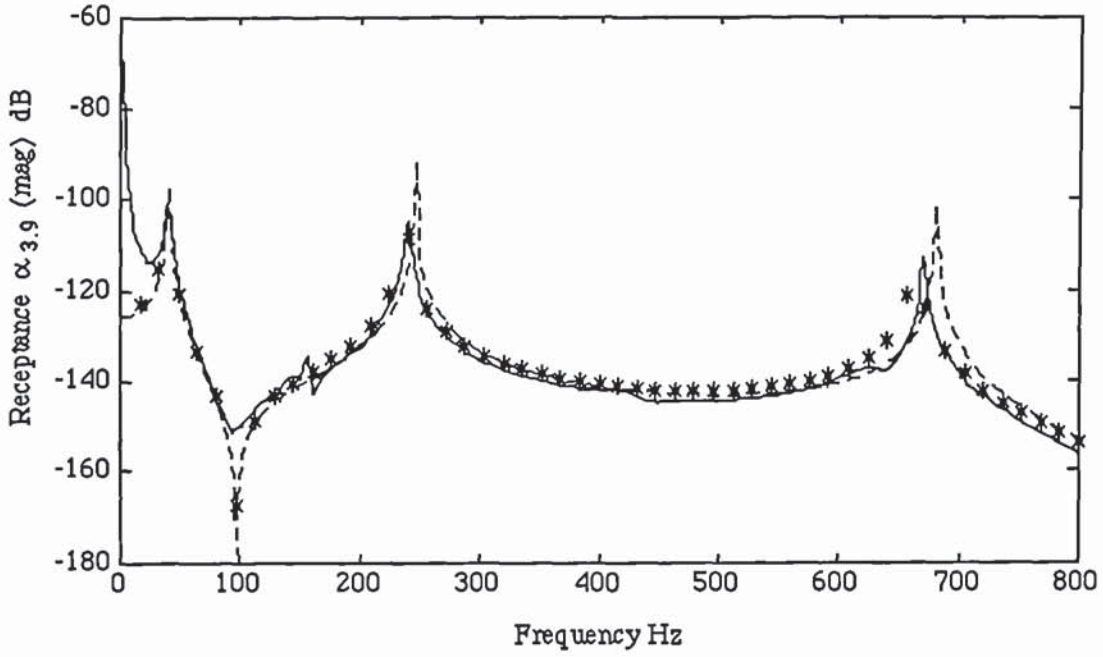

Fig 5.13 Receptance prediction at coordinate 3 of the beam for Case 2.

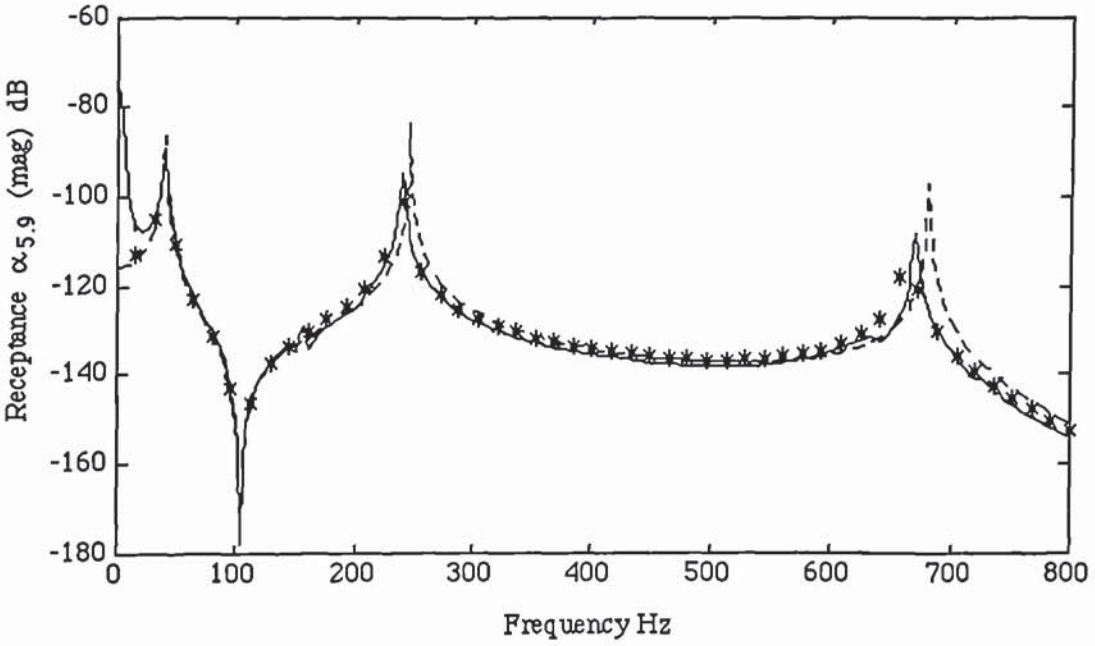

Fig 5.14 Receptance prediction at coordinate 5 of the beam for Case 2.

Experimental data ___ , Initial model - - -, Updated model (Using eigenvalues alone) ***

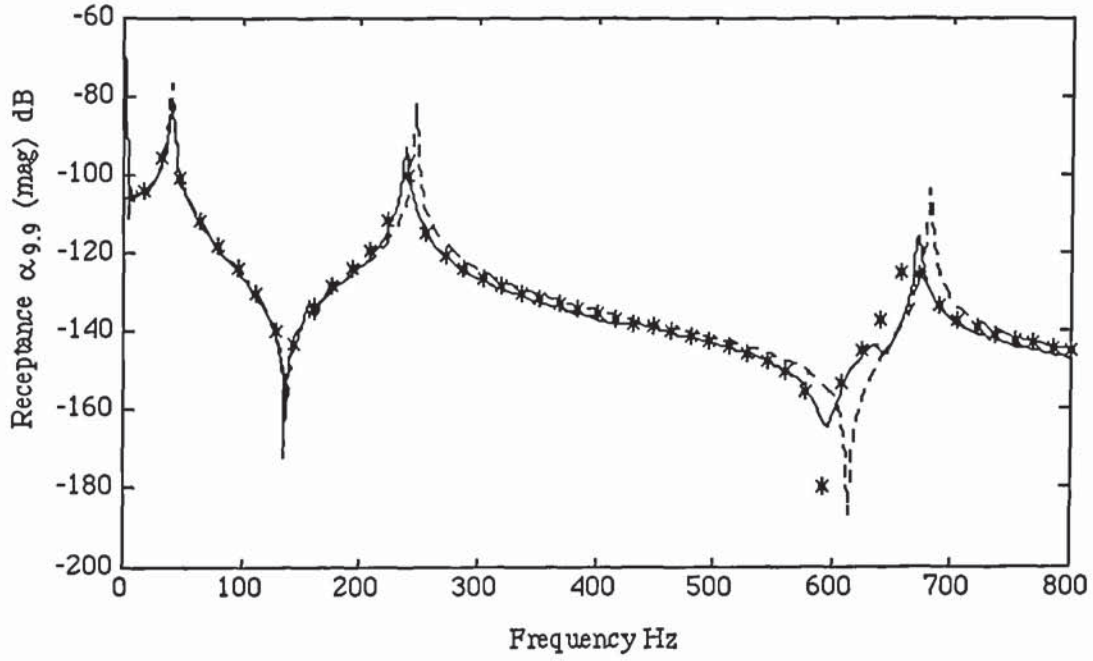

Fig 5.15 Receptance prediction at coordinate 9 of the beam for Case 2.

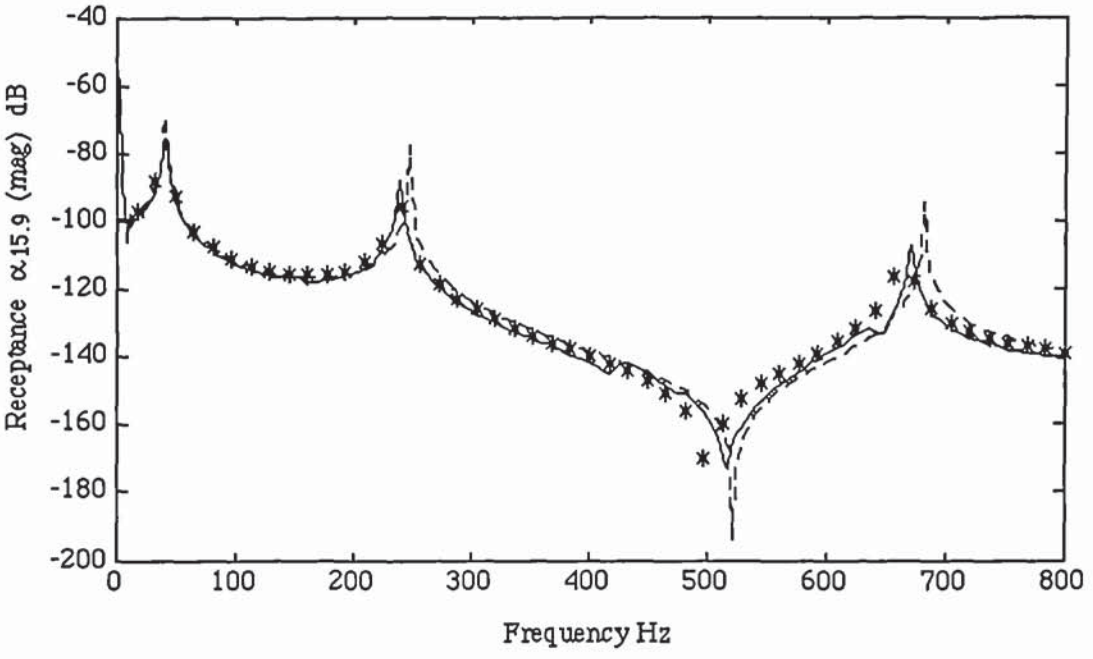

Fig 5.16 Receptance prediction at coordinate 15 of the beam for Case 2.

CASE 3

In Cases 1 and 2, parameters of the initial FE model of the beam were derived based on material and geometry data. As the beam geometry is simple, the uncertainty and hence error in the FE model is low. Case 3 simulates the case of relatively high uncertainty in the FE model parameters, by deliberately using different stiffness parameters in the FE model with high uncertainty. The element parameters were also treated as independent. The objective was to make the updating process slightly difficult and assess the reliability of the technique by comparing the updated model in the two cases. Thus, the following parameters were used for the initial FE model:

$EI_a = 4900$ Nm^2	STD = 300 Nm^2, all elements
$m_{ua} = 3.4$ kg/m	STD = 0.1 kg/m, all elements (as in Case 1)
$k_T = 4.0\text{x}10^7$ N/m	STD = $2.0\text{x}10^7$ N/m
$k_R = 2.0\text{x}10^5$ Nm/Rad	STD = $1.0\text{x}10^5$ Nm/Rad (as in Case 1)
$m_L = 0$	STD = 0.1 kg (as in Case 1)

giving rise to:

$f_{1a} = 39.4$ Hz $\qquad$ $f_{2a} = 245.6$ Hz $\qquad$ $f_{3a} = 674.2$ Hz

Parameter updating was performed by mass addition with the same masses and the same mass addition coordinates as in Cases 1 and 2, using eigenvalues of the first two modes of the perturbed and unperturbed beam (table 5.2). The analytical natural frequencies of the beam with added mass are shown in table 5.3.

Added mass (kg)	Mass addition coordinate (See fig 5.5)	Analytical natural frequencies (Hz) Mode 1	Mode 2
-	-	39.4	245.6
0.199	5	39.3	234.6
	7	39.0	228.1
	11	37.3	243.2
	13	36.0	242.9
0.355	5	39.2	226.8
	7	38.6	217.0
	11	35.8	241.6
	13	33.8	241.4

TABLE 5.3 Analytical natural frequencies of the cantilever beam (Case 3) with added mass.

The updated parameters, after 5 iterations are:

$EI_1 = 4359\ \text{Nm}^2$ $EI_2 = 4666\ \text{Nm}^2$

$EI_3 = 4839\ \text{Nm}^2$ $EI_4 = 4415\ \text{Nm}^2$

$EI_5 = 4028\ \text{Nm}^2$ $EI_6 = 4705\ \text{Nm}^2$

$EI_7 = 4923\ \text{Nm}^2$

$m_{u1} = 3.396\ \text{kg/m}$ $m_{u2} = 3.370\ \text{kg/m}$

$m_{u3} = 3.350\ \text{kg/m}$ $m_{u4} = 3.378\ \text{kg/m}$

$m_{u5} = 3.415\ \text{kg/m}$ $m_{u6} = 3.376\ \text{kg/m}$

$m_{u7} = 3.186\ \text{kg/m}$

$k_T = 5.46\text{x}10^7\ \text{N/m}$ $k_R = 2.03\text{x}10^5\ \text{Nm/Rad}$

$m_L = 0.015\ \text{kg}$

$f_1 = 38.6\ \text{Hz}$ $f_2 = 236.8\ \text{Hz}$ $f_3 = 661.0\ \text{Hz}.$

Figs 5.17-5.20 compares receptance prediction between the initial model, updated model and experimental data at coordinates 3, 5, 9 and 15 of the unperturbed beam.

Experimental data ___ , Initial model - - -, Updated model (Using eigenvalues alone) ***

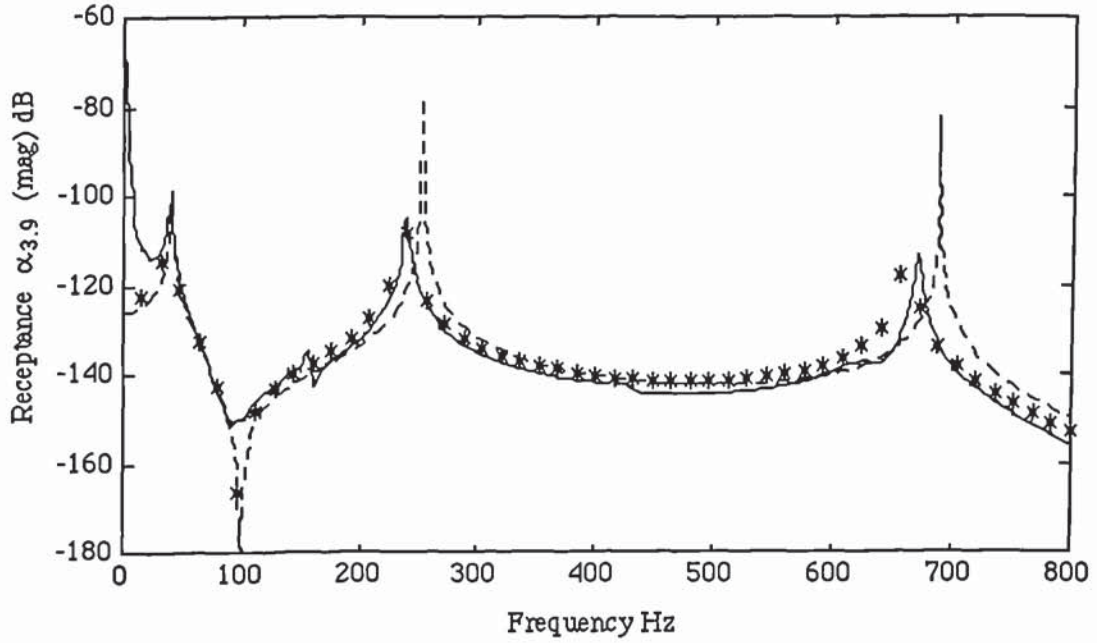

Fig 5.17 Receptance prediction at coordinate 3 of the beam for Case 3.

Experimental data ___ , Initial model - - -, Updated model (Using eigenvalues alone) ***

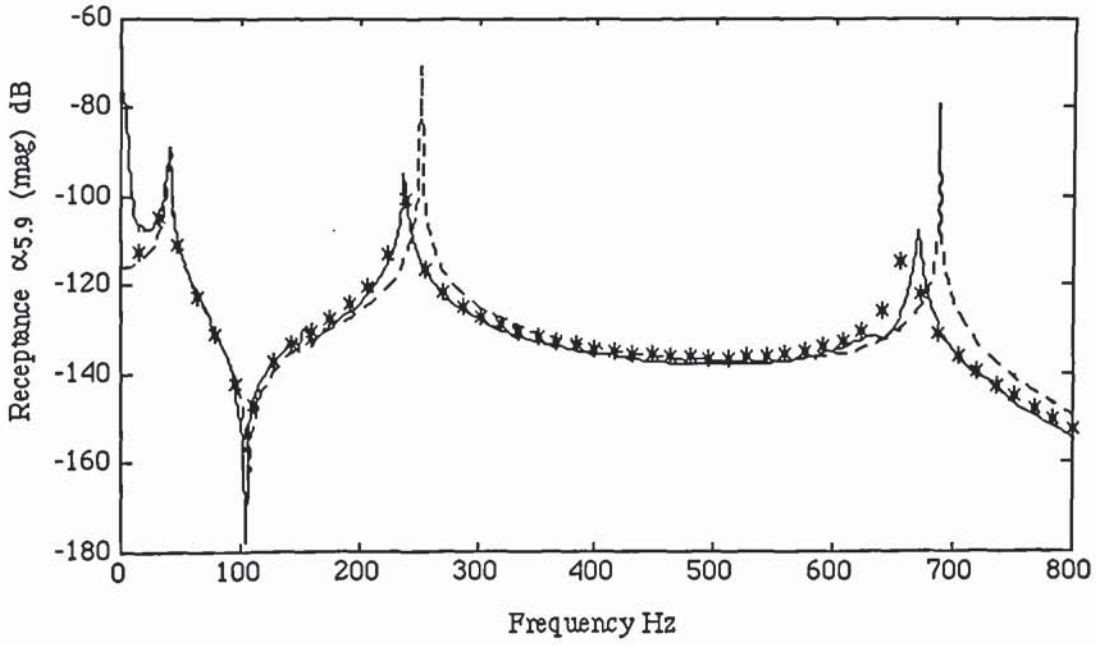

Fig 5.18 Receptance prediction at coordinate 5 of the beam for Case 3.

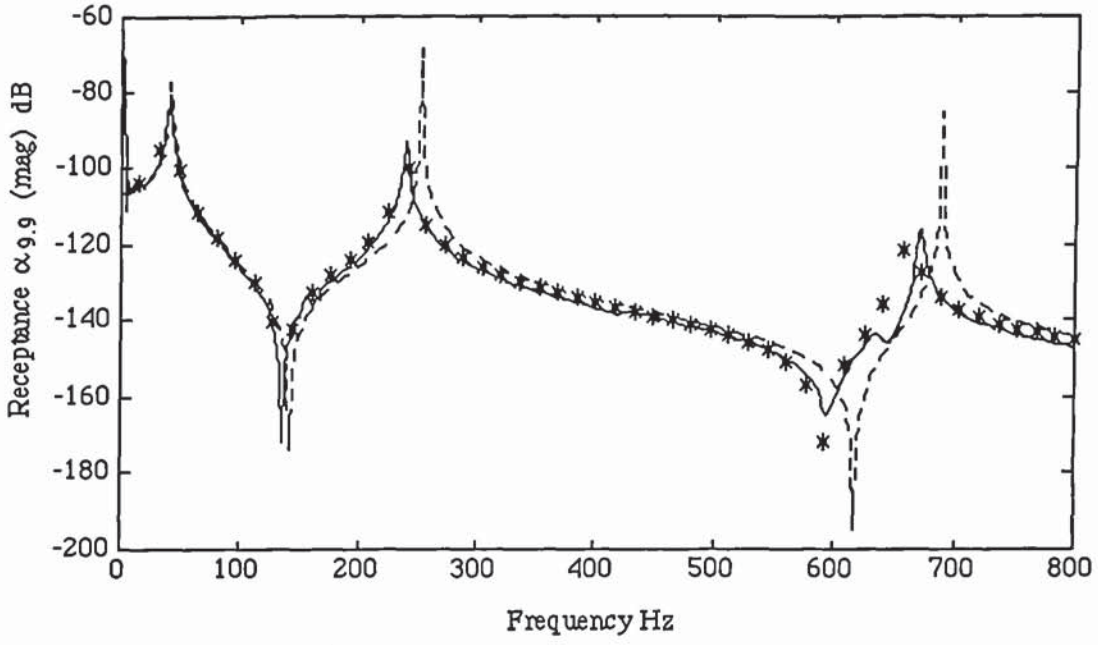

Fig 5.19 Receptance prediction at coordinate 9 of the beam for Case 3.

Experimental data ___ , Initial model - - -, Updated model (Using eigenvalues alone) ***

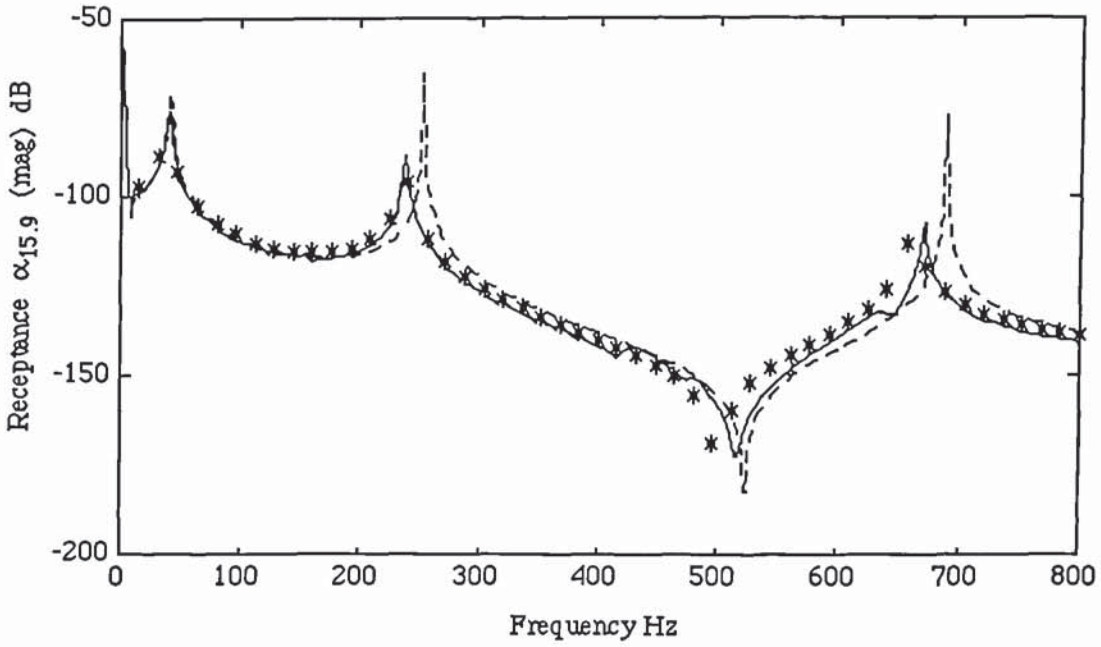

Fig 5.20 Receptance prediction at coordinate 15 of the beam for Case 3.

5.3.2 Updating the FE model of the cantilever beam using both eigenvalues and eigenvectors.

The FE model of the cantilever beam was also updated by mass addition using eigenvalues and eigenvectors. Mass of 0.199 kg was added to coordinates 5 and 11 in turn. In each perturbation, eigenvalues and mode shape data of the first two modes were measured and retained for model updating, together with the modal data of the first two modes of the unperturbed beam. The eigenvalues are a subset of the ones given in table 5.2. The mode shape data used in model adjustment was measured at four translational coordinates. These are coordinates 5, 7, 9 and 11 only. Table 5.4 gives the magnitudes and phase angles of the measured mass-normalized modes. The modes of the unperturbed beam are a subset of the modes given in table 5.1. The modes are of low complexity and were treated as real. The confidence on the mode shape data is expressed by a standard deviation of 0.05 for all measured coordinates. Two updating cases are presented, Case 4 and Case 5. Case 4 consider the fact that the beam is of a uniform geometry, and so the elements are constrained to be identical. Case 5 treats the element parameters as independent unknowns. In each case, the confidence on the initial parameter estimates is the same as in Section 5.2.5.1.

Added mass (kg)	Mass addition coordinate	Measurement coordinate	Measured modes		Analytical modes	
			Mode 1	Mode 2	Mode 1	Mode 2
0	-	5	0.2165 (0.03)	0.6045 (0.01)	0.1671	0.6598
		7	0.3184 (-0.09)	0.8170 (0.01)	0.3361	0.9050
		9	0.4712 (-0.03)	0.7156 (-0.06)	0.5415	0.8171
		11	0.7482 (-0.06)	0.3085 (-0.01)	0.7697	0.3624
0.199	5	5	0.1599 (-0.03)	0.5662 (-0.06)	0.1671	0.6463
		7	0.3157 (-0.02)	0.7405 (-0.07)	0.3357	0.8647
		9	0.4944 (-0.02)	0.6574 (-0.03)	0.5404	0.7607
		11	0.6969 (-0.02)	0.2356 (-0.08)	0.7677	0.3176
0.199	11	5	0.1902 (0.03)	0.5896 (0.08)	0.1586	0.6366
		7	0.3193 (0.01)	0.7825 (0.11)	0.3187	0.8723
		9	0.4490 (-0.04)	0.7523 (0.13)	0.5132	0.7820
		11	0.6523 (-0.04)	0.3404 (0.08)	0.7287	0.3262

TABLE 5.4 Measured and analytical mass-normalized modes with and without added mass (Values in brackets are phase angles in degrees).

CASE 4

When the elements are treated as having non-independent parameters due to the uniformity of the beam, the number of unknowns to update is 5. The two eigenvalues and mode shape vectors measured at four coordinates does, in theory, contain sufficient dynamic characteristic information to update the 5 unknown parameters. The use of mass addition in this case simply increases the

data sample by increasing the total number of data points. The updated parameters, in this case, converged after 5 iterations to:

$EI = 4180\ \text{Nm}^2$ $\quad m_u = 3.28\ \text{kg/m}$

$k_T = 7.79\text{x}10^7$ $\quad k_R = 3.23\text{x}10^5\ \text{Nm/Rad}$

$m_L = 0.019\ \text{kg}$

$f_1 = 38.1\ \text{Hz}$ $\quad f_2 = 237.3\ \text{Hz}$ $\quad f_3 = 661.4\ \text{Hz}.$

Fig 5.21 show the convergence of the mass and stiffness parameters of the beam.

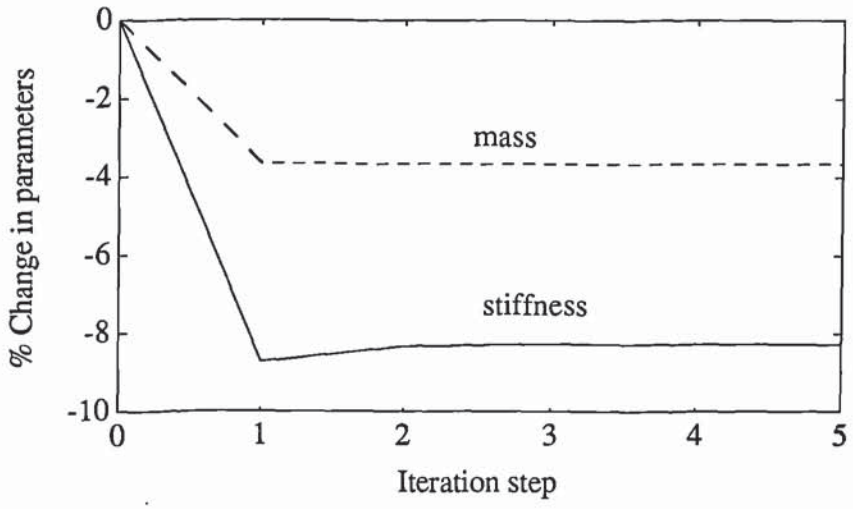

Fig 5.21 Convergence of the mass and stiffness parameters of the uniform cantilever beam for Case 4.

The frequency response functions (receptances) predicted by the updated and the initial models are compared with the experimental data at coordinates 9 and 15 in figs 5.22 and 5.23.

Experimental data __ , Initial model - - - , Updated model (eigenvalues & eigenvectors) ***

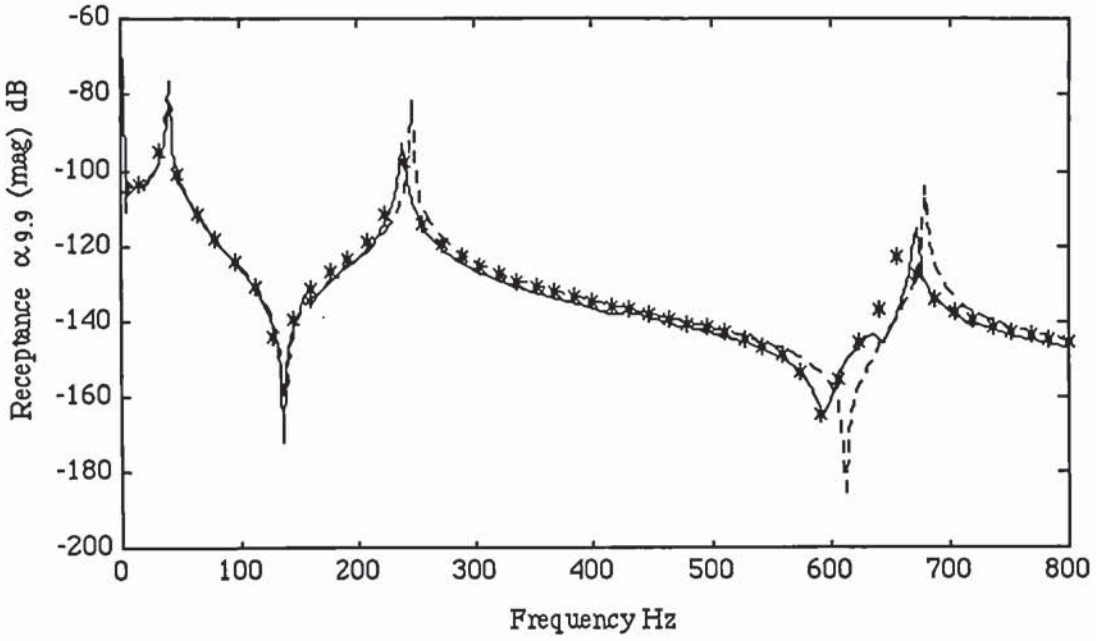

Fig 5.22 Receptance prediction at coordinate 9 of the beam for Case 4.

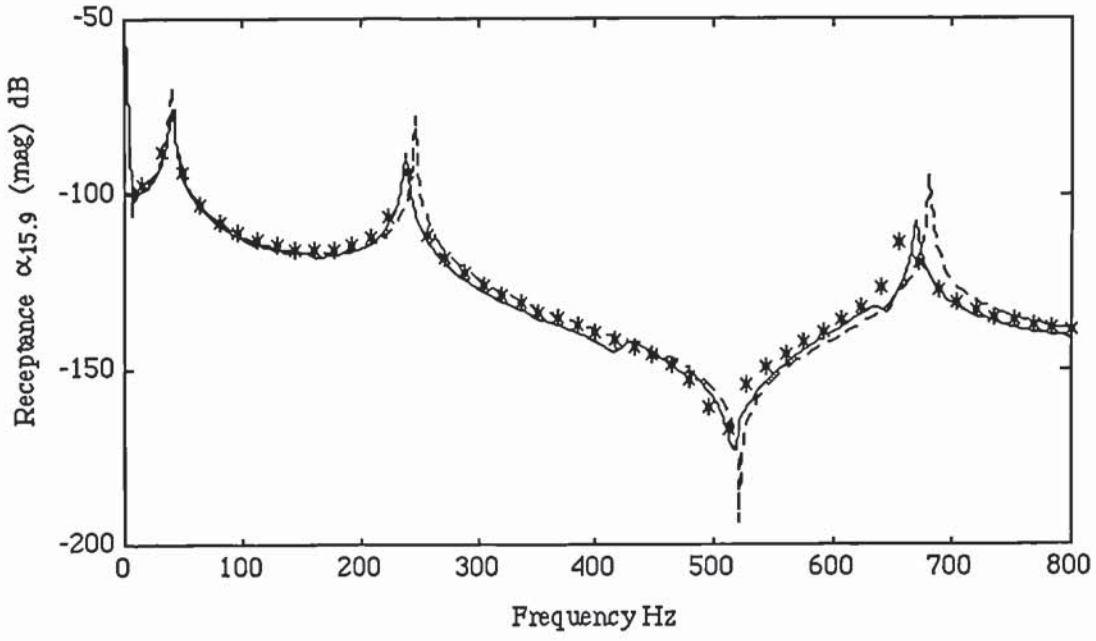

Fig 5.23 Receptance prediction at coordinate 15 of the beam for Case 4.

CASE 5

When the elements were treated as having independent unknown parameters, the updated parameters, after 5 iterations, converged to.

$EI_1 = 4463\ \text{Nm}^2$ $EI_2 = 4485\ \text{Nm}^2$
$EI_3 = 4537\ \text{Nm}^2$ $EI_4 = 4512\ \text{Nm}^2$
$EI_5 = 4375\ \text{Nm}^2$ $EI_6 = 4446\ \text{Nm}^2$
$EI_7 = 4550\ \text{Nm}^2$

$m_{u1} = 3.40$ kg/m $m_{u2} = 3.41$ kg/m
$m_{u3} = 3.42$ kg/m $m_{u4} = 3.42$ kg/m
$m_{u5} = 3.36$ kg/m $m_{u6} = 3.31$ kg/m
$m_{u7} = 3.43$ kg/m

$k_T = 8.05\text{x}10^7$ N/m $k_R = 2.13\text{x}10^5$ Nm/Rad
$m_L = 0.005$ kg
$f_1 = 38.1$ Hz $f_2 = 237.3$ Hz $f_3 = 661.6$ Hz

Figs 5.24 and 5.25 shows the convergence of the mass and stiffness parameters for the first 4 elements starting from the clamped end. Figs 5.26-5.28 compares receptance of the updated model, initial model and experimental data at coordinates 3, 9, and 15.

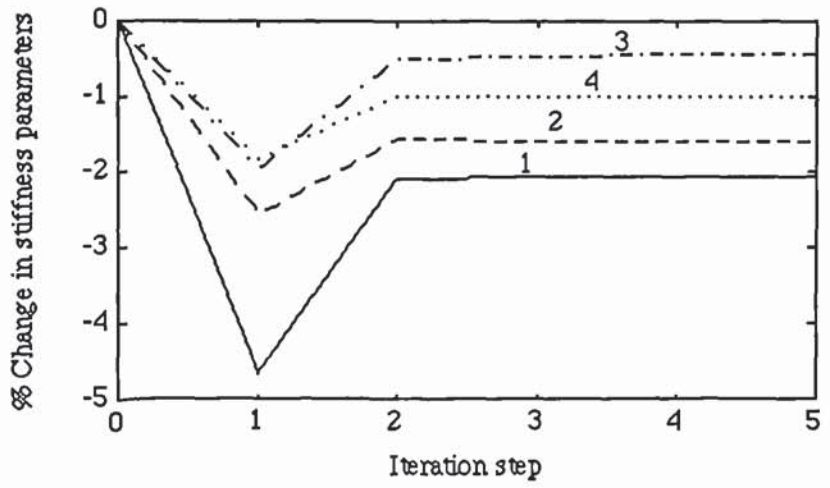

Fig 5.24 Convergence of the stiffness parameters of elements 1-4 of the cantilever beam for Case 5.

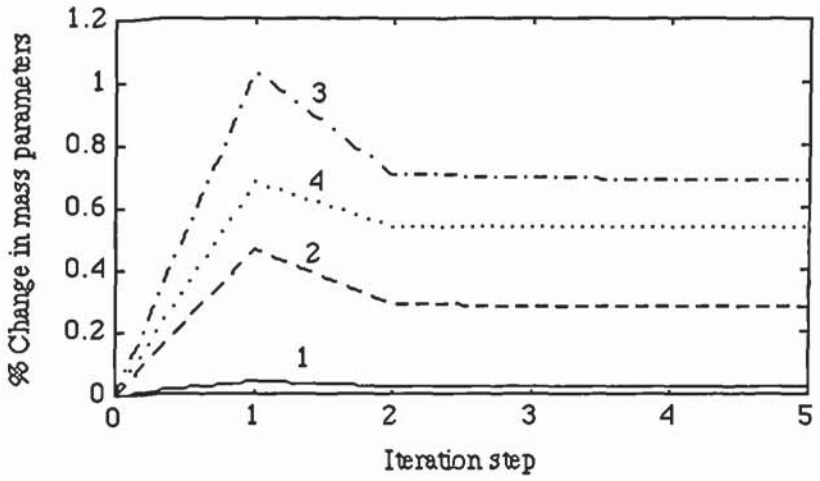

Fig 5.25 Convergence of the mass parameters of elements 1-4 of the cantilever beam for Case 5.

Experimental data __ , Initial model - - - , Updated model (eigenvalues & eigenvectors) ***

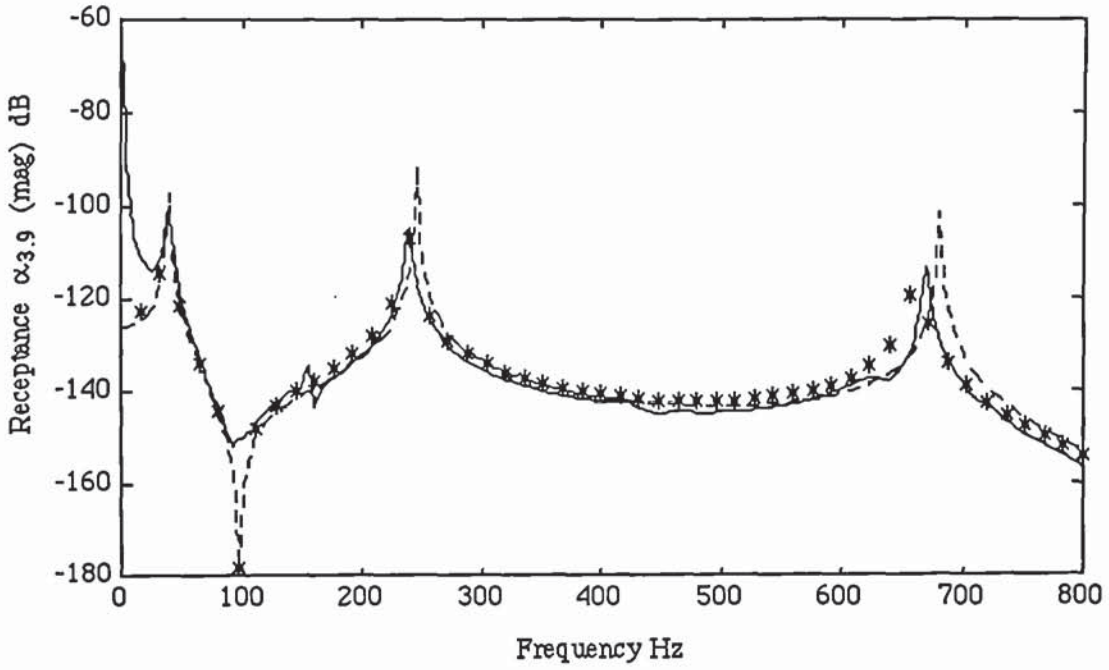

Fig 5.26 Receptance prediction at coordinate 3 of the beam for Case 5.

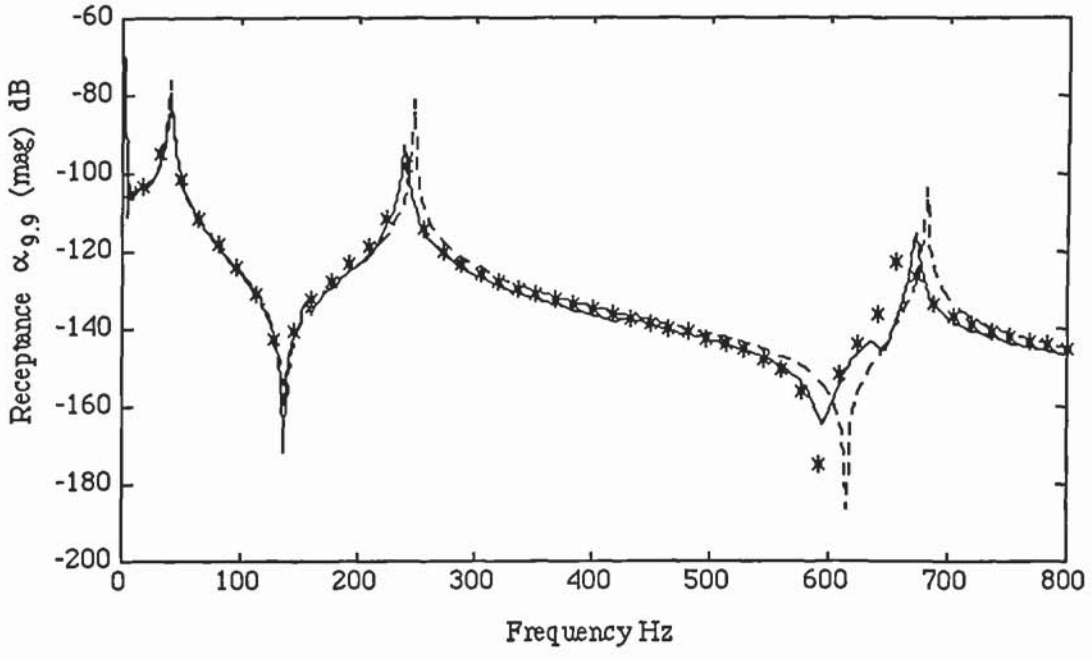

Fig 5.27 Receptance prediction at coordinate 9 of the beam for Case 5.

Experimental data __ , Initial model - - - , Updated model (eigenvalues & eigenvectors) ***

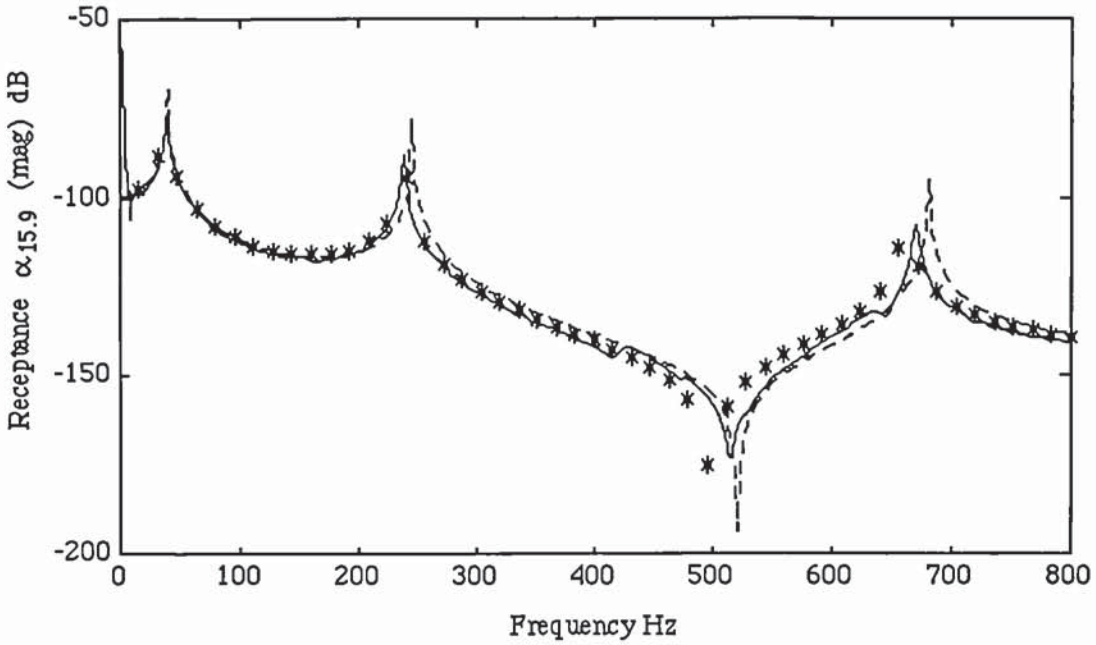

Fig 5.28 Receptance prediction at coordinate 15 of the beam for Case 5.

5.4 Updating a FE model of the free beam using eigenvalues.

The beam of Section 5.2.5 was tested in a free-free configuration and was modelled by an 8 elements, 18 DOF FE model based on a simple beam theory which ignore the effects of rotary inertia and shear deformation. The FE model is shown in fig 5.29, where coordinate 11 is excited. Natural frequencies and damping factors were determined from receptances measured at each translational coordinate.

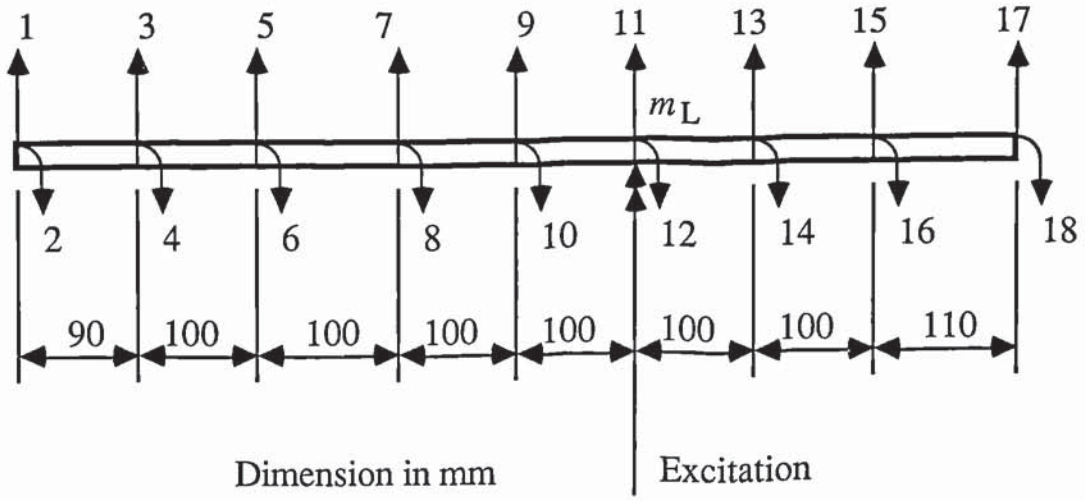

Fig 5.29 Free-free beam

The measurement frequency range was from 0 to 1600 Hz with a resolution of 2 Hz. Measured natural frequencies for the first three elastic modes are:

$$f_1 = 200.1 \text{ Hz} \quad f_2 = 548.4 \text{ Hz} \quad f_3 = 1075 \text{ Hz}$$

Their confidence is expressed by the following estimates of standard deviations.

$$\text{STD}f_1 = 0.5 \text{ Hz} \qquad \text{STD}f_2 = \text{STD}f_3 = 1 \text{ Hz}.$$

There was a considerable variation of the damping factors evaluated from measurements at different coordinates, but they were all very small the maximum being less than 0.002. The natural frequencies were therefore treated as the undamped natural frequencies and the damping factors ignored.

The analytical model had the same initial parameters as the cantilever beam model. Thus (element numbers start from the left-hand-side of fig 5.29):

$$EI_{1a} = \ldots = EI_{8a} = 4557 \text{ Nm}^2, \quad \text{STD } EI_a = 150 \text{ Nm}^2.$$
$$m_{u1,a} = \ldots = m_{u8,a} = 3.4 \text{ kg/m}, \quad \text{STD } m_{ua} = 0.1 \text{ kg/m}$$
$$m_L = 0 \text{ kg}, \qquad \text{STD } m_L = 0.1 \text{ kg}.$$

Resulting in $f_{1a} = 203.7$ Hz $f_{2a} = 561.8$ Hz $f_{3a} = 1103.0$ Hz.

The analytical model was updated by mass addition using eigenvalues of the first two elastic modes only. The 8 elements were treated as having independently unknown parameters. Thus, 16 mass and stiffness parameters of the beam and 1 parameter for the mass loading of the shaker-beam interface were updated.

The added mass was 0.199 kg at each of the translational coordinates giving a total of 20 eigenvalues for the first two elastic modes. Table 5.5 shows measured and analytical natural frequencies of the mass added beam. Standard deviations of 0.5 Hz and 1 Hz for the first and second modes respectively, were also assumed for the natural frequencies of the mass added beam.

The updated parameters, after 4 iterations, are:

$$EI_1 = 4520 \text{ Nm}^2 \qquad EI_2 = 4337 \text{ Nm}^2$$

$EI_3 = 4384\ \text{Nm}^2$ $EI_4 = 4517\ \text{Nm}^2$

$EI_5 = 4450\ \text{Nm}^2$ $EI_6 = 4426\ \text{Nm}^2$

$EI_7 = 4459\ \text{Nm}^2$ $EI_8 = 4529\ \text{Nm}^2$

$m_{u1} = 3.22$ kg/m $m_{u2} = 3.50$ kg/m

$m_{u3} = 3.52$ kg/m $m_{u4} = 3.42$ kg/m

$m_{u5} = 3.41$ kg/m $m_{u6} = 3.41$ kg/m

$m_{u7} = 3.43$ kg/m $m_{u8} = 3.37$ kg/m

$m_L = 0.076$ kg

$f_1 = 199.9$ Hz $f_2 = 545.6$ Hz $f_3 = 1083.4$ Hz

Mass addition coordinate	Measured natural frequencies (Hz)		Analytical natural frequencies (Hz)	
	Mode 1	Mode 2	Mode 1	Mode 2
1	179.3	493.6	183.3	514.1
3	194.1	541.2	198.2	560.6
5	200.1	525.2	203.6	540.4
7	195.2	521.2	198.4	537.6
9	190.8	548.5	194.2	561.5
11	193.9	528.6	197.1	542.8
13	199.7	522.5	203.1	535.3
15	196.2	544.9	200.4	561.7
17	179.1	500.9	183.3	514.0

TABLE 5.5 Measured and analytical natural frequencies of the beam with added mass.

Figs 5.30 and 5.31 shows the convergence of the stiffness and mass parameters of the last four elements as percentage changes from their initial estimates. Figs 5.32 to 5.34 compare receptance prediction between the updated model,

initial model and experimental data at coordinates 1, 9, and 15, when coordinate 11 is excited. The updated model shows a reasonable agreement with the experimental data.

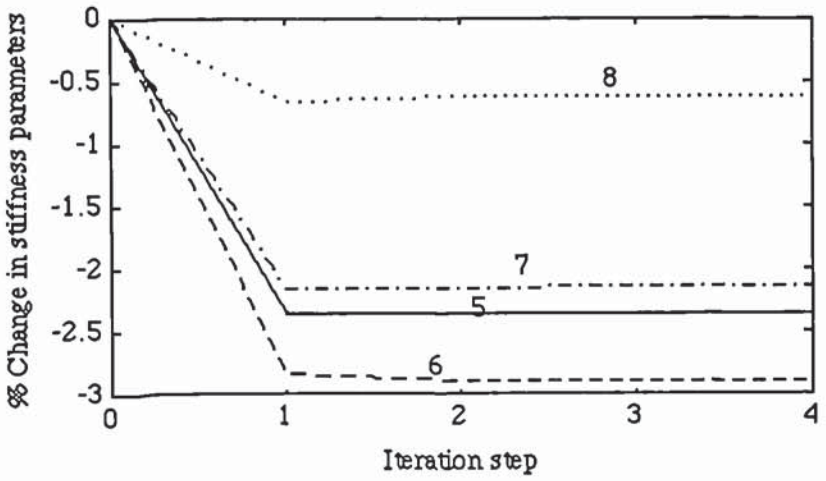

Fig 5.30 Convergence of the stiffness parameters of 4 elements of the free beam.

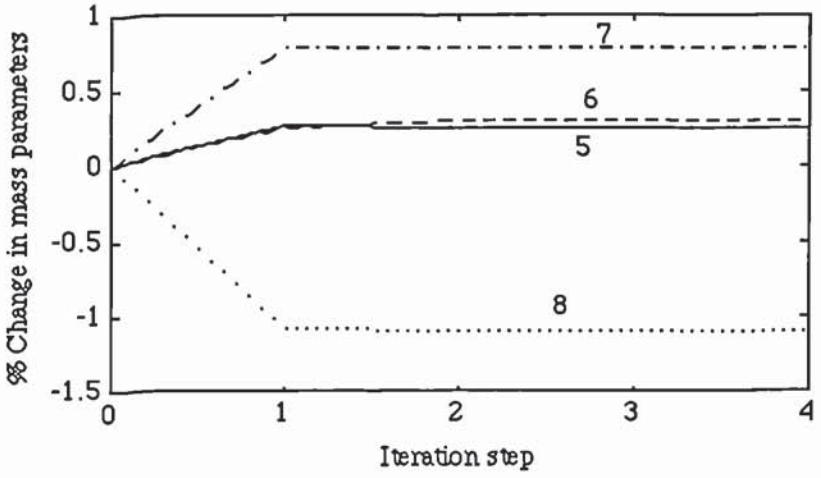

Fig 5.31 Convergence of the mass parameters of 4 elements of the free beam.

Experimental data ___ , Initial model - - -, Updated model (Using eigenvalues alone) * * *

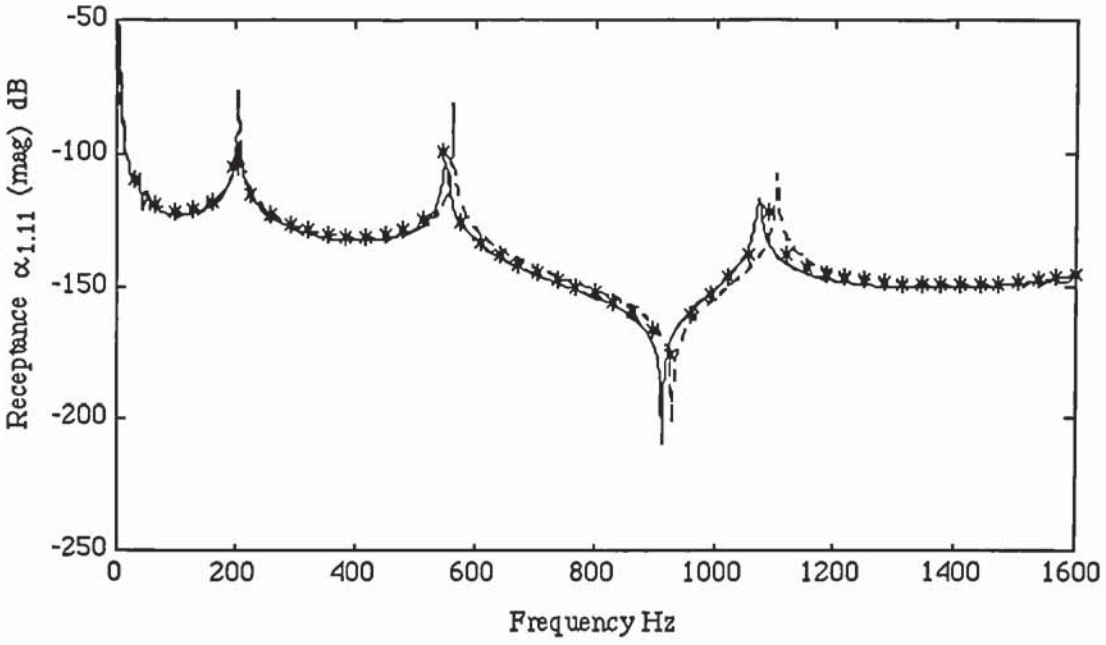

Fig 5.32 Receptance prediction at coordinate 1 of the free beam.

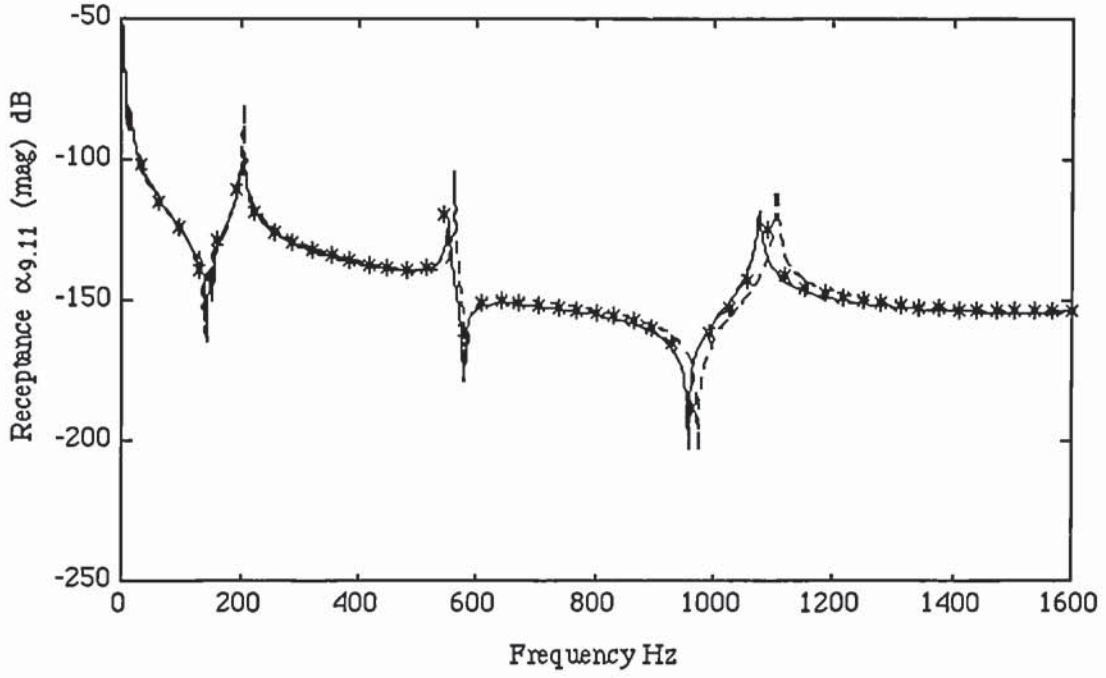

Fig 5.33 Receptance prediction at coordinate 9 of the free beam.

Experimental data ___ , Initial model - - -, Updated model (Using eigenvalues alone) * * *

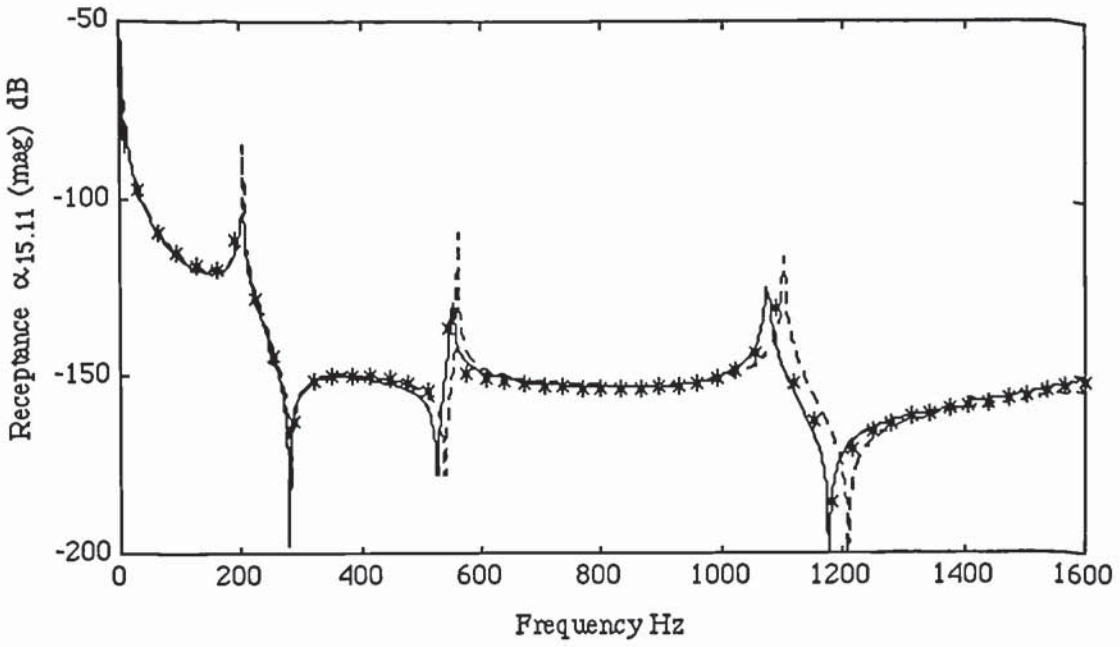

Fig 5.34 Receptance prediction at coordinate 15 of the free beam.

5.5 Discussion.

This chapter is devoted to the application of the mass addition technique in updating a FE model of a laboratory structure. The structure considered is a uniform beam tested in free-free and clamped-free conditions. It was found that, the FE model of the clamped-free beam with an assumption of a rigid boundary condition was not adequate to describe the measured dynamic characteristics. The FE model was improved by considering the flexibility at the clamped end. Since the beam is relatively light, mass loading of the shaker could also affect its eigen-characteristics. The FE model was updated by updating mass and stiffness parameters of the beam, stiffness parameters at the clamped end and mass loading of the shaker-beam interface.

While the beam is uniform, two modelling approaches have been studied. In one case the elements were treated as having independent parameters and in the

other case the uniformity of the beam was maintained by constraining its parameters to be identical. Both approaches resulted in models with improved dynamic characteristics than the initial analytical model. When the beam element parameters were treated as completely independent, the result was a non-uniform beam, in the sense that the elements of the updated model were of different mass and different stiffness parameters. This is to be expected since the measured data is not exact. The updated parameters, therefore, contain errors of varying magnitudes. With an unconstrained parameter estimation algorithm, large unrealistic changes in the parameters could result from very small errors in the measured data. The use here of the minimum cost Bayesian estimator, limits the variation of the parameters to orders of magnitude comparable to the uncertainty specified on the initial estimates. This is consistent with the findings from the numerical simulation in Chapter 4.

In all cases, only the first two elastic modes were used in the updating process. The improvement in the receptance prediction can be observed over a larger frequency range, up to the third mode. This together with the fact that the changes in element parameters are comparable with the uncertainty in the initial parameters suggest that the structure of the model matrices is acceptable for dynamic modelling over the measured frequency range. However, it is reasonable to make use of prior knowledge of the uniformity of the beam and to use this in a practical modelling problem. The models dealt with in this Chapter can be further improved by updating using all three modes in the measured frequency range.

The flexibility at the clamped end of the beam in a clamped-free test was modelled by lumped translational and rotational stiffeners. Since it is difficult to estimate the magnitudes of the lumped stiffeners in the analytical model, some rough values were obtained by trial and error. This is only one possible

modelling approach and its difficulty is in obtaining reasonable values of the stiffeners in the initial model. An alternative is to assume the stiffness parameter of the element next to the clamped end as independent from other elements of otherwise uniform beam. It is not intended to go into the details of analytical modelling techniques, but it is evident that the later approach creates some discomfort on how to visualize the physical interpretation of the parameters.

CHAPTER 6

UPDATING BY SIMULATION OF ADDITIONAL STIFFNESS OR MASS

6.1 Introduction

The technique of model parameter updating by mass or stiffness addition involves perturbing the system and its analytical model, by adding mass or stiffness in order to change the eigen-characteristics. The eigen-data of the perturbed and the unperturbed systems are then used in a model updating algorithm based on sensitivity analysis. The success of the technique depends, among other factors, on the generation of eigen-data which, in general, are different from one perturbation to another. If the added mass or stiffness is relatively small, the eigen-data generated from one mass or stiffness addition to another will be virtually unchanged and the eigen-data sensitivity matrix close to singular. In general, the bigger the changes in the eigen-data, the better. So far, it has been assumed that the simulated systems could be physically perturbed using the assumed additional masses and stiffeners. For small structures, mass addition is practically feasible as demonstrated by laboratory experiments on beams in Chapter 5. For large structures, the size of the additional mass to achieve even small measurable natural frequency changes may be impractical. Furthermore, adding stiffness may not be easy, especially when the unperturbed structure is in a free-free test configuration. In this Chapter, the feasibility of adding stiffness or mass by numerical simulation and determining the eigen-data of the perturbed structure using the FRF of the unperturbed structure is investigated. The simulation of the addition mass or stiffness is based on a structural modification approach to find a new set of eigen-data of a modified system.

6.2 Theoretical derivation

Consider a primary structure, P in fig 6.1, on to which is coupled a secondary structure, S. The secondary structure is the perturbing mass rigidly attached to the primary structure or the perturbing grounded stiffener and the perturbation is at a single degree of freedom, *l*.

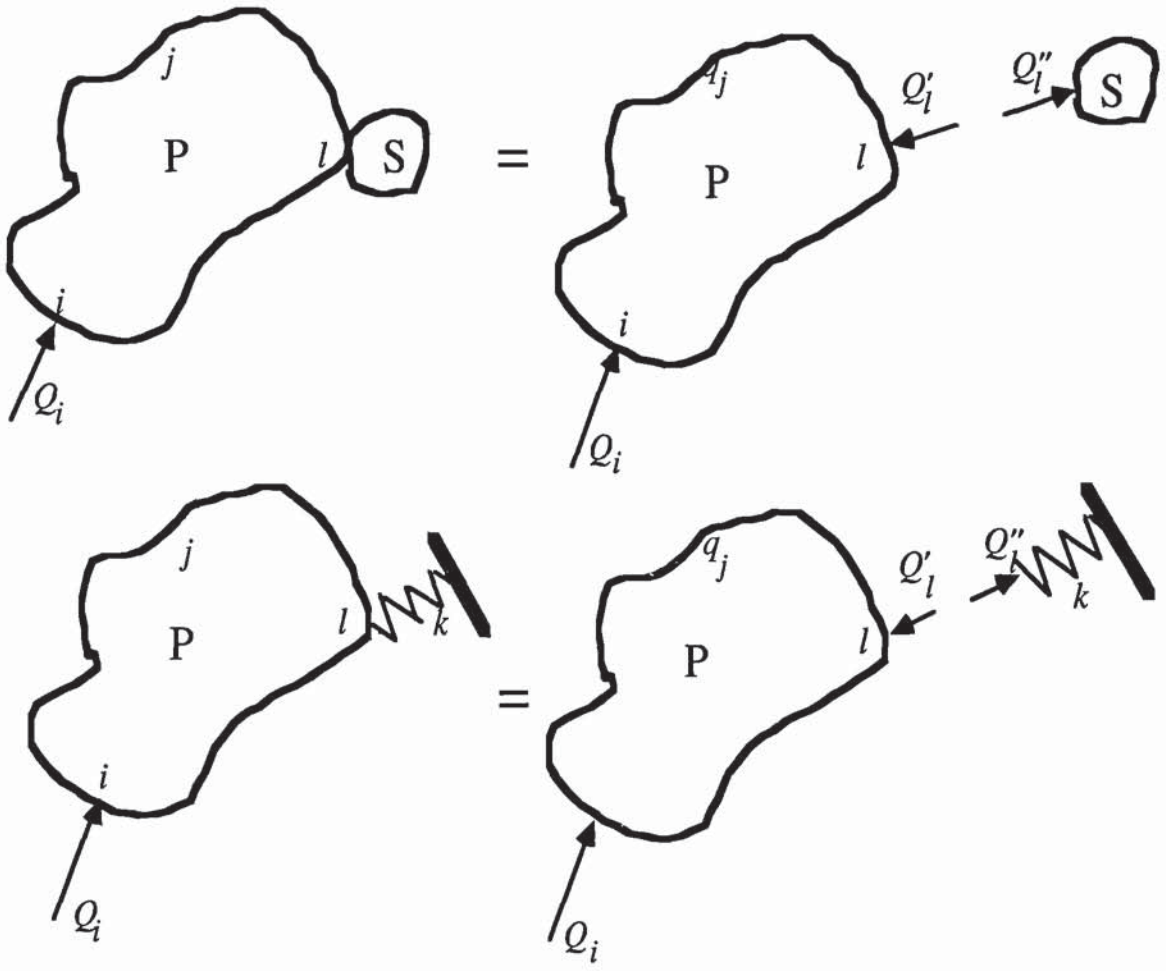

Fig 6.1 Primary structure, P, with mass or stiffness modification at DOF *l*.

Consider the excitation of the perturbed structure at a single coordinate, i. The response, q, at any coordinate j, can be written as,

$$q_j^p = \alpha_{ji} Q_i + \alpha_{jl} Q'_l \tag{6.1}$$

where the response superscript, p, denotes the perturbed system. Q''_l is the force exerted by the primary structure on the secondary structure and Q'_l is the reaction force exerted by the perturbing mass or stiffness on the primary structure at l. The forces exerted on the perturbing mass or stiffness are given by:

Force on the perturbing mass $Q''_l = -\omega^2 m q_l^p$

Force on the perturbing stiffness $Q''_l = k q_l^p$

Therefore

for mass addition $Q'_l = \omega^2 m q_l^p$ (6.2)

for stiffness addition $Q'_l = -k q_l^p$ (6.3)

In the case of stiffness addition, (6.1) becomes:

$$q_j^p = \alpha_{ji} Q_i - \alpha_{jl} k q_l^p \tag{6.4}$$

Divide (6.4) by Q_i and noting $q_j^p/Q_i = \alpha_{ji}^p$ and $q_l^p/Q_i = \alpha_{li}^p$, (6.4) simplifies to:

$$\alpha_{ji}^p = \alpha_{ji} - k\alpha_{jl}\alpha_{li}^p \tag{6.5}$$

Equation (6.5) is not in a convenient form to estimate the FRF, and hence eigen-data, of the perturbed structure as it contains two receptances of the perturbed structure, which are not known. It can be simplified by letting the perturbed coordinate to be the excitation coordinate (Let $l = i$). Therefore:

$$\alpha_{ji}^{p} = \alpha_{ji} - k\alpha_{ji}\alpha_{ii}^{p} \tag{6.6}$$

Equation (6.6) still contains two receptances of the perturbed structure. However, α_{ii}^{p} can be eliminated by expressing it in terms of the receptances of the primary structure, by letting $j = i$, in (6.6).

$$\alpha_{ii}^{p} = \alpha_{ii} - k\alpha_{ii}\alpha_{ii}^{p} \tag{6.7}$$

Therefore:

$$\alpha_{ii}^{p} = \frac{\alpha_{ii}}{1 + k\alpha_{ii}} \tag{6.8}$$

Substitute (6.8) into (6.6), an expression for α_{ji}^{p} is obtained as:

$$\alpha_{ji}^{p} = \alpha_{ji}\left(1 - \frac{k\alpha_{ii}}{1 + k\alpha_{ii}}\right) \tag{6.9}$$

Equations (6.8) and (6.9) could then be used to construct the FRF of the perturbed structure using FRF data of the unperturbed structure. The modal data of the perturbed structure can then be determined from the constructed FRF using any of the established modal analysis algorithms. With error-free data, exact FRF of the perturbed structure will be obtained. Since measured data is always contaminated by measurement errors, the FRF estimated using (6.8) and (6.9) will also contain errors. Since (6.8) and (6.9) are non-linear functions of the FRF of the unperturbed structure, the magnitude of the errors in the constructed FRF varies in a way which is completely different from the errors in α_{ii} and α_{ji}. At frequencies in the vicinity of the natural frequencies of the perturbed structure, small errors in α_{ii} results in large errors in α_{ii}^{p}. This can be seen by deriving expressions for the changes in α_{ii}^{p} and α_{ji}^{p} due to the

changes in α_{ii} and α_{ji}.

$$\Delta\alpha_{ii}^{p} = \frac{\partial\alpha_{ii}^{p}}{\partial\alpha_{ii}}\Delta\alpha_{ii} = \frac{1}{(1+k\alpha_{ii})^{2}}\Delta\alpha_{ii} \tag{6.10}$$

$$\Delta\alpha_{ji}^{p} = \frac{\partial\alpha_{ji}^{p}}{\partial\alpha_{ji}}\Delta\alpha_{ji} + \frac{\partial\alpha_{ji}^{p}}{\partial\alpha_{ii}}\Delta\alpha_{ii}$$

$$= \left(1 - \frac{k\alpha_{ii}}{(1+k\alpha_{ii})}\right)\Delta\alpha_{ji} + \frac{k\alpha_{ji}}{(1+k\alpha_{ii})^{2}}\Delta\alpha_{ii} \tag{6.11}$$

Thus, it may be necessary to consider weighting the data of the constructed FRF in a modal extraction algorithm.

6.3 Simplification for lightly damped structures

There are many types of structures which are so lightly damped that an undamped or a proportionally damped FE model with properly updated parameters could be adequate to describe its dynamic behaviour. A simplification for such systems is possible. This avoids the necessity of constructing FRFs of the perturbed structure and extracting the modal data from the constructed FRFs. The simplified approach cannot extract damping factors of the perturbed structure. Therefore, with proportional damping, the undamped model will first be updated by sensitivity analysis and then updating the damping proportionality constants using the orthogonality equation of the damping matrix with respect to the updated model's real modes.

Recall the expression for point receptance, α_{ii}, of a system with hysteretic

damping:

$$\alpha_{ii} = \sum_{j=1}^{N} \frac{U_{ii}U_{ii}}{\left(\omega_j^2 - \omega^2 + j\eta_j\omega_j^2\right)} \tag{6.12}$$

If the system is undamped, $\eta_j = 0$, receptance amplitude is infinity at the natural frequencies of the system ($\omega = \omega_j$). Likewise, receptance of the perturbed undamped system will become infinity at frequencies corresponding to the natural frequencies of the perturbed system. Therefore, from (6.8):

$$1+k\alpha_{ii} = 0 \quad \text{at} \quad \omega = \omega_j^p. \tag{6.13}$$

Thus, it is possible to determine the natural frequencies, ω_j^p, of the perturbed structure, using (6.13), by simply determining the frequencies at which α_{ii} of the unperturbed structure is equal to $-1/k$. If mode shape of the perturbed structure is also required, it is simply given by the deflection shape at ω_j^p. The deflection shape can be determined from the receptances, which at ω_j^p determines the mode shape.

$$V_j = \{\alpha(\omega_j^p)\} \tag{6.14}$$

Mode shapes determined in this way are only arbitrary scaled, whereas mode shapes required in parameter estimation are mass normalized. As the modal masses are not known, modal masses of the current analytical model will be used in the normalization. The analytical modal masses will be updated after each iteration until convergence in the mass and stiffness parameters is reached. At that point, the mass normalized modes of the updated system will, hopefully, also converge towards the true mass normalized modes of the real system. However, this requires the non-mass normalized modes determined by

(6.14) to be scaled in the same way as the non-mass normalized modes of the analytical model, before mass normalization is effected. A simple way is to scale each vector such that the biggest term for the mode shape displacement of the perturbed structure (defined at the measurement coordinates) is unity. The analytical modes are then scaled such that coordinates corresponding to unity in the structure's modes are also scaled to unity.

Thus, lets redefine $V_{mm,j}$ to be the jth mode shape of the perturbed structure (at the measurement coordinates) determined from (6.14) and scaled such that the biggest term is unity. Let $V_{a,j}$ be the jth mode shape of the perturbed analytical model. The mass normalized mode shape of the analytical model, $U_{a,j}$, and an estimate of the mass normalized mode of the perturbed structure, at the current iteration, $U_{mm,j}$, will be given by dividing $V_{a,j}$ and $V_{mm,j}$ by the square root of $V_{a,j}^T \mathbf{M}_a V_{a,j}$. This approach inevitably results in the errors in the analytical model being transmitted to the estimated mass normalized modes of the perturbed structure and contributes to non-random errors in $U_{mm,j}$. Non-random errors result in biased estimates, but the degree of bias is reduced by the iteration process which updates $U_{mm,j}$. The convergence rate, however, will be relatively slower than in the case where eigenvalues alone are used.

It should be noted that the frequency is measured at discrete intervals, and therefore it is difficult to solve (6.13) exactly for a given k and a given FRF ($\alpha_{ii}(\omega)$), even if data for $\alpha_{ii}(\omega)$ is exact. Thus small errors in the data, due to frequency resolution, are inevitable. This type of error, however, is not very important as it can be minimized to negligible levels by zooming and increasing the resolution around the estimated resonance zone. An alternative idea is to curve fit the FRF over the zone expected to contain the natural frequency of interest using a low order polynomial. Curve fitting using a first order polynomial (linear interpolation) is discussed in section 6.3.1.

6.3.1 Simulation examples: Undamped system.

EXAMPLE 6.1

Consider the beam of example 4.1. The beam is 1 m long and is made of uniform geometry and material with the following structural parameters, EI = 5000 Nm^2 and m_u = 3.5 kg/m.

Consider the idealization of the beam into a free-free configuration and let its dynamic characteristics be, for simplicity, adequately modelled by a 4 elements 10 DOF finite element model with elements of equal length, fig 6.2. The first three natural frequencies are:

f_1 = 134.73 Hz $\qquad$ f_2 = 373.30 Hz $\qquad$ f_3 = 733.05 Hz.

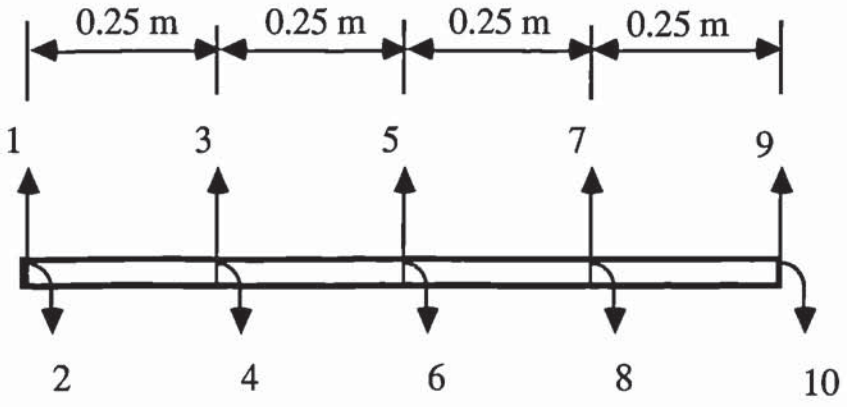

Fig 6.2 Simulated undamped free beam

The 4 element model will be used to simulate the error-free FRF of the physical structure. Let the analytical model have the following parameters, where it is considered that elements may not have identical parameters and therefore a total of 8 parameters are to be updated (element numbers starts

from the left end of the beam).

$EI_{1,a} = 5300\ \text{Nm}^2$ $EI_{2,a} = 4800\ \text{Nm}^2$ $EI_{3,a} = 5200\ \text{Nm}^2$
$EI_{4,a} = 4900\ \text{Nm}^2$ $m_{u1,a} = 3.3\ \text{kg/m}$ $m_{u2,a} = 3.3\ \text{kg/m}$
$m_{u3,a} = 3.3\ \text{kg/m}$ $m_{u4,a} = 3.3\ \text{kg/m}$.

$f_{1a} = 138.76\ \text{Hz}$ $f_{2a} = 385.53\ \text{Hz}$ $f_{3a} = 758.45\ \text{Hz}$

The analytical model will now be updated by numerical simulation of the additional stiffness. The eigen-data of the perturbed beam will be determined from the FRF of the unperturbed beam. In this case the beam is undamped and the FRF will not be contaminated by errors, hence accurate parameters should be identified using an unconstrained least square solution of the sensitivity equations. Two studies are performed, using eigenvalues alone and using both eigenvalues and eigenvectors.

UPDATING USING EIGENVALUES

There are 8 parameters to update. Let coordinates 3 and 5 be perturbed analytically by stiffness addition and use the first three eigenvalues of the perturbed and unperturbed system in the updating process. The stiffeners are $2.0\text{x}10^6$ N/m and $1.0\text{x}10^7$ N/m. There will therefore be a total of 15 equations in 8 unknowns. Since coordinates 3 and 5 are perturbed, these coordinates must also be excited. The eigenvalues of the perturbed beam will be determined from the point receptances simulated to have been measured at coordinates 3 and 5, using (6.13). Figs 6.3 and 6.4 shows the point receptances as well as the point receptances of the analytical model, at a resolution of 2 Hz.

The natural frequencies of the perturbed beam are given by locating the

frequencies at which the point receptances are given by $-1/k$. Since 0 dB represent a receptance magnitude of 1 m/N (reference 1 m/N), stiffness addition of $2x10^6$ N/m and $1.0x10^7$ N/m, corresponds to receptances, in dB, of $20\log_{10}(0.5x10^{-6})$ = -126.0206 dB and $20\log_{10}(10^{-7})$ = -140 dB respectively of the unperturbed beam. These are points where the two horizontal lines in figs 6.3 and 6.4, drawn at -126.0206 dB and -140 dB, intercept the receptance curve on the right-hand-side of each resonance peak. The actual points are close to the points indicated by a1. . . d3.

It can be seen that the second elastic mode does not appear in fig 6.4. This suggests that the excitation coordinate 5 is at the node of the second elastic mode of the unperturbed beam, and therefore this mode is not excited. As a result, adding a stiffness to coordinate 5 does not affect the eigenvalue of the second mode. The frequency located at d1 in fig 6.4 corresponds to the new natural frequency of the originally first mode, when coordinate 5 is perturbed by a stiffness of $1.0x10^7$ N/m.

To improve the accuracy of the estimated eigenvalues, the FRF was zoomed around each of points a1 to d3, at a resolution of 0.1 Hz. Tables 6.1 and 6.2 shows some values of the receptances and their corresponding frequencies of the zoomed FRF, around each of points a1 to d3. The natural frequencies were then determined by inspection, by locating the frequencies at which the receptance data is closest to -126.0206 dB and -140 dB respectively. This exercise results in the establishment of the natural frequencies of the stiffness added beam with an uncertainty of 0.1 Hz, table 6.3.

Simulated system receptance ____ , Receptance of the initial analytical model - - - -

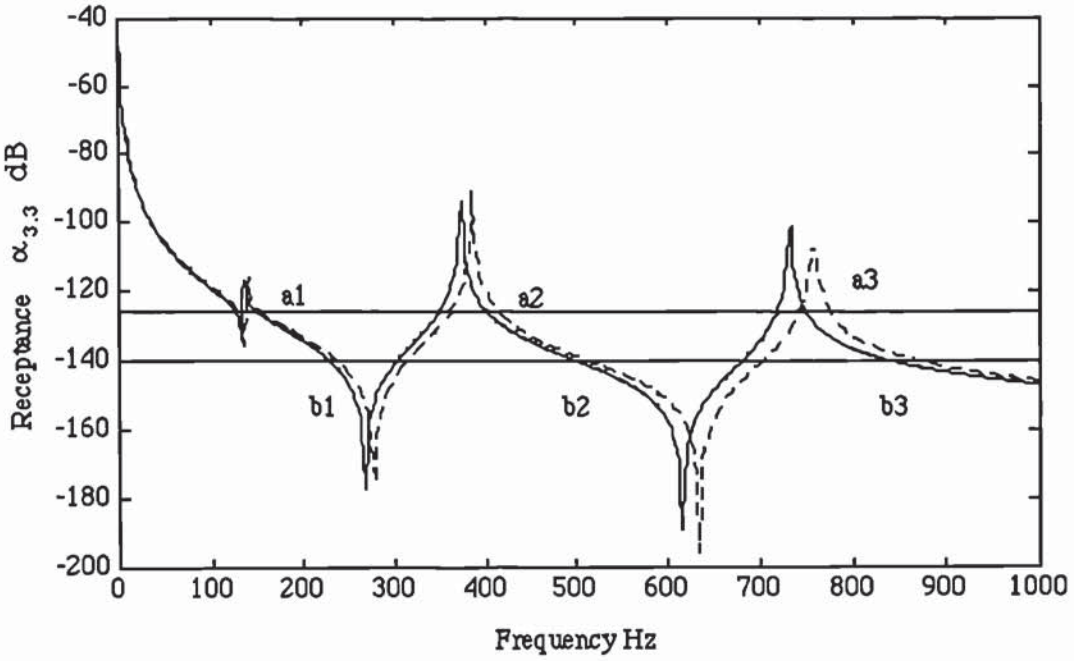

Fig 6.3 Point receptance of the undamped beam: Excitation at coordinate 3.

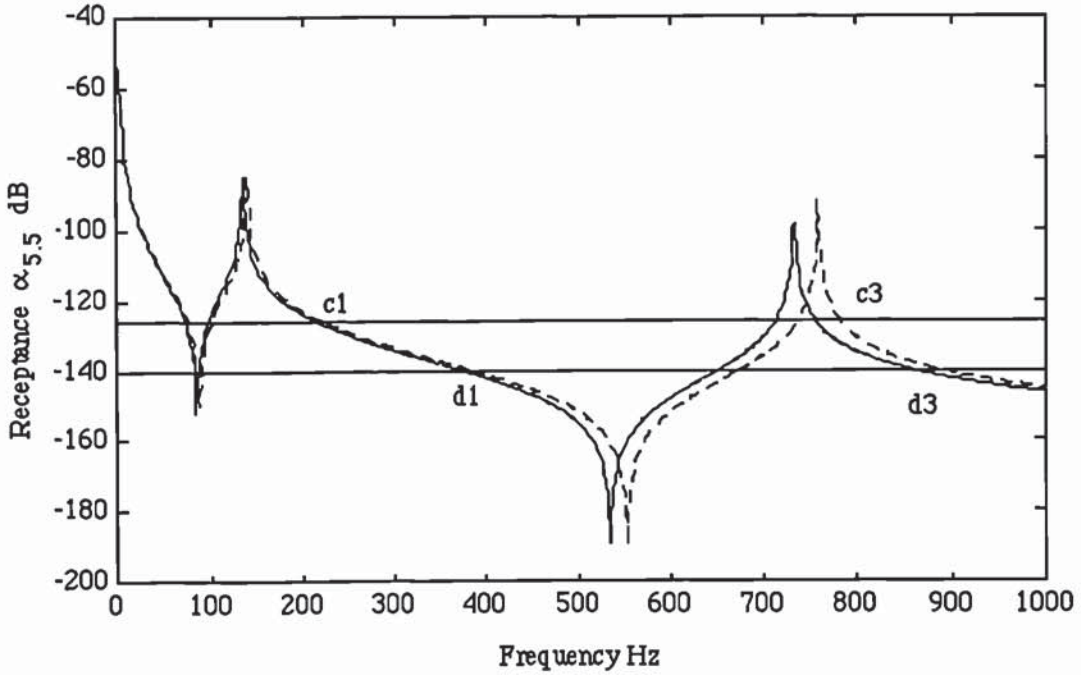

Fig 6.4 Point receptance of the undamped beam: Excitation at coordinate 5.

	$k = 2.0\text{x}10^6$ N/m		$k = 1.0\text{x}10^7$ N/m	
	Frequency (Hz)	Receptance (dB)	Frequency (Hz)	Receptance (dB)
Mode 1	151.3	-126.0014	231.0	-139.9634
	151.4	-126.0212	231.1	-139.9879
	151.5	-126.0409	231.2	-140.0124
	151.6	-126.0405	231.3	-140.0369
Mode 2	402.2	-125.9871	500.8	-139.9878
	402.3	-126.0161	500.9	-139.9980
	402.4	-126.0451	501.0	-140.0081
	402.5	-126.0739	501.1	-140.0183
Mode 3	750.0	-125.9433	842.3	-139.9900
	750.1	-125.9907	842.4	-139.9966
	750.2	-126.0378	842.5	-140.0031
	750.3	-126.0846	842.6	-140.0162

TABLE 6.1 Receptance-frequency data (error-free): Excitation at coord. 3.

	$k = 2.0\text{x}10^6$ N/m		$k = 1.0\text{x}10^7$ N/m	
	Frequency (Hz)	Receptance (dB)	Frequency (Hz)	Receptance (dB)
Mode 1	215.5	-126.0086	371.1	-139.9876
	215.6	-126.0212	371.2	-139.9955
	215.7	-126.0338	371.3	-140.0035
	215.8	-126.0464	371.4	-140.0114
Mode 3	755.2	-125.9626	857.7	-139.9891
	755.3	-126.0002	857.8	-139.9955
	755.4	-126.0376	857.9	-140.0019
	755.5	-126.0748	858.0	-140.0084

TABLE 6.2 Receptance-frequency data (error-free): Excitation at coord. 5.

Added stiffness (N/m)	Stiffness added coordinate	Natural frequency in Hz		
		Mode 1	Mode 2	Mode 3
2.0×10^6	3	151.4	402.3	750.2
	5	215.6	373.3	755.4
1.0×10^7	3	231.1	500.9	842.5
	5	371.3	373.3	857.9

TABLE 6.3 Estimated natural frequencies of the stiffness added beam.

The estimated natural frequencies of the perturbed beam together with the correct natural frequencies of the unperturbed beam were then used in an unconstrained weighted least squares updating algorithm.

The updated parameters, after 6 iterations are:

$EI_1 = 5012$ Nm^2 $EI_2 = 4992$ Nm^2 $EI_3 = 5004$ Nm^2

$EI_4 = 4989$ Nm^2 $m_{u1} = 3.503$ kg/m $m_{u2} = 3.497$ kg/m

$m_{u3} = 3.503$ kg/m $m_{u4} = 3.495$ kg/m.

$f_1 = 134.72$ Hz $f_2 = 373.29$ Hz $f_3 = 733.07$ Hz

Figs 6.5 and 6.6 shows the convergence of the stiffness and mass parameters. The updated parameters are reasonably accurate. This has to be expected since the estimated natural frequencies, table 6.3, are reasonably accurate. As no measurement error was simulated in the receptance data, the accuracy of the estimated natural frequencies is of the order of the resolution in the frequency axis (0.1 Hz).

Element 1 __ , element 2 - - -, element 3 . . . . . , element 4 -.-.-.-.

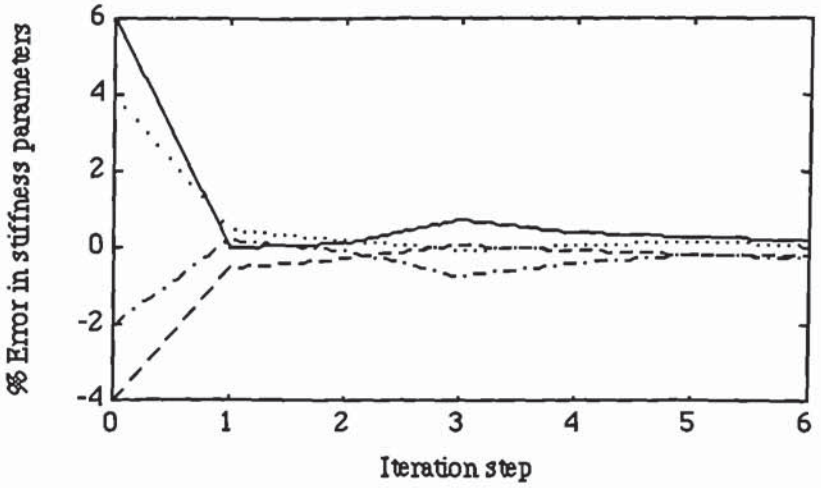

Fig 6.5 Convergence of the stiffness parameters
(using eigenvalues alone; modes 1-3)

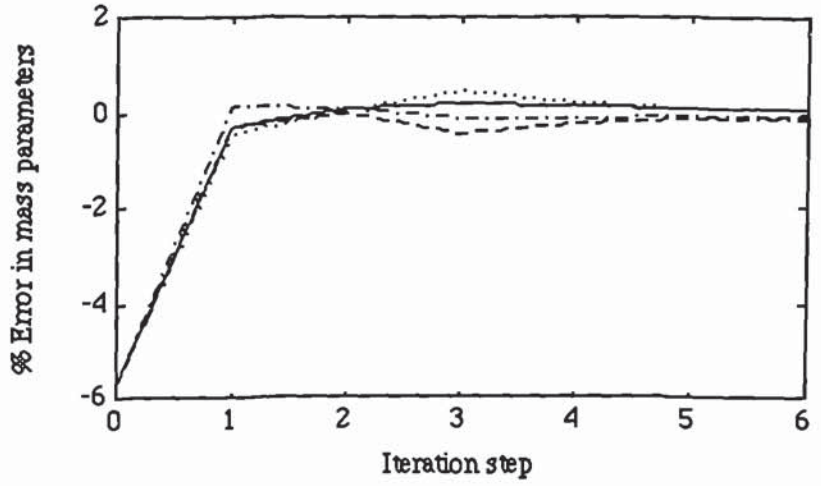

Fig 6.6 Convergence of the mass parameters.
(using eigenvalues alone; modes 1-3)

UPDATING USING EIGENVALUES AND EIGENVECTORS

The beam is now updated using eigenvalues and eigenvectors of the first two elastic modes. The eigenvectors are simulated to have been measured at two

translational coordinates, whereas stiffness additions of $2x10^6$ N/m and $1.0x10^7$ N/m are made at a single coordinate, 3. Measurement coordinates are 3 and 7. Thus, the required FRFs are, point receptance at coordinate 3 (fig 6.3) and transfer receptance at coordinate 7 with an excitation at 3 (fig 6.7).

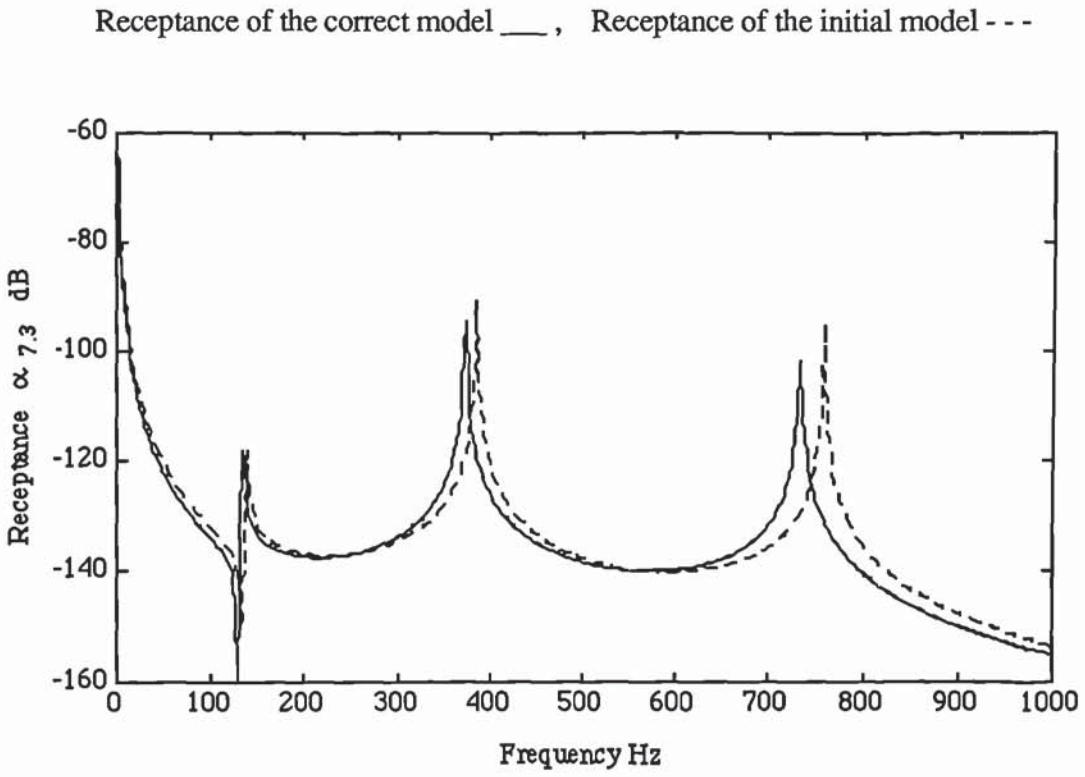

Fig 6.7 Receptance at coordinate 7 with an excitation at 3.

The eigenvalues of the beam with added stiffness, in this case, are determined from the natural frequencies shown in table 6.3, since the same stiffness additions were also made in the first case when eigenvalues only were used. The eigenvectors are given by the receptance vectors evaluated at the measurement coordinates for each established natural frequency of the perturbed beam. Table 6.4 shows the frequencies and their corresponding receptances and hence eigenvectors normalized to the highest displacement of unity in each eigenvector. The eigenvectors of the unperturbed beam were determined by solving the eigenvalue problem.

Simulated additional stiffness (N/m)	Measurement coordinate	Frequency (Hz)	Receptance ($x10^{-7}$ m/N)	Estimated eigenvectors
$2.0x10^{6}$	3	151.4	4.9997	1.0000
	5		2.0528	0.4106
	3	402.3	5.0030	1.0000
	5		-4.6984	-0.9391
$1.0x10^{7}$	3	231.1	1.0010	0.7256
	5		1.3796	1.0000
	3	500.9	1.0000	-0.8190
	5		-1.2210	1.0000

TABLE 6.4 Estimated eigenvectors of the perturbed beam.

Parameters of the analytical model were updated by an unconstrained weighted least squares algorithm. The eigenvalue weighting matrix was based on a standard deviation of 0.1 Hz in the natural frequencies. The eigenvector weighting matrix was based on a standard deviation of 0.01 for the non-mass normalized eigenvector data of table 6.4. This value is an approximation decided by inspection of the variation of the eigenvector data between the upper and lower frequency bounds. The upper and lower frequency bounds are determined by the uncertainty in the estimated natural frequencies of the perturbed beam, which is +(-) 0.1 Hz. The standard deviation of the mass normalized eigenvectors, which is the one to be used in the eigenvector weighting matrix, is then computed by dividing the standard deviation of the non-mass normalized vectors (0.01), by the analytical modal mass for the mode in question.

Figs 6.8 and 6.9 shows the convergence of the stiffness and mass parameters.

Element 1 ___ , element 2 - - - , element 3 . . . . , element 4 -.-.-.-.

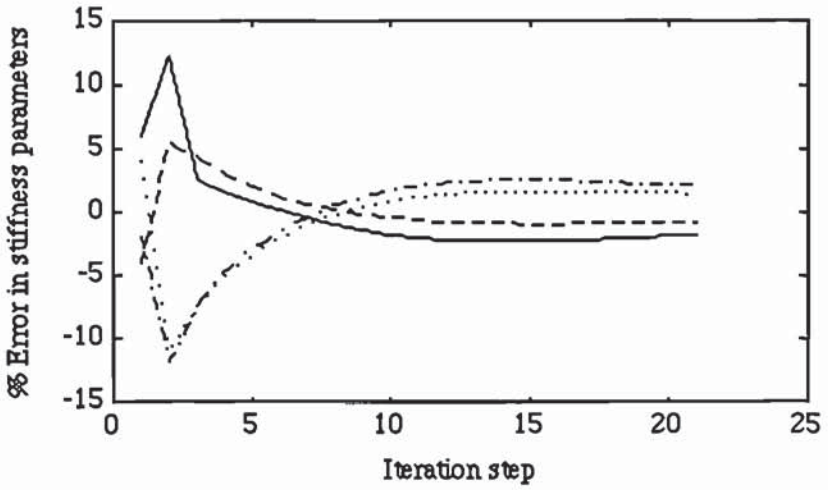

Fig 6.8 Convergence of the stiffness parameters
(using eigenvalues and eigenvectors; modes 1 and 2)

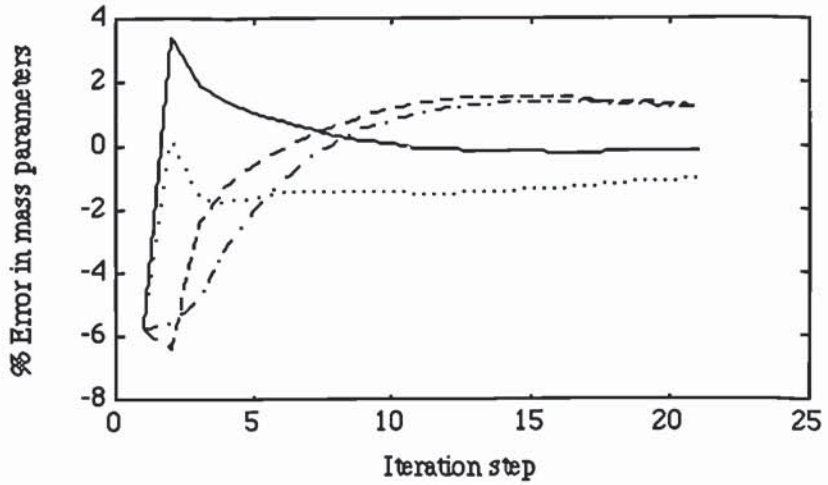

Fig 6.9 Convergence of the mass parameters
(using eigenvalues and eigenvectors; modes 1 and 2)

The updated parameters after 21 iterations are:

$EI_1 = 4912$ Nm^2 $EI_2 = 4963$ Nm^2 $EI_3 = 5075$ Nm^2

$EI_4 = 5107$ Nm^2 $m_{u1} = 3.495$ kg/m $m_{u2} = 3.543$ kg/m

$m_{u3} = 3.465$ kg/m $m_{u4} = 3.542$ kg/m

$f_1 = 134.73$ Hz $\qquad$ $f_2 = 373.30$ Hz.

It can be seen that although the updated parameters are of acceptable accuracy, they are less accurate than when eigenvalues alone were used and the convergence rate is considerably slower. The FRF prediction of the updated model is acceptable, fig 6.10. It should also be noted that only the first two elastic mode shapes and eigenvalues of the beam before and after stiffness addition were used as opposed to the first three eigenvalues in the previous case.

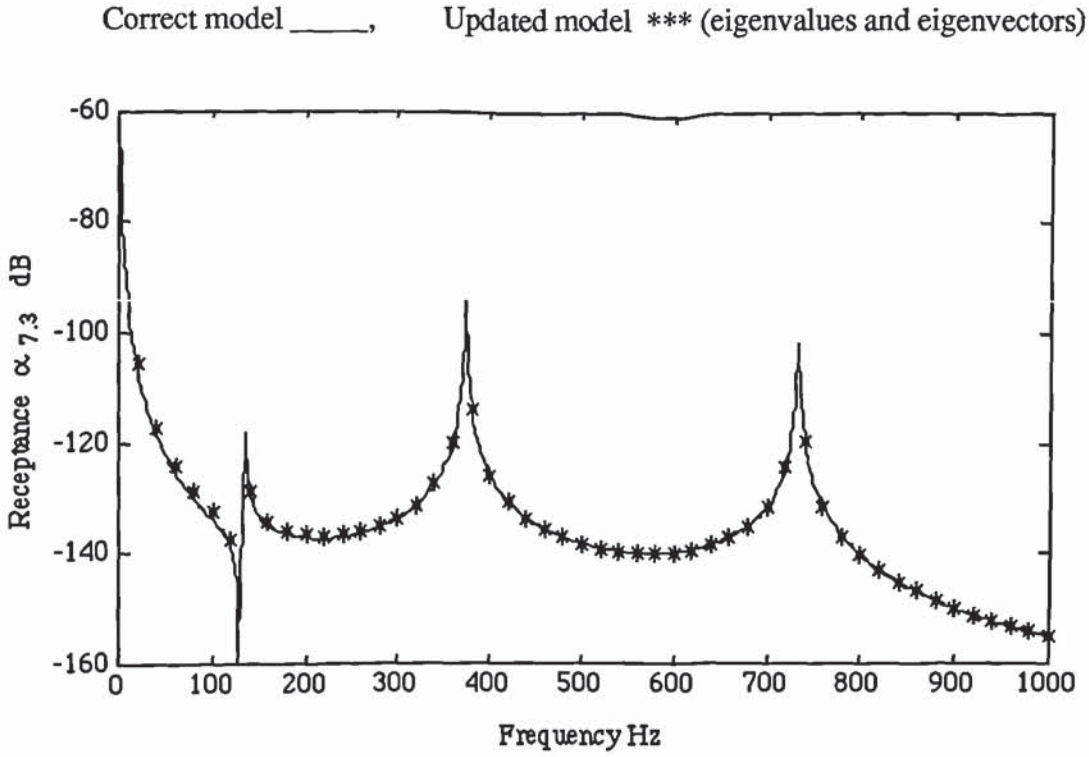

Fig 6.10 Comparing receptance prediction

The previous example considered updating a model by numerical simulation of the additional stiffness using the FRF data of the unperturbed structure. The updating was performed using an unconstrained optimization and no errors were simulated in the FRF data. The only errors involved are associated with

frequency resolution as the FRF data is simulated at discrete frequency intervals, and the errors associated with the use of analytical modal masses (iterated) in the normalization of the mode shape vectors. These errors are shown in tables 6.5 - 6.7. Table 6.8 shows the computed standard deviation estimates of the mass-normalized eigenvectors.

Added stiffness at coordinate 3 (N/m)	Natural frequency estimate (Hz)		Natural frequency error (Hz)	
	Mode 1	Mode 2	Mode 1	Mode 2
$2x10^6$	151.4	402.3	-0.003	0.015
$1x10^7$	231.1	500.9	0.049	0.020

TABLE 6.5 Errors in the estimated natural frequencies of the beam with added stiffness.

Added stiffness at coordinate 3 (N/m)	Measurement coordinate	Eigenvector estimate $U_{mm} = \frac{V_{mm}}{(V_a^T M_a V_a)^{1/2}}$		Error in eigenvector estimate $U_{exact} - U_{mm}$	
		Mode 1	Mode 2	Mode 1	Mode 2
0	3	0.1130	-0.6584	-0.0067	0.0239
	5	0.1130	0.6584	-0.0067	-0.0239
$2x10^6$	3	0.5308	0.7040	-0.0178	-0.0138
	5	0.2179	-0.6611	-0.0073	0.0129
$1x10^7$	3	0.2632	-0.5986	-0.0088	0.0172
	5	0.3627	0.7309	-0.0117	-0.0213

TABLE 6.6 Errors in the estimated mass-normalized eigenvectors at the begining of the first iteration.

Added stiffness at coordinate 3 (N/m)	Measurement coordinate	Eigenvector estimate $U_{mm} = \frac{V_{mm}}{(V_a^T M_a V_a)^{1/2}}$		Error in eigenvector estimate $U_{exact} - U_{mm}$	
		Mode 1	Mode 2	Mode 1	Mode 2
0	3	0.1072	-0.6340	-0.0009	-0.0005
	5	0.1072	0.6340	-0.0009	0.0005
$2x10^6$	3	0.5120	0.6899	0.0010	0.0003
	5	0.2102	-0.6479	0.0004	0.0003
$1x10^7$	3	0.2550	-0.5802	-0.0006	-0.0012
	5	0.3514	0.7084	-0.0004	0.0012

TABLE 6.7 Errors in the estimated mass-normalized eigenvectors at the begining of the final iteration (21st iteration).

	Computed STD of U_{mm}= Estimated STD of V_{mm} divide by $(V_a^T M_a V_a)^{1/2}$					
	$k = 0$		$k = 2x10^6$ N/m		$k = 1x10^7$ N/m	
	Mode 1	Mode 2	Mode 1	Mode 2	Mode 1	Mode 2
Start of first iteration	0.0011	0.0066	0.0053	0.0070	0.0036	0.0073
Start of final iteration	0.0011	0.0073	0.0051	0.0069	0.0035	0.0071

TABLE 6.8 Computed STD of mass-normalized eigenvectors at the start of the first and the final iterations.

The following example consider the effects of measurement errors in the FRF and updating will be performed using the minimum cost Bayesian estimator.

EXAMPLE 6.2

The beam receptances of example 6.1 are now simulated at 0.25 Hz resolution, with additional errors. The errors are simulated as random with zero mean and standard deviation of 5% of the respective FRF data at each frequency. The FRF data will then be used in the estimation of the natural frequencies and eigenvectors of the perturbed beam, using a different set of stiffness added at coordinates 3 and 5. Parameters will then be updated using eigenvalues alone and using both eigenvalues and eigenvectors. In both cases, the minimum cost Bayesian estimator will be used, with the following estimates of the standard deviations of the initial parameters:

$$\text{STD } EI = 200 \text{ Nm}^2 , \text{ STD } m_u = 0.2 \text{ kg/m} \qquad \text{(all parameters).}$$

UPDATING USING EIGENVALUES

Figs 6.11 and 6.12 shows the point receptances at coordinates 3 and 5 respectively, with additional random errors with standard deviation of 5% of the FRF data. From these two FRFs, an estimate is made of the natural frequencies of the beam if stiffness of 2.5×10^6 N/m and 8.0×10^6 N/m are grounded in turn, at each of coordinates 3 and 5. The natural frequencies are given by the points defined by $\alpha = -1/k$, which in this case corresponds to -127.9588 dB and -138.0618 dB on the right-hand-side of each resonance peak in figs 6.11 and 6.12.

Because of errors in the FRF data, the location of the appropriate point is not obvious. By inspecting the FRF data, one should be able to determine the zone

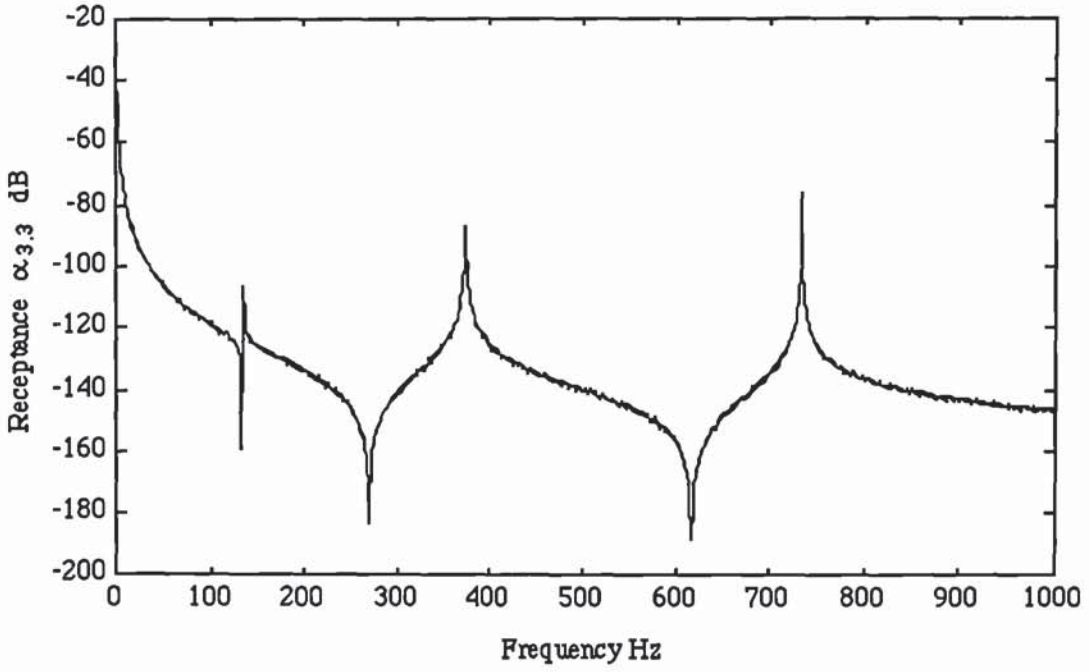

Fig 6.11 Point receptance at coordinate 3, with errors (5% STD).

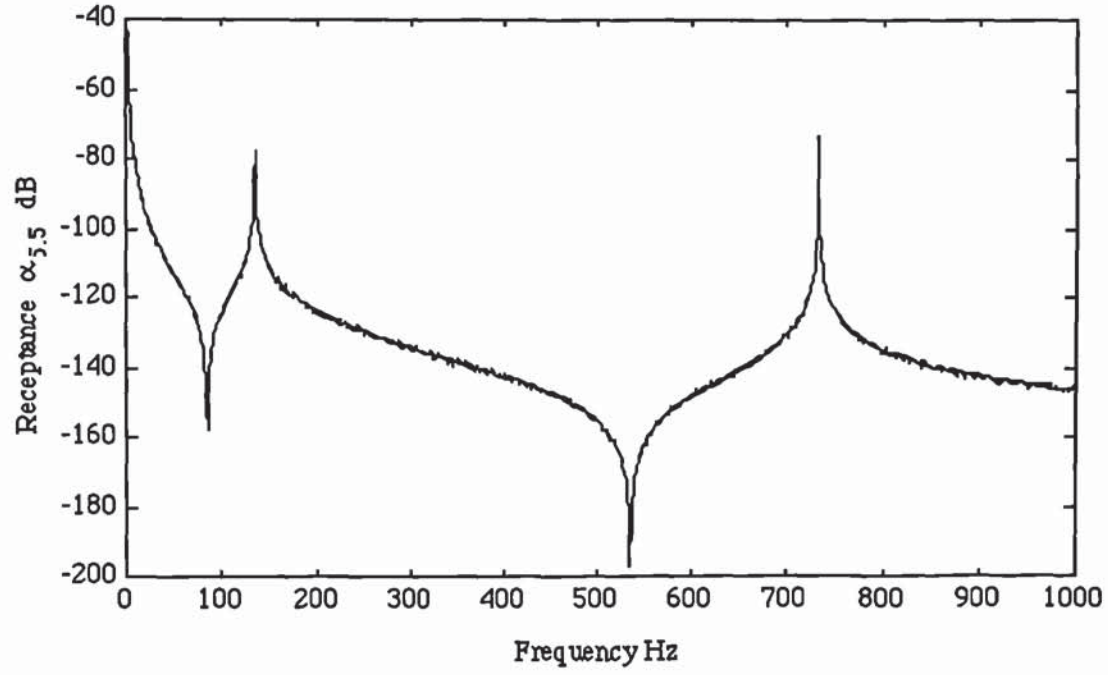

Fig 6.12 Point receptance at coordinate 5, with errors (5% STD).

which most likely contain the appropriate point. From this zone, the upper and lower frequency bounds can be determined as well as the best guess of the natural frequency of the perturbed structure. The upper and lower frequency bounds could then be used to estimate the natural frequency uncertainty and compute the eigenvalue weighting factor.

Tables 6.9 to 6.12 shows the frequency and receptance data determined from the FRFs contaminated with random errors (figs 6.11 and 6.12). The tables shows the way the receptance data changes through the zones which most likely contains the natural frequencies of the perturbed beam.

Tables 6.9 and 6.10 are for the point receptances at coordinate 3. They will be used to estimate the natural frequencies of the beam, when coordinate 3 is perturbed by a grounded stiffness of 2.5×10^6 N/m (α = -127.9588 dB) and 8.0×10^6 N/m (α = -138.0618 dB) respectively. The first, second and third frequency-receptance columns contain data to estimate the new natural frequencies of the initially first, second and third elastic modes of the unperturbed beam.

Tables 6.11 and 6.12 are for the point receptances at coordinate 5. They will be used to estimate the natural frequencies of the beam when coordinate 5 is perturbed by a grounded stiffness of 2.5×10^6 N/m and 8.0×10^6 N/m respectively. The first and second frequency-receptance columns contains data to estimate the new natural frequencies of the initially first and third elastic modes of the unperturbed beam. The second elastic mode of the unperturbed beam is unchanged by stiffness addition at coordinate 5, since this coordinate is at the node and excitation of coordinate 5 does not excite this mode.

Frequency (Hz)	Receptance (dB)	Frequency (Hz)	Receptance (dB)	Frequency (Hz)	Receptance (dB)
156	-127.2879	405	-126.8381	750	-126.5936
157	-126.9985	406	-126.4369	751	-125.8006
158	-127.4498	407	-128.2685	752	-127.0408
159	-127.8606	408	-127.6271	753	-126.9857
160	-127.4510	409	-127.0961	754	-127.3033
161	-127.7230	410	-128.2835	755	-128.3544
162	-128.4316	411	-129.4890	756	-128.0611
163	-127.8416	412	-129.6331	757	-129.6888
164	-128.4315	413	-129.1859	758	-129.4080
165	-127.7756	414	-129.0285	759	-129.6689

TABLE 6.9 Receptance-frequency data: Excitation and measurement at 3.
(used to estimate the natural frequencies for $k = 2.5 \times 10^6$ N/m at 3)

Frequency (Hz)	Receptance (dB)	Frequency (Hz)	Receptance (dB)	Frequency (Hz)	Receptance (dB)
220	-137.1220	476	-137.3232	813	-137.5945
221	-137.7533	477	-138.3337	814	-137.6231
222	-139.1250	478	-137.0606	815	-137.7708
223	-137.7693	479	-137.6513	816	-137.3065
224	-137.9020	480	-138.0254	817	-138.2195
225	-137.8957	481	-137.5899	818	-138.5557
226	-138.7479	482	-138.1333	819	-138.8515
227	-139.6161	483	-137.9780	820	-138.4141
228	-139.4183	484	-139.1104	821	-138.8901
229	-139.2276	485	-138.1499	822	-138.6642

TABLE 6.10 Receptance-frequency data: Excitation and measurement at 3.
(used to estimate the natural frequencies for $k = 8.0 \times 10^6$ N/m at 3)

Frequency (Hz)	Receptance (dB)	Frequency (Hz)	Receptance (dB)
228	-127.8455	756	-126.0470
229	-127.3450	757	-126.7895
230	-127.4389	758	-127.0789
231	-127.4656	759	-127.6993
232	-127.5609	760	-127.8497
233	-128.4708	761	-128.3980
234	-128.2305	762	-128.0497
235	-127.7833	763	-128.5686
236	-128.8645	764	-129.3462
237	-128.6633	765	-128.9297

TABLE 6.11 Receptance-frequency data: Excitation and measurement at 5.
(used to estimate the natural frequencies for $k = 2.5\text{x}10^6$ N/m at 5)

Frequency (Hz)	Receptance (dB)	Frequency (Hz)	Receptance (dB)
341	-137.4715	824	-137.0517
342	-137.8329	825	-138.8693
343	-137.5394	826	-138.2031
344	-137.3313	827	-137.8143
345	-139.3196	828	-138.3880
346	-138.0933	829	-137.8733
347	-138.0164	830	-137.3525
348	-137.7034	831	-137.6860
349	-134.9004	832	-138.0508
350	-137.5768	833	-138.2185
351	-138.5325	834	-138.0948
352	-138.7568	835	-138.1620
353	-138.4149	836	-138.8460
354	-137.9511	837	-138.4890

TABLE 6.12 Receptance-frequency data: Excitation and measurement at 5.
(used to estimate the natural frequencies for $k = 8.0\text{x}10^6$ N/m at 5)

From tables 6.9 to 6.12, natural frequencies of the beam with added stiffness have been estimated by inspection, with uncertainties represented by standard deviation of 2 Hz for all the frequencies. The estimated natural frequencies are shown in table 6.13.

Added stiffness (N/m)	Stiffness addition coordinate	Estimated natural frequencies (Hz)		
		Mode 1	Mode 2	Mode 3
$2.5\text{x}10^6$	3	161	408	754
	5	232	373	760
$8.0\text{x}10^6$	3	224	480	817
	5	349	373	832

TABLE 6.13 Estimated natural frequencies of the beam with added stiffness.

The estimated natural frequencies of the beam with added stiffness, and the natural frequencies of the unperturbed beam (obtained by solving the eigenvalue problem) were used to update the mass and stiffness parameters, using the minimum cost Bayesian estimator. A standard deviation of 0.25 Hz was assumed for the natural frequencies of the unperturbed beam whereas a standard deviation of 2 Hz was used for all the frequencies of the perturbed beam (estimated with the aid of tables 6.9 to 6.12). The standard deviations in the natural frequencies were used to compute the eigenvalues weighting matrix.

The updated parameters, after 4 iterations, are:

$$EI_1 = 5222 \text{ Nm}^2 \qquad EI_2 = 4825 \text{ Nm}^2 \qquad EI_3 = 5101 \text{ Nm}^2$$
$$EI_4 = 4740 \text{ Nm}^2 \qquad m_{u1} = 3.504 \text{ kg/m} \qquad m_{u2} = 3.512 \text{ kg/m}$$

$m_{u3} = 3.444$ kg/m $\qquad$ $m_{u4} = 3.440$ kg/m.

Figs 6.13 and 6.14 shows the convergence of the stiffness and mass parameters as percentage changes from their initial estimates.

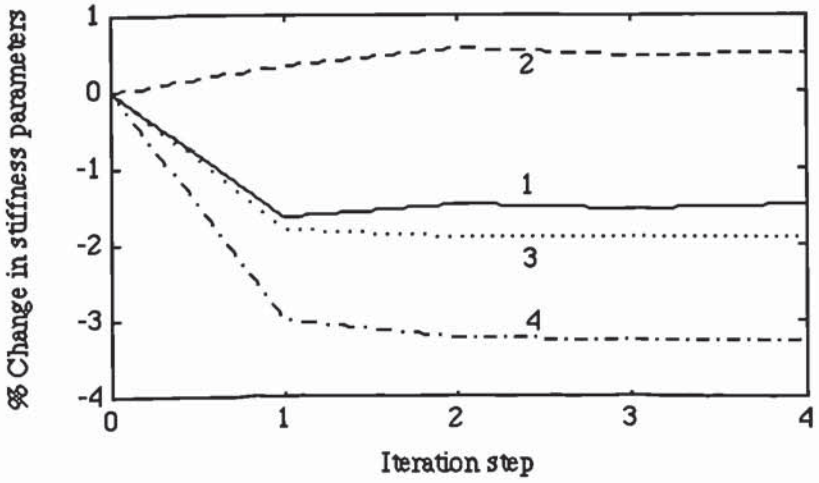

Fig 6.13 Convergence of the stiffness parameters.
(using eigenvalues; modes 1-3)

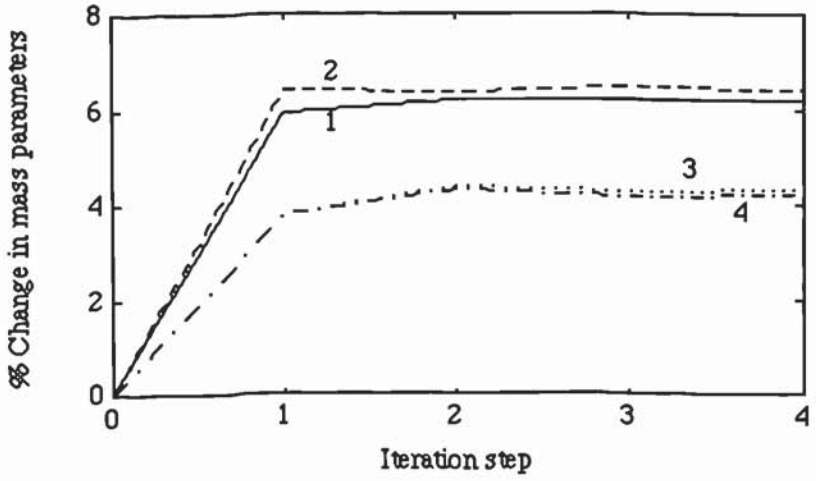

Fig 6.14 Convergence of the mass parameters.
(using eigenvalues; modes 1-3)

Fig 6.15 compares receptance prediction between the simulated system, initial model and the updated model at coordinate 3. Fig 6.16 compares prediction of the rotational receptance at coordinate 8 with an excitation at coordinate 3. The receptance data for coordinate 8 was not used in the updating process. The updated model is accurate enough to predict the FRF of the unmeasured coordinate.

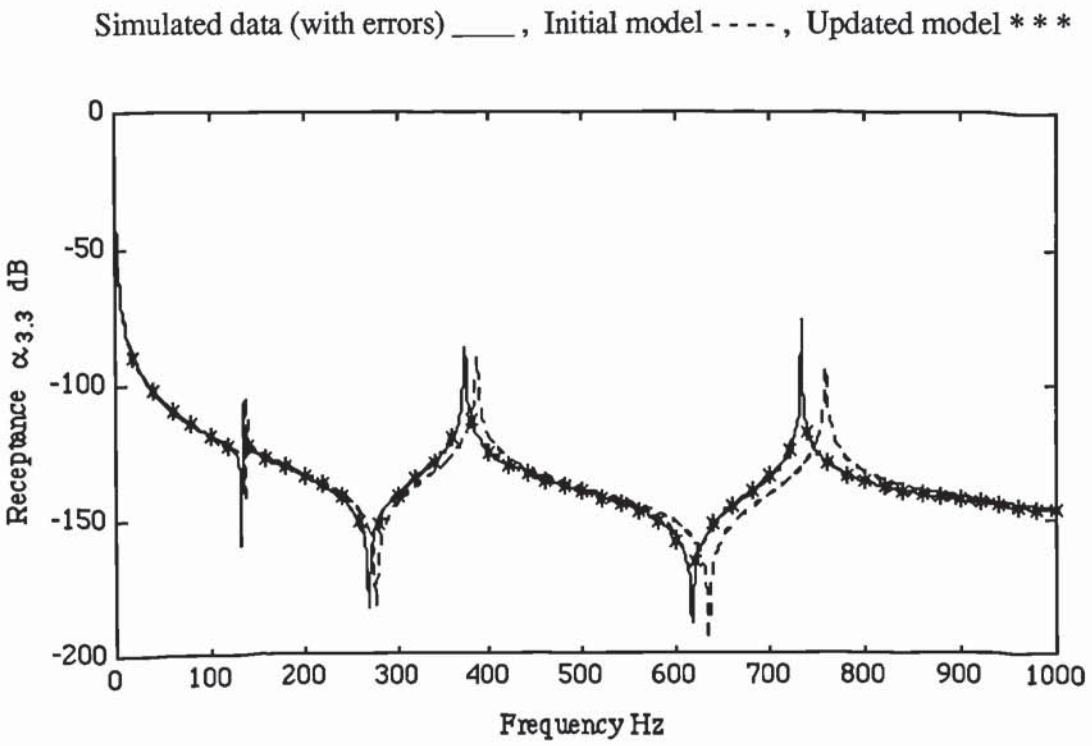

Fig 6.15 Receptance comparison at the excitation coordinate 3.

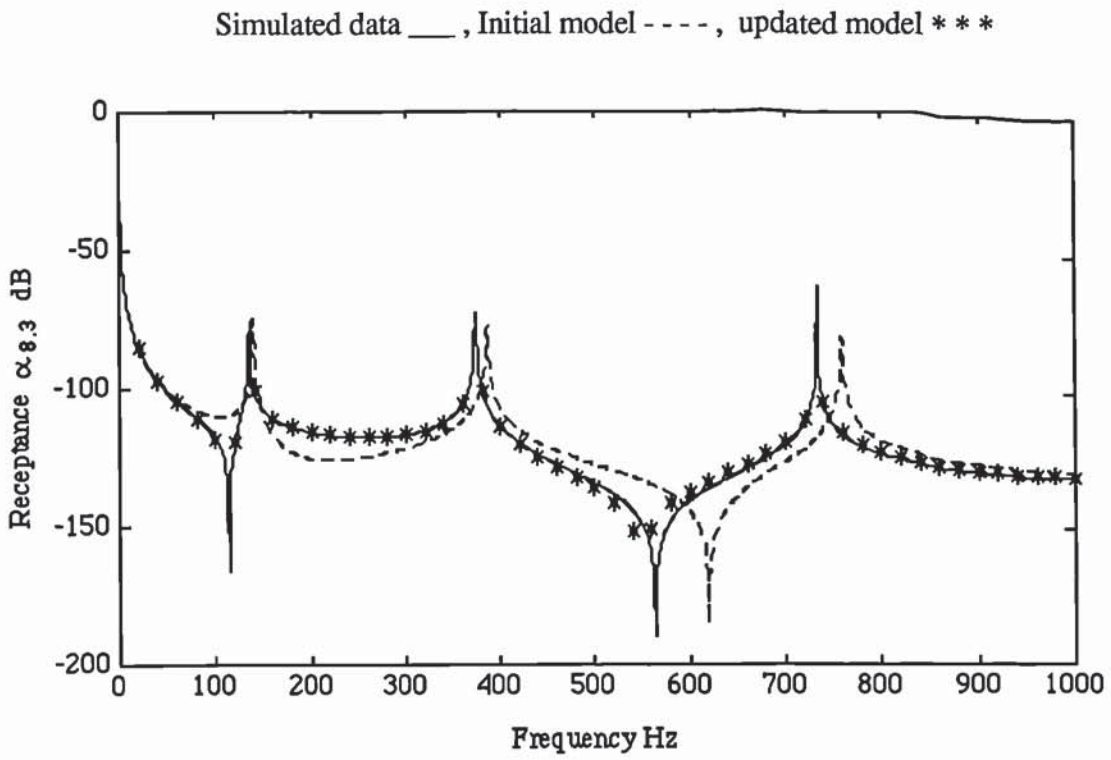

Fig 6.16 Rotational receptance prediction at coordinate 8.

UPDATING USING EIGENVALUES AND EIGENVECTORS

The analytical model is now to be updated using eigenvalues and eigenvectors with stiffness additions of 2.5×10^6 N/m and 8.0×10^6 N/m at coordinate 3 only. Only the first two elastic modes of the unperturbed beam and their corresponding modes of the perturbed beam will be used in the updating process. The mode shape data is measured at coordinates 3 and 7 only. The eigen-data of the perturbed beam is to be determined from the FRF data of the unperturbed beam, contaminated with random errors with zero mean and standard deviation of 5%. The FRF data are the point receptance at coordinate 3 (fig 6.11) and the transfer receptance at coordinate 7 for an excitation at coordinate 3 (fig 6.17). To determine the mode shape data, the natural frequencies are to be established first from the point receptance data.

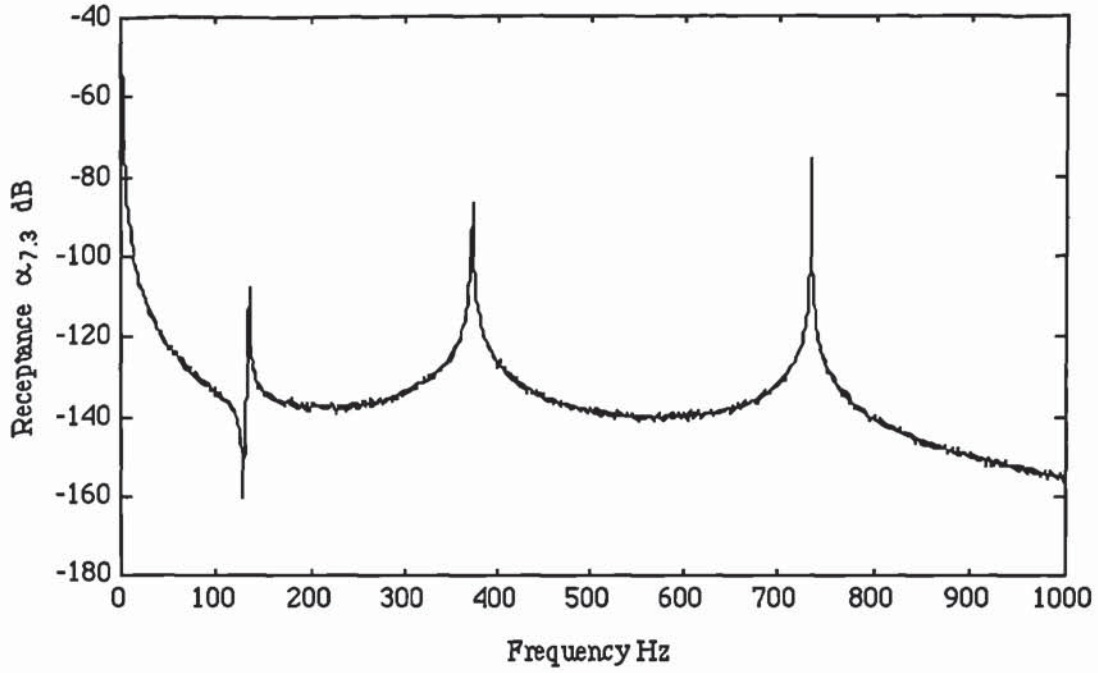

Fig 6.17 Receptance at coordinate 7(with random errors), excitation at 3.

The natural frequencies are a subset of the natural frequency data determined in the previous case, when eigenvalues alone were used in the updating process, and are given in table 6.13. Using this natural frequency data, the mode shapes of the perturbed beam, arbitrarily scaled, are determined from the FRFs at coordinates 3 and 7. The mode shapes are given by the receptance vectors at frequencies corresponding the estimated natural frequencies of the perturbed beam. Table 6.14 shows the mode shape data (receptance data of the unperturbed beam) and estimates of the upper and lower bounds. The upper and lower bounds of the mode shape data are determined by the upper and lower bounds of the estimated natural frequencies (2 Hz from the nominal values). The differences between the upper and the nominal values and between the nominal and the lower values of the mode shape data are averaged out and treated as standard deviations, which will be used in the formulation of the eigenvector weighting matrix. As the modal masses are not known, the analytical model's modal masses (updated after each iteration) will be used in

Stiffness at coordinate 3 ($x10^6$ N/m)	Estimated natural frequency (Hz)	Mode shape data at coordinate 3 (receptance data) $x10^{-7}$			Mode shape data at coordinate 7 (receptance data) $x10^{-7}$		
		Nominal value	lower limit	upper limit	Nominal value	lower limit	upper limit
2.5	161	4.121	3.890	4.365	1.778	1.698	1.862
	408	4.169	3.715	4.677	-4.169	-4.518	-3.846
8.0	224	1.274	1.202	1.349	1.380	1.303	1.460
	480	1.259	1.189	1.334	-1.334	-1.445	-1.230

TABLE 6.14 Mode shape data estimated using receptance data.

the normalization of the mode shape vectors. The standard deviations are normalized too. Before this is effected, the estimated mode shape vectors (receptance data) are to be scaled such that the highest term in each vector is unity. The analytical modal masses will then be determined using analytical eigenvectors scaled such that the coordinates corresponding to unity displacements in the estimated modes of the perturbed system, are also unity in the analytical vectors. This ensures some compatibility between the estimated eigenvectors and the normalizing modal masses.

Table 6.15 shows the estimated mode shape vectors of the perturbed and unperturbed beam normalized to maximum displacements of unity, as well as their corresponding standard deviations. In a practical situation, the eigen-data of the unperturbed structure will be determined by conventional modal analysis methods. In this numerical example, the eigenvectors and natural frequencies used for the unperturbed beam are the true values determined by

solving the eigenvalue problem, but they are assumed to have uncertainty expressed by assumed standard deviations of 0.01 in the eigenvector data and 0.25 Hz in the natural frequencies.

		$k = 2.5\text{x}10^6$ (N/m)		$k = 8.0\text{x}10^6$ (N/m)	
Frequency (Hz)		161	408	224	480
Mode shape data	Coordinate 3	1 (0.06)	1 (0.12)	0.923 (0.05)	-0.9437 (0.06)
	Coordinate 7	0.4315 (0.02)	-1 (0.08)	1 (0.06)	1 (0.07)

TABLE 6.15 Mode shapes of the beam with added stiffness (normalized to highest displacements of unity): values in brackets are STD estimates.

The following parameters were obtained by updating the initial analytical model, using the minimum cost Bayesian estimator, in 10 iteration steps.

$EI_1 = 5154\ \text{Nm}^2$ $EI_2 = 4850\ \text{Nm}^2$ $EI_3 = 5079\ \text{Nm}^2$
$EI_4 = 4761\ \text{Nm}^2$

$m_{u1} = 3.494$ kg/m $m_{u2} = 3.478$ kg/m
$m_{u3} = 3.400$ kg/m $m_{u4} = 3.513$ kg/m

$f_1 = 134.7$ Hz $f_2 = 373.3$ Hz

Figs 6.18 and 6.19 shows the convergence of the stiffness and mass parameters as percentage changes from their initial estimates.

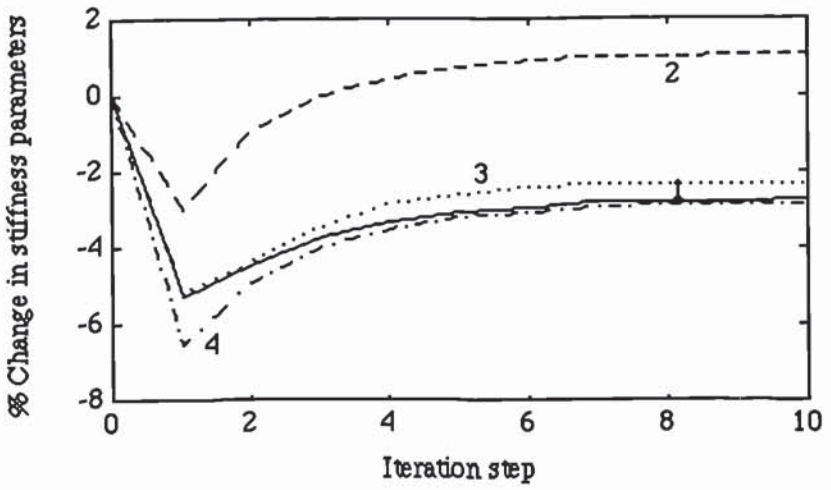

Fig 6.18 Convergence of the stiffness parameters .
(using eigenvalues and eigenvectors; modes 1 and 2)

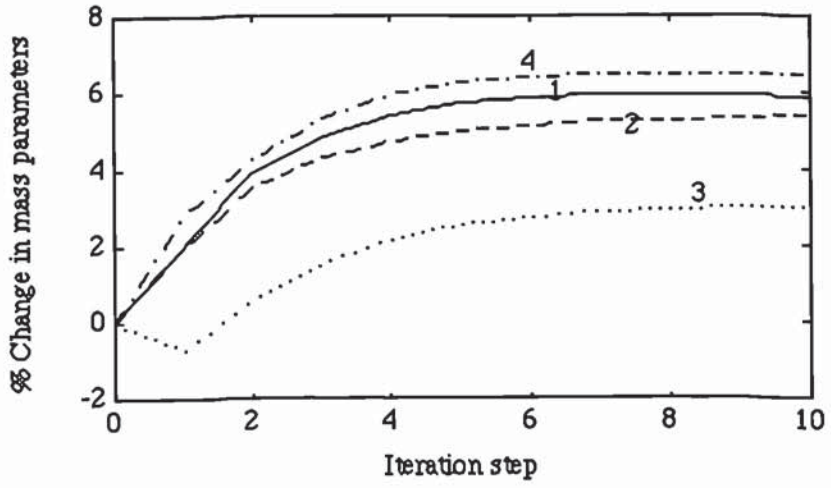

Fig 6.19 Convergence of the mass parameters.
(using eigenvalues and eigenvectors; modes 1 and 2)

It can be seen that, the accuracy of the updated parameters is not very much different from the previous case when eigenvalues only were used. Parameter convergence rate, however, is much slower although there is a slight improvement from example 6.1, where an unconstrained optimization was used.

The dynamic behaviour prediction of the updated model will now be tested in two simulated cases. First, coordinate 7 is excited and coordinate 3 is measured. Secondly, the beam is configured as an 8 DOF cantilever with its left end fixed, fig 6.20. Coordinate 1 of the cantilever beam is then excited and rotational coordinate 4 is measured. The receptance predictions are compared between the model based on correct parameters, initial parameters and the updated parameters. Figs 6.21 and 6.22 shows the comparison for the first and second cases respectively and both shows good agreement with the simulated FRF.

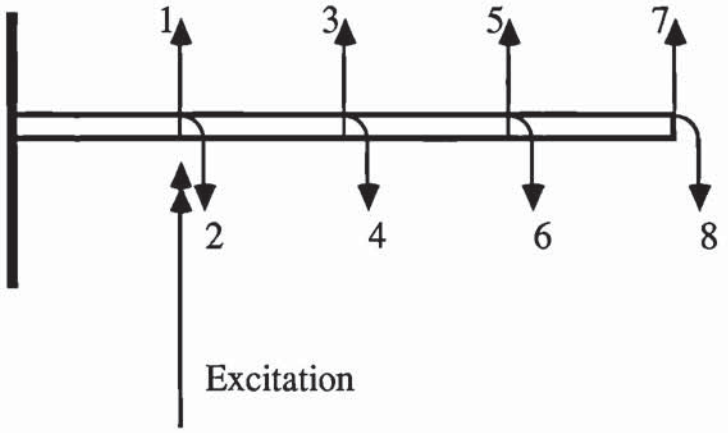

Fig 6.20 Cantilever beam

Correct model ____ , Initial model - - - - , Updated model * * *

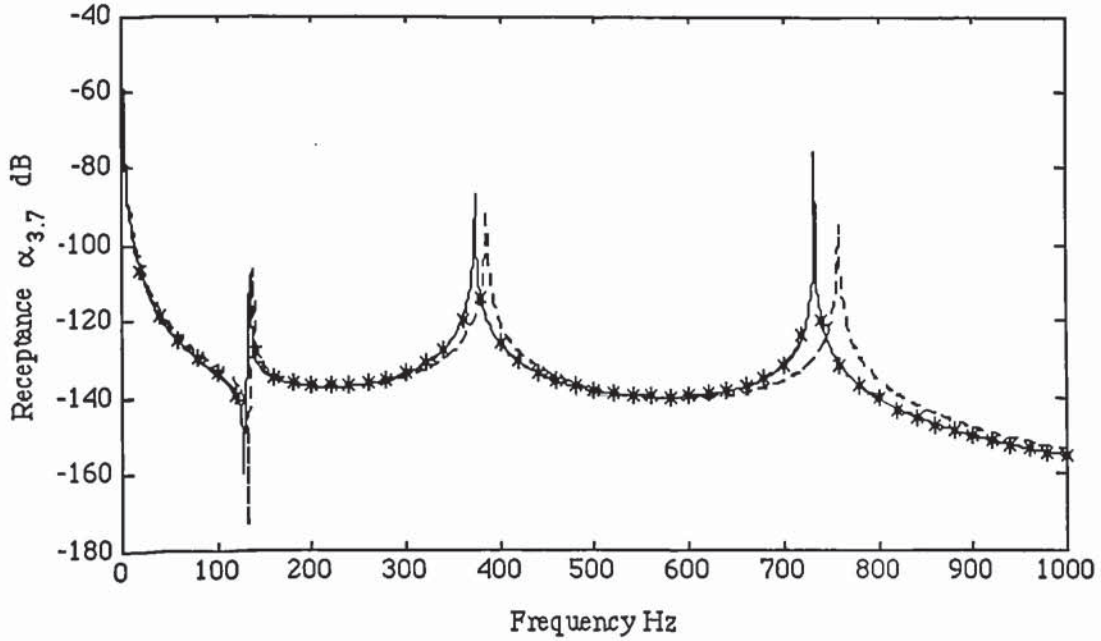

Fig 6.21 Receptance prediction at coordinate 3 of the free beam.

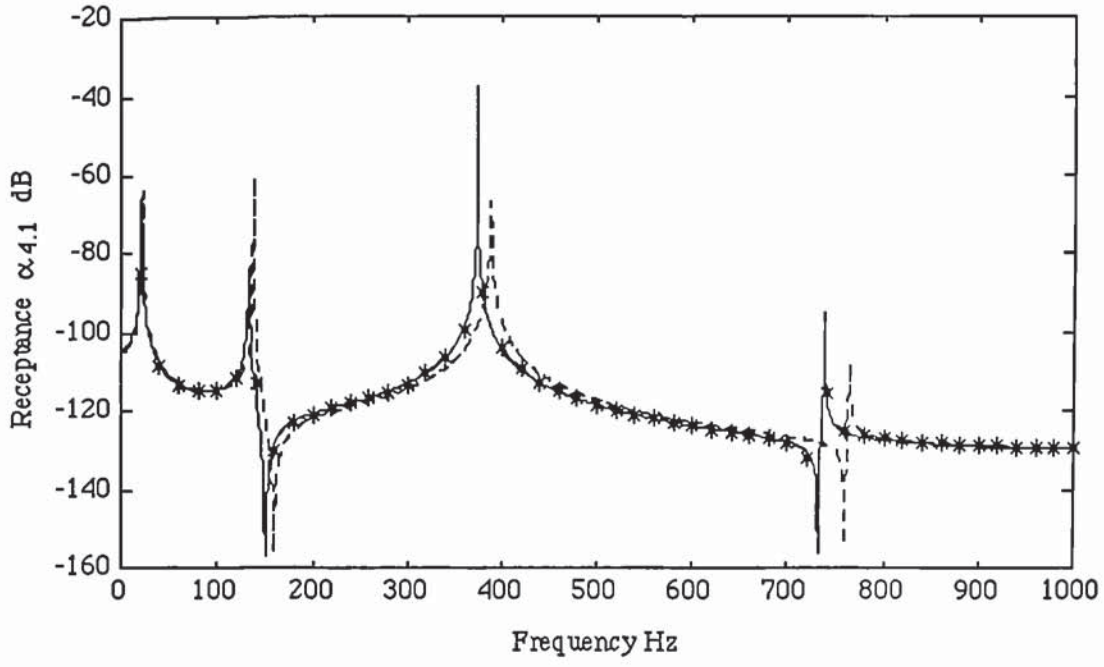

Fig 6.22 Receptance prediction at coordinate 4 of the cantilever beam.

In example 6.2, the natural frequencies of the perturbed beam were determined by inspecting the point receptance data of the unperturbed beam, and establish the value of f for which $\alpha = -1/k$. Problems of accuracy may arise if the randomness of the data is such that it is difficult to confine the zone containing the required natural frequency over a narrow frequency range. Improvements could be possible by employing a curve fitting technique over the zoomed frequency range of interest for the natural frequency of interest. It is fairly reasonable to assume that the FRF over this range can be adequately expressed by a low order polynomial. The adequacy of fitting a first order polynomial by a least squares method will be investigated. Thus once the zone containing the natural frequency of interest is identified, by inspection of the receptance data, a curve fitting process is performed over this zone. The natural frequency is then computed by substituting $-1/k$ for α in the curve fitted expression. This approach enables the automation of the process for obtaining the natural frequencies of the perturbed structure.

Consider the frequency-receptance data of tables 6.9 to 6.12, which corresponds to the point receptances at coordinates 3 and 5 of the free beam and stiffness additions of 2.5×10^6 N/m and 8.0×10^6 N/m at these coordinates. By least squares fitting of the data, using a first order polynomial, the natural frequencies of the beam with added stiffness were determined. Table 6.16 show the natural frequencies determined by curve fitting, as compared to the natural frequencies determined by inspection and exact natural frequencies determined by solving the perturbed eigenvalue problem. The designations first mode, second mode and third mode, in the table, refers to the natural frequencies of the modes which were the first, second and third elastic modes of the unperturbed beam. Figs 6.23 to 6.28 show the curve fitted plots, where the dashed lines represents the regenerated FRF data. For brevity, only the plots for coordinate 3 are shown.

	Added stiffness ($x10^6$ N/m)	Stiffness addition coordinate	Natural frequencies (Hz)		
			Estimated by inspection	Estimated by curve fitting	Exact
First mode	2.5	3	161.0	162.60	162.35
		5	232.0	232.44	232.09
	8.0	3	224.0	222.68	222.56
		5	349.0	348.12	346.59
Second mode	2.5	3	408.0	408.78	409.82
		5	-	-	-
	8.0	3	480.0	481.63	481.94
		5	-	-	-
Third mode	2.5	3	754.0	754.66	754.86
		5	760.0	760.76	761.2
	8.0	3	817.0	816.71	816.56
		5	832.0	832.09	831.03

TABLE 6.16 Estimated and exact natural frequencies of the beam with added stiffness.

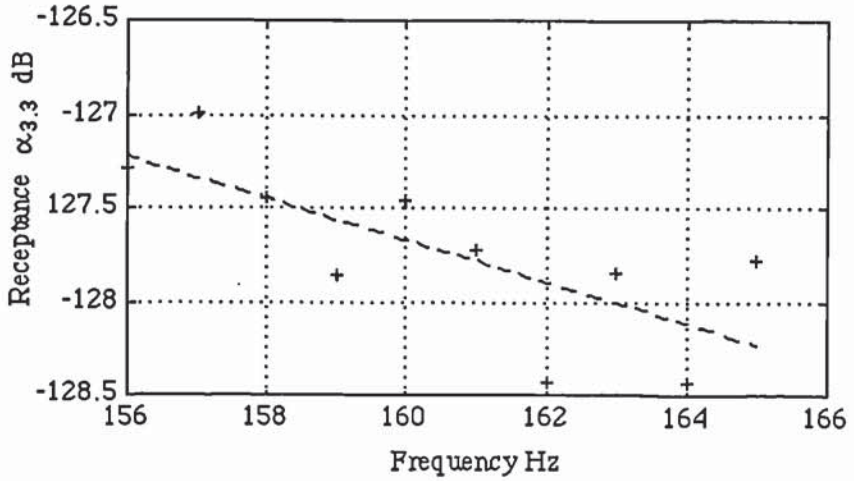

Fig 6.23 Curve fitting the FRF data at coordinate 3.
($k = 2.5x10^6$ N/m, frequency range: 156 Hz to 165 Hz).

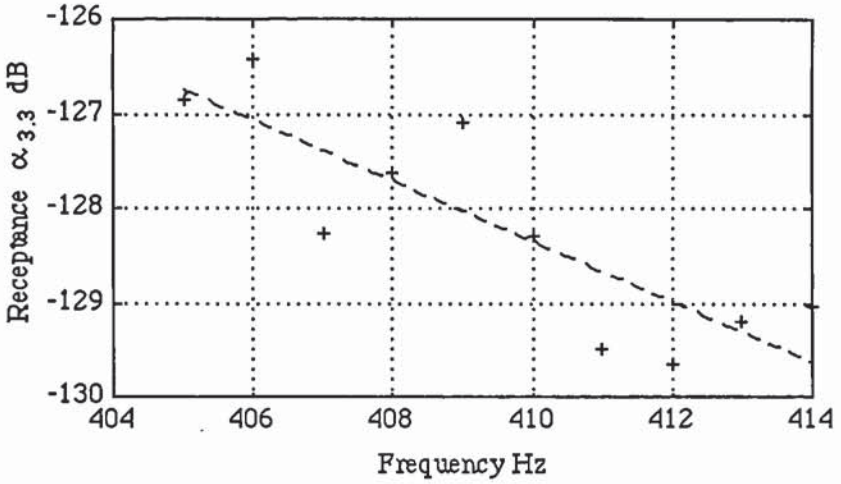

Fig 6.24 Curve fitting the FRF data at coordinate 3.
(k = 2.5x10^6 N/m, frequency range: 405 Hz to 414 Hz).

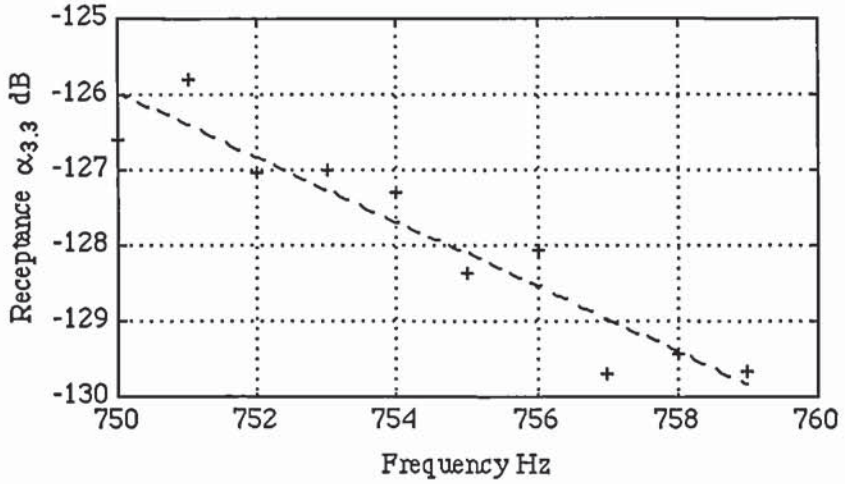

Fig 6.25 Curve fitting the FRF data at coordinate 3.
(k = 2.5x10^6 N/m, frequency range: 750 Hz to 759 Hz)

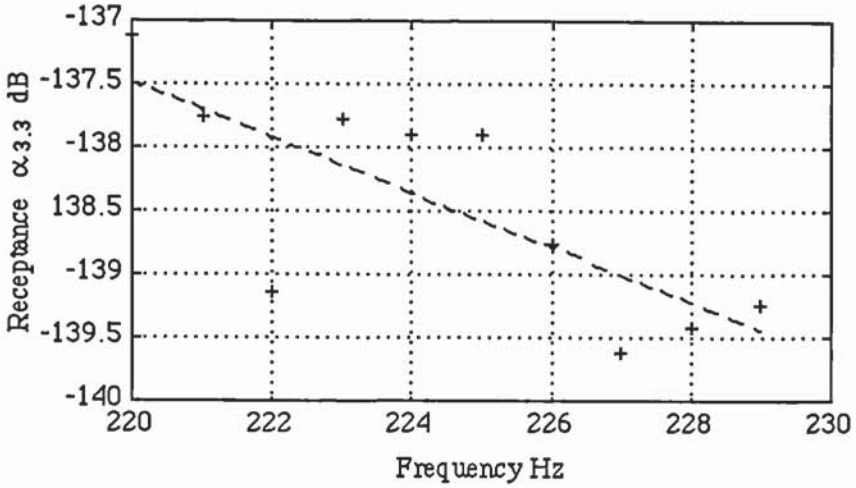

Fig 6.26 Curve fitting the FRF data at coordinate 3.
(k = 8.0x10^6 N/m, frequency range: 220 Hz to 229 Hz)

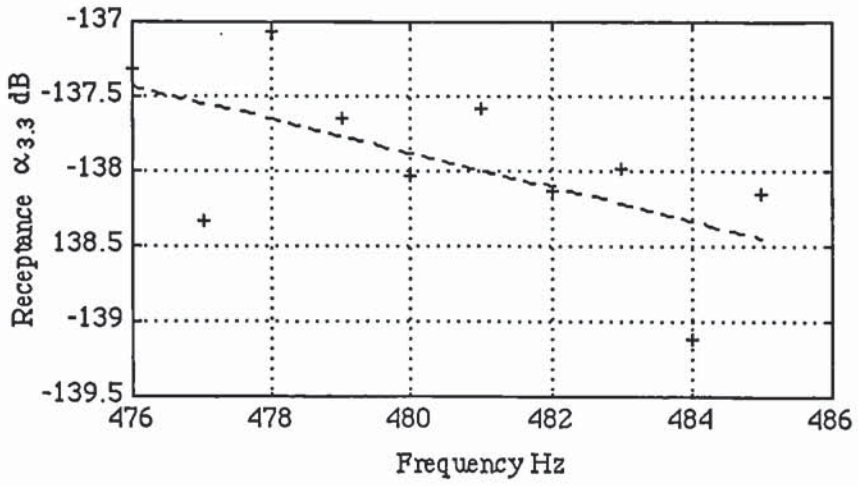

Fig 6.27 Curve fitting the FRF data at coordinate 3.
(k = 8.0x10^6 N/m, frequency range: 476 Hz to 485 Hz)

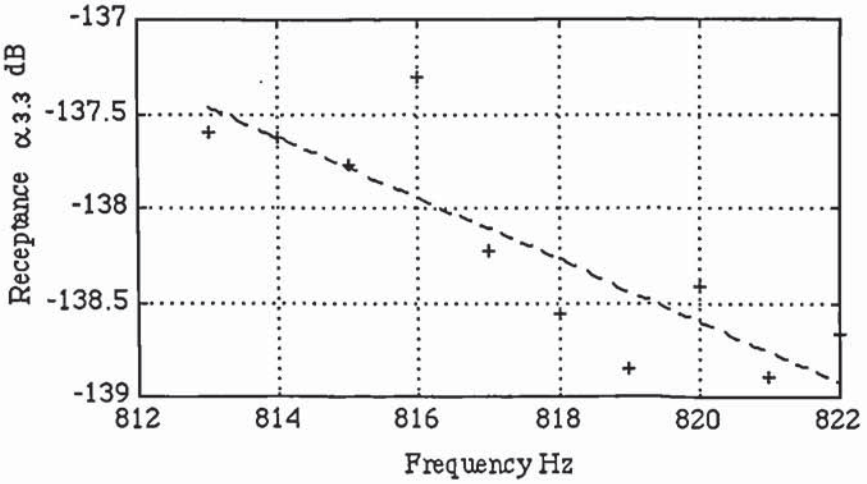

Fig 6.28 Curve fitting the FRF data at coordinate 3.
(k = 8.0x10^6 N/m, frequency range: 813 Hz to 822 Hz)

EXAMPLE 6.3

A plane frame, modelled by a 39 DOF FE model, is shown in fig 6.29 where only motion in the plane of the frame is considered. The frame is unrestrained and is made of 5 beam members, denoted by B1, . . B5. Table 6.17 show the mass and stiffness data of the beam members, used to simulate a physical system. The mass and stiffness data corresponds to a frame made of steel and with cross-sectional dimensions given in the last column in the table. Using this data, the natural frequencies of the first five elastic modes are:

f_1 = 56.07 Hz $\quad$ f_2 = 58.95 Hz $\quad$ f_3 = 70.50 Hz
f_4 = 98.21 Hz $\quad$ f_5 = 109.75 Hz.

The initial analytical model is formulated using the parameters shown in table 6.18 and results in the following natural frequencies:

f_{1a} = 54.60 Hz $\quad$ f_{2a} = 61.34 Hz $\quad$ f_{3a} = 74.04 Hz

f_{4a} = 96.37 Hz f_{5a} = 110.55 Hz.

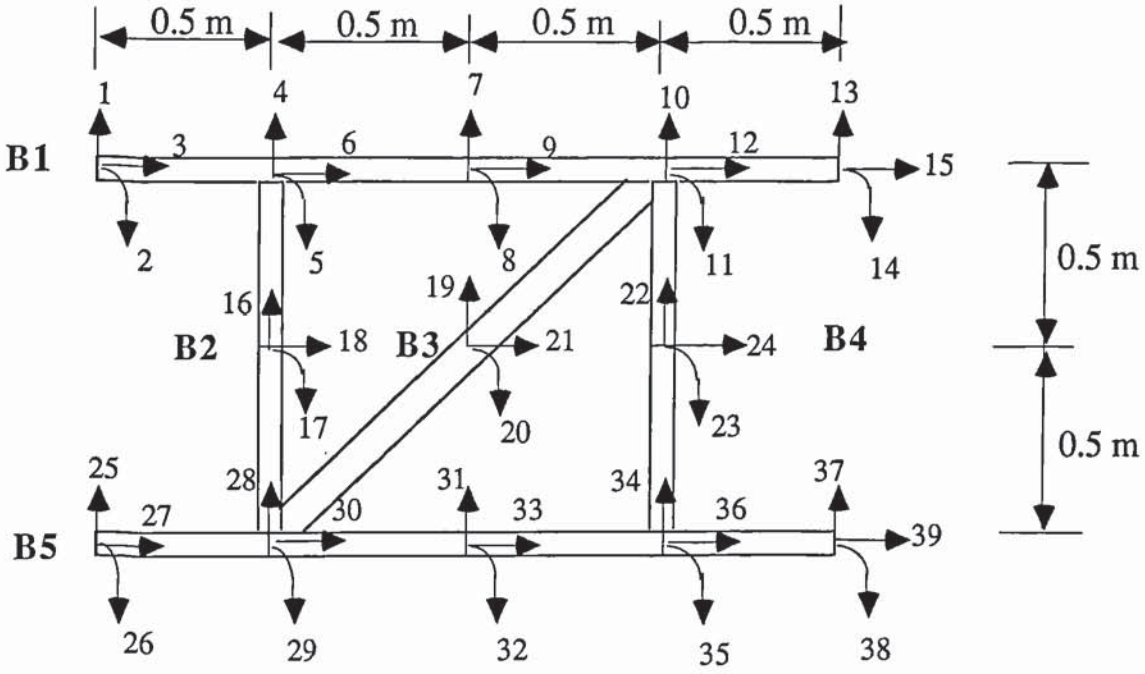

Fig 6.29 Plane frame model.

	EI (Nm^2)	m_u (kg/m)	EA (x10^8 N)	Cross-section (mm x mm)
B1	21333	6.28	1.6	20x40
B2	5208	3.925	1.0	20x25
B3	14292	5.495	1.4	20x35
B4	9000	4.71	1.2	20x30
B5	9000	4.71	1.2	20x30

TABLE 6.17 Parameters of the simulated frame.

	EI Nm^2	m_u kg/m	EA $x10^8N$
B1	25000 (5000)	6.0 (0.5)	1.6
B2	6000 (500)	3.5 (0.5)	1.0
B3	10000 (3000)	5.0 (0.5)	1.4
B4	11000 (2000)	5.5 (0.5)	1.2
B5	11000 (2000)	5.5 (0.5)	1.2

TABLE 6.18 Initial parameters and their standard deviation in brackets.

In this example, correct values of the axial stiffness parameters in the analytical model have been assumed and are not updated. It should be noted that in this example and in many other practical cases, axial flexibility of the beam elements usually have very little influence on the dynamic characteristics in the frequency range of interest and are therefore not updated.

Figs 6.30 and 6.31 show the point receptances of the simulated system and the initial analytical model, at coordinates 24 and 31. To simulate measurement errors, the receptances of the simulated system have been contaminated by random errors with zero mean and standard deviation of 10%.

The analytical model is to be updated using the simulated point receptances at coordinates 24 and 31 by numerical simulation of additional stiffeners at these coordinates (figs 6.30 and 6.31). With error-free data, the parameters should converge to the exact values, if coordinates 24 and 31 are perturbed physically, see Friswell, Nalitolela and Penny (1990) for a very similar example.

Simulated system (with 10% random errors) _____ , Initial model - - - -

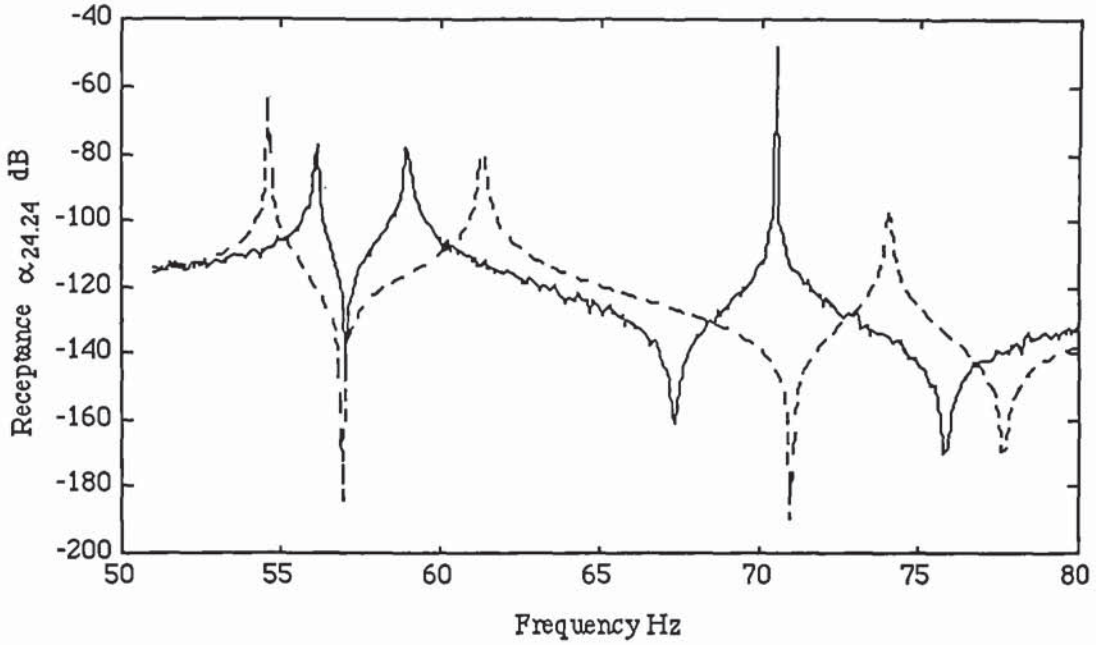

Fig 6.30 Simulated and initial model point receptances at coordinate 24.

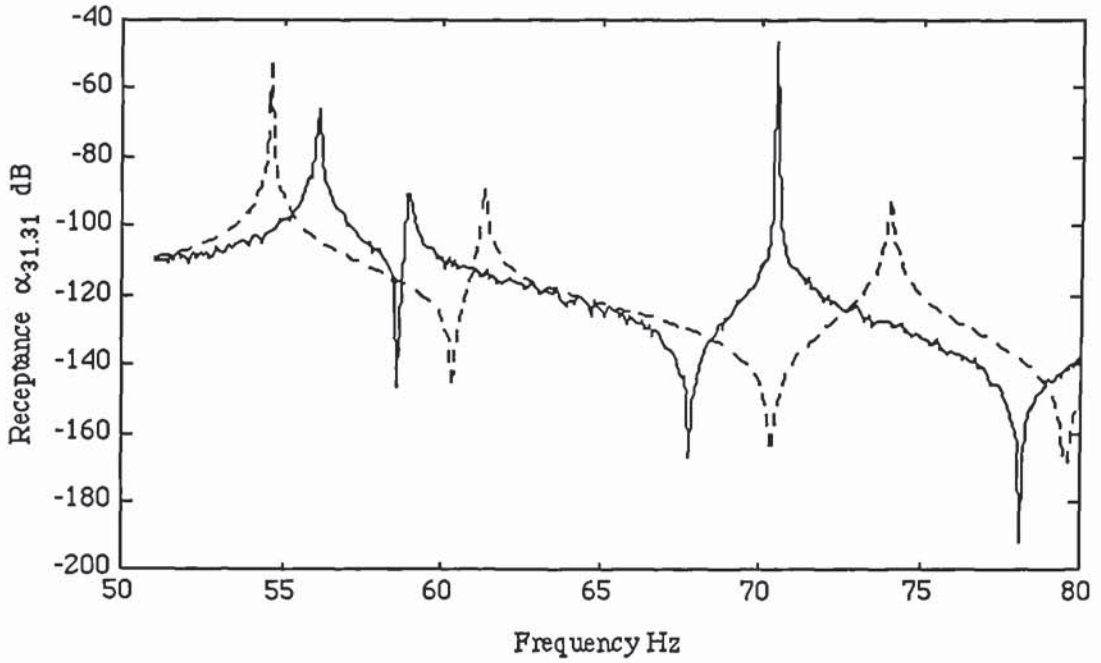

Fig 6.31 Simulated and initial model point receptances at coordinate 31.

In this example, numerical simulation of the additional stiffness is to be performed using the receptance data contaminated by random errors. Four different stiffness additions will be simulated at each of coordinates 24 and 31. Eigenvalues of two modes of the unperturbed structure and two modes of the perturbed structure, for each added stiffness, will be used in the updating process. These are the eigenvalues of the second and third elastic modes of the unperturbed structure and their corresponding new eigenvalues when the structure is perturbed. The perturbing stiffness are $4.0\text{x}10^5$ N/m, $1.0\text{x}10^6$ N/m, $2.5\text{x}10^6$ N/m and $8.0\text{x}10^6$ N/m. The natural frequencies of the frame with added stiffness are given by the frequencies at which the point receptances are equal to $-1/k$. The exact location of the natural frequencies are between the resonance peak and its next antiresonance, for the second and third elastic modes (figs 6.30 and 6.31) and are given by the following receptance magnitudes:

$k = 4.0\text{x}10^5$ N/m	$\alpha_{ii} = 2.5\text{x}10^{-6}$ m/N
$k = 1.0\text{x}10^6$ N/m	$\alpha_{ii} = 1.0\text{x}10^{-6}$ m/N
$k = 2.5\text{x}10^6$ N/m	$\alpha_{ii} = 4.0\text{x}10^{-7}$ m/N
$k = 8.0\text{x}10^6$ N/m	$\alpha_{ii} = 1.25\text{x}10^{-7}$ m/N

Tables 6.19 to 6.22 show the frequency-receptance (magnitude) data at 0.1 Hz resolution zoomed across the zones which, by inspection, the natural frequencies of the frame with added stiffness are most likely to be.

From the tables, the natural frequencies of the frame with added stiffness and their standard deviations were estimated and are shown in table 6.23. The standard deviations, which are used to compute the eigenvalue variances (weighting factors), have been simply approximated by taking the difference between the estimated nominal frequencies and their upper/lower bounds.

$1/k$ ($\times 10^{-6}$ m/N)	Frequency (Hz)	Receptance magnitude ($\times 10^{-6}$ m/N)	$1/k$ ($\times 10^{-6}$ m/N)	Frequency (Hz)	Receptance magnitude ($\times 10^{-6}$ m/N)
2.5	60.6	3.5575	0.4	64.8	0.6278
	60.7	3.3987		64.9	0.5148
	60.8	2.9055		65.0	0.4457
	60.9	2.9489		65.1	0.3711
	61.0	2.6076		65.2	0.4484
	61.1	2.6424		65.3	0.5105
	61.2	2.1166		65.4	0.4152
	61.3	2.0959		65.5	0.4112
	61.4	2.4562		65.6	0.3513
	61.5	1.9266		65.7	0.3718
1.0	62.9	1.2504	0.125	66.2	0.2402
	63.0	1.1524		66.3	0.2498
	63.1	0.9299		66.4	0.1963
	63.2	1.0557		66.5	0.1914
	63.3	1.0225		66.6	0.1357
	63.4	0.9088		66.7	0.1520
	63.5	0.9382		66.8	0.1370
	63.6	1.1023		66.9	0.0902
	63.7	0.8054		67.0	0.0678
	63.8	0.6811		67.1	0.0496

TABLE 6.19 Receptance data of the frame at excitation coordinate 24.

This data is for the estimation of the new natural frequencies of the originally second elastic mode of the unperturbed free frame, when stiffness additions are simulated at coordinate 24.

$1/k$ ($x10^{-6}$ m/N)	Frequency (Hz)	Receptance magnitude ($x10^{-6}$m/N)	$1/k$ ($x10^{-6}$ m/N)	Frequency (Hz)	Receptance magnitude ($x10^{-6}$m/N)
2.5	70.7	6.0719	0.4	72.3	0.5341
	70.8	3.3062		72.4	0.4506
	70.9	2.3233		72.5	0.4130
	71.0	1.9681		72.6	0.3581
	71.1	1.8267		72.7	0.3737
	71.2	1.6085		72.8	0.3967
1.0	71.3	1.3466		72.9	0.3827
	71.4	1.1369		73.0	0.3954
	71.5	1.2348		73.1	0.3424
	71.6	0.8850		73.2	0.2424
	71.7	0.8708	0.125	74.3	0.1615
	71.8	0.7323		74.4	0.1536
				74.5	0.1144
				74.6	0.1102
				74.7	0.0888
				74.8	0.0888

TABLE 6.20 Receptance data of the frame at the excitation coordinate 24.

This data is for the estimation of the new natural frequencies of the originally third elastic mode of the unperturbed free frame, when stiffness additions are simulated at coordinate 24.

$1/k$ ($\times 10^{-6}$ m/N)	Frequency (Hz)	Receptance magnitude ($\times 10^{-6}$ m/N)	$1/k$ ($\times 10^{-6}$ m/N)	Frequency (Hz)	Receptance magnitude ($\times 10^{-6}$ m/N)
2.5	60.4	3.1965	0.4	65.7	0.5613
	60.5	2.7300		65.8	0.4929
	60.6	2.7281		65.9	0.4629
	60.7	2.1998		66.0	0.4091
	60.8	2.1895		66.1	0.4418
	60.9	2.2284		66.2	0.3593
	61.0	2.2946		66.3	0.3942
	61.1	1.9017		66.4	0.3662
1.0	63.1	1.1388	0.125	66.8	0.2664
	63.2	1.0529		66.9	0.2198
	63.3	1.0439		67.0	0.2043
	63.4	0.8578		67.1	0.1623
	63.5	1.0735		67.2	0.1410
	63.6	1.0643		67.3	0.1439
	63.7	0.8903		67.4	0.1006
	63.8	0.9647		67.5	0.1072
	63.9	0.9894		67.6	0.0537
	64.0	0.9501		67.7	0.0307

TABLE 6.21 Receptance data of the frame at excitation coordinate 31.

This data is for the estimation of the new natural frequencies of the originally second elastic mode of the unperturbed free frame, when stiffness additions are simulated at coordinate 31.

$1/k$ ($x10^{-6}$ m/N)	Frequency (Hz)	Receptance magnitude ($x10^{-6}$ m/N)	$1/k$ ($x10^{-6}$ m/N)	Frequency (Hz)	Receptance magnitude ($x10^{-6}$ m/N)
2.5	70.8	5.3455	0.4	73.5	0.5195
	70.9	3.5175		73.6	0.3963
	71.0	2.8195		73.7	0.4325
	71.1	2.4282		73.8	0.4930
	71.2	2.0963		73.9	0.4211
	71.3	1.8056		74.0	0.4256
	71.4	1.5898		74.1	0.4256
	71.5	1.7024		74.2	0.3190
1.0	71.6	1.2105		74.3	0.3140
	71.7	1.1410	0.125	76.0	0.1738
	71.8	1.1668		76.1	0.1433
	71.9	1.0132		76.2	0.1476
	72.0	1.0891		76.3	0.1108
	72.1	1.0680		76.4	0.1070
	72.2	0.9147		76.5	0.1022
	72.3	0.8957		76.6	0.0901
	72.4	0.7251		76.7	0.0875

TABLE 6.22 Receptance data of the frame at excitation coordinate 31.

This data is for the estimation of the new natural frequencies of the originally third elastic mode of the unperturbed free frame, when stiffness additions are simulated at coordinate 31.

Added stiffness ($x10^6$ N/m)	Stiffness addition coordinate	Estimated natural frequency (Hz) and standard deviation.			
		f_2	STDf_2	f_3	STDf_3
4.0	24	61.1	0.2	70.9	0.1
	31	60.7	0.2	71.1	0.1
1.0	24	63.3	0.2	71.5	0.1
	31	63.5	0.3	72.0	0.2
2.5	24	65.2	0.3	72.7	0.3
	31	66.1	0.2	73.9	0.2
8.0	24	66.7	0.2	74.5	0.2
	31	67.4	0.1	76.3	0.2

TABLE 6.23 Natural frequency and standard deviation estimates of the frame with added stiffness.

The correct natural frequencies of the unperturbed frame (second and third elastic modes only) were taken to represent measured natural frequencies, obtained by modal analysis, but with an uncertainty represented by a standard deviation of 0.1 Hz.

Using the natural frequencies of the frame with added stiffness, table 6.23, and of the unperturbed frame, mass and stiffness parameters were determined by the minimum cost Bayesian approach. The following updated parameters were obtained in 5 iteration steps. The natural frequencies of the first three elastic modes of the updated model are also given (second and third modes were used in the updating process).

EI_{B1}=19690 Nm^2 EI_{B2}= 5932 Nm^2 EI_{B3} = 14045 Nm^2

EI_{B4} = 9380 Nm^2 EI_{B5} = 9349 Nm^2

$m_{u,B1}$ = 6.11 kg/m $m_{u,B2}$ = 3.31 kg/m $m_{u,B3}$ = 5.56 kg/m

$m_{u,B4}$ = 5.07 kg/m $m_{u,B5}$ = 4.88 kg/m.

$f_1 = 52.22$ Hz $\qquad$ $f_2 = 58.94$ Hz $\qquad$ $f_3 = 70.52$ Hz.

Figs 6.32 and 6.33 show the convergence of the mass and stiffness parameters as percentage changes from their initial estimates. Fig 6.34 to 6.36 compare receptance prediction of the analytical model, the updated model and the simulated system at coordinates different from the ones used in the updating process. These are the translational receptance at coordinate 4, and rotational receptances at coordinates 5 and 11. In each case, 31 is the excitation coordinate. It can be seen that the updated model's receptance prediction is good. Note that, the frequency range used in the updating process is between 58 Hz and 77 Hz approximately.

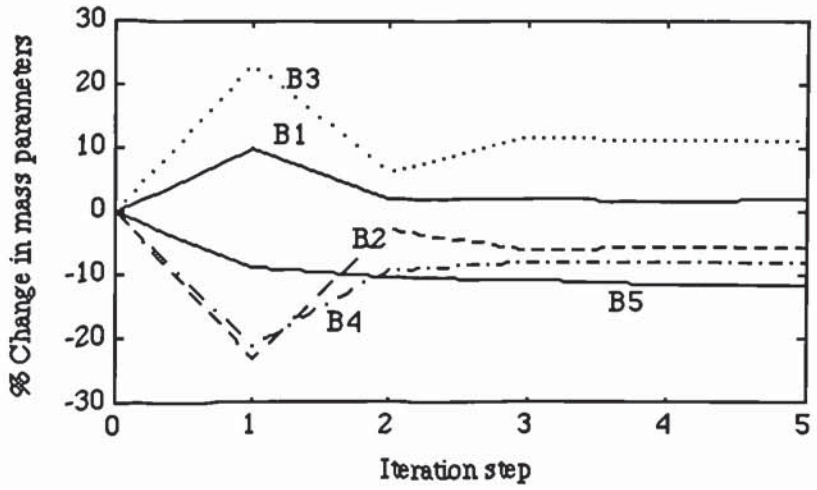

Fig 6.32 Convergence of the mass parameters of the frame.

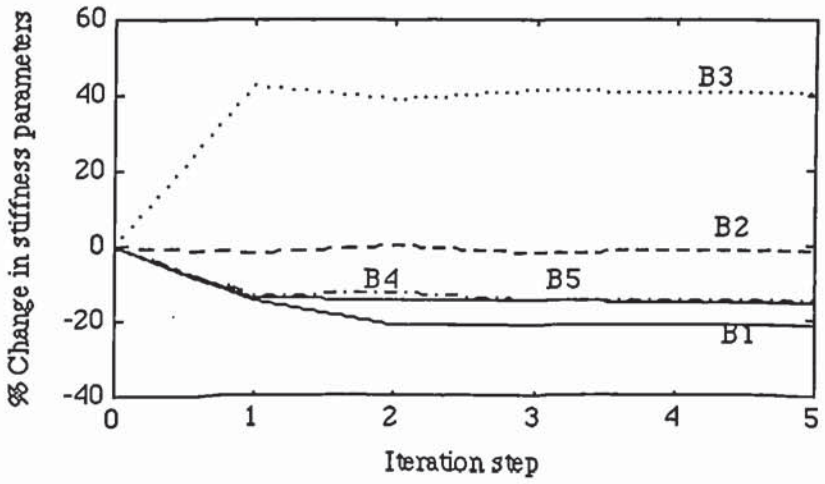

Fig 6.33 Convergence of the stiffness parameters of the frame.

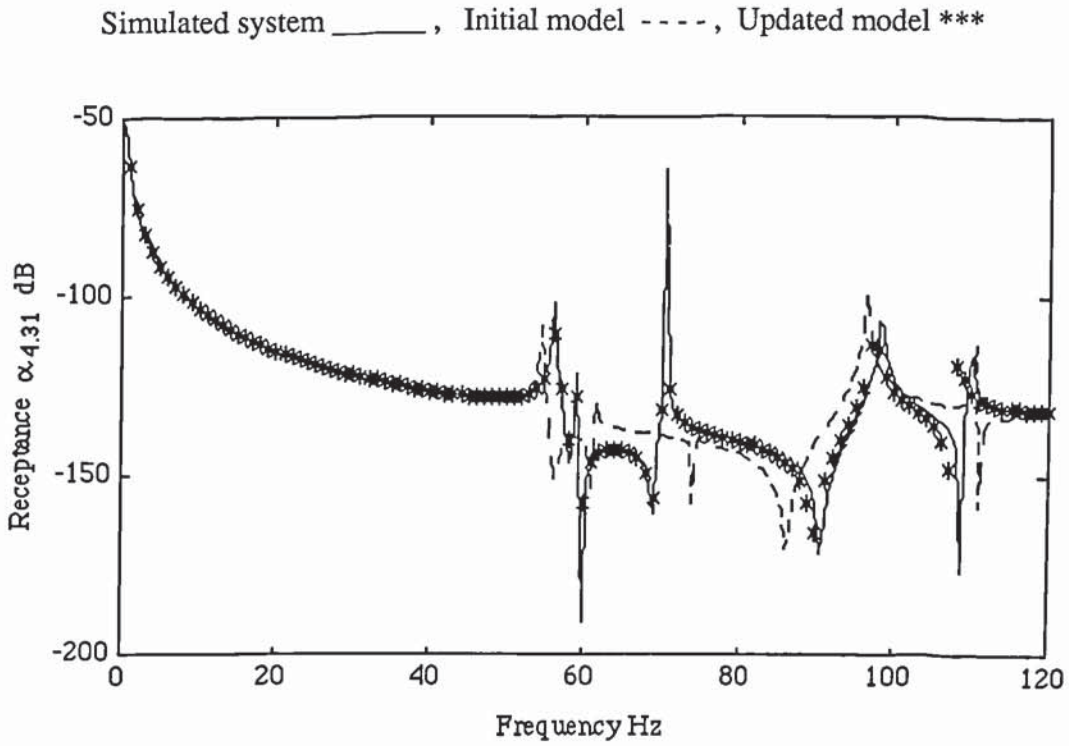

Fig 6.34 Translational receptance prediction at coordinate 4.

Simulated system _____ , Initial model - - - - , Updated model ***

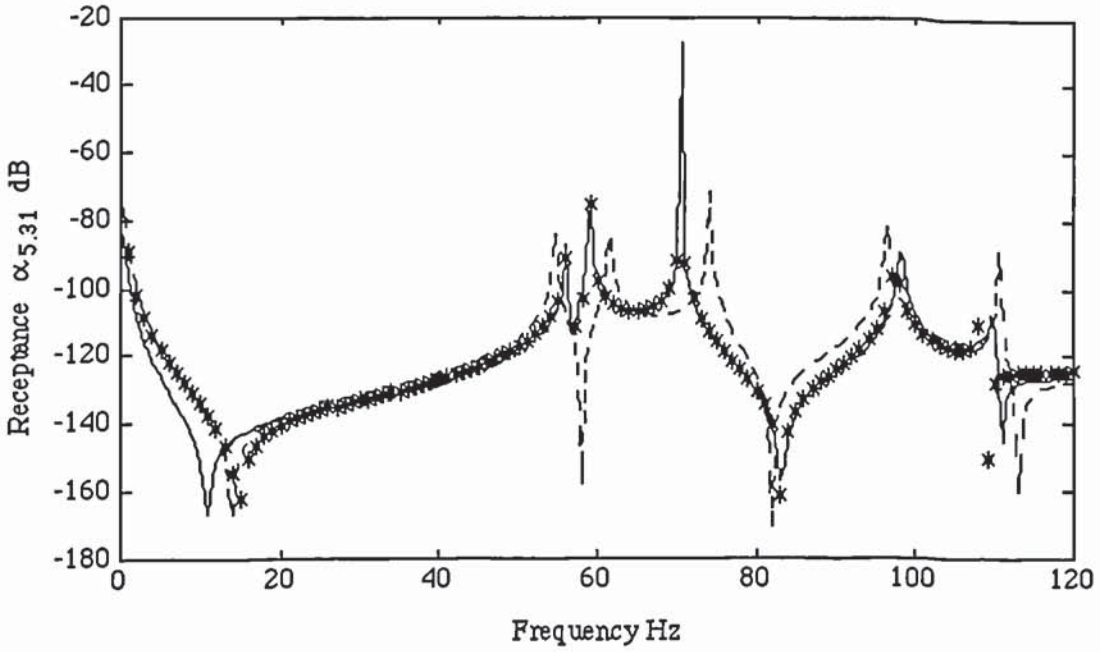

Fig 6.35 Rotational receptance prediction at coordinate 5.

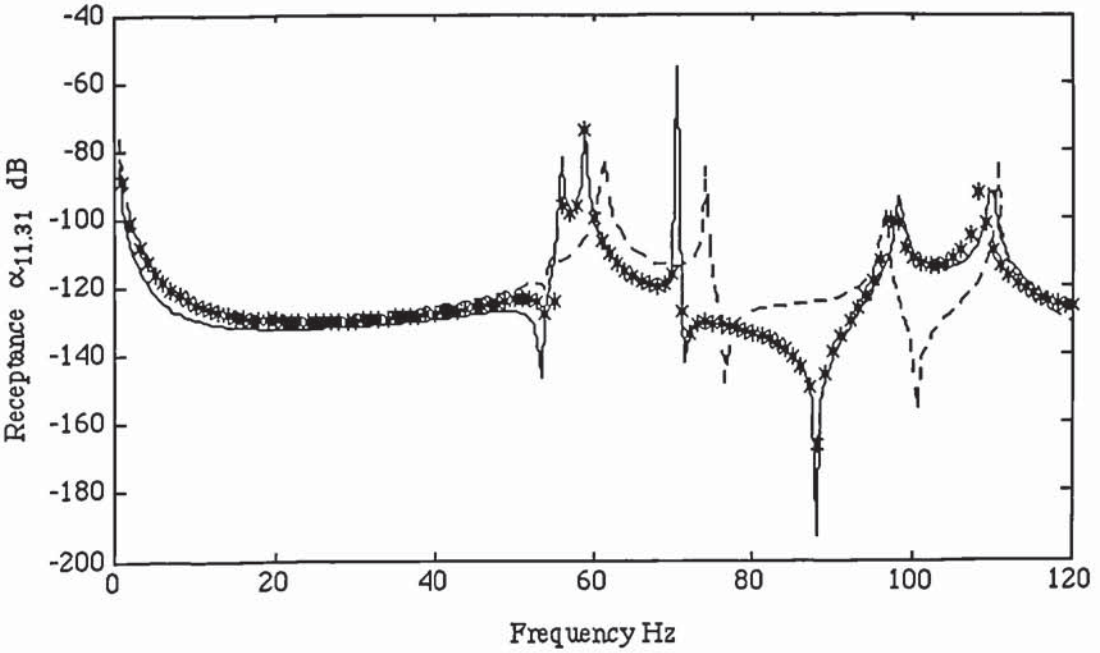

Fig 6.36 Rotational receptance prediction at coordinate 11.

6.3.2 Simulation example: Lightly damped structure.

So far, the numerical examples have assumed that the system under investigation is undamped and therefore the natural frequencies of the system when perturbed by real stiffness are simply obtained from a solution of (6.13). Equation (6.13) is based on the fact that at resonant frequency, the receptance of an undamped system becomes infinity. Practical structures are always damped and (6.13) is therefore not applicable since η is not zero. Indeed, it can be seen that, the receptances of practical structures are complex and (6.13) cannot be solved for a real k. However, an approximation is feasible by considering the fact that, for lightly damped structures, at frequencies away from resonance and antiresonance, its receptance amplitude is usually very close to the receptance of the undamped system and α_{ii} is almost real. Thus, as the phase angle in α_{ii} approaches zero (or 180°), α_{ii} approaches the receptance of the undamped system. In this case, (6.13) can be used to estimate the natural frequencies of the undamped system with added stiffness. Once the natural frequencies of the undamped system are determined, an undamped model can be established. If the system can be adequately represented by a proportionally damped model, the updated undamped model can be used to determine the damping matrix by using orthogonality equations. If damping levels are high such that the undamped approximation is not practical, then a more generalized approach to determine the eigen-data of the perturbed system has to be used. This involves computation of the FRF of the perturbed system using the FRF of the unperturbed system, and finding the eigen-data using a modal analysis algorithm.

It is difficult to give rigid rules on the choice of the limiting phase angles in α_{ii} before which the undamped approximation should not be used, as it also depends on the degree of demanded accuracy. It is reasonable, however, to use

a figure of +(-)10° of the in-phase or out-of-phase condition, as is commonly used in deciding whether measured modes could be treated as real modes.

EXAMPLE 6.4

The 4 elements, 10 DOF free beam of example 6.1 is now simulated with a damping matrix proportional to the stiffness matrix. The damping proportionality factor, which in this case is the same as the damping loss factor, is 0.02. The error-free point receptances (magnitude and phase plots) at coordinates 3 and 5 are shown in figs 6.37 to 6.40. It is required to update the initial model, given in example 6.1, by stiffness addition where the natural frequencies of the beam with added stiffness are to be estimated from the receptance data of the unperturbed beam. Let the added stiffness and the stiffness addition coordinates be the same as in example 6.1 ($2x10^6$ N/m and $1.0x10^7$ N/m at coordinates 3 and 5).

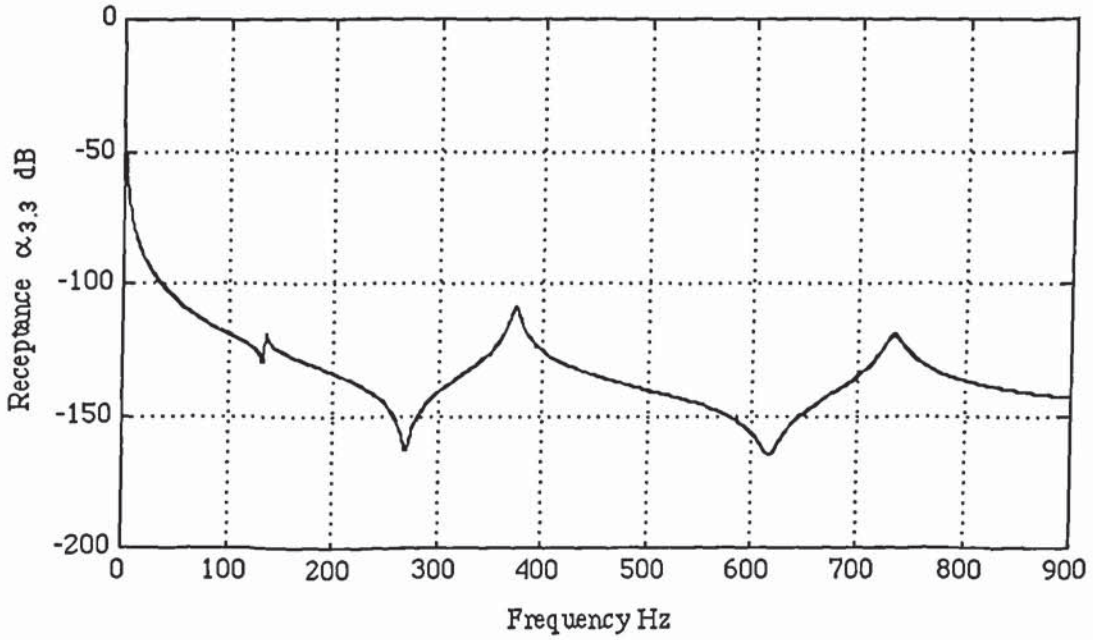

Fig 6.37 Point receptance (magnitude) at coordinate 3.

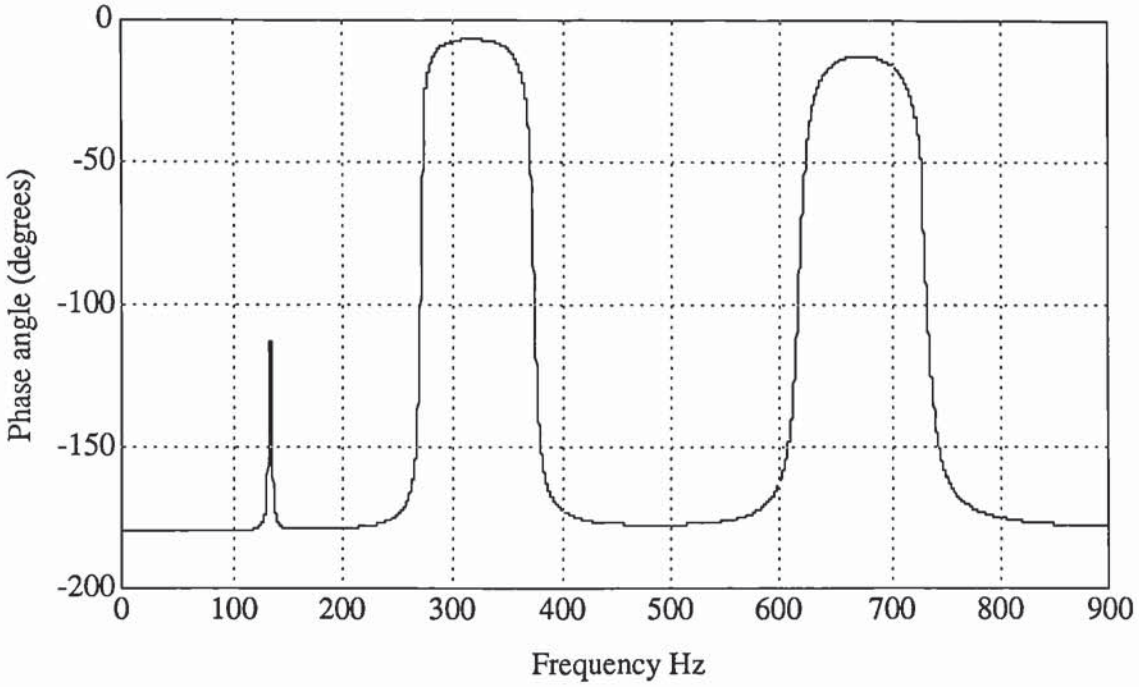

Fig 6.38 Phase angles for the point receptance at coordinate 3.

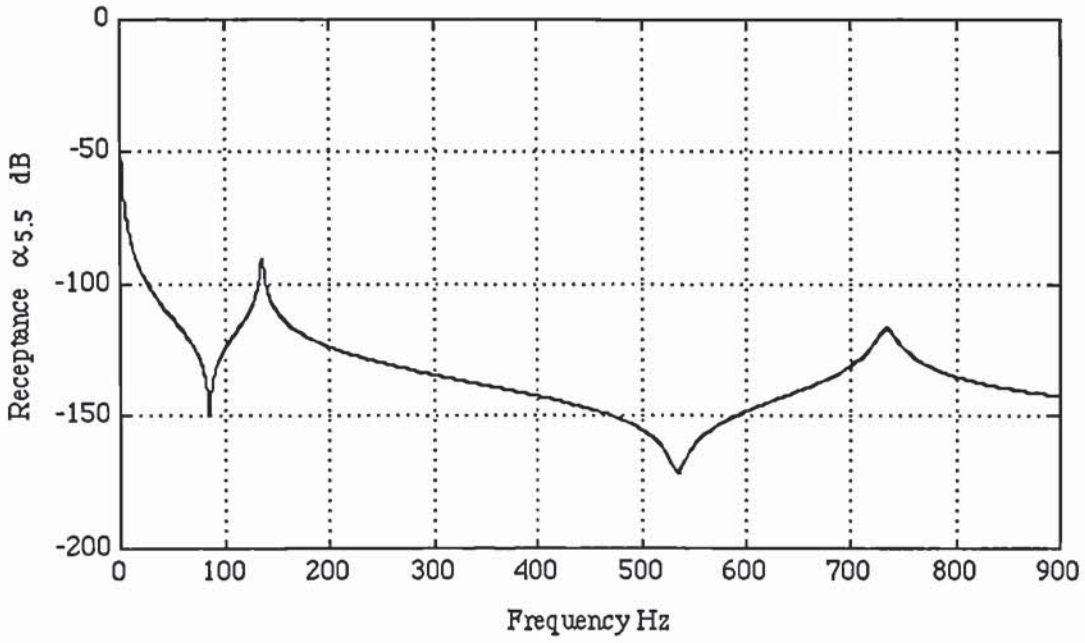

Fig 6.39 Point receptance (magnitude) at coordinate 5.

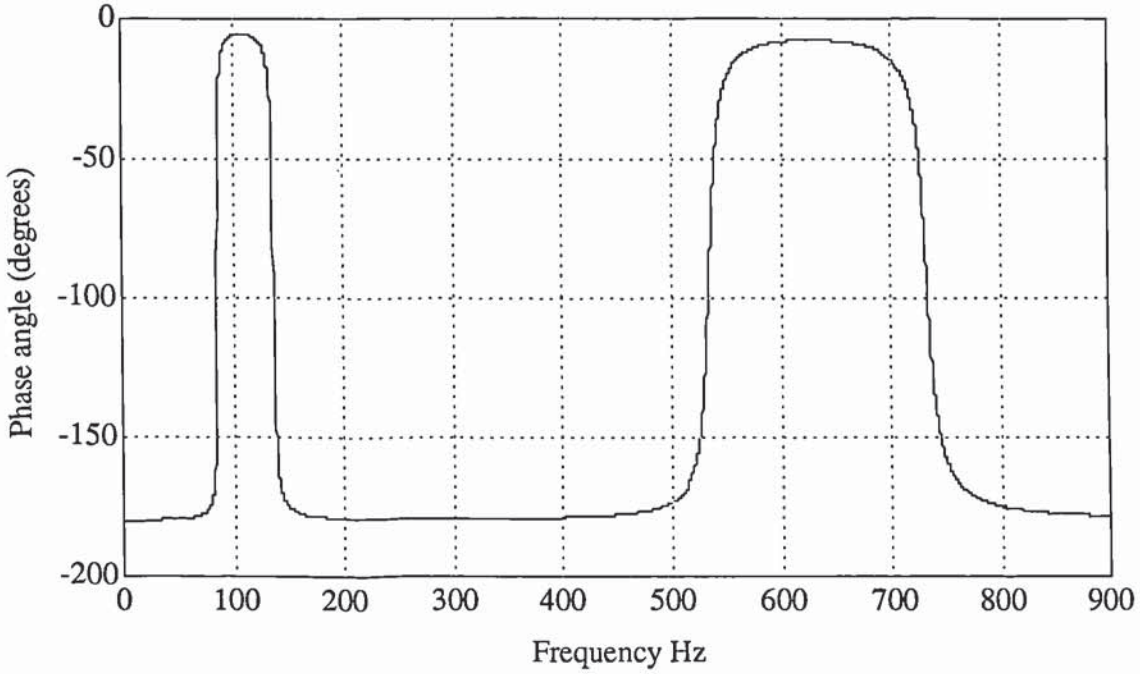

Fig 6.40 Phase angles for the point receptance at coordinate 5.

By inspection of the receptance data, at 0.25 Hz resolution, the natural frequencies of the beam with added stiffness are estimated as shown in table 6.24. Both the natural frequency estimates and phase angles in the corresponding receptance data are tabulated. It can be seen that the phase angles in the receptance data for the estimation of the new natural frequencies of the originally third elastic mode, with stiffness addition of $2x10^6$ N/m, are more than the 10^o limit of the out-of-phase or in-phase condition. Consequently the estimated natural frequencies of this mode are likely to contain the biggest errors. This is confirmed by comparing table 6.24 with table 6.25 (columns 2,4,5 and 7), where the later table gives the correct natural frequencies of the beam with added stiffness as determined by solving the eigenvalue problem. Note that, in these tables, there is no entry for the natural frequencies of mode 2 when stiffness is added at coordinate 5. This coordinate is a node for the mode in question and there is no change in natural frequency from the unperturbed case.

	Excitation and measurement at coordinate 3				Excitation and measurement at coordinate 5			
	$k = 2x10^6$ (N/m)		$k = 1x10^7$ (N/m)		$k = 2x10^6$ (N/m)		$k = 1x10^7$ (N/m)	
	f (Hz)	Phase (deg.)	f (Hz)	Phase (deg.)	f (Hz)	Phase (deg.)	f (Hz)	Phase (deg.)
Mode 1	151.5	-179.2	231.25	2.6	215.50	-179.4	371.25	0.8
Mode 2	402.0	-173.4	501.00	2.2	-	-	-	-
Mode 3	748.5	-157.0	842.25	2.5	754.25	-162.2	857.75	2.5

TABLE 6.24 Natural frequency estimates of the beam with added stiffness. (light proportional damping, $k = 2x10^6$ N/m and $1x10^7$ N/m)

	Stiffness addition at coordinate 3			Stiffness addition at coordinate 5		
	$k = 2x10^6$ (N/m)	$k = 8x10^6$	$k = 1x10^7$ (N/m)	$k = 2x10^6$ (N/m)	$k = 8x10^6$ (N/m)	$k = 1x10^7$ (N/m)
	f (Hz)	f (Hz)	f (Hz)	f (Hz)	f (Hz)	f (Hz)
Mode 1	151.39	222.57	231.16	215.59	346.61	371.27
Mode 2	402.31	481.95	500.93	-	-	-
Mode 3	750.17	816.55	842.44	755.35	831.03	857.86

TABLE 6.25 Correct natural frequencies of the beam with added stiffness.

To minimize errors, the selection of the additional stiffness should ensure that the frequencies which become the new natural frequencies of the perturbed structure, correspond to point receptance data which is very close to the in-

phase or out-of-phase condition. For example, if we select stiffness addition of $8x10^6$ N/m instead of $2.0x10^6$ N/m, the estimated natural frequencies and the receptance phase angles at coordinates 3 and 5 are now shown in table 6.26. It can be seen that the phase angles are much smaller and the errors in the estimated natural frequencies are much reduced. Even without comparing with the correct natural frequencies in table 6.25, it can now be reasonably assumed that the natural frequencies in table 6.26 are a good approximation of the natural frequencies of the undamped beam with added stiffness.

	Excitation and measurement at coordinate 3				Excitation and measurement at coordinate 5			
	$k = 8x10^6$ (N/m)		$k = 1x10^7$ (N/m)		$k = 8x10^6$ (N/m)		$k = 1x10^7$ (N/m)	
	f (Hz)	Phase (deg.)	f (Hz)	Phase (deg.)	f (Hz)	Phase (deg.)	f (Hz)	Phase (deg.)
Mode 1	222.25	1.9	231.25	2.6	346.5	0.6	371.25	0.8
Mode 2	482.00	2.1	501.00	2.2	-	-	-	-
Mode 3	816.25	3.5	842.25	2.5	830.75	3.3	857.75	2.5

TABLE 6.26 Natural frequency estimates of the beam with added stiffness.
(light proportional damping, $k = 8x10^6$ N/m and $1x10^7$ N/m)

Although the FRF data is simulated error-free, the natural frequencies obviously contains errors of a magnitude which is at least of the order of magnitude as the resolution of the frequency axis (0.25 Hz in this case). Assume in this case, the standard deviation in the natural frequency data is given by 0.25 Hz. Using an unconstrained weighted least squares solution method, the following updated parameters (of an undamped model) were

obtained in five iteration steps.

$EI_1 = 4840$ Nm^2	$EI_2 = 5147$ Nm^2	$EI_3 = 4776$ Nm^2
$EI_4 = 5068$ Nm^2	$m_{u1} = 3.452$ kg/m	$m_{u2} = 3.548$ kg/m
$m_{u3} = 3.477$ kg/m	$m_{u4} = 3.414$ kg/m.	
$f_1 = 134.77$ Hz	$f_2 = 373.02$ Hz	$f_3 = 732.96$ Hz.

As damping is "proportional", the undamped model's eigenvectors are the same as the eigenvectors of the damped model. Using the damping factors measured on the unperturbed structure, and the updated undamped model matrices and eigen-data, a least squares solution for the damping proportionality constants with respect to the mass and stiffness matrices can be determined from (6.17). Note that (6.17) is derived from (6.15), and U_j, ω_j^2 are the eigen-data of the undamped updated model, whereas η_j are the damping factors measured on the unperturbed structure.

$$U_j^T \mathbf{H} U_j = \eta_j \omega_j^2 \tag{6.15}$$

$$U_j^T \left[\chi_k \mathbf{K} + \chi_m \mathbf{M}\right] U_j = \eta_j \omega_j^2 \tag{6.16}$$

$$\chi_k \omega_j^2 + \chi_m = \eta_j \omega_j^2 \tag{6.17}$$

The number of measured modes is usually greater than one, and (6.17) can therefore be assembled in a matrix equation for all measured modes of the unperturbed structure, and solved for the proportionality constants χ_m and χ_k. In this example, three modes of the unperturbed beam were simulated to have been measured, with η_j ($j = 1, 2, 3$) of 0.02. Using the computed eigenvalues of the first three elastic modes of the updated, undamped model, the following

damping proportionality constants are obtained:

$$\chi_k = 0.0200 \qquad \chi_m = -7.27\text{x}10^{-11}.$$

χ_m is practically zero. Thus an updated model is obtained with a damping matrix proportional to the stiffness matrix, by a factor of 0.02.

Figs 6.41 and 6.42 compare receptance prediction (magnitude) between the initial model, the updated model and the simulated system at coordinates 3 and 9, with an excitation at coordinate 3. They both show good agreement in the FRFs between the simulated and the updated models.

System (damped) ____ , Initial model (undamped) - - - - , Updated model (damped) * * *

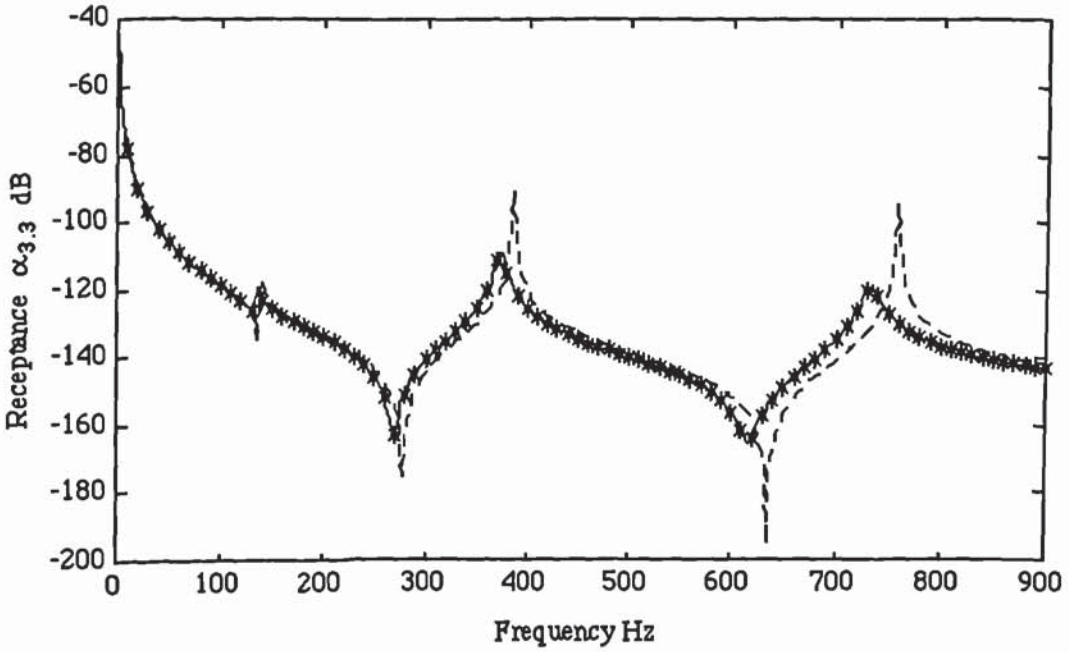

Fig 6.41 Comparing receptance prediction at coordinate 3.

System (damped) ____ , Initial model (undamped) - - - - , Updated model (damped) * * *

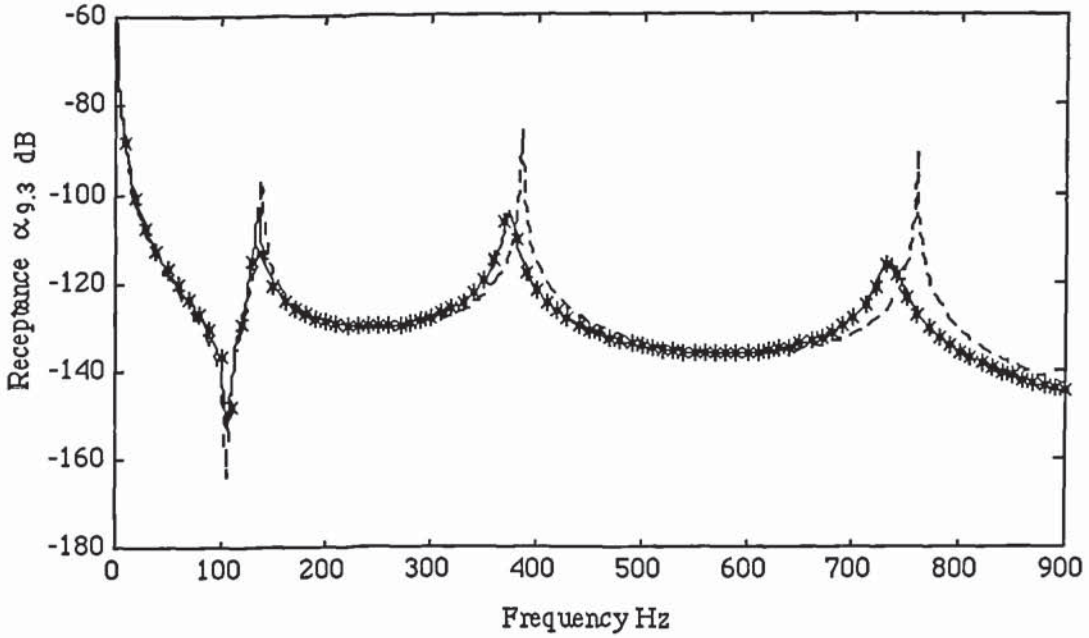

Fig 6.42 Comparing receptance prediction at coordinate 9.

6.4 Generalization for system with damping.

6.4.1 Extraction of the eigen-data of the perturbed structure.

A simplified procedure of extracting the eigen-data of the perturbed structure using FRF data of the unperturbed structure has been presented in Section 6.3. The procedure, which is based on solving (6.13) or a similar expression for mass addition, by inspection of the point receptance data is most suitable for systems with very light damping. Its main difficulty is that α_{ii} is generally complex, and for a real additional stiffness or mass, a solution of (6.13) is generally not possible. The simplified procedure assumes that if the phase angle in α_{ii} is close to zero or 180°, its magnitude is very close to that of an undamped structure. The natural frequencies of the perturbed undamped structure may therefore be determined by replacing the complex α_{ii} by its magnitude and solve the real equation for ω. The application of this simplified procedure is feasible for lightly damped structures only since for relatively high damping levels, it is usually the case that the zone over which the receptance magnitude of the damped and undamped systems are in agreement, is rather limited.

A generalized procedure of extracting eigen-data of the perturbed system using FRF data of the unperturbed system, irrespective of the damping levels and non-proportionality is now investigated. It is based on the reconstruction of the FRF of the perturbed structure from the FRF data of the unperturbed structure using (6.8) or (6.9). The eigen-data is then extracted from the reconstructed FRF using a modal analysis algorithm. Any of the well established modal analysis algorithms may be used, but attention has to be paid to the fact that random errors in the reconstructed FRF may not have the same distribution as random errors in the FRF data of the unperturbed structure. In

this case, (6.10) and (6.11) may be used to estimate the weighting factors of the reconstructed FRF data.

6.4.2 Parameter estimation.

The generalized method will extract natural frequencies and damping factors and, if needed, mode shape vectors of the perturbed structure. If a model with a damping matrix is desired, the sensitivity matrix, which now includes the sensitivity of the eigen-data with respect to the damping parameters, will generally become complex. Consider the matrix equation (6.18), where **G** is the eigenvalue (or both eigenvalue and eigenvector) sensitivity matrix, and b is the vector of difference between the eigenvalues (or both eigenvalues and eigenvectors) of the system and the analytical model (before as well as after mass or stiffness addition).

$$\mathbf{G}\{\Delta s\} = b \tag{6.18}$$

Both **G** and b are generally complex. Equation (6.18) can be written as a set of two real matrix equations by equating, separately, the real parts on both sides of the equation and the imaginary parts. The two sets of the equations can be combined into a single overdetermined equation, (6.19).

$$\begin{bmatrix} \text{Real}(\mathbf{G}) \\ \text{Imag}(\mathbf{G}) \end{bmatrix} \{\Delta s\} = \begin{Bmatrix} \text{Real}(b) \\ \text{Imag}(b) \end{Bmatrix} \tag{6.19}$$

Parameter update on the current analytical model, can be determined using the minimum cost Bayesian estimator, derived in Chapter 4, by making the following substitution in (4.15).

$$\begin{bmatrix} \mathbf{J}_\lambda \\ \mathbf{J}_U \end{bmatrix} \text{ is replaced by } \begin{bmatrix} \text{Real}(\mathbf{G}) \\ \text{Imag}(\mathbf{G}) \end{bmatrix}$$

$$\begin{Bmatrix} \Delta\lambda \\ \Delta U \end{Bmatrix} \text{ is replaced by } \begin{Bmatrix} \text{Real}(b) \\ \text{Imag}(b) \end{Bmatrix}$$

$\mathbf{W}_{\lambda,U}$ is replaced by a diagonal weighting matrix, whose terms in the first half of its main diagonal are reciprocals of the variances of the real parts of the eigen-data of the structure, and the terms in the second half of its main diagonal are reciprocals of the variances of the imaginary parts.

Partitioning the matrix equation into real and imaginary parts and reassembling into a single overdetermined equation, in the form of (6.18), is not a new approach. In this work, this approach is adopted in the context of a new concept of how to use the experimental data to update an analytically derived model. Since parameter estimation is based on iterative adjustments of the initial analytical model, it is necessary that initial damping parameters are available. The determination of a reasonable initial damping matrix by theoretical considerations alone is difficult. The finite element model is typically undamped. As many structural systems may be adequately represented by a system with proportional damping, some possibilities do exist to get around this difficulty.

One possibility is to assume initial damping proportionality constants of zero. The updating process is then performed to improve on the initial estimates.

A second possibility is to use the analytical model and measured damping factors to find some estimates of the damping proportionality constants by solving, in a least squares sense, the orthogonality equation of the damping

matrix with respect to the analytical eigenvectors. This is effectively using (6.17), or a similar expression in case of proportional viscous damping, where ω_j are derived from the initial analytical model and η_j are measured. χ_k and χ_m becomes the initial estimates.

A third possibility is to estimate the undamped eigen-data of the structure from measured eigen-data of the perturbed and unperturbed structure. For structures which are very close to being proportionally damped, the errors involved in the estimation are usually very small. The estimated eigen-data of the undamped structure is then used to update the undamped analytical model. The updated analytical model and measured damping factors are then used to find a least squares solution of the damping proportionality constants using orthogonality equation (6.15) which results in (6.17). This method is similar to that used in example (6.4). The advantage of this method is, the damping parameters are not determined by an iterative updating. The equation used to determine the damping parameters, (6.17), involves only two unknowns and tends to be numerically more stable. Unconstrained least squares solution method can be used and therefore the weighting factors for the initial damping parameters need not be assumed.

For systems which have to be modelled by a model with non-proportional damping, progress is difficult since determining initial analytical damping parameters of practical structures is difficult and there is no reliable method. The work reported in this thesis does not involve the details of analytical modelling of the damping matrix, as that is a rather special problem. However, a simulation study will be performed, by assuming initial damping model/parameters are available.

6.4.3 Simulation example

EXAMPLE 6.5

The 4 elements, 10 DOF free beam of example 6.1 (fig 6.2), is simulated with non-proportional hysteretic damping. Each element damping matrix is assumed to be proportional to element stiffness matrix. Damping matrix non-proportionality is achieved by using different proportionality constants for different elements. Thus, the system is simulated by replacing the real stiffness parameters by complex stiffness parameters, which are given as:

$$EI_1 = 5000(1+j0.002)\ \text{Nm}^2 \qquad EI_2 = 5000(1+j0.05)\ \text{Nm}^2$$
$$EI_3 = 5000(1+j0.002)\ \text{Nm}^2 \qquad EI_3 = 5000(1+j0.05)\ \text{Nm}^2.$$

The FE model, to be updated by stiffness addition, is the same as in example 6.1. The additional stiffness are $2\text{x}10^6$ N/m and 10^7 N/m at coordinates 3 as well as 5. These are the same stiffness as in example 6.1 with the same stiffness addition coordinates. In this case, the FRF for the beam with added stiffness at the excitation coordinate (coordinate 3 and then 5) will be derived from the FRF of the beam without additional stiffness. The excitation coordinates are the coordinates to be perturbed. The eigen-data of the beam before and after adding stiffness will be determined by modal analysis, using Dobson's method (Dobson 1986, 1987). To test the idea, no error is added to the FRF data. Any errors that may arise in the eigen-data should be due to the modal analysis algorithm and are expected to be very small. Therefore an unconstrained least squares solution method, in this case, should result is accurate parameters. Figs 6.43 and 6.44 shows the point receptances at coordinates 3 and 5. Figs 6.45-6.46 and figs 6.47-6.48 shows the reconstructed receptances with stiffness addition of $2\text{x}10^6$ N/m and 10^7 N/m respectively.

Simulated system (damped) _____ , Initial model (undamped) - - - -

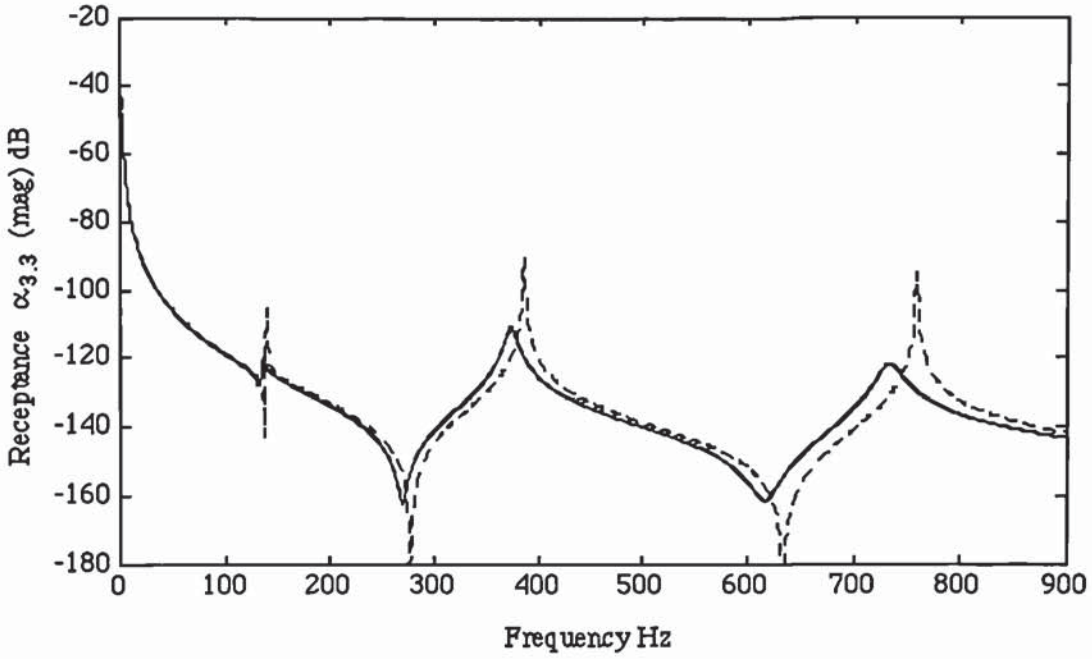

Fig 6.43 Point receptances of the beam (non-proportional damping) and the initial model at coordinate 3.

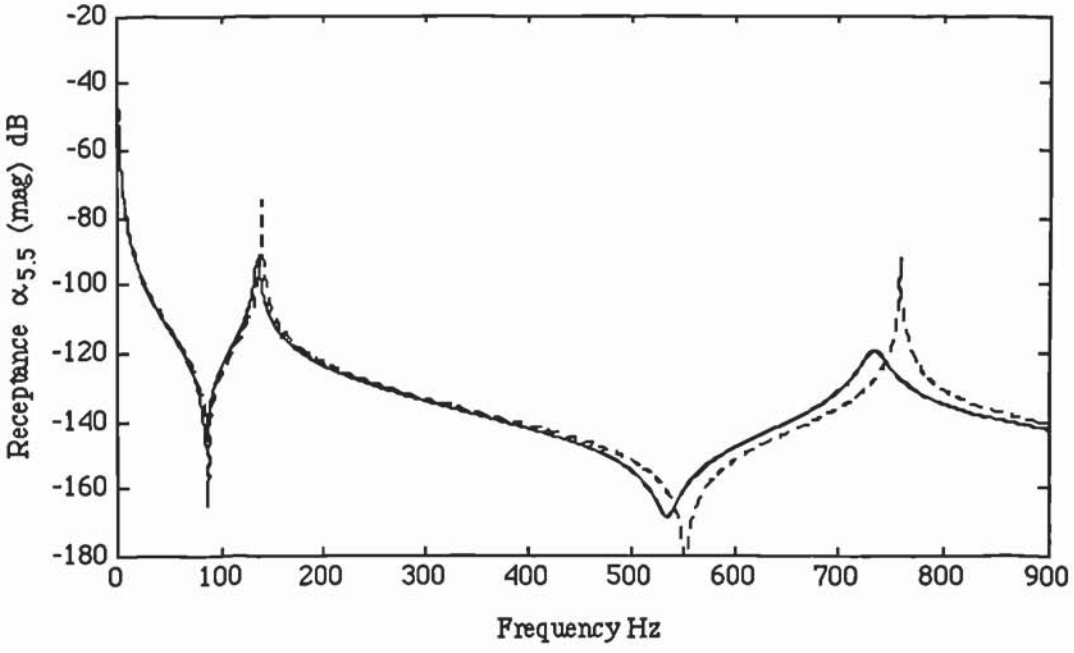

Fig 6.44 Point receptances of the beam (non-proportional damping) and the initial model at coordinate 5.

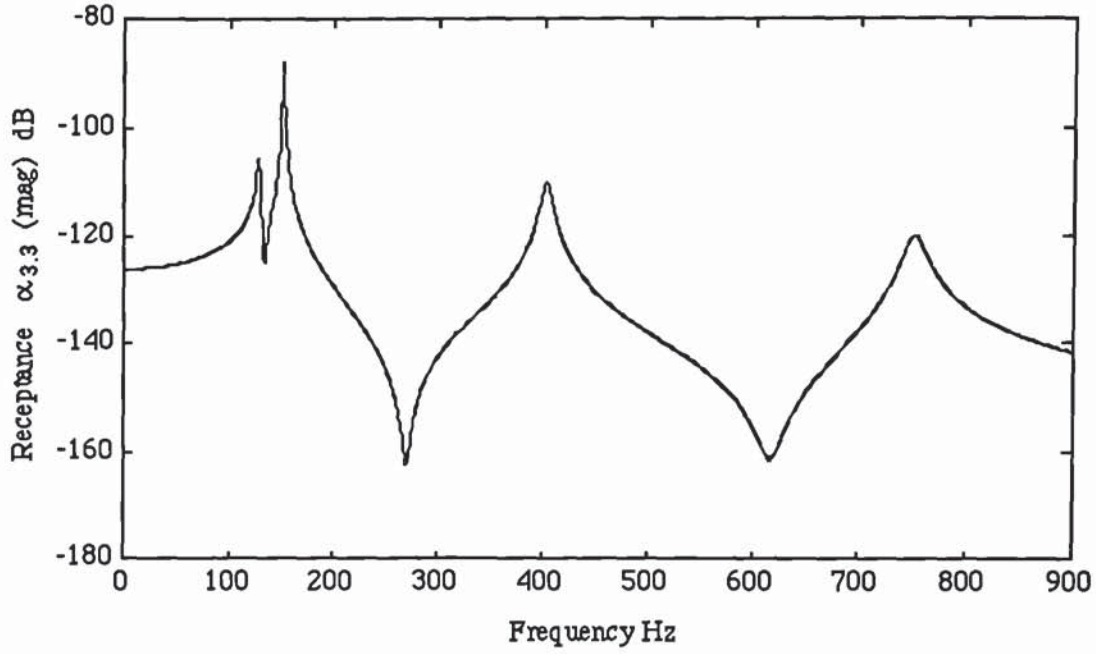

Fig 6.45 Reconstructed beam receptance at coordinate3.
(non-proportional damping, $k = 2\text{x}10^6$ N/m)

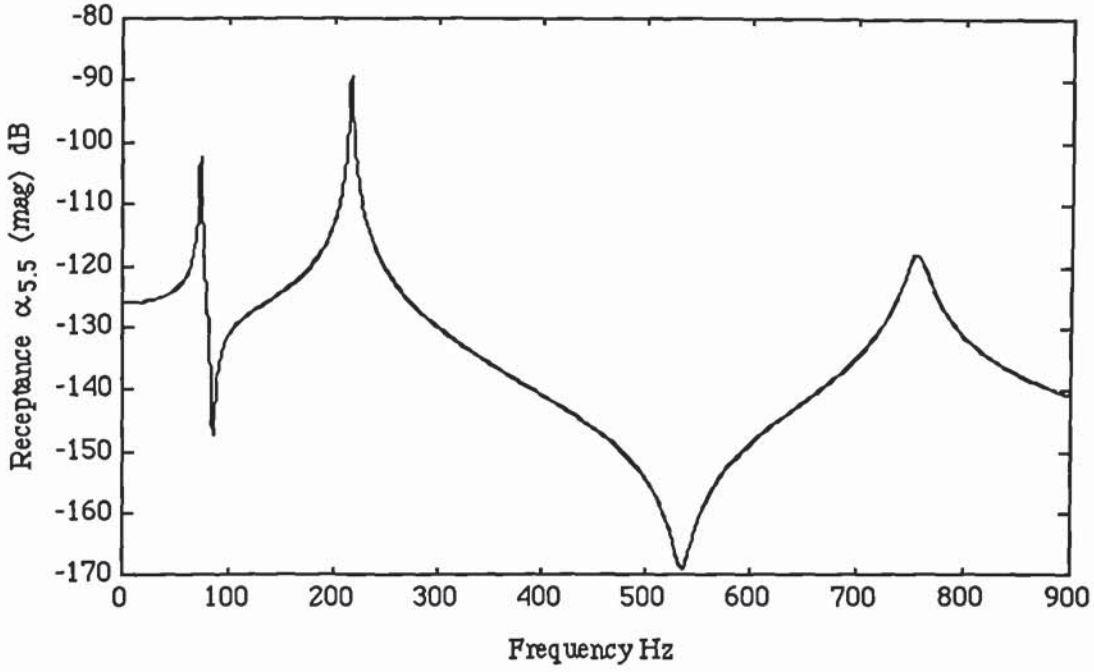

Fig 6.46 Reconstructed beam receptance at coordinate 5.
(non-proportional damping, $k = 2\text{x}10^6$ N/m)

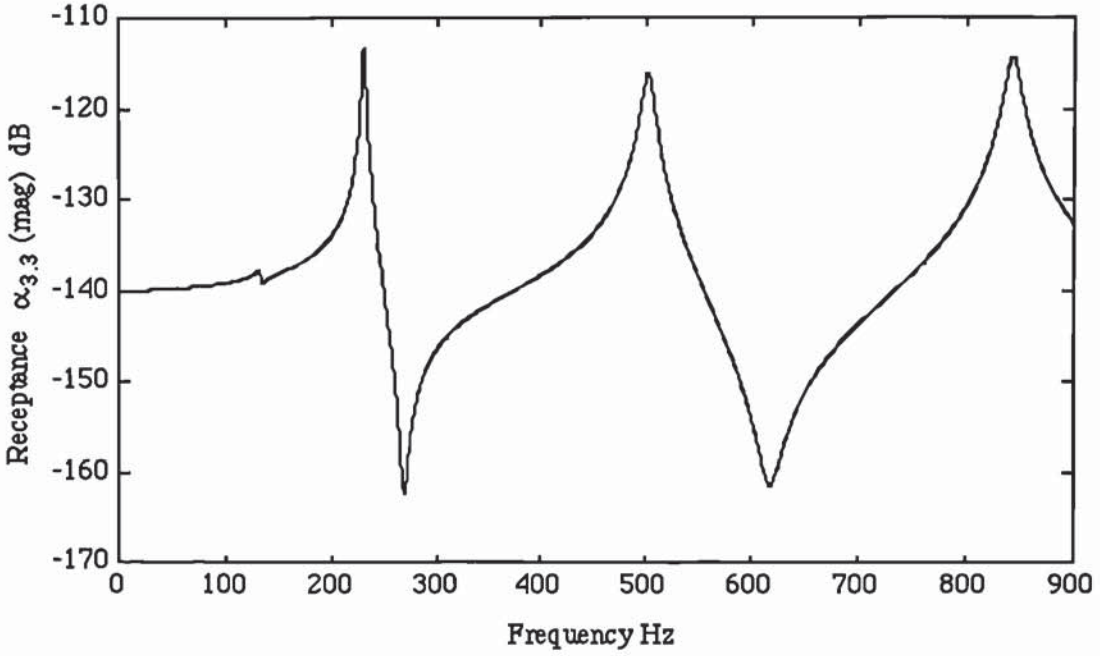

Fig 6.47 Reconstructed beam receptance at coordinate 3.
(non-proportional damping, $k = 10^7$ N/m).

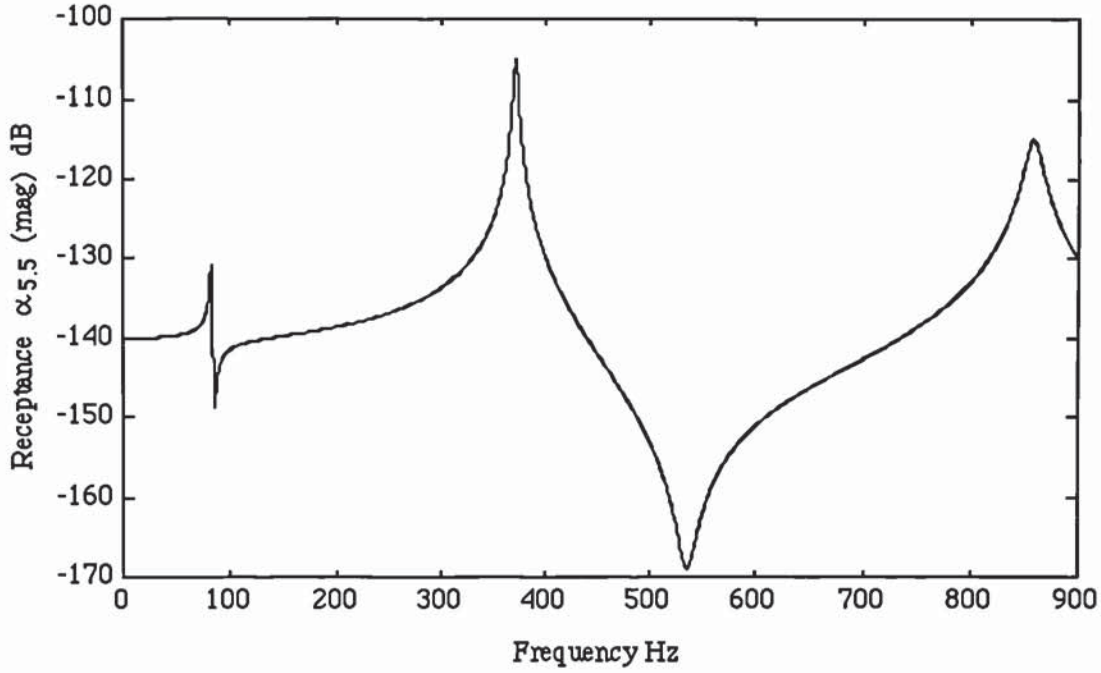

Fig 6.48 Reconstructed beam receptance at coordinate 5.
(non-proportional damping, $k = 10^7$ N/m).

Table 6.27 shows the identified natural frequencies and damping loss factors of the system before and after stiffness addition. The identified natural frequencies and damping factors were used to update the initial model mass and complex stiffness parameters of the four beam elements. As the initial model is undamped, the initial stiffness parameters are all real. The updated parameters, after 5 iterations, are:

$EI_1 = 4997(1+j0.0020)\ \text{Nm}^2$ $\quad$ $EI_2 = 5005(1+j0.0493)\ \text{Nm}^2$

$EI_3 = 4994(1+j0.0023)\ \text{Nm}^2$ $\quad$ $EI_4 = 5002(1+j0.0502)\ \text{Nm}^2$

$m_{u1} = 3.499\ \text{kg/m}$ $\quad$ $m_{u2} = 3.501\ \text{kg/m}$ $\quad$ $m_{u3} = 3.500\ \text{kg/m}$

$m_{u4} = 3.500\ \text{kg/m}$

It can be seen that the updated parameters, which were obtained using an ordinary least squares solution without weighting, are reasonably accurate. The result confirm that the eigen-data of the perturbed structure could be determined without physical addition of the stiffness or mass to the structure. In a practical situation with measurement noise, the identification of sufficiently accurate eigen-data simply depends on the capability of the modal analysis algorithm in coping with measurement noise. Usually this is feasible, as it will be shown in the experimental example.

Additional Stiffness (N/m)	Stiffness addition coordinate	Natural frequency (Hz) and damping factor (in bracket)		
		f_1	f_2	f_3
0	-	134.77 (0.0259)	373.39 (0.0259)	733.26 (0.0259)
$2x10^6$	3	151.39 (0.0071)	402.40 (0.0236)	750.35 (0.0242)
	5	215.62 (0.0093)	373.39 (0.0259)	755.55 (0.0243)
$1x10^7$	3	231.20 (0.0139)	501.04 (0.0218)	842.59 (0.0162)
	5	371.34 (0.0105)	373.39 (0.0259)	858.01 (0.0178)

TABLE 6.27 Natural frequencies and damping factors identified from FRFs. (non-proportionally damped beam)

6.5 Experiment on an H frame.

6.5.1 Initial FE model

An H-frame was made by bolting together three Aluminium beam members, using two Brass screws of size 5/16BSW and length 50mm on each joint. The beams are of uniform cross-section of 50x25mm. The frame was modelled with a free boundary condition, using 17 elements, with 37 DOF by considering only motion in the plane of the frame. The FE model assumed the frame joints to be perfectly rigid and for the purpose of dynamic analysis in the frequency range of interest (0 - 600 Hz), axial flexibility of the beam elements has been ignored. The FE model with frame dimensions is shown in fig 6.49, where the shorter sides of the cross-sections of the vertical legs and the cross-beam are parallel to the plane of the frame. The mass per unit length and flexural rigidities of the beam elements, determined from material and

geometry data, are:

$EI_a = 4557\ \text{Nm}^2$ $\quad m_{u,a} = 3.4\ \text{kg/m}$ (for all elements).

The FE model result in the following natural frequencies of the first 5 elastic modes:

$f_{1a} = 54\ \text{Hz}$ $\quad f_{2a} = 119.3\ \text{Hz}$ $\quad f_{3a} = 133.8\ \text{Hz}$

$f_{4a} = 187.1\ \text{Hz}$ $\quad f_{5a} = 500.9\ \text{Hz}$

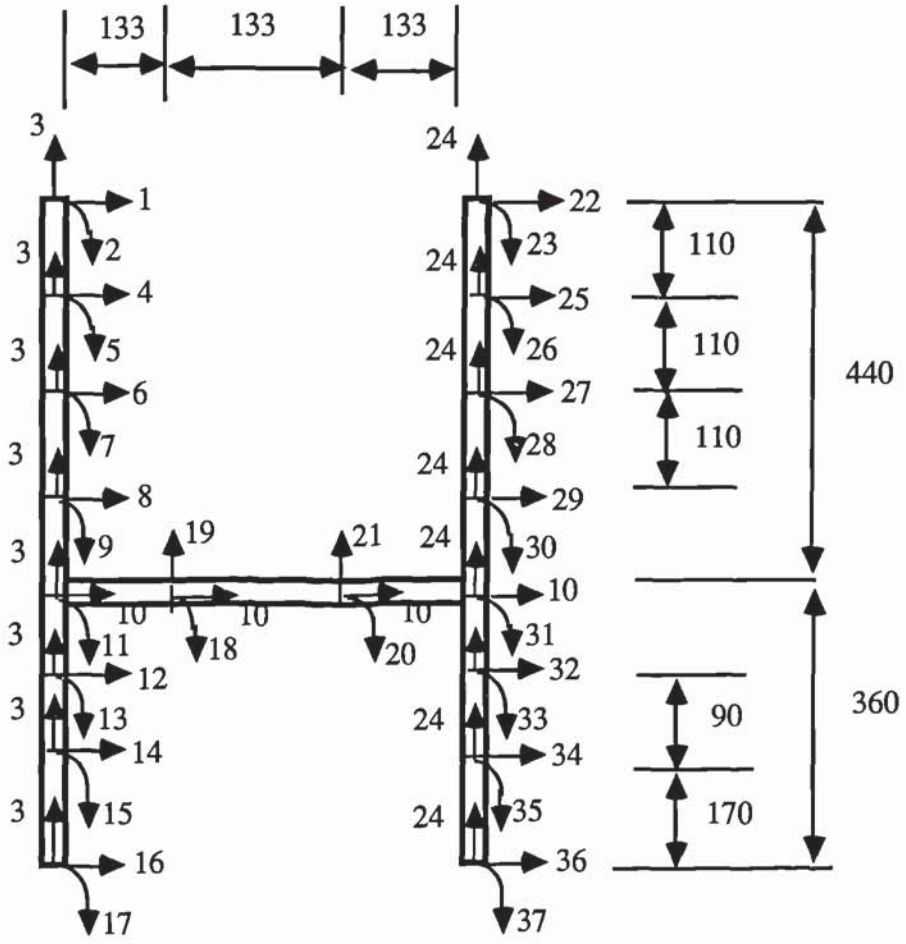

Fig 6.49 H-frame model (dimension in mm).

6.5.2 Vibration testing

The frame was suspended in a free configuration and excited at coordinate 14, using an electrodynamic shaker. The excitation was performed using random noise generated by a B&K dual channel signal analyser type 2034. A force transducer and an accelerometer were used to pickup the excitation and response signals. The response and forcing signals were then processed by the signal analyser to generate spectral data and this was fed to the computer for further processing, using SPIDERS signal processing and modal analysis package. The instrumentation layout and signal processing involved is similar to that used with beam experiments in Chapter 5 (fig 5.3). The H-frame test configuration is shown in fig 6.50. Fig 6.51 shows the magnitude of the receptance measured at the excitation coordinate as compared to the receptance of the FE model. A plot of the phase angle of the measured receptance is shown in fig 6.52.

The FRF show 5 modes in the frequency range 50-500 Hz with the following measured natural frequencies and damping factors.

$f_1 = 52.6$ Hz	$f_2 = 106.9$ Hz	$f_3 = 136.7$ Hz
$f_4 = 192.1$ Hz	$f_5 = 489.8$ Hz	
$\eta_1 = 0.0142$	$\eta_2 = 0.0237$	$\eta_3 = 0.0038$
$\eta_4 = 0.0085$	$\eta_5 = 0.0051$.	

These modes correspond to the first five elastic modes of the FE model. In addition, there is another mode at about 23 Hz which is far away from any natural frequency of the FE model. The appearance of this additional mode may be due to a gross mismatch between the FE model and the actual frame under test, or imperfect boundary conditions. Gross-mismatch between the

system and the model is unlikely to be the explanation in this particular case because the geometry of the structure is simple. Further examination of the setup suggest that the frame is not perfectly unrestrained in the vertical direction. The excitation of the frame in the horizontal direction induces vibration in the vertical direction which is transmitted as transverse vibration of the pushrod which connects the frame to the shaker. As the shaker is fixed, rather than suspended, and the pushrod is not perfectly free to undergo transverse oscillations, there is some restraint. The appearance of a low frequency mode could therefore be explained by the finite flexibility of the pushrod in its transverse direction.

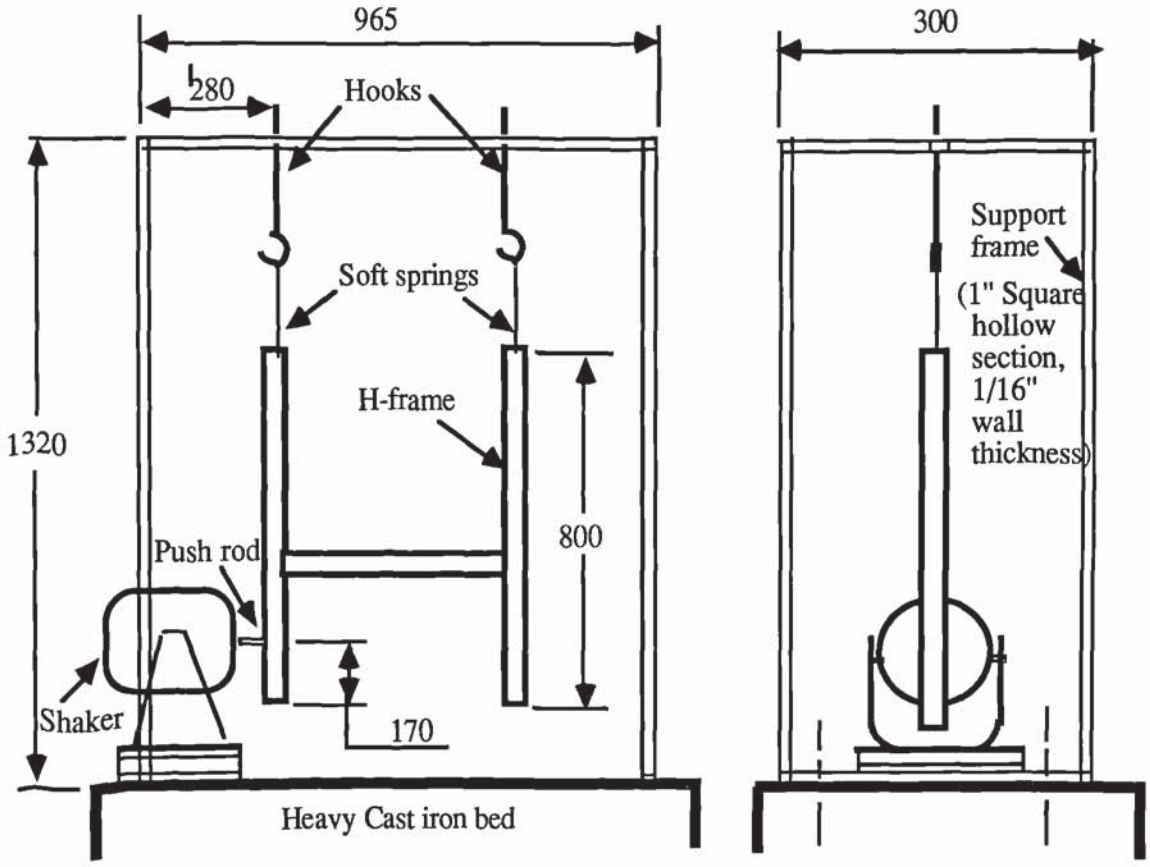

Fig 6.50 H-frame test configuration (unspecified dimension in mm).

Measured Frame receptance _____ , Receptance of the initial FE model - - - -

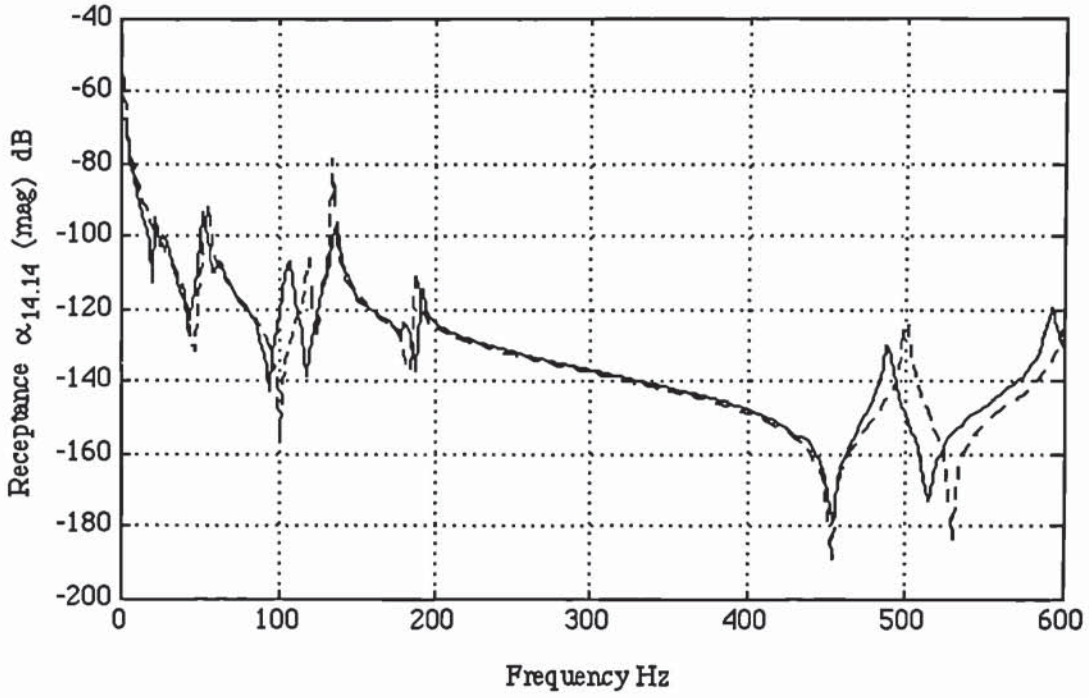

Fig 6.51 Measured and initial model's point receptances at coord. 14.

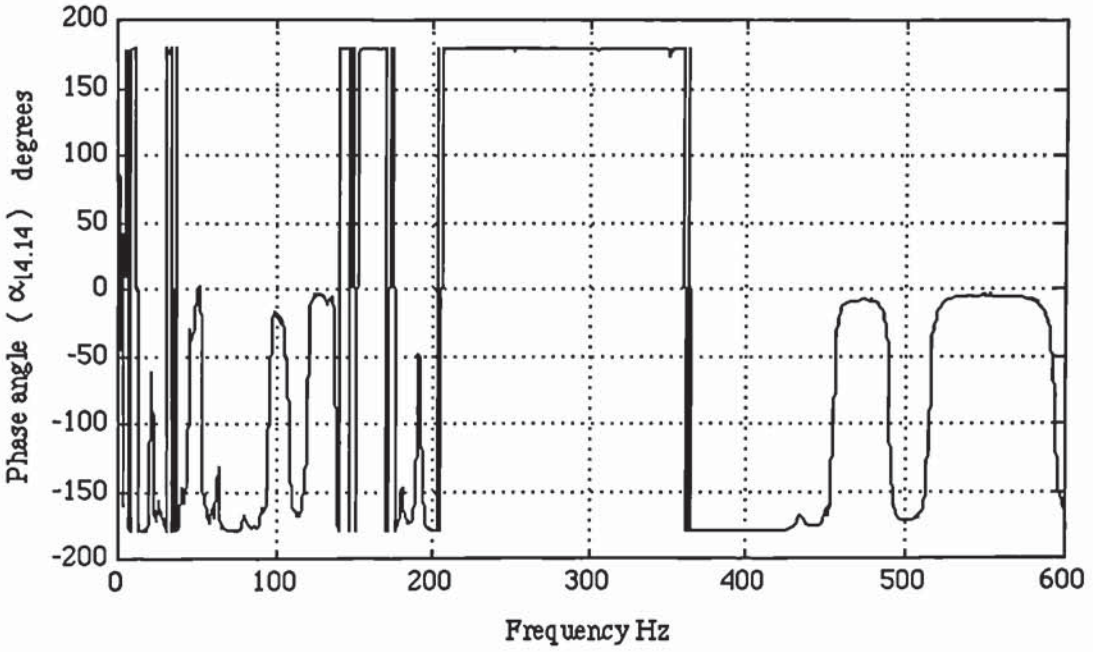

Fig 6.52 Phase angle of measured point receptance (degrees).

It will be assumed that the effect of such low stiffness restraint is considerably reduced at higher frequency and therefore the other five measured modes are a reasonably correct representation of the modes of the frame. Figs 6.53-6.57 shows the Nyquist plots around each of the five resonance zones, at 1 Hz resolution.

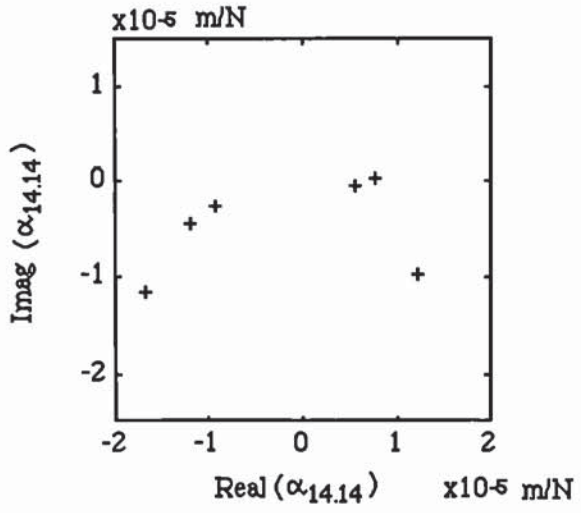

Fig 6.53 Nyquist plot of the H-frame around f_1 = 52.6 Hz.

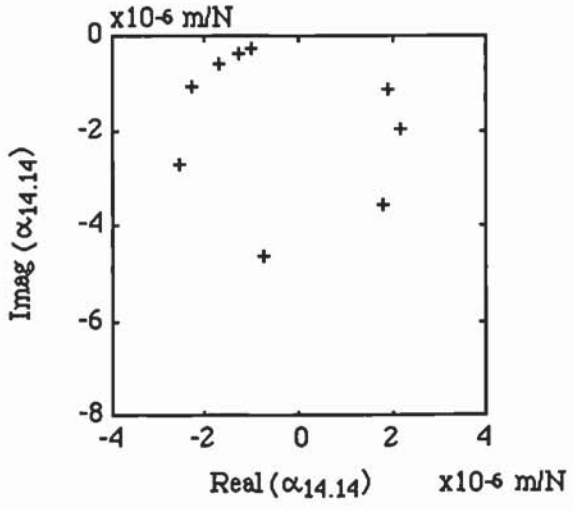

Fig 6.54 Nyquist plot of the H-frame around f_2 = 106.9 Hz.

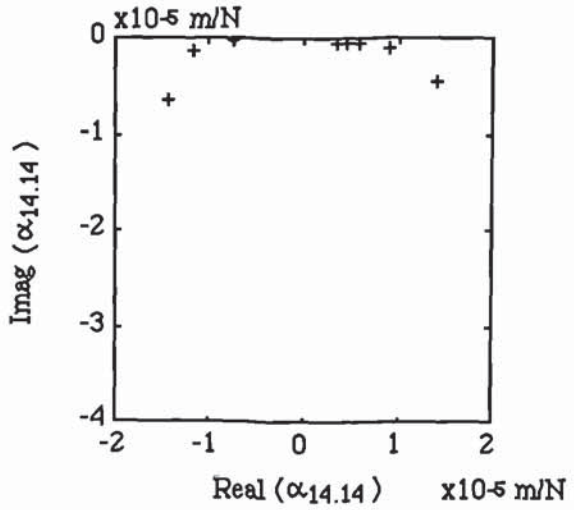

Fig 6.55 Nyquist plot of the H-frame around f_3 = 136.7 Hz.

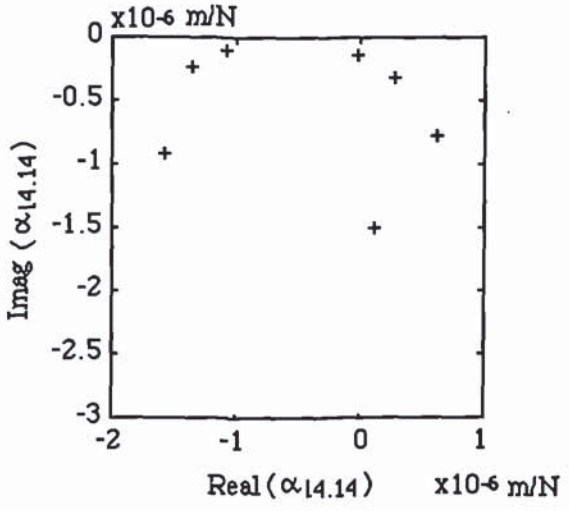

Fig 6.56 Nyquist plot of the H-frame around f_4 = 192.1 Hz.

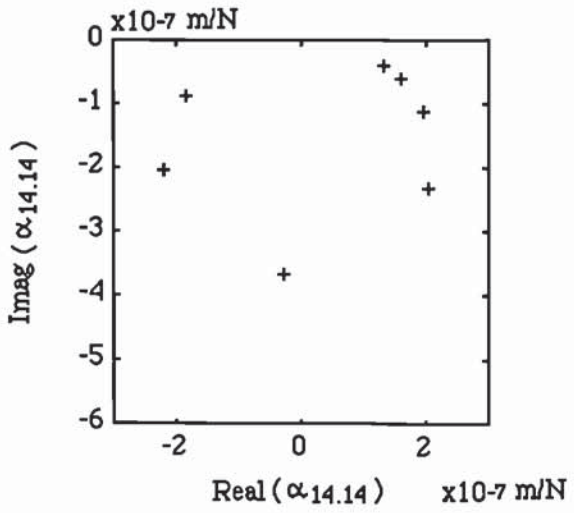

Fig 6.57 Nyquist plot of the H-frame around f_5 = 489.8 Hz.

6.5.3 Updating the FE model by simulation of additional stiffness.

6.5.3.1 Introduction

The FE model will now be updated without modification for the effects of boundary conditions. A damping matrix proportional to the mass and stiffness matrices will be assumed, and therefore real parts of measured eigenvalues will be treated as the eigenvalues of the undamped system. Model updating will be performed by stiffness addition using eigenvalues alone. The stiffness will be simulated to have been added at two coordinates. These are the excitation coordinate, 14, and coordinate 36. Thus, coordinate 36 must be excited also, and the eigenvalues of the frame with added stiffness will be determined from the point receptance data at coordinates 14 and 36. The point receptance and phase angle at coordinate 36 are shown in figs 6.58 and 6.59. It can be seen that in addition to the mode at 23 Hz, there is another mode at 67 Hz which did not show up properly in the FRF at coordinate 14. Since the mass or stiffness addition technique could make use of a few measured modes, there is no need

to use all the modes in the measured frequency range. Extra modes which are generated as a result of imperfect boundary condition, as well as modes which are degraded by noise should preferably be omitted. An alternative is to improve the experimental setup so as to achieve the desired boundary conditions. This is not always easy and in some cases, is time consuming, expensive and may not be necessary. Thus it was decided to use only those modes in the frequency range between 100-560 Hz. These are the four modes whose natural frequencies are referred to, in Section 6.5.2, as f_2, f_3, f_4 and f_5, and relate to f_{2a}, f_{3a}, f_{4a}, and f_{5a} of the initial FE model.

The updating process involves:

(i) The construction of the FRF of the frame with added stiffness at the excitation coordinates (coordinate 14 and then 36) using measured receptance data.

(ii) Identification of the eigenvalues of the frame with added stiffness.

(iii) Updating an undamped model using the minimum cost Bayesian estimator.

(iv) Finding the stiffness and mass proportionality constants for the proportional damping matrix using orthogonality equations and the updated model's mode shape vectors (real modes).

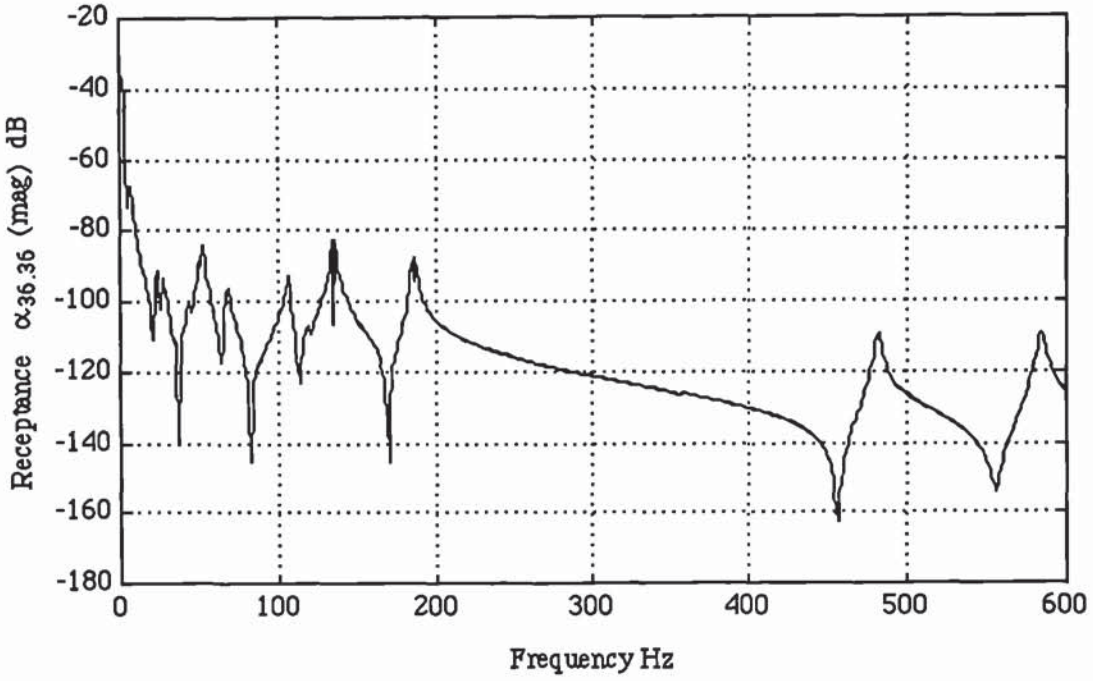

Fig 6.58 Measured receptance at the excitation coordinate 36.

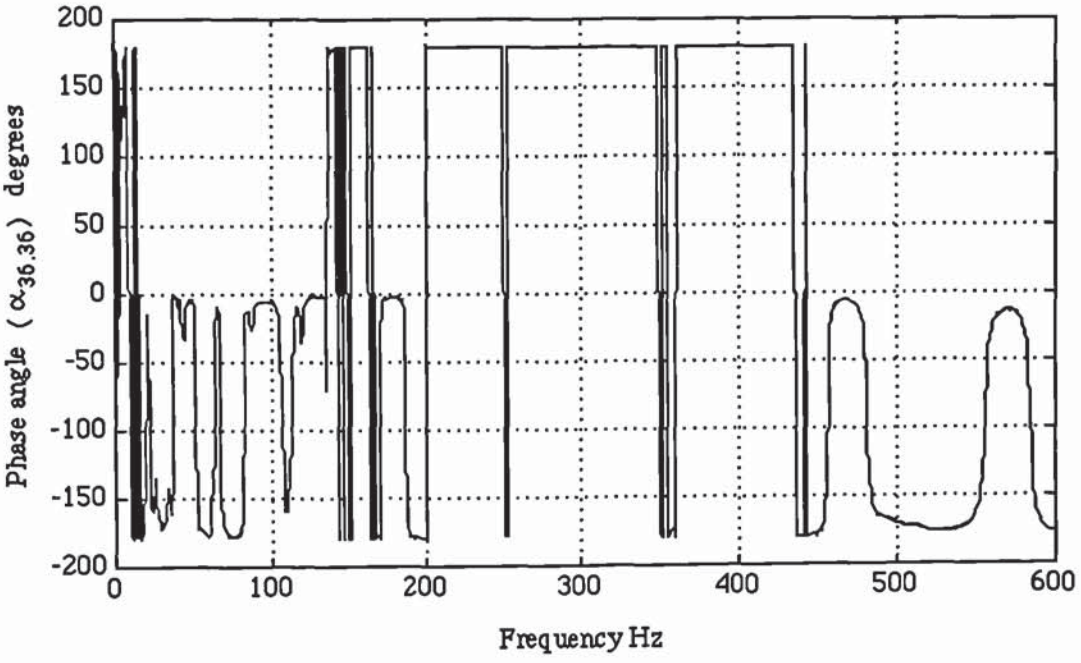

Fig 6.59 Phase angle of measured receptance at coord. 36 (degrees).

6.5.3.2 Construction of the FRFs of the frame with added stiffness.

Four stiffeners were simulated to have been added in turn at coordinates 14 and 36. They are given by:

Stiffness addition at coordinate 14:	$5x10^5$ N/m	$2x10^6$ N/m
	$1x10^7$ N/m	$5x10^6$ N/m
Stiffness addition at coordinate 36:	$5x10^5$ N/m	$1x10^6$ N/m
	$1x10^7$ N/m	$5x10^7$ N/m.

The FRF of the frame with added stiffness at coordinate 14 and at coordinate 36 were constructed from point receptances using (6.8). Figs 6.60-6.63 shows the constructed FRF (point receptance) at coordinate 14. Figs 6.64-6.67 shows the constructed point receptances at coordinate 36. For brevity only the magnitudes are shown.

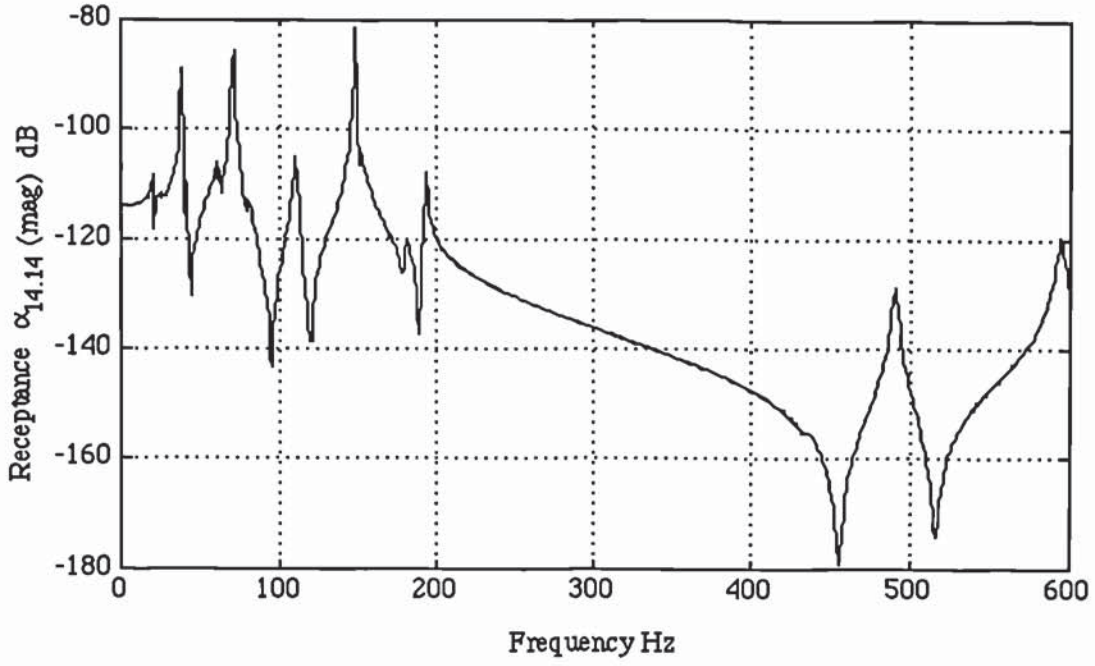

Fig 6.60 Point receptance at coordinate 14 ($k = 5x10^5$ N/m)

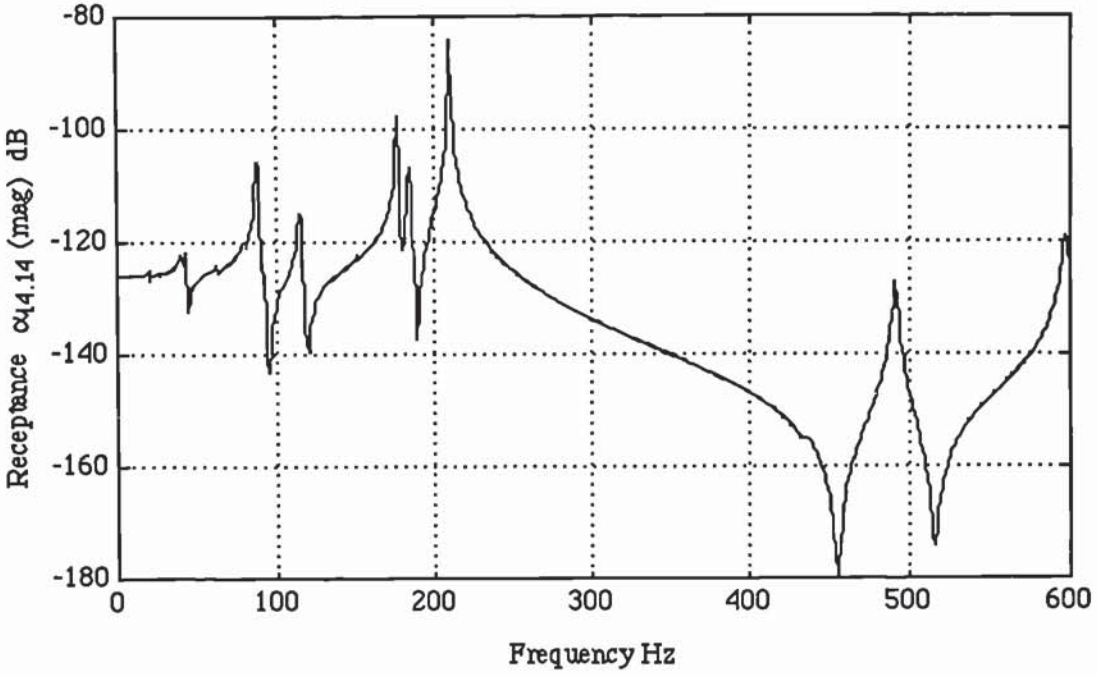

Fig 6.61 Point receptance at coordinate 14 ($k = 2\text{x}10^6$ N/m)

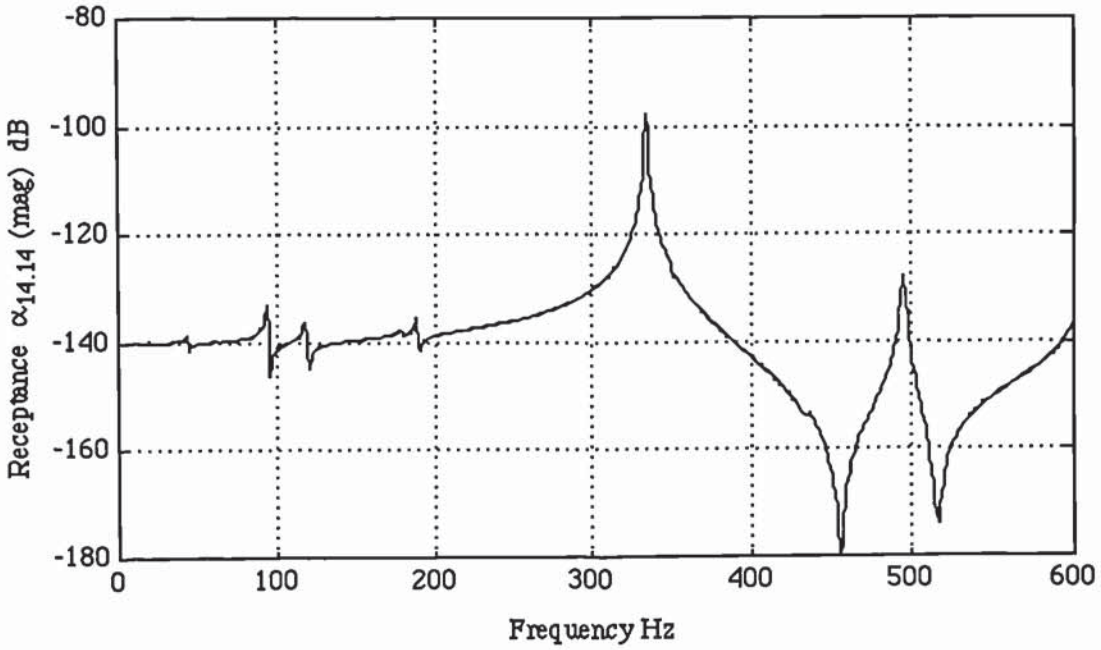

Fig 6.62 Point receptance at coordinate 14 ($k = 10^7$ N/m).

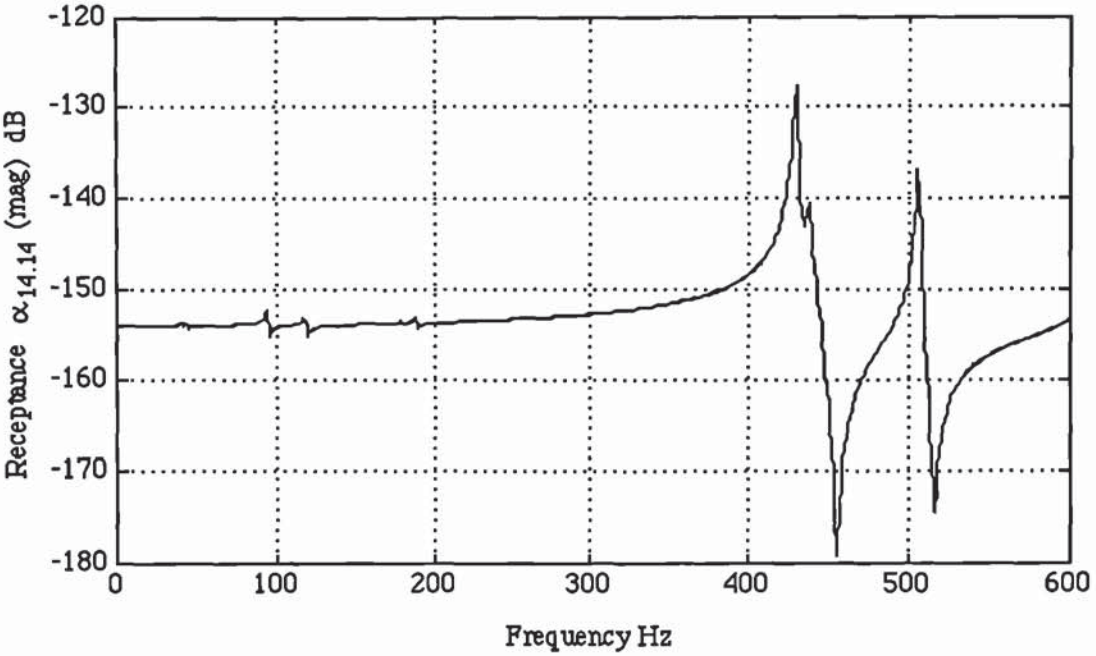

Fig 6.63 Point receptance at coordinate 14 ($k = 5\text{x}10^7$ N/m)

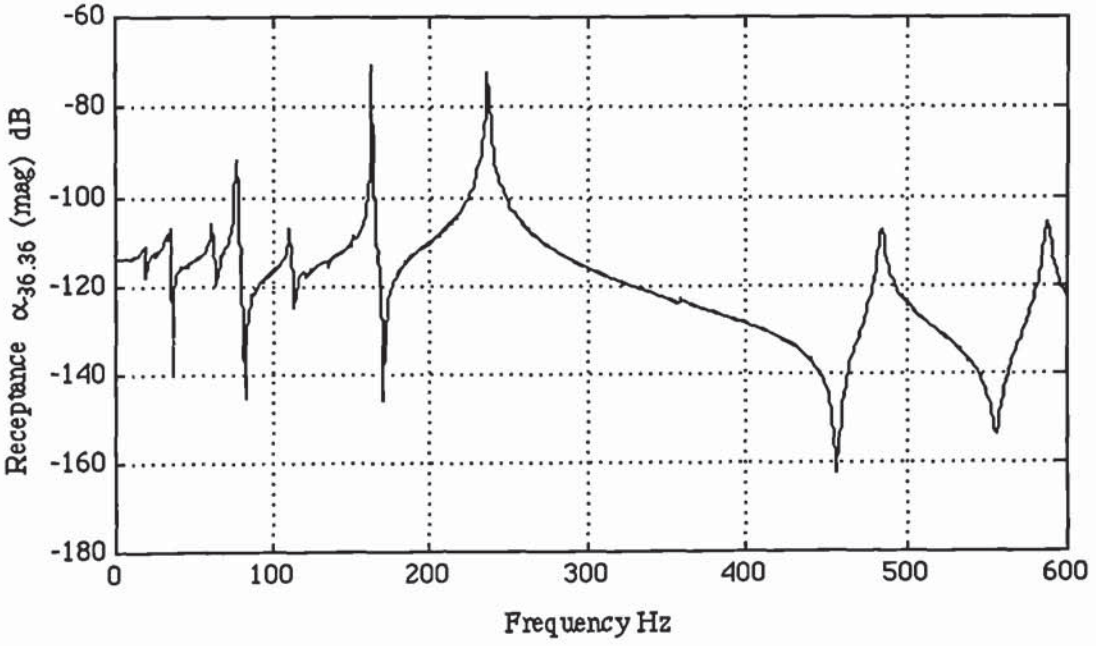

Fig 6.64 Point receptance at coordinate 36 ($k = 5\text{x}10^5$ N/m)

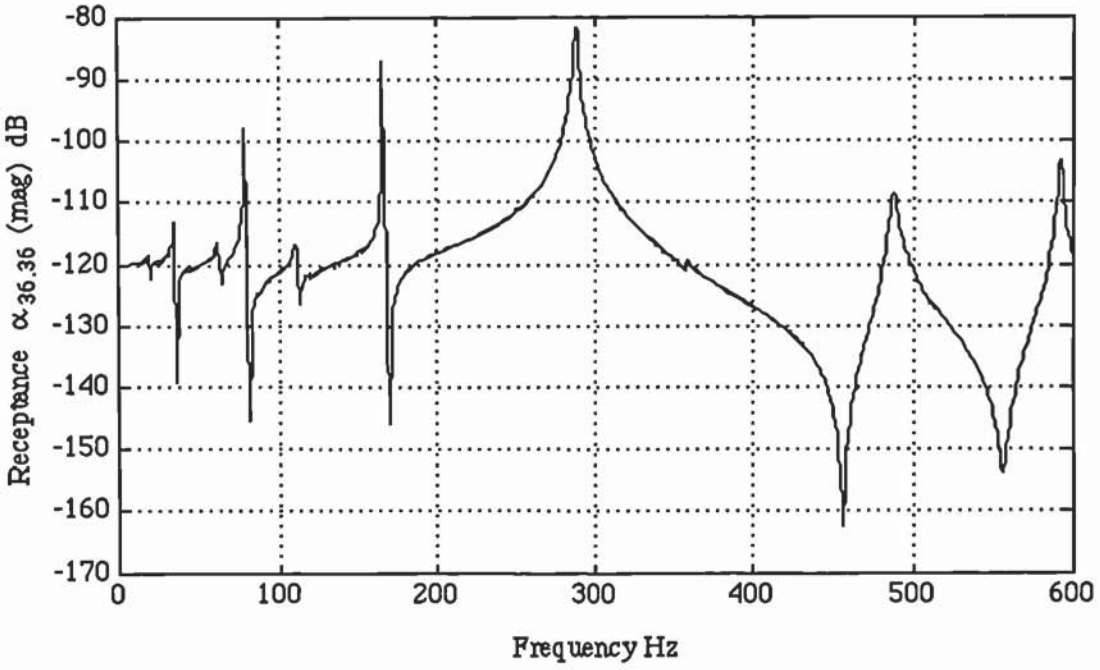

Fig 6.65 Point receptance at coordinate 36 ($k = 10^6$ N/m)

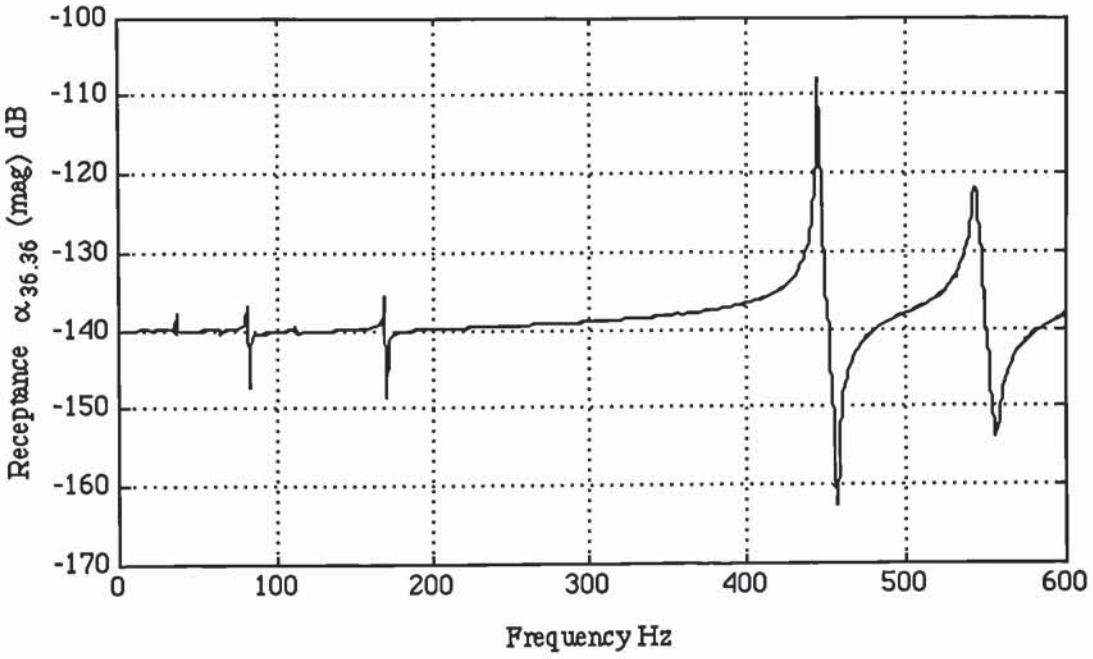

Fig 6.66 Point receptance at coordinate 36 ($k = 10^7$ N/m)

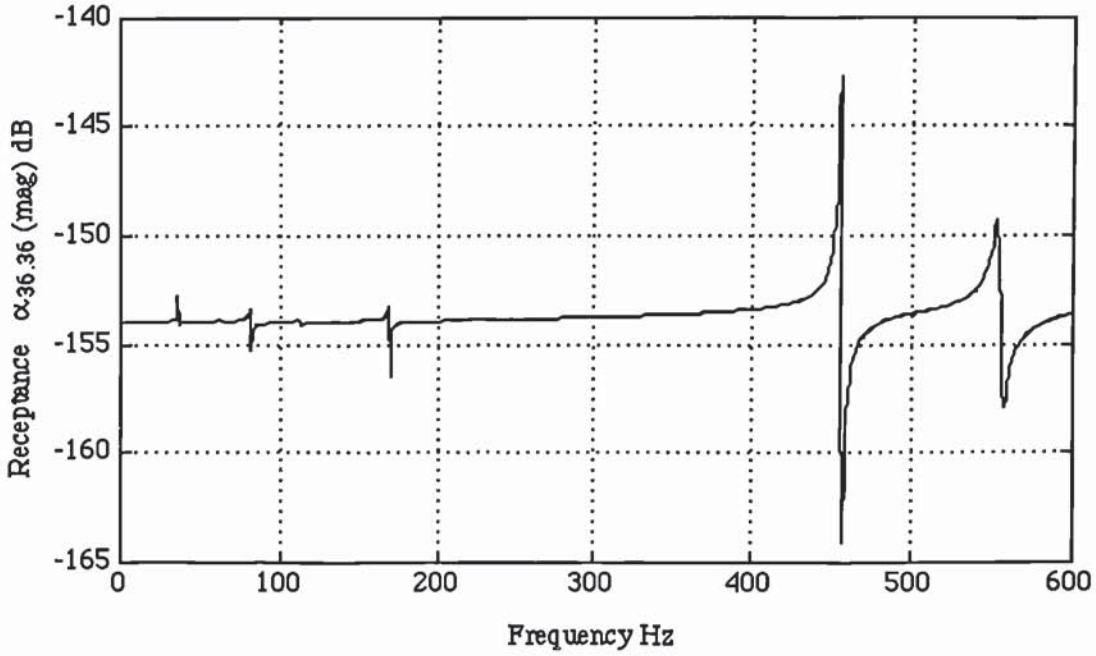

Fig 6.67 Point receptance at coordinate 36 ($k = 5\text{x}10^7$ N/m)

6.5.3.3 Identification of modal data of the frame with added stiffness.

Eigenvalues were identified from the point receptances at coordinates 14 and 36 of the frame with added stiffness (fig 6.59-6.67) using Dobson's modal analysis algorithm. It was found that the Nyquist plots around resonances of the frame with added stiffness were close to circular arcs or circles. The degree of randomness, due to measurement errors for example, was very small indeed to the extent that weighting the data was not necessary. In fact, the Nyquist plots were of the same order of accuracy as the Nyquist plots of the unperturbed frame. Generally, better plots were obtained from those modes which were strongly excited. Figs 6.68-6.71 shows the Nyquist plots, of one case of the frame with added stiffness at coordinate 36, around the four resonances corresponding to f_2, f_3, f_4 and f_5. The added stiffness is $5\text{x}10^7$ N/m,

and the magnitude-frequency plot is shown in fig 6.67. It should be noted that this is a representative of the difficult cases, as the lower modes are only weakly excited. Table 6.28 show the natural frequencies of the frame with added stiffness, identified from the constructed FRF.

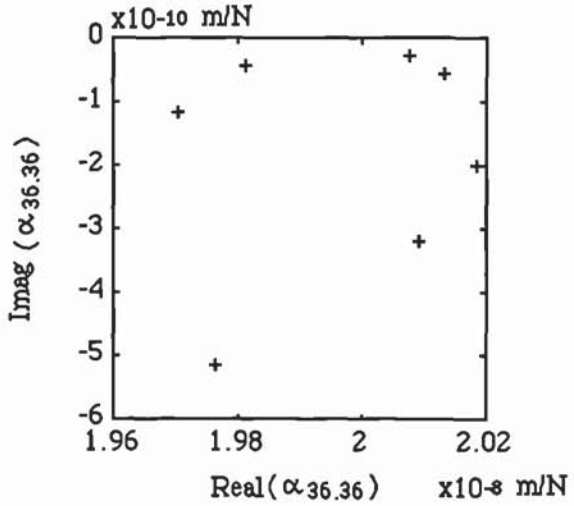

Fig 6.68 Nyquist plot at coordinate 36 around f_2 = 112.4 Hz
(H-frame with simulated additional stiffness, $k = 5\text{x}10^7$ N/m)

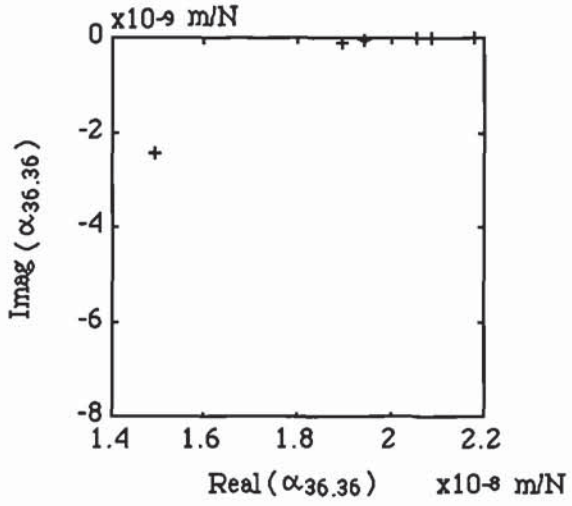

Fig 6.69 Nyquist plot at coordinate 36 around f_3 = 169.7 Hz
(H-frame with simulated additional stiffness, $k = 5\text{x}10^7$ N/m)

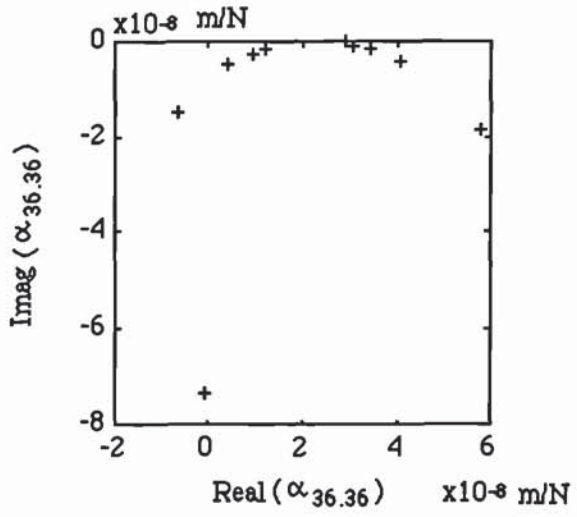

Fig 6.70 Nyquist plot at coordinate 36 around $f_4 = 454.8$ Hz
(H-frame with simulated additional stiffness, $k = 5\text{x}10^7$ N/m)

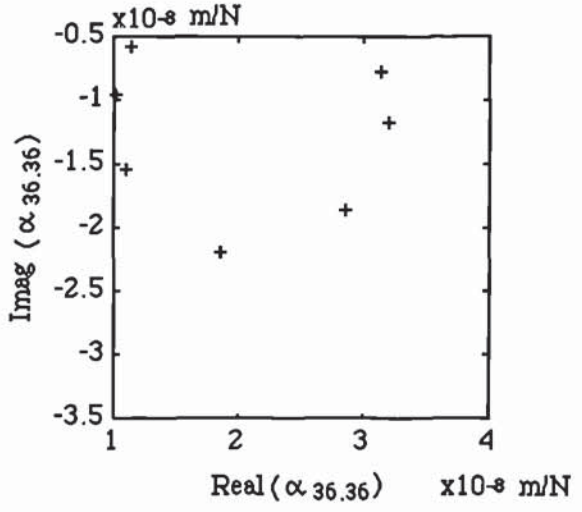

Fig 6.71 Nyquist plot at coordinate 36 around $f_5 = 553.4$ Hz.
(H-frame with simulated additional stiffness, $k = 5\text{x}10^7$ N/m)

Added stiffness x10^6 (N/m)	Stiffness addition coordinate	Identified Natural frequency (Hz)			
		f_2	f_3	f_4	f_5
0.5	14	109.8	147.8	193.4	490.0
	36	110.2	161.9	236.2	484.0
2.0	14	114.7	175.9	209.6	490.9
1.0	36	111.0	166.1	288.3	488.0
10.0	14	117.9	188.4	334.2	494.6
	36	112.4	169.5	445.2	543.5
50.0	14	118.6	188.7	428.9	505.2
	36	112.4	169.8	454.8	553.5

TABLE 6.28 Natural frequencies of the H-frame with added stiffness.

6.5.3.4 Parameter updating.

Parameter updating was performed using the minimum cost Bayesian estimator. Updating was performed by dividing the element parameters into a group of parameters defined as follow:

EI_1, m_{u1} : Stiffness and mass parameter of elements of the legs and cross beam, away from the joints.

EI_2, m_{u2} : Stiffness and mass parameter of the elements of the vertical legs next to the joints.

EI_3, m_{u3} : Stiffness and mass parameter of elements of the cross beam, next to the joints.

For the purpose of computing the weighting matrices $\mathbf{W}_\lambda$ and $\mathbf{W}_a$, the following standard deviations were assumed.

PAGE
MISSING

vibration amplitudes are expected. It will be assumed that, the natural frequency and damping factors measured at coordinate 14, are a fair representation of the natural frequencies and damping factors of the unperturbed frame and boundary condition effects will be ignored.

Using the minimum cost Bayesian estimator, the following parameters of an undamped model were obtained in 4 iteration steps,

$EI_1 = 4370\ \text{Nm}^2$ $EI_2 = 4912\ \text{Nm}^2$ $EI_3 = 2841\ \text{Nm}^2$

$m_{u1} = 3.295\ \text{kg/m}$ $m_{u2} = 3.139\ \text{kg/m}$ $m_{u3} = 4.421\ \text{kg/m}$

and result in the following natural frequencies:

$f_1 = 48.4\ \text{Hz}$ $f_2 = 105.8\ \text{Hz}$ $f_3 = 137.9\ \text{Hz}$

$f_4 = 187.6\ \text{Hz}$ $f_5 = 490\ \text{Hz}.$

Figs 6.72 and 6.73 shows the convergence of the H-frame parameters.

		f_2 (Hz)	f_3 (Hz)	f_4 (Hz)	f_5 (Hz)
Excitation coordinate 14	Measurement coordinate 19	106.8 (η= 0.028)	136.6 (η= 0.005)	191.9 (η = 0.008)	489.8 (η = 0.005)
	Measurement coordinate 25	106.7 (η = 0.027)	136.6 (η= 0.004)	192.0 (η = 0.009)	490.0 (η= 0.005)
Excitation coordinate 36	Measurement coordinate 36	106.0 (η= 0.019)	136.1 (η= 0.002)	186 (η= 0.004)	481.5 (η = 0.006)

TABLE 6.29 H-frame natural frequencies and damping factors (in bracket) identified from different measurement and excitation coordinates.

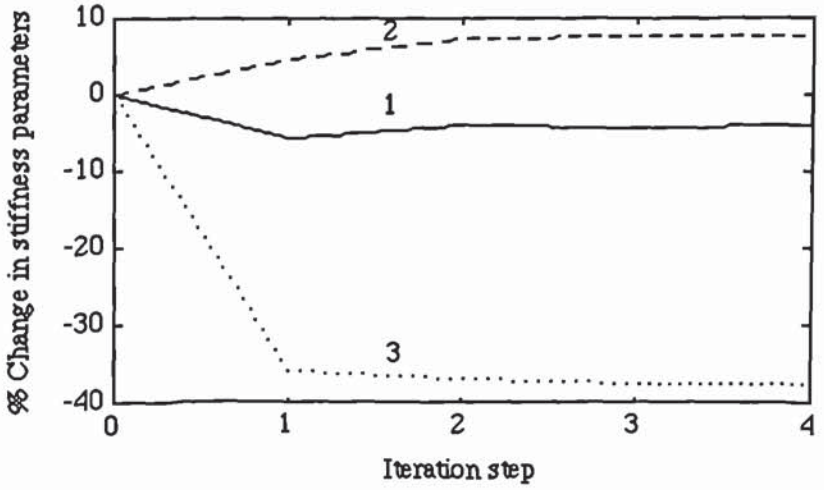

Fig 6.72 Convergence of the stiffness parameters of the H-frame.

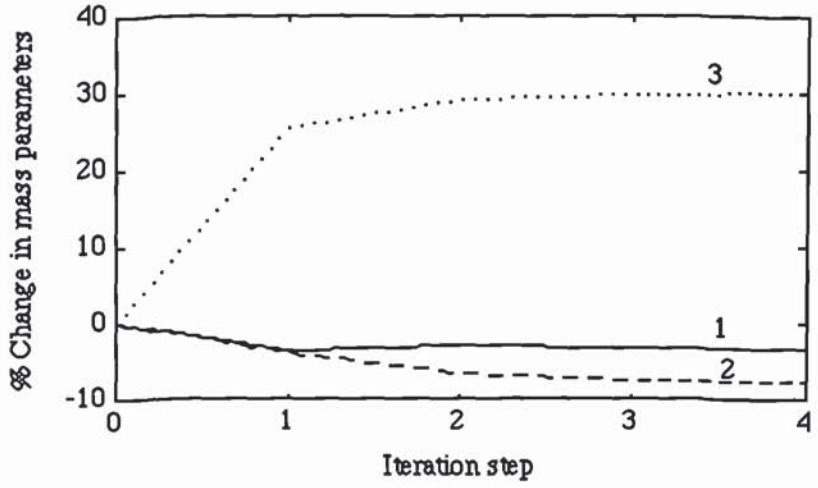

Fig 6.73 Convergence of the mass parameters of the H-frame.

To find the damping matrix proportionality constants, measured damping factors of the unperturbed frame, η_2 - η_4, and eigenvalues of the updated, undamped model were used in a least squares solution of (6.17). The following

damping proportionality constants (with respect to the stiffness and mass matrices) and damping loss factors of the first five elastic modes of the updated, proportionally damped model were obtained:

$\chi_k = 0.0046$ $\chi_m = 4.4x10^3$

$\eta_1 = 0.052$ $\eta_2 = 0.0146$ $\eta_3 = 0.0105$

$\eta_4 = 0.0078$ $\eta_5 = 0.005$

Figs 6.74-6.78 shows the comparison of the FRFs (magnitude), with excitation at coordinate 14, between the experimental data, the initial FE model and the damped (proportional) updated model, at coordinates 1, 14, 19, 21 and 29.

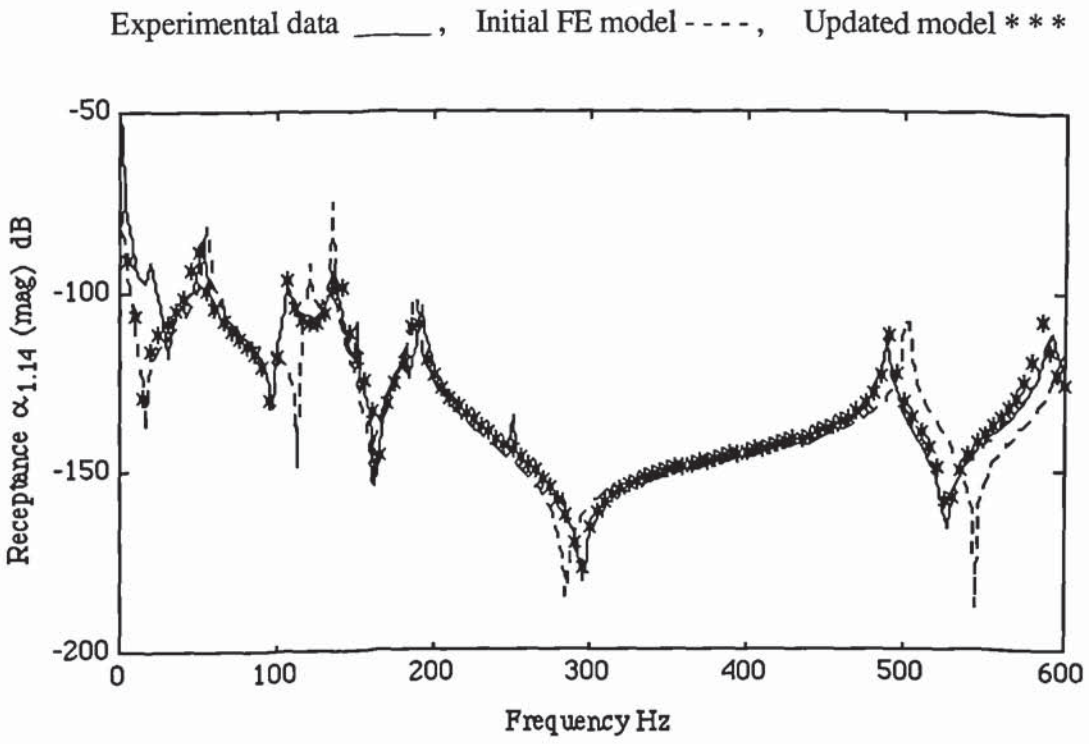

Fig 6.74 Comparing receptance prediction at coordinate 1.

Experimental data _____ , Initial FE model - - - - , Updated model * * *

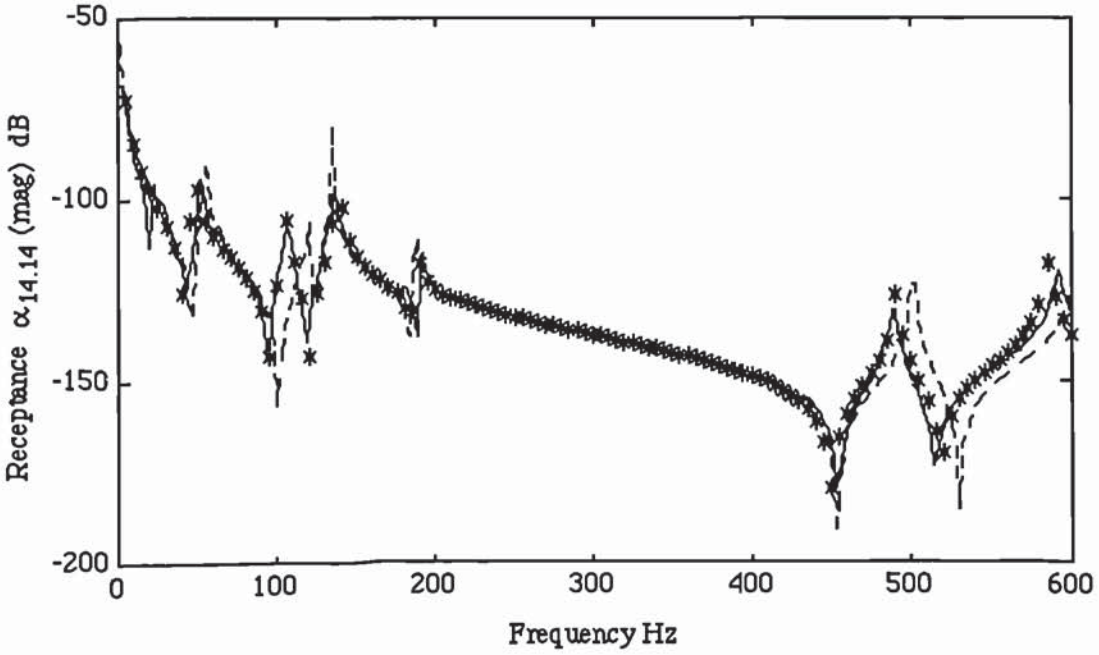

Fig 6.75 Comparing receptance prediction at coordinate 14.

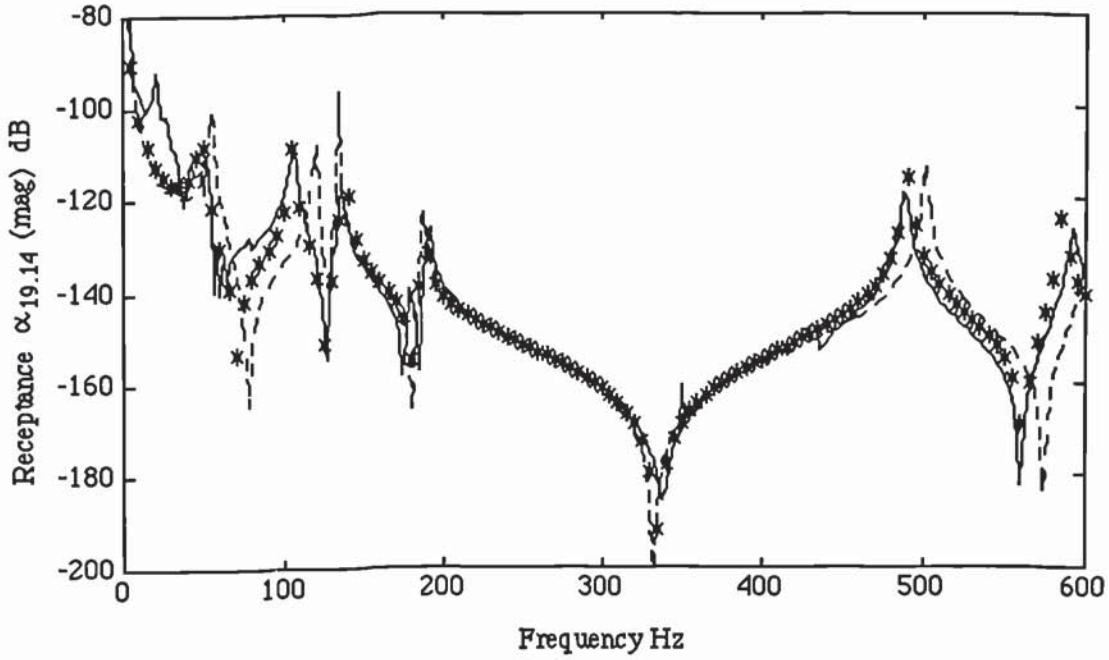

Fig 6.76 Comparing receptance prediction at coordinate 19.

Experimental data _____, Initial FE model - - - -, Updated model * * *

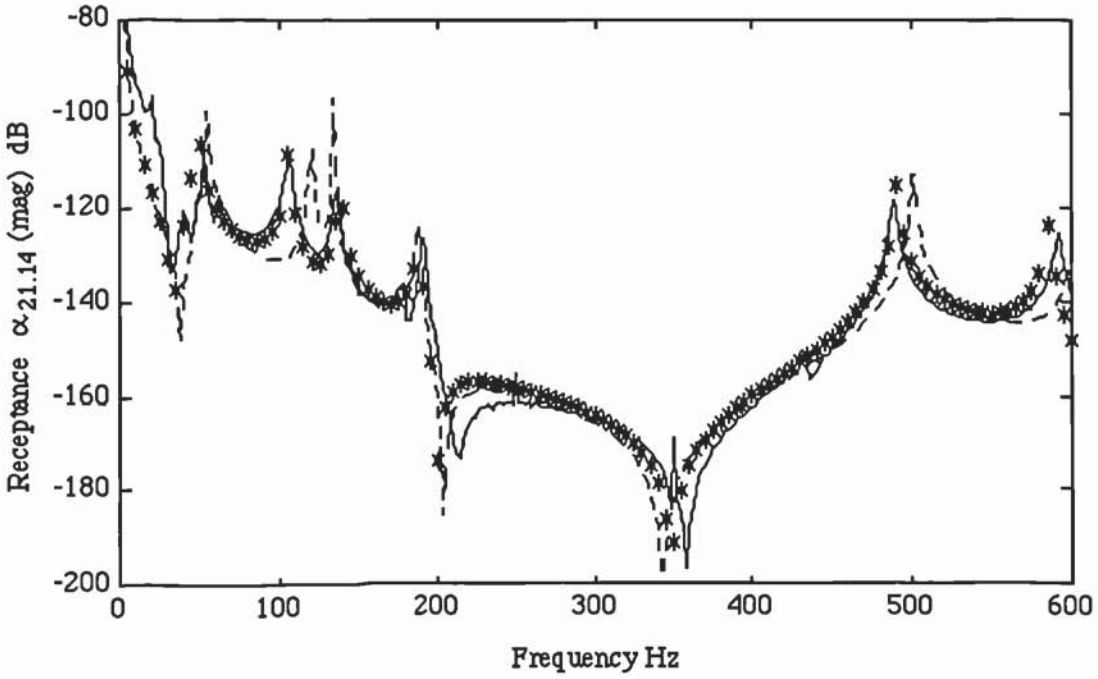

Fig 6.77 Comparing receptance prediction at coordinate 21.

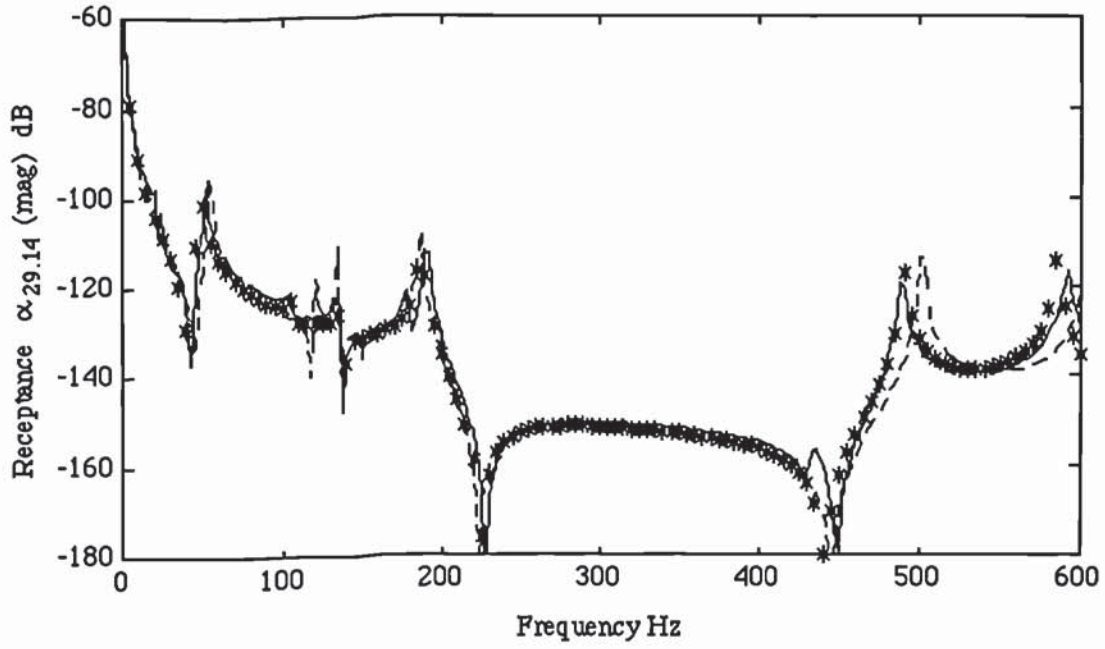

Fig 6.78 Comparing receptance prediction at coordinate 29.

6.6 Discussion

This Chapter has considered the use of a simple structural modification approach to predict the eigen-data of a modified structure, and uses the eigen-data of the modified structure in a model updating exercise. The modifications are performed on one coordinate at a time and are based on the FRF of the unmodified structure. The eigen-data to be used may be the eigenvalues or both eigenvalues and eigenvectors. In either case, the minimum requirement is the measurement of the point receptance at each modification coordinate. Two alternative approaches have been presented.

(i) The natural frequencies of the structure with added stiffness (or mass) are determined from the point receptance data at the modification coordinates, by solving (6.13) or a similar expression for mass addition.

(ii) The natural frequencies (and possibly damping factors) are determined from the simulated FRF of the stiffness (or mass) added structure, where the simulated FRF is computed from the FRF of the unmodified structure.

The first approach requires solving an equation, the solution of which is generally feasible for real receptances, at the modification coordinates. Since measured receptances of real systems are generally complex, its validity depends on the approximation which uses receptance magnitudes, and bear the signs of the real part of the complex receptance. Thus, while this approach could, theoretically, be an exact approach for determining the eigenvalues of an undamped system with additional mass or stiffness, it is an approximate method for real systems which involves damping. It has been shown, however,

for systems with very light damping, which can be adequately modelled by an undamped or proportionally damped model, the errors introduced are in practice small. This approach, therefore, has a practical value when eigenvalues alone are to be used.

When both eigenvalues and eigenvectors are to be used, the mode shape vectors of the structure with added stiffness (or mass) are given by the deflection shape of the unmodified structure, at frequencies corresponding to the natural frequencies of the modified structure. The deflection shape is therefore easily determined from the receptance data at the measurement coordinates. The main difficulty, however, is that the mode shapes determined in this way are not mass normalized. Parameter updating requires mass normalized mode shapes. The use of analytical modal masses, updated after each iteration, to normalize the mode shapes of the structure have been investigated. It has been found that the convergence rate is much slower, although there is no significant reduction in the overall accuracy of the updated parameters when the minimum cost Bayesian approach was used.

The second approach is a more generalized technique of finding the eigen-data of the structure with added stiffness (or mass) . Both damping and natural frequency data of the modified structure can be identified using well established modal analysis algorithms. While the technique could also be applicable to systems with highly non-proportional damping, parameter updating is the main problem due to the difficulty in formulating an initial damping model. A simulation example with non-proportional hysteretic damping and error-free FRF data was used to verify the technique. Accurate convergence to the correct mass, stiffness and damping parameters was obtained.

For structures which have to be modelled with non-proportional damping, practical application of the parameter updating technique is likely to be feasible if reasonable estimates of the damping parameters in the analytical model are available.

For structures which could be adequately described by a model with proportional damping, reasonable initial estimates of the initial damping parameters may not be a necessity. The unknown parameters of the damping matrix, in this case, are the proportionality constants with respect to the stiffness and mass matrices, (χ_k and χ_m). It has been shown, by simulation example 6.4 and experimental H-frame example, that the damping parameters of such structures could be identified from orthogonality of the damping matrix with respect to the eigenvectors of the updated model. Since the updated model is to have proportional damping, its eigenvectors are the same as the eigenvectors of its undamped model. The updating process will therefore involve updating an undamped model, and use the undamped model's eigenvectors in the orthogonality equation (6.15)-(6.17), so as to solve for the unknown damping parameters.

To update an undamped model requires eigenvalues of the undamped system before and after stiffness (or mass) addition. The eigenvalues of the unmodified and undamped system are simply the real parts of measured eigenvalues, since damping is proportional. With a stiffness or mass addition, the damping matrix will not strictly remain proportional, since the relationship between the damping matrix and the mass/stiffness matrices is disturbed by the additional stiffness or mass. However, as the mass or stiffness matrix is modified one coordinate at a time, it can be assumed that the non-proportionality introduced by the additional lumped stiffness or mass is very small such that the system after mass or stiffness addition is still treated as

proportional. Thus, the real parts of measured eigenvalues of the structure with added stiffness (or mass) will be treated as the eigenvalues of the undamped modified structure, provided a proportional damping model is adequate to describe the dynamic behaviour of the unmodified structure. This approach was used in example 6.4 and the H-frame experiment with satisfactory results.

As an additional example consider the 10 DOF, 4 element model of example 6.4. A hysteretic damping matrix proportional to the stiffness matrix is simulated with a much larger damping loss factor, $\eta = 0.1$. Thus let,

$$EI = 5000(1+j0.1)\ \text{Nm}^2 \quad \text{for all elements.}$$

Fig 6.79 shows the point receptance at coordinate 3 as compared to that of an undamped model.

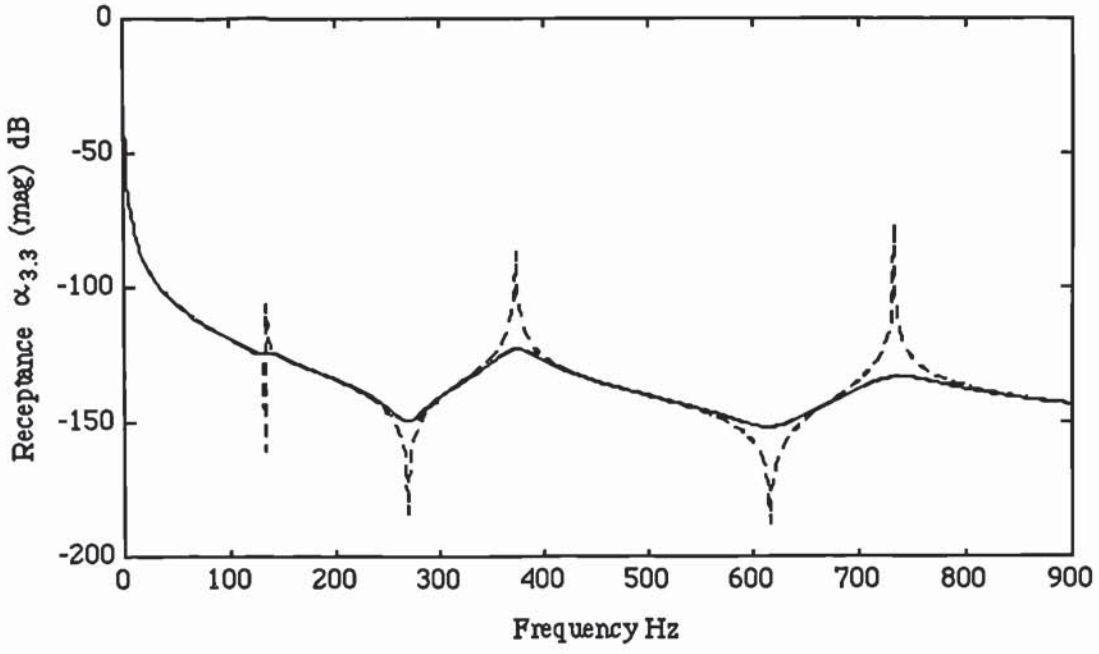

Fig 6.79 Receptance of the beam with proportional damping ($\eta = 0.1$) as compared to the undamped beam.

Let stiffnesses (N/m) of $2x10^6$, 10^7 and 10^8 be added at coordinate 3. Table 6.30 shows the correct and the estimated natural frequencies of the undamped beam with added stiffness. The estimated natural frequencies were obtained by assuming the real parts of the eigenvalues of the beam with added stiffness as the eigenvalues of the undamped beam with added stiffness. It can be seen that the difference between the two is very small.

	Estimated natural frequencies (Hz)			Correct natural frequencies (Hz)		
	f_1	f_2	f_3	f_1	f_2	f_3
$k = 2x10^6$	151.3	402.3	750.1	151.4	402.3	750.2
$k = 1x10^7$	231.4	501.3	842.2	231.1	500.9	842.5
$k = 1x10^8$	265.4	605.2	1292.5	265.4	605.1	1292.0

TABLE 6.30 Correct and estimated natural frequencies of the modified beam. (heavy proportional damping)

The H-frame experiment verifies the feasibility of using the FRF of a practical structure to simulate the FRF of the modified structure for model updating purposes. The smoothness of the simulated FRF of the frame with added stiffness and the reasonable Nyquist plots suggest that the degree of randomness in the measured data is not a crucial problem. No remarkable degradation of the Nyquist plot due to the simulation process was found. However, with large stiffness additions, lower modes tend to be less excited. As is usually the case with classical experimental modal analysis, modal identification of the weakly excited modes becomes relatively difficult. This is indicated, for example, by relatively less pronounced circles in figs 6.68 and

6.69 as compared to figs 6.70 and 6.71. An alternative option is to ignore the weakly excited modes as the additional stiffness becomes large or those modes which are obviously contaminated by noise. In the H-frame example, all four modes in the range 100-560 Hz were used with satisfactory results.

Whilst the technique of simulating the FRF of the structure with added stiffness (or mass) can be extended to transfer receptances, using (6.9), if both eigenvalues and eigenvectors are to be used, it is believed that eigenvalues are usually identified more accurately than eigenvectors. Hence, emphasis in this work has been on the use of point receptances and updating using eigenvalues.

A possible area of difficulty is the effect of shaker (push rod) loading on the structural dynamic characteristics of the structure under test. Since the point receptance at each modification coordinate has to be measured, the difficulty may be apparent as inconsistency in the global properties of the structure (in particular natural frequencies). Thus, large structures, which are least affected by small mass loading, are most suited to this technique if correction for mass loading has to be avoided. On the other hand, this difficulty is a useful warning that something has been overlooked.

CHAPTER 7

DISCUSSION AND CONCLUSION

7.1 Comparison with other methods

A technique of parametric adjustment of a FE model, based on eigenvalue or eigenvalue and eigenvector sensitivity analysis, has been developed. The technique, which utilizes the eigen-data of the system before and after the system is perturbed by adding lumped masses or grounded stiffnesses, can also be extended to a system modelled by lumped stiffness and a diagonal lumped mass matrix. Practical application of the technique requires the confidence on the parameters of the initial model, given as a diagonal variance matrix, to be available. The updated parameters are then determined by the minimum cost Bayesian approach which takes into consideration the confidence on the initial parameters as well as the measurements.

One of the difficulties experienced in previous parameter estimation methods, based on eigenvalues, is the incomplete dynamic characteristic information of the structure from eigenvalues alone. There is generally an infinite number of models that will reproduce a given set of measured eigenvalues. This problem is evident from the rank deficiency of the Jacobian matrix based on eigenvalue sensitivity. The Bayesian and similar approaches, which impose constraints on the changes of the parameters of the analytical model, have often been used to facilitate a solution for the parameter updates (see for example Collins *et al* 1974, Chen and Garba 1980). The Bayesian approach will always yield a solution even if only one eigenvalue is measured.

The idea behind the mass and stiffness addition technique is to develop a method that will result, theoretically, in convergence to the exact parameters,

provided the model structure is correct and the experimental data is error-free. Since neither the experimental data nor the model structure is likely to be error-free in practice, use is made of the Bayesian approach to limit excessive changes in the parameters. A technique which will result in the convergence of the parameters to their correct values, using an ordinary least squares solution method, if the experimental data were error-free, is considered to be more credible than the one with an infinity of solutions. Such a technique is also possible by using both eigenvalues and eigenvectors of an unperturbed system or the FRF data.

Most of the published methods are based on using both eigenvalues and eigenvectors or FRF data. If both eigenvalues and eigenvectors are used, a significant number of coordinates have to be measured, so that the number of sensitivity equations is at least as large as the number of parameters to update. Even in this case, the choice of the parameters to update and the choice of measurement coordinates could have an influence on the identification of the correct parameters with error-free data. Quite often, it has been assumed that a unique solution exists provided the number of eigenvalue and eigenvector sensitivity equations is at least as large as the number of parameters to update. The work reported in this thesis has attempted to find a method of assessing the adequacy of a given set of measurement coordinates. It is apparent, from Chapter 3, that if the parameters to be updated are the coefficients of the element mass and/or stiffness matrices, the choice of the measurement coordinates is generally not so crucial. If the lumped mass and stiffness of a lumped parameter model are to be updated, it is not enough for the number of eigenvalue and eigenvector sensitivity equations to be equal to or greater than the number of parameters. The choice of the measurement coordinates, in this case, is usually important.

Since natural frequencies are generally measured with higher accuracy than mode shape displacements, the mass and stiffness addition technique developed in this thesis can take advantage of this fact, as parameter updating is possible using eigenvalues alone. In addition, this new technique is attractive because it is possible to generate a much larger data base of eigenvalues of the mass or stiffness added structure, than the data base which can practically be measured using eigenvalues and eigenvectors without mass or stiffness addition.

Methods based on the FRF falls into two main groups. The equation error methods (Natke *et al* 1984,1985,1986,1988, Fritzen 1986, Mottershead 1988, Friswell 1989, 1990) and the output error methods (Cottin *et al* 1984, Natke 1988, Fritzen *et al* 1988). The equation error methods utilize directly the frequency domain equation of motion and attempts to find the parameters which, with the given response vector, the forcing vector is reproduced in a least squares sense. The equation error method has attracted more interest than the output error method due to the linear appearance of the parameters in the equations. A major draw back is that the equation error formulation requires response data at each DOF to be measured. Since this is not possible, a practical alternative has been to estimate the responses of the unmeasured DOF in terms of the analytical mode shape vectors or model reduction to the measurement DOF. Model reduction is based on transformation of coordinates where the response vector is expressed as a linear combination of the mode shape vectors. The eigenvectors of the analytical model are used in the transformation and it effectively involves expressing the unmeasured response vector in terms of the analytical model. This obviously is not exact and introduce errors which, in addition to the experimental errors in the measured data, contribute to biased estimates because the coefficients in the equations are computed using the contaminated data. The degree of errors introduced depends on how close are the analytical eigenvectors to the correct system

eigenvectors. An improved approach (Friswell 1989, 1990) has been to iterate, where after each parameter estimation, the new analytical model is used to find improved estimates of the responses of the unmeasured DOF. However, methods based on the equation error do not directly minimize the prediction, between the updated model and the system, in the dynamic characteristics for the parameters of interest.

The advantage of the present technique is that the optimization is performed with respect to the minimization of an error quantity of a dynamic characteristic which is of primary interest. Since the FRF data can be converted into modal data for the structure with added mass or stiffness, by the method of Chapter 6, the updating process attempts to fit the model to the modal data and also to the FRF data of the structure. Better convergence in the FRF is most likely to be ensured than with the frequency domain equation error approach, where parameters are optimized by minimizing the error between the computed and the experimental forcing vectors.

It can be argued that the mass or stiffness addition technique offers an alternative approach to fitting the FRF, where a well known eigen-data sensitivity algorithm is used. In fact, with this technique, both negative and positive stiffness addition is possible, so as to cover a large proportion of the FRF, although this is usually not necessary.

A well known technique of fitting directly to the FRF is the frequency domain output error approach. This technique is based on expressing the response vector in terms of the forcing vector, usually normalized to unity, and the unknown parameters. The resulting equation is non-linear in the parameters and a non-linear optimization algorithm is used. This is usually achieved by using a first order Taylor's expansion, based on parameter estimates of the

analytical model, and iteratively updating. The frequency domain output error algorithm, however, is potentially numerically unstable and is susceptible to divergence problems.

7.2 Some limitations and suggestions for further investigation

The mass or stiffness addition method is a modal based technique and therefore it shares some inherent limitations with other modal based updating techniques. One of the limitations is that the eigenvalue problem of the current analytical model has to be solved after each iteration and this consumes time. This limitation, however, is apparent in other non-modal but iterative methods.

Another limitation is the necessity to match the eigenvalues of the analytical model to those of the structure. As in other modal based methods, the eigenvalue of each structure mode which is to be used in the updating process has to be matched to the eigenvalue of the corresponding analytical mode. There are many systems where it is not difficult to match the two simply by inspection. In the numerical and experimental examples given in this thesis, it was not difficult (for those modes of interest) to decide which structure mode relates to which analytical mode. There are also many systems, for example with closely coupled modes, where matching by inspection alone may not be easy. The modal assurance criterion (MAC) is a reliable tool which can be used to match the analytical and the experimental modes (MAC is discussed by Ewins 1985). The use of the MAC, however, requires the eigenvectors of the structure. It means therefore, even if updating is to be based on eigenvalues alone, more coordinates will have to be measured so as to extract eigenvectors to be used in the MAC. For example, in the H-frame experiment, the measurement of the two excitation coordinates would be sufficient to extract eigenvalues of the

perturbed and unperturbed structure but would not be sufficient if MAC has to be used. The advantage of the possibility of measuring the structure at a smaller number of coordinates when eigenvalues alone are used is therefore diluted by the fact that more coordinates have to be measured so that MAC can be used to match the analytical and the experimental eigenvalues.

The technique developed in this thesis is modal based and has been developed from sensitivity analysis using well known equations of sensitivities of the eigenvalue and eigenvectors with respect to structural parameter changes. The eigenvectors in the sensitivity equations are mass-normalized. Almost all modal based methods uses mass-normalized modes. A possible area of improvement which is worth further investigation is the use of the sensitivity of the non-mass normalized modes. If the sensitivities of the arbitrarily normalized modes are derived then it should be possible, some how, to use the mass/stiffness addition technique based on these sensitivities. Since the mode shapes of the perturbed structure can be derived from the FRF of the unperturbed structure if the natural frequencies of the perturbed structure are known (Chapter 6) then the sensitivities of the FRF may be derived by treating the FRF as arbitrarily scaled mode shapes of the perturbed structure. If this is possible then it may be possible to formulate an algorithm which involves the FRF vectors rather than the mass-normalized eigenvectors. Such an algorithm may not require an eigensolution with each added mass/stiffness because the modes are replaced by the FRF vectors and some computational time may be saved. This is effectively using the stiffness addition technique to derive a frequency domain algorithm by, some how, getting rid of the normalizing modal masses from the mode shapes.

The method developed in this thesis is parametric in the sense that it estimates parameters of a model of a given structure. The structure of the model

matrices is determined by the analytical idealization of the physical system. When the idealization is not exact, the parameters will start to lose their physical meaning. Consequently the confidence expressed in, for example, flexural rigidity values, also lose their meaning. A difficulty will occur if the confidence in the initial parameters have been assigned based on the expected uncertainty in computing the true physical flexural rigidity of the beam element, while the model structure ignores flexibility of a joint in the structure. Fortunately the difficulty will become apparent by the unexpectedly large or unacceptable changes in the parameters from their initial estimates. Such unacceptable parameter changes may not necessarilly be localized to areas of modelling difficulties, but may be distributed in a way which is difficult to relate to the areas of errors in the model structure. When inaccuracy in the model structure is expected due to joint flexibility, those elements next to the joints have to be allowed to be more flexible than their actual physical flexibility suggest. Large parameter changes will therefore be localized to such elements. This seem to be a logical approach with any parametric updating method. The difficulty however, is how much flexibility should be allowed. For example, in the H-frame experiment, the elements of the cross-beam next to the joints were allowed to be more flexible than others by assigning an assumed standard deviation of twice as large as others. This was assigned by feeling as there is no proper method. As the prospects of updating the parameters using unconstrained algorithms are not very good, methods based on a form of Bayesian approach will continue to dominate. Investigation on systematic methods of assigning initial parameters weighting factors is therefore important.

7.3 Conclusion

A technique to update the parameters of a dynamic model has been developed. It is based on sensitivity analysis of the eigenvalues or both eigenvalues and eigenvectors before and after the system and its analytical model are perturbed by adding lumped mass or grounded stiffness. It has been shown that the eigen-data of the structure with added mass or stiffness can be successfully determined from its simulated FRF. The FRF of the structure with added mass or stiffness is simulated using the FRF measured from the structure without added mass or stiffness. Thus, mass or stiffness do not have to be added physically. The derivation of the method has been based on updating the coefficients of the element mass and stiffness matrices of a FE model or lumped mass and stiffness of a lumped parameter model with a diagonal mass (or stiffness) matrix. Due to the experimental errors in the modal data and possible inaccuracy in the model structure, parameter updating of a practical structure has to be performed by incorporating a constraint of minimum changes of the parameters from the initial estimates. It has been shown that with error-free data and a correct model structure, parameter convergence to the exact solution is possible, even by using eigenvalues alone or eigenvalues and incomplete mode shapes. Hence, the method forms a more rational basis of applying the constraint of minimum parameter changes from the initial estimates, than with methods which have infinite number of solutions with error-free data. The minimum conditions with respect to the choice of mass or stiffness addition coordinates as well as the choice of mode shape measurement coordinates have been derived. These conditions are not crucial for a FE model, due to the smaller number of parameters to update in comparison to the order of the model.

Since the technique is based on eigen-data sensitivities, to derive a set of

equations linear in the parameters, the coefficients are calculated using data from the analytical model only. Thus, biased errors associated with correlation of the equation errors are not encountered. It has also been shown that gross inaccuracy in the model structure results in unexpected large parameter changes from the initial estimates. This effect can also be brought about by poor assignment of the relative weighting of the eigen-data and the initial parameters. However, in many cases, reasonable assignment of the relative weighting is usually possible, and therefore large unexpected changes in the parameters is usually a warning of a gross inaccuracy in the model structure. If this is the case, the analytical model structure has to be re-examined. A major shortcoming of the technique is that an eigenvalue problem has to be solved, not only after each iteration, but also with each added mass or stiffness. A suggestion for further improvement has been put forward.

REFERENCE

Badenhauser K, 1986, *"Time domain identification of incomplete physical system matrices using a condensed estimation equation."* Proceedings of the 4th IMAC **1** 402-408.

Baruch M, Bar-Itzhack YB, 1978, *"Optimal weighted orthogonalization of measured modes."* AIAA Journal **16** 4 346-351.

Berman A, 1979, *"Comment on optimal weighted orthogonalization of measured modes."* AIAA Journal **17** 8 927-928.

Berman A, Flannelly WG, 1971, *"Theory of incomplete models of dynamic structures."* AIAA Journal **9** 8 1481-1487.

Berman A, Nagy EJ, 1983, *"Improvement of a large analytical model using modal test data."* AIAA Journal **21** 8 1168-1173.

Chen JC, Garba JA, 1980, *"Analytical model improvement using modal test results."* AIAA Journal **18** 6 684-690.

Collins JD, Hart CG, 1974, Hasselman TK, Kennedy B, *"Statistical identification of structures."* AIAA Journal **12** 2 185-190.

Collins JD, Young JP, Kiefling L, 1972, *"Methods and application of system identification of vibrating structures."* ASME winter annual meeting 45-71.

Dobson BJ, 1984, *"Modification of FE models using experimental modal analysis."* Proceedings of the 2nd IMAC, Florida USA, 593-601.

Dobson BJ, 1986, *"Model parameter estimation using difference equations."* Proceedings of the 4th IMAC, Los Angeles CA, 1006-1010.

Dobsob BJ, 1987, *"A straight line technique for extracting modal properties from frequency response data."* Mechanical systems and signal processing, **1** 1 29-40.

Edwards CH, 1973, *"Advanced calculus of several variables."* Academic press.

Ewins DJ, 1985, *"Modal testing: Theory and practice."* Research studies Press.

Ewins DJ, Sidhu J, 1984, *"Correlation of FE and modal test studies of a practical structure."* Proceedings of the 2nd IMAC, Florida USA, 756-762.

Fox RL, Kapoor MP, 1968, *"Rates of change of eigenvalues and*

eigenvectors." **AIAA** Journal **6** 2 2425-2429.

Friswell MI, 1989a, *"The adjustment of structural parameters using a minimum variance estimator."* Mechanical Systems and Signal Processing, 3(2), 143-155.

Friswell MI, 1989b, *"Updating physical parameters from frequency response function data."* Proceedings of the 12th Biennial Conference on Mechanical Vibration and Noise, Montreal Canada. DE-Vol 18-4: Vibration analysis-Techniques and applications, 393-400.

Friswell MI, Nalitolela NG, Penny JET, 1990, *"Updating the parameters of a finite element model."* Proceedings of the 15th Inter. Seminar on Modal Analysis, Katholieke Universiteit, Leuven Belgium,173-188.

Friswell MI, Penny JET, 1990, *"Updating model parameters directly from frequency response function data."* Proceedings of the 8th IMAC, Florida USA, 843-849.

Fritzen CP, 1986, *"Identification of Mass, Damping and Stiffness matrices of mechanical systems."* J. of Vibration, Acoustics, Stress and Reliability in Design **108** 9-16.

Fritzen CP, Zhu S, 1989, *"Systematic updating of finite element models by means of measured transfer functions."* Proceedings of the 12th Biennial Conference on Mechanical Vibration and Noise, Montreal Canada. DE-Vol 18-4: Vibration analysis-Techniques and applications, 363-369.

Gravitz SI, 1958, *"An analytical procedure for the orthogonalization of experimentally measured modes."* Journal of Aerospace Sciences, 721-722.

Guyan RJ, 1965, *"Reduction of stiffness and mass matrices."* AIAA Journal **3** 378.

Gysin H, 1986, *"Critical application of the error matrix method for localisation of FE modelling inaccuracies."* Proceedings of the 4th IMAC, Los Angeles CA, 1339-1343.

Gysin H, 1990, *"Comparison of expansion methods for finite element modelling error localization."* Proceedings of the 8th IMAC, Florida USA, 195-204.

Heylen W, 1986, *"Model optimization with measured modal data by mass and stiffener changes."* Proceedings of the 4th IMAC, Los Angeles CA, 94-100.

Ibrahim SR, 1983a *"Computation of normal modes from identified complex*

modes." AIAA Journal **21** 3 446-451.

Ibrahim SR, 1983b *"Dynamic modelling of structures from measured complex modes."* AIAA Journal **21** 6 893-901.

Ibrahim S, Fissette E, 1987, *"Error location and updating of analytical model using a force balance approach."* Proceedings of the 5th IMAC London 1183-1190.

Irons P, 1965, *"Structural eigenvalue problem, elimination of unwanted variables."* AIAA Journal **3.**

Joeng WB, Okuma M, Nagamatsu A, 1989, *"Experimental identification of mechanical structure with characteristic matrices."* JSME International Journal **32** 1 30-35.

Kidder RL, 1973, *"Reduction of structural frequency equations."* AIAA Journal **11** 6 892.

McGrew J, 1969, *"Orthogonalization of measured modes and calculation of influence coefficients."* AIAA Journal **16** 4 774-776.

Miller CA, 1980, *"Dynamic reduction of structural models."* ASCE Journal, 2097-2108.

Mottershead JE, 1988, *"A unified theory of recursive frequency domain filters with application to system identification in structural dynamics."* J of Vibration, Acoustics, Stress and Reliability in Design **110** 360-365.

Mottershead JE, Stanway R, 1986. *"Identification of structural vibration parameters by using a frequency domain filter."* Journal of Sound and Vibration **109** 3 495-506.

Nalitolela NG, Penny JET, Friswell MI, 1990b *"Updating structural parameters of a finite element model by adding mass or stiffness to the system."* Proceedings of the 8th IMAC, Florida USA, 836-842.

Natke HG, Cottin N, 1985, *"Updating mathematical models on the basis of vibration and modal test data: A review of experience."* Proceedings of the 2nd International Symposium on Aeroelasticity and Structural dynamics, Aachen Germany 625-631.

Natke HG, Hoff C, 1988, *"Correction of a finite element model by Input-Output measurement with application to Radar tower."* Proceedings of the 6th IMAC 658-666.

Natke HG, Cottin N, 1986, *"On the parameter identification of elasto-Mechanical systems using weighted input and modal residuals."* Ingenieur Archiv, **56** 106-113.

O'Callahan J, Avitable P, Lieu I, Madden R, 1984, *"An efficient method of determining rotational degrees-of-freedom from analytical and experimental data."* Proceedings of the 2nd IMAC Florida USA 50-58.

O'Callahan J, Milani J, 1989a, *"Comparison of system characteristics using various model reduction techniques."* Proceedings of the 7th IMAC Las Vegas Nevada, **2** 1109-1115.

O'Callahan J, Pan ED, 1989b, *"Effects of various model reduction techniques on computed system response."* Proceedings of the 7th IMAC Las Vegas Nevada, **2** 777-785.

Paz M, 1984, *"Dynamic condensation."* AIAA Journal **22** 724-727.

Richardson M, Potter R, 1974, *"Mass, stiffness and damping matrices from measured modal parameters."* International Instrumentation: Automation Conference, New York.

Rodden WP, 1967, *"A method for deriving structural influence coefficients from vibration tests."* AIAA Journal **5** 991-1000.

Ronald LH, Xu M, 1986, *"Modelling and parameter identification of vibrating systems in dynamic space."* Proceedings of the 4th IMAC Los Angeles CA, 422-426.

Ross GR, 1971, *"Synthesis of stiffness and mass matrices from experimental vibration modes."* SAE paper 710787.

Targoff WP, 1976, *"Orthogonal check and correction of measured modes."* AIAA Journal **14** 164-167.

Thoren AR, 1972, *"Derivation of mass and stiffness matrices from dynamic test data."* AIAA paper 72-346, 13th Structures, structural dynamics and materials conference, San Antonio Texas.

Tlusty J, Ismail F, 1980, *"Dynamic structural identification: Tasks and methods."* Annals of the CIRP, **29** 1 251-255.

Wang IC, Max L Wei, Jong-Chun Wei, 1986, *"Comparison of FE method and experimental modal analysis of a T plate with various boundary conditions."* Proceedings of the 4th IMAC Los Angeles CA, 748-753.

Wong KY, Polak E, 1987, *"Identification of linear discrete time systems using the Instrumental variable method."* IEEE Trans. on Automatic control **12** 6 707-717.

Young JP, On FJ, 1969, *"Mathematical modelling via direct use of vibration data."* SAE paper 690615, Los Angeles CA.

Young PC, 1970, *"An Instrumental variable method for real-time identification of a noisy process."* Automatica **6** 271-287.

Zhang Q, Lallement G, 1989, *"Selective structural modifications: Applications to problems of eigensolutions sensitivity and model adjustment."* Mechanical systems and Signal processing **3** 1 55-69.

Zhang Q, Lallement G, Fillod R, Piranda J, 1987, *"A complete procedure for the adjustment of a mathematical model from the identified complex modes."* Proceedings of the 5th IMAC London, 1183-1190.

APPENDIX A

MATHEMATICAL PROOFS

Appendix A1

Let **R** and **S** be *N*th order arbitrary but non-singular matrices such that:

$$\mathbf{R}\Delta\mathbf{M}\mathbf{S} = \Delta\mathbf{M} \tag{A1.1}$$

Let **R**, **S** and $\Delta\mathbf{M}$ be partitioned as follow:

$$\mathbf{R}=\begin{bmatrix} \mathbf{R}_{11} & \mathbf{R}_{12} & \mathbf{R}_{13} \\ \mathbf{R}_{21} & \mathbf{R}_{ii} & \mathbf{R}_{23} \\ \mathbf{R}_{31} & \mathbf{R}_{32} & \mathbf{R}_{33} \end{bmatrix}, \quad \mathbf{S}=\begin{bmatrix} \mathbf{S}_{11} & \mathbf{S}_{12} & \mathbf{S}_{13} \\ \mathbf{S}_{21} & \mathbf{S}_{ii} & \mathbf{S}_{23} \\ \mathbf{S}_{31} & \mathbf{S}_{32} & \mathbf{S}_{33} \end{bmatrix}, \quad \Delta\mathbf{M}=\begin{bmatrix} 0 & 0 & 0 \\ 0 & \delta m_i & 0 \\ 0 & 0 & 0 \end{bmatrix} \tag{A1.2}$$

where $\mathbf{R}_{ii}$, $\mathbf{S}_{ii}$ and δm_i are 1x1 submatrices.

Then: $\mathbf{S}_{ii} = \mathbf{R}_{ii}^{-1}$, $\mathbf{R}_{12} = \mathbf{R}_{32} = 0$, $\mathbf{S}_{21} = \mathbf{S}_{23} = 0$.

PROOF:

Substitute for **R**, **S** and $\Delta\mathbf{M}$ into (A1.1).

$$\begin{bmatrix} \mathbf{R}_{11} & \mathbf{R}_{12} & \mathbf{R}_{13} \\ \mathbf{R}_{21} & \mathbf{R}_{ii} & \mathbf{R}_{23} \\ \mathbf{R}_{31} & \mathbf{R}_{32} & \mathbf{R}_{33} \end{bmatrix}\begin{bmatrix} 0 & 0 & 0 \\ 0 & 1 & 0 \\ 0 & 0 & 0 \end{bmatrix}\begin{bmatrix} \mathbf{S}_{11} & \mathbf{S}_{12} & \mathbf{S}_{13} \\ \mathbf{S}_{21} & \mathbf{S}_{ii} & \mathbf{S}_{23} \\ \mathbf{S}_{31} & \mathbf{S}_{32} & \mathbf{S}_{33} \end{bmatrix}\delta m_i, = \begin{bmatrix} 0 & 0 & 0 \\ 0 & 1 & 0 \\ 0 & 0 & 0 \end{bmatrix}\delta m_i \tag{A1.3}$$

$$\begin{bmatrix} 0 & \mathbf{R}_{12} & 0 \\ 0 & \mathbf{R}_{ii} & 0 \\ 0 & \mathbf{R}_{32} & 0 \end{bmatrix}\begin{bmatrix} \mathbf{S}_{11} & \mathbf{S}_{12} & \mathbf{S}_{13} \\ \mathbf{S}_{21} & \mathbf{S}_{ii} & \mathbf{S}_{23} \\ \mathbf{S}_{31} & \mathbf{S}_{32} & \mathbf{S}_{33} \end{bmatrix} = \begin{bmatrix} 0 & 0 & 0 \\ 0 & 1 & 0 \\ 0 & 0 & 0 \end{bmatrix} \tag{A1.4}$$

$$\begin{bmatrix} \mathbf{R}_{12}\mathbf{S}_{21} & \mathbf{R}_{12}\mathbf{S}_{ii} & \mathbf{R}_{12}\mathbf{S}_{23} \\ \mathbf{R}_{ii}\mathbf{S}_{21} & \mathbf{R}_{ii}\mathbf{S}_{ii} & \mathbf{R}_{ii}\mathbf{S}_{23} \\ \mathbf{R}_{32}\mathbf{S}_{21} & \mathbf{R}_{32}\mathbf{S}_{ii} & \mathbf{R}_{32}\mathbf{S}_{23} \end{bmatrix} = \begin{bmatrix} 0 & 0 & 0 \\ 0 & 1 & 0 \\ 0 & 0 & 0 \end{bmatrix} \tag{A1.5}$$

From (A1.5):

$$\mathbf{R}_{ii}\mathbf{S}_{ii} = 1 \qquad \mathbf{R}_{ii}\mathbf{S}_{21} = 0$$
$$\mathbf{R}_{ii}\mathbf{S}_{23} = 0 \qquad \mathbf{R}_{12}\mathbf{S}_{21} = 0$$

$$\mathbf{R}_{12}\mathbf{S}_{ii} = 0 \qquad \mathbf{R}_{12}\mathbf{S}_{23} = 0$$
$$\mathbf{R}_{32}\mathbf{S}_{21} = 0 \qquad \mathbf{R}_{32}\mathbf{S}_{ii} = 0$$
$$\mathbf{R}_{32}\mathbf{S}_{23} = 0$$

But $\mathbf{R}_{ii}$ and $\mathbf{S}_{ii}$ cannot be zero. Therefore:

$$\mathbf{R}_{12} = \mathbf{R}_{32} = 0,$$
$$\mathbf{S}_{21} = \mathbf{S}_{23} = 0$$
$$\mathbf{S}_{ii} = \mathbf{R}_{ii}^{-1}.$$

Appendix A2

Let **T** and **L** be *N*th order arbitrary but non-singular matrices given by

$$\mathbf{T} = \begin{bmatrix} \mathbf{T}_{11} & \mathbf{T}_{12} \\ 0 & \mathbf{T}_{22} \end{bmatrix}, \qquad \mathbf{L} = \begin{bmatrix} \mathbf{T}_{11}^{-1} & 0 \\ \mathbf{L}_{21} & \mathbf{L}_{22} \end{bmatrix}$$

and such that $\mathbf{T}_{11}$ is an N_{pc}xN_{pc} diagonal submatrix with at least one of its elements as unity. Let **T** and **L** satisfy the determinant expression (A2.1),

$$\text{Det}(\mathbf{T} [\mathbf{K} - \lambda (\mathbf{M} + \Delta\mathbf{M})] \mathbf{L}) = 0 \qquad \text{(A2.1)}$$

where **K**, **M** and $\Delta\mathbf{M}$ ($\Delta\mathbf{M} = 0$ represent the case with no added mass to the system) are symmetrical matrices and

$$\mathbf{K}_x = \mathbf{TKL} \quad , \quad \mathbf{M}_x + \Delta\mathbf{M} = \mathbf{T} [\mathbf{M} + \Delta\mathbf{M}] \mathbf{L}$$

are also symmetrical matrices. Then

$$\mathbf{L} = \mathbf{T}^T \quad \text{and} \quad \mathbf{T}_{11}^2 = \mathbf{I} \qquad \text{(A2.2)}$$

PROOF

Consider the following equation of motion,

$$[\mathbf{K}_x - \lambda (\mathbf{M}_x + \Delta\mathbf{M})] \mathbf{V}^P_x = 0 \qquad \text{(A2.3)}$$

where $\mathbf{V}^P_x$ is an eigenvector of a system with mass matrix $[\mathbf{M}_x + \Delta\mathbf{M}]$ and stiffness matrix $\mathbf{K}_x$. But (A2.3) can be written as:

$$\mathbf{T} [\mathbf{K} - \lambda (\mathbf{M} + \Delta\mathbf{M})] \mathbf{L} \mathbf{V}^P_x = 0 \qquad \text{(A2.4)}$$

Pre-multiply (A2.4) by $\mathbf{T}^{-1}$ to obtain:

$$[\mathbf{K} - \lambda (\mathbf{M} + \Delta\mathbf{M})] \mathbf{L} \mathbf{V}^P_x = 0 \qquad \text{(A2.5)}$$

From symmetry

$$\mathbf{K}_x = \mathbf{L}^T \mathbf{K} \mathbf{T}^T \, , \qquad \mathbf{M}_x = \mathbf{L}^T \mathbf{M} \mathbf{T}^T$$

Therefore (A2.3) can also be written as:

$$\mathbf{L}^T [\mathbf{K} - \lambda (\mathbf{M} + \Delta\mathbf{M})] \mathbf{T}^T \mathbf{V}^P_x = 0 \qquad \text{(A2.6)}$$

Pre-multiply (A2.6) by $\mathbf{L}^{-T}$ to obtain:

$$[\mathbf{K} - \lambda (\mathbf{M} + \Delta\mathbf{M})] \mathbf{T}^T \mathbf{V}^P_x = 0 \qquad \text{(A2.7)}$$

From (A2.5) and (A2.7), $\mathbf{L}\mathbf{V}^P_x$ and $\mathbf{T}^T\mathbf{V}^P_x$ are eigenvectors of identical systems with stiffness matrix $\mathbf{K}$ and mass matrix $[\mathbf{M} + \Delta\mathbf{M}]$. Assuming d distinct eigenvalues ($d <$ or $= N$), the eigenvectors $\mathbf{L}\mathbf{V}^P_x$ and $\mathbf{T}^T\mathbf{V}^P_x$ which corresponds to the distinct eigenvalues are therefore related by scaler multipliers μ_j. Thus, for any jth of these eigenvectors,

$$\mathbf{L}\{\mathbf{V}^P_x\}_j = \mu_j \mathbf{T}^T \{\mathbf{V}^P_x\}_j$$

$\{\mathbf{V}^P_x\}_j$ can be partitioned into subvectors corresponding to the partitioning of $\mathbf{T}$ and $\mathbf{L}$. Therefore

$$\begin{bmatrix} \mathbf{T}_{11}^{-1} & 0 \\ \mathbf{L}_{21} & \mathbf{L}_{22} \end{bmatrix} \begin{Bmatrix} \mathbf{V}^P_{1,x} \\ \mathbf{V}^P_{2,x} \end{Bmatrix}_j = \mu_j \begin{bmatrix} \mathbf{T}_{11}^T & 0 \\ \mathbf{T}_{12}^T & \mathbf{T}_{22}^T \end{bmatrix} \begin{Bmatrix} \mathbf{V}^P_{1,x} \\ \mathbf{V}^P_{2,x} \end{Bmatrix}_j \qquad \text{(A2.8)}$$

From (A2.8):

$$\mathbf{T}_{11}^{-1} \left\{\mathbf{V}^P_{1,x}\right\}_j = \mu_j \mathbf{T}_{11}^T \left\{\mathbf{V}^P_{1,x}\right\}_j \qquad \text{(A2.9)}$$

But $\mathbf{T}_{11}$ is a diagonal submatrix with one of its elements as unity. Therefore, from (A2.9), for i = 1 to N_{pc}:

$$\mu_j T_{11}^2 = \mu_j T_{22}^2 = . . = \mu_j T_{ii}^2 = ... = \mu_j = 1 \qquad \text{(A2.10)}$$

$$T_{ii} = 1/T_{ii} \qquad \text{(A2.11)}$$

Therefore, from (A2.11) $\mathbf{T}_{11}^{\ 2} = \mathbf{I}$.

For the $d$vectors which corresponds to the distinct eigenvalues:

$$\begin{bmatrix} \mathbf{T}_{11}^{-1} & 0 \\ \mathbf{L}_{21} & \mathbf{L}_{22} \end{bmatrix} \begin{bmatrix} \mathbf{V}^P_{1,x} \\ \mathbf{V}^P_{2,x} \end{bmatrix} = \begin{bmatrix} \mathbf{T}_{11}^T & 0 \\ \mathbf{T}_{12}^T & \mathbf{T}_{22}^T \end{bmatrix} \begin{bmatrix} \mathbf{V}^P_{1,x} \\ \mathbf{V}^P_{2,x} \end{bmatrix} \qquad \text{(A2.12)}$$

Similarly, consider (A2.7) for $\Delta\mathbf{M} = 0$ and let $\mathbf{V}_x$ be an eigenvector of the system with stiffness and mass matrices $\mathbf{K}_x$ and $\mathbf{M}_x$ respectively ($\Delta\mathbf{M} = 0$). By the same arguments

$$\begin{bmatrix} \mathbf{T}_{11}^{-1} & 0 \\ \mathbf{L}_{21} & \mathbf{L}_{22} \end{bmatrix} \begin{bmatrix} \mathbf{V}_{1,x} \\ \mathbf{V}_{2,x} \end{bmatrix} = \begin{bmatrix} \mathbf{T}_{11}^{T} & 0 \\ \mathbf{T}_{12}^{T} & \mathbf{T}_{22}^{T} \end{bmatrix} \begin{bmatrix} \mathbf{V}_{1,x} \\ \mathbf{V}_{2,x} \end{bmatrix} \tag{A2.13}$$

where the eigenvector matrix is associated with the distinct eigenvalues. Equations (A2.12) and (A2.13) can be combined as

$$\mathbf{L}[\mathbf{V}_x \mathbf{V}^P{}_x] = \mathbf{T}^T[\mathbf{V}_x \mathbf{V}^P{}_x] \tag{A2.14}$$

Assuming the total number of distinct eigenvalues of $[\mathbf{M} + \Delta\mathbf{M}]^{-1}\mathbf{K}$ and $\mathbf{M}^{-1}\mathbf{K}$ is greater or equal to N, then (A2.14) results in

$$\mathbf{L} = \mathbf{T}^T \tag{A2.15}$$

Appendix A3

Let $\mathbf{K}$ and $\mathbf{M}$ be Nth order symmetrical stiffness and mass matrices and $\mathbf{T}$ an Nth order non-singular matrix in the form of (A3.1),

$$\mathbf{T} = \begin{bmatrix} \mathbf{T}_{11} & \mathbf{T}_{12} \\ 0 & \mathbf{T}_{22} \end{bmatrix} \tag{A3.1}$$

where $\mathbf{T}_{12}$ and $\mathbf{T}_{22}$ are arbitrary and $\mathbf{T}_{11}$ is diagonal with at least one element as unity but otherwise arbitrary.

Let
$$\mathbf{K}_x = \mathbf{T}\mathbf{K}\mathbf{T}^T \tag{A3.2}$$
$$\mathbf{M}_x = \mathbf{T}\mathbf{M}\mathbf{T}^T \tag{A3.3}$$

If $\mathbf{K}_x = \mathbf{K}$ and $\mathbf{M}_x = \mathbf{M}$ then

$$\mathbf{T} = \mathbf{I} \tag{A3.4}$$

PROOF

Let $\mathbf{V}_x$ and Λ_x be eigenvector and eigenvalue matrices of $\mathbf{M}_x^{-1}\mathbf{K}_x$ where the eigenvectors are orthogonal with respect to the mass ($\mathbf{M}_x$) and stiffness ($\mathbf{K}_x$) matrices. $\mathbf{M}_x^{-1}\mathbf{K}_x$ can be written in terms of its eigenvalue and eigenvector matrices as:

$$\mathbf{M}_x^{-1}\mathbf{K}_x = \mathbf{V}_x\Lambda_x\mathbf{V}_x^{-1} \tag{A3.5}$$

Using (A3.2) and (A3.3) in (A3.5) results in

$$\mathbf{M}_x^{-1}\mathbf{K}_x = \mathbf{T}^{-T}\mathbf{M}^{-1}\mathbf{K}\mathbf{T}^T = \mathbf{V}_x\Lambda_x\mathbf{V}_x^{-1} \tag{A3.6}$$

From (A3.6)

$$\mathbf{M}^{-1}\mathbf{K} = \mathbf{T}^T\mathbf{V}_x\Lambda_x(\mathbf{T}^T\mathbf{V}_x)^{-1} \tag{A3.7}$$

Equation (A3.7) is an eigenvalue problem with $\mathbf{T}^T\mathbf{V}_x$ as an eigenvector matrix of $\mathbf{M}^{-1}\mathbf{K}$.

$$(\mathbf{T}^T\mathbf{V}_x)^T\mathbf{M}(\mathbf{T}^T\mathbf{V}_x) = \mathbf{V}_x{}^T\mathbf{T}\mathbf{M}\mathbf{T}^T\mathbf{V}_x = \mathbf{V}_x{}^T\mathbf{M}_x\mathbf{V}_x = \text{diagonal} \tag{A3.8}$$

$$(\mathbf{T}^T\mathbf{V}_x)^T\mathbf{K}(\mathbf{T}^T\mathbf{V}_x) = \mathbf{V}_x{}^T\mathbf{T}\mathbf{K}\mathbf{T}^T\mathbf{V}_x = \mathbf{V}_x{}^T\mathbf{K}_x\mathbf{V}_x = \text{diagonal} \qquad \text{(A3.9)}$$

Thus, the eigenvectors in $\mathbf{T}^T\mathbf{V}_x$ are also orthogonal with respect to **M** and **K**. If $\mathbf{K}_x = \mathbf{K}$ and $\mathbf{M}_x = \mathbf{M}$ then $\mathbf{T}^T\mathbf{V}_x$ and $\mathbf{V}_x$ are both eigenvectors of the same system and from (A3.8) and (A3.9) they are related by

$$\mathbf{T}^T\mathbf{V}_x = \mathbf{V}_x\mu \qquad \text{(A3.10)}$$

where μ = square root of **I**. But **T** has at least one element as +1 in its diagonal submatrix $\mathbf{T}_{11}$. Thus,

$$\mu = \mathbf{I} = \mathbf{T} \qquad \text{(A3.11)}$$

APPENDIX B

COMPUTER PROGRAM

This appendix describes the computer program written during the course of the research. The program has been used in the simulation and experimental model updating examples. It has been written in MATLAB language based on the flow diagrams shown in figs B1.1 and B1.2. For the sake of clarity, the flow diagrams shows unconstrained optimization using eigenvalues alone. However, both unconstrained and constrained optimization using eigenvalues and using both eigenvalues and eigenvectors have been implemented in the program. The flow diagrams shows two options for sensitivity analysis. One option is sensitivity analysis based on the full order model. The other option for sensitivity analysis is based on the reduced order model.

The first option is based on the derivatives of the eigenvalues (and both eigenvalues and eigenvectors) as presented by Fox and Kapoor (1968). The second option is based on exact expression for the reduced equation of motion, which results in frequency dependent reduced mass and stiffness matrices and is described by Nalitolela *et al* (1990). The second option was first used in an attempt to avoid the problem of mismatch in the number of DOF between the FE model and the experimental modal model, but was later realised that the sensitivity data for the two options is the same and results in the same updated model. The first option was therefore introduced due to computational advantage. However, due to the limitations of MATLAB within the 640 Kbytes RAM, memory problems were experienced when updating large models (> 20 DOF). Memory restrictions were not experienced with model reduction. The reduction option was therefore restored due to its better utilization of memory in the MATLAB environment within the 640 Kbytes RAM. It is not intended, however, that the reduction option should be prefered in the general sense.

The program is made up of the following modules.

(i) ngdisc.m	Main module. The FE model employs 2 dimensional beam elements. The lumped parameter model is of a spring-mass system with diagonal mass matrix and the masses possess translational motion only.
(ii) ngdisc1.m	Module for assembling the mass and stiffness matrices.
(iii) ngdisc2.m	Module to perform differentiation of the matrices with respect to the parameters.
(iv) ngdisc3.m	Module to assemble the sensitivity matrix, **J**.

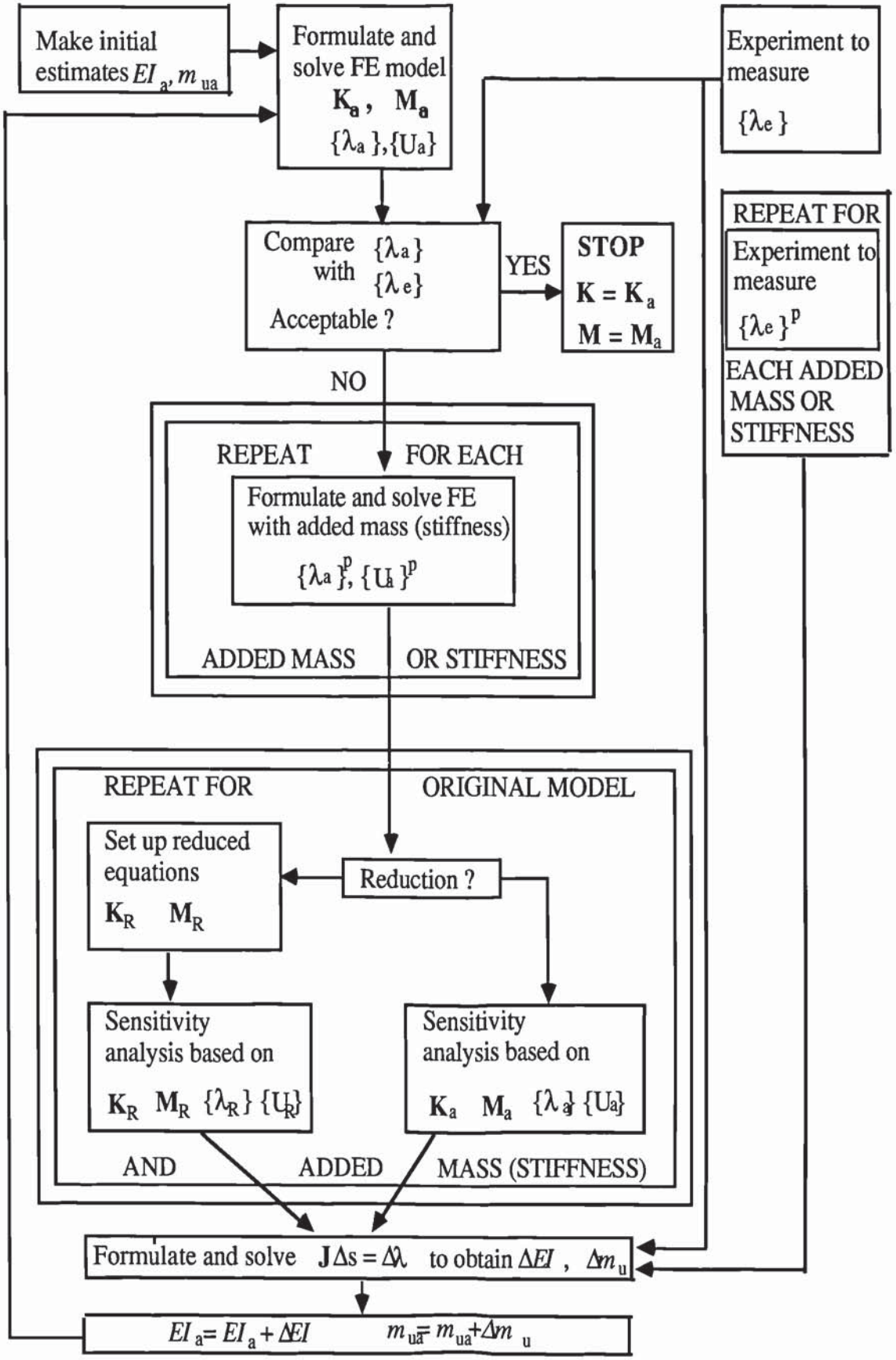

Fig B1.1 Flow diagram for updating by physical mass or stiffness addition.

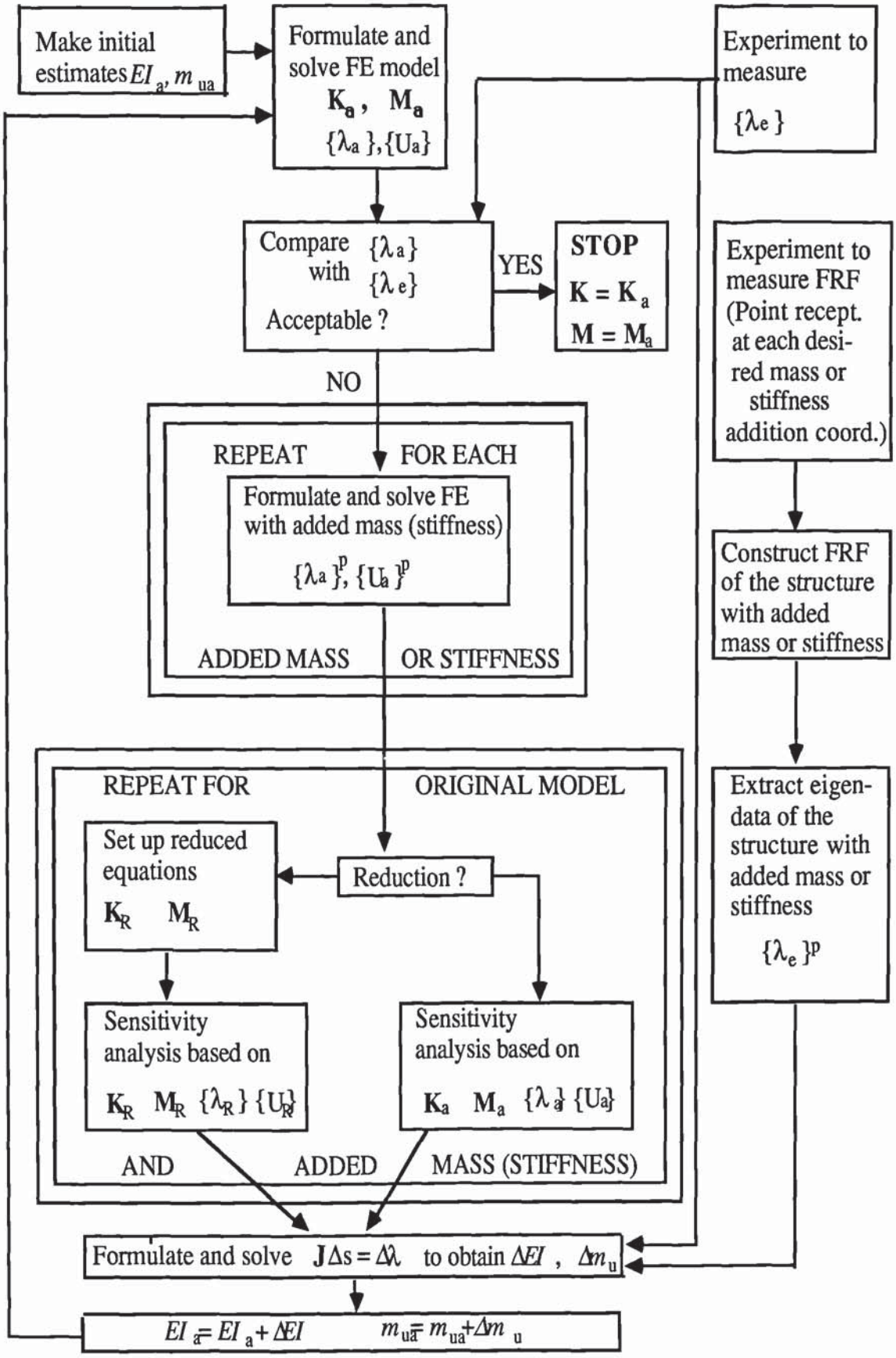

Fig B1.2 Flow diagram for updating by simulation of added stiffness or mass.

DATA INPUT

To run the program, MATLAB is invoked, then the name of the main program without the extension (ngdisc) is typed on the MATLAB work space followed by RETURN. Data is then input by responding to the questions as they are displayed on the screen, one after another. It is usually more convenient to prepare, in advance, some of the data as variables on the MATLAB work space before the program is run. Data input will therefore require typing in the variables corresponding to the required data.

Data associated with the eigenvalues should be saved as variables in a MATLAB file ngnval100.mat. The variables are: (i) lbe; eigenvalue data (ii) sw1; estimates of the STD of the errors in the natural frequencies. There is also an option of loading these variables in the MATLAB work space instead of saving them in a matlab file.

Data associated with the eigenvectors should be saved as variables in a file ngvec100.mat. The variables are: (i) ue; mass normalized eigenvectors (ii) su1; estimates of the STD of the errors in the mass normalized eigenvectors. These data may, instead, also be loaded in advance in the Matlab work space.

In case of analytical mass or stiffness addition using the simplified approach (see Chapter 6, section 6.3 equation 6.14), the non-mass normalized modes can be measured by simply reading the receptance data of the unperturbed structure, at frequencies corresponding to the estimated natural frequencies of the perturbed structure. In this case, the variables are (i) vee; non-mass normalized modes (ii) sv1; estimates of the STD of the errors in vee (iii) cee; vector defining coordinates with highest measured displacement for each vector in vee. The variables vee, cee and sv1 must be save in a data file ngvec100.mat. The updated parameters, at the end of iterations, will be recovered from the following variables

eee	Stiffness parameters, EI, of the FE model for all iteration steps.
mmm	Mass parameters, m_u, of the FE model for all iteration steps.
bbb	Lumped mass and stiffness parameters for all iteration steps.

The following section list the questions displayed by the program, required data, prefered variable names for some of the data, the structure of the data and describe the best way of data input. The questions are shown in *italics* and the responses in plain text. The questions shown with an asterik, *, require the data to be prepared in advance on the MATLAB work space and assigned a variable name which is to be typed in when responding to the questions. The prefered variable names are shown. The structure of the data in the variables is given in the section on data structure.

Discrete of continuous system ? *enter 0 (discrete) or 1 (continuous)*	Enter 0 for lumped spring-mass system or 1 for a FE model
Number of DOF ?	Enter the number of DOF.
Number of measured modes ?	Enter the appropriate number.
Number of rigid body modes ?	Enter the appropriate number.
Number of finite elements ?	Enter the appropriate number. This question will only appear if you have responded to the first question by entering 1
**Enter elements code matrix ?*	Enter nc (prefered variable 'nc', this question will only appear if you have responded to the first question by entering 1).
**Enter global coordinate code matrix*	Enter ng (prefered variable 'ng', this question will only appear if you have responded to the first question by entering 1).
Element type ? 0-beam 1-plate	Enter 0. (This question will only appear if your response to the first question is1).
Number of measurement coordinates ?	Enter the appropriate number
Model reduction yes (1) or no (0) ?	Enter 0 if model reduction is not required or 1 if model reduction is to be performed. (Model reduction, if specified, will only be performed to the measurement coordinates).
**Enter vector of measured coordinates*	Enter nvm. (Prefered variable 'nvm'. This question will be asked if model reduction has not been specified in the previous question).
Total number of discrete elements	Enter the appropriate number

**Enter elements data matrix*	Enter nd. (prefered variable nd. This question will only be asked if you have answered 1 to the first question)
**Enter discrete parameter matrix*	Enter bcm. (prefered variable 'bcm'. This question is asked if you have entered the total number of discrete elements greater than zero)
Number of discrete stiffness if any ?	Enter the appropriate number
**Enter matrix of parameter definition*	Enter pd (prefered variable 'pd'. This question will only appear if you have answered 1 to the first question).
**Enter vector of measured coordinates*	Enter nm (prefered variable is 'nm'. This question will only appear if model reduction is to be performed).
**Enter vector of unmeasured coordinates*	Enter ns (prefered variable is 'ns'. This question will only appear if model reduction is to be performed).
Number of mass/stiffness addition coord.?	Enter the appropriate number
Number of mass/stiffness addition per coord?	Enter the appropriate number
Eigenvalues (0) or eigenvalues + eigenvectors (1) ?	Enter 0 if eigenvalues alone are used or 1 if both eigenvalues and eigenvectors are used.
Analytical (1) or physical (0) mass or stiffness addition ?	Enter 1 if mode shapes are determined by a simplified approach of reading the receptances corresponding to the natural frequencies of the structure with added mass or stiffness (see equation 6.14 in

	Chapter 6, section 6.3). Otherwise enter 0 (this question is only asked if both eigenvalues and eigenvectors are used).
Want to use initial par in optimization ? Yes (1) No (0)	Enter 1 if the minimum cost Bayesian approach is to be used. Enter 0 if an unconstrained weighted least squares solution method is to be used.
**Enter mass/stiff addition matrix*	Enter my (Prefered variable is 'my').
Enter 0 or 1 for mass or stiffener additions	Enter 0 if mass addition. Enter 1 if stiffness addition.
Want to use existing file of eigendata ? Yes (1) No (0)	Enter 1 if eigenvalue data is already saved in a MATLAB file called ngnval100.mat and eigenvector data (if mode shapes are also used) in a file called ngvec100.mat Enter 0 if the eigendata variables are not saved in files but loaded in the MATLAB work space.
Enter simulation error in natural freq.	Enter the simulated STD error, in Hz, of the natural frequencies if the eigenvalue data is not already contaminated by measurement errors. If already contaminated, enter a very small number, close to zero, but not zero. You may enter 0 if the eigenvalue data is error-free and no error is to be simulated.
**Enter eigenvalue matrix*	Enter lbe (Prefered variable is 'lbe'. This question is asked if the eigenvalue data is not save as a variable in a MATLAB file ngnval100.mat).

**Enter matrix of STD for natural freq.*	Enter sw1 (Prefered variable is 'sw1'. This question is asked if the eigenvalue data, including natural freq STD, is not saved as variables in a MATLAB file ngnval100.mat).
**Enter eigenvector matrix*	Enter ue.(Prefered variable is 'ue'. This question is asked if eigenvectors are also used and the data is not saved as variables in a file ngvec100.mat. NOT applicable for qq1=1.)
**Enter vector of STD for the eigenvectors*	Enter su1 (Prefered variable is 'su1'. This question is asked if eigenvectors are also used and the eigenvector data, including its STD data to be used in the weighting matrix, is not saved in a file ngvec100.mat. NOT applicable for qq1=1.)
Enter simulation eigenvector error	Enter the simulated error for the mass normalized eigenvectors if the eigenvectors are not already contaminated by measurement errors. If the eigenvectors are already contaminated, enter a number close to 0, but not 0. You may enter 0 if the data is error free and no error is to be simulated.
Enter total no of unknown parameters	Enter the appropriate number
**Enter vector of initial estimates for optimization*	Enter nduo (Prefered variable is 'nduo'. This question is only asked if the minimum cost Bayesian approach is to be used).
**Enter STD of initial estimates*	Enter c2 (Prefered variable c2).

ADDITIONAL VARIABLES

The program can be terminated at any time by pressing Cntrl Break, and recover the variables containing the updated parameters (nd, bcm) from the Matlab work space. In addition to the variables 'eee' and 'mmm', new variables will be generated. The ones of interest are:

lb	Matrix of eigenvalues of the current analytical model.
ua	Matrix of mass-normalized eigenvectors of the current analytical model.
bbb	Matrix of lumped mass and stiffness (where appropriate) from the begining of the first iteration.
ue	Matrix of estimated mass-normalized modes (a new varible if the simplified approach, with non-mass normalized experimental modes, is used)
su1	Row vector of STD estimates of the errors in 'ue' above.

DATA STRUCTURE

Element code matrix (nc):

This matrix specifies the orientation of the element coordinates with respect to the local coordinate axes. The refence local coordinate axes are shown in fig B1.3.

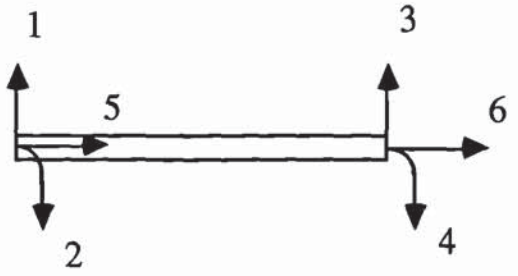

Fig B1.3 Local coordinate system (node 1 is on the left and node 2 on the right)

The element code matrix (nc) must consist of as many rows as the number of elements. Each row must have six entries which relate to the 6 coordinates shown in fig B1.3 and in the same order. Coordinates which are fixed must have an entry of 0. Coordinates which are not fixed but are in opposite directions to the local reference axes must have an entry of -1. A coordinate in the same direction as its corresponding local reference axis must have an entry of 1. For coordinates which are at an angle to the local reference axes, the global reference axes at that node have to be rotated so that the global coordinates are parallel to the local coordinate system shown in fig B1.3, before assigning an entry of -1 or 1. The direction of rotation determines the sign of the angle of rotation and will be required as input data for the element data matrix 'nd'. The sign convention is +ve if rotated anticlockwise.

Global coordinate code matrix (ng):

This matrix must have 6 columns and as many rows as the number of elements. Each row defines all the global coordinates associated with one element. The order at which the elements are defined is not important but must be the same as in the definition of 'nc'. The order at which the global coordinates (for each element) are defined must be similar to the order at which their corresponding local coordinates are defined (fig B1.3). Enter 0 if a coordinate is fixed.

Element data matrix (nd):

This matrix must have 6 columns and as many rows as the number of elements. The order at which the elements are defined (the order at which the rows appear) is not important but must be the same as in the definition of 'nc' and 'ng'. The six columns are defined as follow:

1st column:	Stiffness parameters, *EI*, of all elements starting with element 1.
2nd column:	Axial stiffness *EA*
3rd column:	Mass parameters, m_u(mass per unit length of the beam elements)
4th column:	Element lengths.
5th column:	Angle in degrees for which the global reference axes at node 1 have to be rotated so as to be parallel to the local reference axes. Sign convention is +ve in the anticlockwise direction.
6th column:	Angle in degrees for which the global reference axes at node 2 have to be rotated so as to be parallel to the local reference axes.

Discrete parameter matrix (bcm):

This matrix defines the lumped masses and stiffnesses and must have 4 columns and as many rows as the number of lumped mass and stiffnesses. The stiffenesses are defined first and then the masses. The stiffnesses are defined as follow:

1st column:	The DOF in consideration.
2nd column:	Value of the stiffness (N/m).
3rd column:	Must be 0.
4th column:	The DOF at which the defined stiffness is connected to. Enter 0 if grounded.

The masses are defined as follow:

1st column:	The DOF in consideration
2nd column:	Must be zero.
3rd column:	Value of the mass in Kg
4th column:	Must be 0.

Matrix of parameter definition (pd):

This is a matrix with 2 rows and as many columns as the number of elements. The first row consist of numbers starting with 1 and ending with the number of elements. The second row defines which elements are to be treated as having independent parameters and which elements are to be treated as having identical parameters. Thus,

$$\text{pd} = \begin{bmatrix} 1 & 2 & 3 & 4 & 5 & 6 & 7 & 8 \\ 1 & 2 & 2 & 2 & 1 & 3 & 4 & 1 \end{bmatrix}$$

means the system has 8 finite elements. Elements 1, 5, and 8 are to be treated as having identical parameters denoted by EI_1, m_{u1}. Elements 2, 3 and 4 have identical parameters denoted by EI_2, m_{u2}. Elements 6 and 7 have independent parameters denoted by EI_3,m_{u3} and EI_4, m_{u4} respectively.

Vector of measured coordinates (nm or nvm):

This is a row matrix containing the measurement DOF. The variable name 'nm' must be used if model reduction option is used. Otherwise use the variable name 'nvm'.

Vector of unmeasured coordinates (ns):

A row matrix containing the unmeasured DOF.

Mass/stiffness addition matrix (my):

This matrix specifies which coordinates are perturbed and the value of the perturbing mass (kg) or stiffness (N/m). It consist of as many columns as the number of perturbed coordinates. The first row lists the perturbing coordinates. The second row lists the perturbing mass or stiffness for each specified perturbing coordinates in the first perturbation. The next rows lists the perturbing masses or stiffnesses for the next rounds of mass or stiffness additions. Thus,

$$\text{my} = \begin{bmatrix} 3 & 5 & 11 \\ 0.25 & 0.25 & 0.25 \\ 0.35 & 0.35 & 0.05 \end{bmatrix}$$

means coordinates 3, 5 and 11 are perturbed. The perturbing masses are 0.25 kg at each of the three coordinates, 0.35 kg at coordinates 3 and 5 only and 0.5 kg at coordinate 11.

Eigenvalues matrix (lbe):

This is a matrix made of diagonal submatrices of measured eigenvalues and is of the following format:

$$lbe = \left[\Lambda_1\ \Lambda_2\ \Lambda_3\ \Lambda_4\ \Lambda_5 \ldots\right]$$

The first submatrix consist of eigenvalues of the unperturbed structure. The other submatrices consists of eigenvalues of the perturbed structure arranged in an order similar to the order of the perturbing masses/stiffnesses in 'my'.

Matrix of STD for the natural frequencies (sw1):

This is a matrix of the same format as 'lbe' but the diagonal submatrices of measured eigenvalues are replaced by diagonal submatrices of the estimated standard deviations of the natural frequencies in Hz.

Eigenvector matrix (ue):

This matrix has a similar format to 'lbe' but the diagonal submatrices of measured eigenvalues are replaced by submatrices of measured eigenvactors (mass-normalized).

Vector of STD for the eigenvectors (su1):

This is a row vector of the estimated standard deviations for the measured eigenvectors. It is assumed, for simplicity, that the mode shape displacements for a given mode at all measured coordinates are of the same standard deviation. Thus, each entry in 'su1' is a STD for the mode shape displacements of the mode in the corresponding position in 'ue'.

Vector of initial estimates for optimization (nduo):

This is a column vector of the parameters of the initial analytical model. The FE parameters are entered first, and then lumped stiffness parameters, if any, and finally lumped masses. The format for 'nduo' is illustrated by the following example for a system with 3 independent sets of element parameters, 3 lumped stiffness and 2 lumped masses.

$$\text{nduo} = \begin{bmatrix} EI_1 \\ m_{u1} \\ EI_2 \\ m_{u2} \\ EI_3 \\ m_{u3} \\ k_1 \\ k_2 \\ k_3 \\ m_1 \\ m_2 \end{bmatrix}$$

STD of initial estimates (c2):

This is a column vector of the same format as 'nduo' but the parameters are replaced by their respective standard deviation estimates.

PROGRAM LISTING

MAIN MODULE: ngdisc.m

```
%ngdisc.m
clc
disp('**************************************************      ')
disp(' NGDISC / NGDISC1 / NGDISC2 / NGDISC3 ')
disp('    ----------------------------------    ')
disp('UPDATING CONTINUOUS PLANE FRAME STRUCTURES WITH 2D FE
BEAM ELEMENTS')
disp(' AND DISCRETE SYSTEMS ( Lumped Spring-Mass systems ) ')
disp('**************************************************      ')
disp(' ')
disp(' Discrete or Continuous system ? ')
ds=input('Enter 0 ( Discrete ) or 1 ( Continuous ) ');
ty=2;
if ds==0
ne=0;
end
dof=input('Number of DOF ? ');
r=input('Number of measured modes ? ');
rg=input('Number of rigid body modes (unperturbed structure) ? ');
disp(' ')
if ds==1
ne=input('Number of finite elements ? ');
nc=input('Enter elements code matrix. ');
ng=input('Enter global coordinate code matrix (0 for fixed nodes) ');
disp(' ')
ty=input('Element type ? 0-beam 1-plate ');
end
nr=input('Number of measurement coordinates ? ');
drf=input('Model reduction(to the measurement coord) yes (1) or no (0)
? ');
if drf==0
nm=[1:dof];
ns=[];
nnr=nr;
nr=dof;
nvm=input('Enter vector of measured coodinates ? ');
end
bct=input('Total number of discrete elements if any ? ');
bcn=bct;
if ty==0
```

```
nd=input('Enter elements data matrix [ei ea mu la Angle1 Angle2] ')
end
if bcn>0
bcm=input('Enter discrete parameter matrix [coord stiff mass coord]
');
end
bck=input('Number of discrete stiffness if any ');
if ds~=0
pd=input('Enter matrix of param definition (pd) [elem nos;ident nos] ');
end
if drf==1
nm=input('Enter vector of measured coordinates (global) ');
ns=input('Enter vector of unmeasured coordinates (global) ');
end
p=input('Number of mass/stiffener addition coordinates ? ');
q=input('Number of stiffener/mass additions per coordinate ? ');
p3=input('Eigenvalues (0) or eigenvalues+vectors (1) ? ');
if p3==1
qq1=input('Analytical (1) or Physical (0) mass/stiffness addition ? ');
if qq1==1
clc
disp('REMEMBER THAT EIGENVECTORS vee SHOULD BE NON MASS
NORMALIZED')
disp(' ')
disp('press any key to continue ')
pause
end
end
pp1=input('Want to use initial par in optimization ? yes(1) no(0) ');
my=input('Enter mass/stiff addition matrix [coords;sttiffener/mass]
');
ms=input('Enter 0 or 1 for mass or stiffener additions ');
iii=input('Want to use existing file of eigendata ? YES(1) NO(0) ');
sw=input('Enter simulation error in natural freq (STD Hz) ? ');
if iii==1
load ngnval100
if p3==1
load ngvec100
end
end
if iii==0
lbe=input('Enter eigenvalue matrix [lbe] ');
sw1=input('Enter matrix of STD for natural freq (Hz) ');
```

```
if p3==1
ue=input('Enter eigenvector matrix [ue] ');
su1=input('Enter row vector of STD for eigenvectors ');
end
end
if p3==1
su=input('Enter simulation eigenvector error (mass normalized) ');
end
iii=input('Enter total no of unknown structural parameters ');
if pp1==1
nduo=input('Enter vector of initial estimate for optimization ');
c2=input('Enter STD of initial estimates ');
c2=inv(diag(c2,0));
end
yy=1;
z2=1;
z1=100;
while abs((z1-z2)/z1)>0.01
if ty~=1
ngdisc1 % ***** element matrices & assembling process
end
if yy>1
z2=z1;
end
[v,l]=eig(k,m); % ********* eigen sol of unperturbed structure
[kv,kl]=sort(diag(l));
l=real(diag(kv,0));
v=real(v(:,kl));
if qq1==1 % &&&&&&&& renormalization of eigenvectors
s=1;
for i=rg+1:rg+r
v(:,i)=v(:,i)/v(cee(s),i);
s=s+1;
end
end % &&&&&&&&&
for i=1:dof
u(1:dof,i)=v(:,i)/sqrt(v(:,i)'*m*v(:,i));
end
u=real(u);
uax=u(:,rg+1:rg+r);
lb=l(rg+1:rg+r,rg+1:rg+r);
if qq1==1 % &&&&& modal mass calc
maa=v(:,rg+1:rg+r)'*m*v(:,rg+1:rg+r);
```

```
maa=diag(maa);
end % &&&&&&&&&&&&&&&
save ngdata k m l v % *************** end of eigen sol
j=r;
for ii=2:q+1 % *********to calculate eigendata of added structure
for i=1:p
if ms==0
m(my(1,i),my(1,i))=m(my(1,i),my(1,i))+my(ii,i);
end
if ms==1
k(my(1,i),my(1,i))=k(my(1,i),my(1,i))+my(ii,i);
end
[v,l]=eig(k,m);
[kv,kl]=sort(diag(l));
v=real(v(:,kl));
l=real(diag(kv,0));
if qq1==1 % &&&&&&&&&&&& renormalization of the eigenvectors
for jj=rg+1:rg+r
v(:,jj)=v(:,jj)/v(cee(s),jj);
s=s+1;
end
end % &&&&&&&&&&&&
for t=1:dof
u(1:dof,t)=v(:,t)/sqrt(v(:,t)'*m*v(:,t));
end
u=real(u);
uax(1:dof,j+1:j+r)=u(:,rg+1:rg+r);
lb(1:r,j+1:j+r)=l(rg+1:rg+r,rg+1:rg+r);
if qq1==1 % &&&&&&&&&&&&&& modal mass calc
maa2=v(:,rg+1:rg+r)'*m*v(:,rg+1:rg+r);
maa2=diag(maa2);
maa=[maa;maa2];
end % &&&&&&&&&&&&
if ms==0
m(my(1,i),my(1,i))=m(my(1,i),my(1,i))-my(ii,i);
end
if ms==1
k(my(1,i),my(1,i))=k(my(1,i),my(1,i))-my(ii,i);
end
j=j+r;
end % ******************* end of next i
end % ******************* end of next ii
if qq1==1 % &&&&&&&&& computing mass normalized modes
```

```
for  i=1:r+p*q*r
ue(:,i)=vee(:,i)/sqrt(maa(i));
su1(i)=sv1(i)/sqrt(maa(i));
end
end % &&&&&&&&
if  nr<dof
for  i=1:nr
ua(i,1:j)=uax(nm(i),:);
end
end
if  nr==dof
ua(1:dof,1:j)=uax(1:dof,:);
end
if  p3==1
for  i=1:r+p*q*r
if  drf==0
for  ii=1:nnr
d2(ii,1)=ue(ii,i)-ua(nvm(ii),i);
d3(ii,1)=ue(ii,i)+ua(nvm(ii),i);
end
end
if  drf==1
d2=ue(:,i)-ua(:,i);
d3=ue(:,i)+ua(:,i);
end
if  max(abs(d2))>max(abs(d3))
ua(:,i)=-ua(:,i);
end
end
end
clear  uax  u  v  l  % ************* end of eigen data calc
%  ******************  calculating  reduced  matrices
if  nr<dof
for  i=1:nr
for  ii=1:nr
k11(i,ii)=k(nm(i),nm(ii));
m11(i,ii)=m(nm(i),nm(ii));
end
end
for  i=1:nr
for  ii=1:dof-nr
k12(i,ii)=k(nm(i),ns(ii));
m12(i,ii)=m(nm(i),ns(ii));
```

```
end
end
k21=k12';
m21=m12';
for  i=1:dof-nr
for  ii=1:dof-nr
k22(i,ii)=k(ns(i),ns(ii));
m22(i,ii)=m(ns(i),ns(ii));
end
end
end     %     ***************************************************
if  nr==dof
k11=k;
k12=zeros(nr,nr);
k21=k12;
k22=k12;
m11=m;
m12=zeros(nr,nr);
m21=m12;
m22=m12;
end
nne=(iii-bct)/2;
clear k  m
clc
disp('BUSY BUSY BUSY BUSY BUSY  BUSY sensitivity analysis')
jx=1;
for so=1:1+p3
ss=1; zz=2;
for s=1:1+p*q % ******** mass/stiff add & Jacobian matrices
s
yy
xx=zeros(dof,dof);
if s>1
xx(my(1,ss),my(1,ss))=my(zz,ss);
ss=ss+1;
end
if ss>p
ss=1;
zz=zz+1;
end
if  nr<dof
for  i=1:nr
for  ii=1:nr
```

```
mx(i,ii)=xx(nm(i),nm(ii));
end
end
end
if nr==dof
mx=xx;
end
clear xx
if ms==0
m11=m11+mx;
end
if ms==1
k11=k11+mx;
end
for j=1:r
a=(s-1)*r+j;
a4=-lb(j,a)*m12+k12;
if nr<dof
a5=inv(-lb(j,a)*m22+k22);
end
if nr==dof
a5=diag(ones(nr,1),0);
end
a6=-lb(j,a)*m21+k21;
kr=k11-a4*a5*k21-k12*a5*a6+a4*a5*k22*a5*a6;
mr=m11-a4*a5*m21-m12*a5*a6+a4*a5*m22*a5*a6;
[v,lx]=eig(kr,mr);
[kv,kl]=sort(diag(lx));
lx=real(diag(kv,0));
v=real(v(:,kl));
for i=1:nr
ux(1:nr,i)=v(:,i)/sqrt(v(:,i)'*mr*v(:,i));
end ii=0; % ********
if j>nr
lx=[lx  zeros(nr,j-nr);zeros(j-nr,j)];
ux=[ux  zeros(nr,j-nr)];
end
for i=1:nr
if  abs(lb(j,a)-lx(i,i))<1
lz=lx(j,j);
uz=ux(:,j);
lx(j,j)=lx(i,i);
lx(i,i)=lz;
```

```
ux(:,j)=ux(:,i);
ux(:,i)=uz;
clear uz lz
ii=ii+1;
end
end
nnk=0;
nnm=0;
if yy==1 % ************ rand error generator
if s==1 & j==1
if so==1
rand('normal')
rn1=rand(r+p*q*r,1);
end
if so==2
rn2=rand(nr*p*q*r+r*nr,1);
end
end
end % ******************** end of rand error generat
if so==1
dd(a,1)=lbe(j,a)-lb(j,a)+4*pi*sqrt(lbe(j,a))*sw*rn1(a);
w1(a,1)=1/(4*pi*sqrt(lbe(j,a))*sw1(j,a));
if sw==0
w1(a,1)=1;
end
end
for jj=1:nne+bct % ****** ****** ******** ******
dk=zeros(dof,dof);
dm=zeros(dof,dof);
if jj<nne+1
if ty~=1
b=2*(jj-1);
end
end
if jj==nne+1
if ty==0
b=b+2+1;
end
if ty==2
b=1;
end
end
if jj>nne+1
```

```
b=b+1;
end
if ty~=1
ngdisc2 % **** formulating dk,dm,dk11. . . . dm22 matrices
end
d2=ua(:,a)-ux(:,j);
d3=ua(:,a)+ux(:,j);
if max(abs(d2))>max(abs(d3))
ux=-ux;
end
clear d2 d3
if ty~=1
ngdisc3 % ******** actual calc of jacobian matrices
end
end % ****** * ******** ********** ** end of next jj
if so==2 % ********** if eigenvectors are also used
uz=ua(:,a)-su*rn2((s-1)*nr*r+(j-1)*nr+1:(s-1)*nr*r+j*nr,1);
if drf==1
ddd=ue(:,a)-uz;
w3=ones(nr,1)/su1(a);
d=diag(w3,0)*d;
ddd=diag(w3,0)*ddd;
end
if drf==0
du=zeros(nnr,iii);
dddu=zeros(nnr,1);
for ji=1:nnr
du(ji,:)=d(nvm(ji),:);
dddu(ji,1)=ue(ji,a)-uz(nvm(ji),1);
end
w3=ones(nnr,1)/su1(a);
d=diag(w3,0)*du;
ddd=diag(w3,0)*dddu;
end
d2=0;
if s==1 & j==1
d1=d'*d;
ddd1=d'*ddd;
d2=1;
end
if d2==0
d1=d1+d'*d;
ddd1=ddd1+d'*ddd;
```

```
clear d  ddd
end
cz=diag(w1(1:jx),0)*c(1:jx,:);
rk=rank(d1+cz(1:jx,:)'*cz(1:jx,:));
rkd=rank(d1);
if  jx==1
rnk=[jx;rkd;rk];
end
if  jx>1
rnk=[rnk  [jx;rkd;rk]];
end
rnk
jx=jx+1;
end  %  ********** end  of  if  so==2
j
end  %  ********************************  end  of  next  j
if  ms==0
m11=m11-mx;
end
if  ms==1
k11=k11-mx;
end
end  %  **********************  end  of  next  s
end  %  ************************  end  of  next  so
z1=max(abs(dd));
if  pp1==0
c=diag(w1,0)*c;
dd=diag(w1,0)*dd;
end
if  pp1==1
c=[diag(w1,0)  zeros(r+p*q*r,iii);zeros(iii,r+p*q*r)  c2]*c;
dd=[diag(w1,0)  zeros(r+p*q*r,iii);zeros(iii,r+p*q*r)  c2]*dd;
end
cd=c'*c;
cdd=c'*dd;
clear  dd
if  p3==1
cd=cd+d1;
cdd=cdd+ddd1;
end
x=inv(cd)*cdd;
for  i=1:10
ii=cdd-cd*x;
```

```
x=x+inv(cd)*ii;
end
for  i=1:iii
x(i)=x(i)/ao(i);
end
if  yy==1
if  ds==1
eee=nd(:,1);
mmm=nd(:,3);
end
if  bct>0  %  **********
bbb=bcm(:,2:3);
end   %   ******************
end
ii=1;
jj=1;
if   ty==0   %   ************************
for  i=1:ne
nd(i,1)=nd(i,1)+x(2*pd(2,i)-1);
nd(i,3)=nd(i,3)+x(2*pd(2,i));
end
for  i=1:bcn
if  bcm(i,2)~=0
bcm(i,2)=bcm(i,2)+x(2*pd(2,ne)+ii);
ii=ii+1;
end
if  bcm(i,3)~=0
bcm(i,3)=bcm(i,3)+x(2*pd(2,ne)+bck+jj);
jj=jj+1;
end
end
end  %  ************  end  of  ty=0
if   ty==2   %   ****************
for  i=1:bcn
if  bcm(i,2)~=0
bcm(i,2)=bcm(i,2)+x(ii);
ii=ii+1;
end
if  bcm(i,3)~=0
bcm(i,3)=bcm(i,3)+x(bck+jj);
jj=jj+1;
end
end
end
```

```
end % ********** end of ty=2
if ds==1
eee=[eee nd(:,1)];
mmm=[mmm nd(:,3)];
end
if bct>0
bbb=[bbb bcm(:,2:3)];
end
if ds==1
nd(:,1)
nd(:,3)
end
if ds==0
bcm(1:bck,2)
bcm(bck+1:bct,3)
end
yy=yy+1;
clear dk dkk dk11 dk12 dk21 dk22 dm dmm dm11 dm12 dm21 dm22
clear k11 k12 k21 k22 m11 m12 m21 m22 kv kl ux
clear ndu % &&&&&&&&&&&
end
clc
disp(' FINISH ********** FINISH ')
yy=yy-1;
break
```

MODULE ngdisc1.m

```
% ngdisc1.m
clc
disp('BUSY BUSY BUSY BUSY BUSY assembly full matrices')
k=zeros(dof,dof);
m=zeros(dof,dof);
if ds==1
for j=1:ne
ei=nd(j,1); % ******************** formulating element matrices
ea=nd(j,2);
mu=nd(j,3);
la=nd(j,4);
t1=nd(j,5)*pi/180;
t2=nd(j,6)*pi/180;
keb=(ei/(la^3))*[12 6*la -12 6*la;6*la 4*la^2 -6*la 2*la^2;-12 -6*la
12 -6*la; 6*la 2*la^2 -6*la 4*la^2];
meb=(mu*la/420)*[156 22*la 54 -13*la;22*la 4*la^2 13*la -3*la^2;
54 13*la 156 -22*la;-13*la -3*la^2 -22*la 4*la^2];
kea=(ea/la)*[1 -1;-1 1];
mea=(mu*la/6)*[2 1;1 2];
ke=[keb zeros(4,2);zeros(2,4) kea];
me=[meb zeros(4,2);zeros(2,4) mea];
dc=diag(ones(6,1),0);
for i=1:6
if nc(j,i)==-1
dc(i,i)=-1;
end
end
ke=dc'*ke*dc;
me=dc'*me*dc;
dc=diag(ones(6,1),0);
dc(1,1)=cos(t1);
dc(1,5)=-cos(pi/2-t1);
dc(3,3)=cos(t2);
dc(3,6)=-cos(pi/2-t2);
dc(5,1)=cos(pi/2-t1);
dc(5,5)=cos(t1);
dc(6,3)=cos(pi/2-t2);
dc(6,6)=cos(t2);
ke=dc'*ke*dc;
me=dc'*me*dc;
for i=1:6 % ******************** assembly
```

```
for ii=1:6
if ng(j,i)~=0 & ng(j,ii)~=0
k(ng(j,i),ng(j,ii))=ke(i,ii)+k(ng(j,i),ng(j,ii));
m(ng(j,i),ng(j,ii))=me(i,ii)+m(ng(j,i),ng(j,ii));
end
end
end
end %****************** end of next j
end % ***** end of ds==1
if bcn>0 % ********** adding boundary stiffeners/masses ****
for i=1:bcn
if bcm(i,4)==0
k(bcm(i,1),bcm(i,1))=k(bcm(i,1),bcm(i,1))+bcm(i,2);
m(bcm(i,1),bcm(i,1))=m(bcm(i,1),bcm(i,1))+bcm(i,3);
end
if bcm(i,4)>0
k(bcm(i,1),bcm(i,1))=k(bcm(i,1),bcm(i,1))+bcm(i,2);
k(bcm(i,4),bcm(i,4))=k(bcm(i,4),bcm(i,4))+bcm(i,2);
k(bcm(i,1),bcm(i,4))=k(bcm(i,1),bcm(i,4))-bcm(i,2);
k(bcm(i,4),bcm(i,1))=k(bcm(i,4),bcm(i,1))-bcm(i,2);
end
end
end % ***************** end of boundary add *****
disp('return to main program')
return % ******* return to ngdisc.m
```

MODULE ngdisc2.m

```
% ngdisc2.m
% Performing diff of matrices. dk,dm,dk11 . . . dm22, beam elements
if jj<nne+1
%      ************************************************
for o=1:ne
if pd(2,o)==jj
dkk=zeros(dof,dof);
dmm=zeros(dof,dof);
ea=nd(o,2);
mu=nd(o,3);
la=nd(o,4);
t1=nd(o,5)*pi/180;
t2=nd(o,6)*pi/180;
dkb=(1/(la^3))*[12 6*la -12 6*la;6*la 4*la^2 -6*la 2*la^2; -12 -6*la
12 -6*la;6*la 2*la^2 -6*la 4*la^2];
dmb=(la/420)*[156 22*la 54 -13*la;22*la 4*la^2 13*la -3*la^2; 54
13*la 156 -22*la;-13*la -3*la^2 -22*la 4*la^2];
dka=zeros(2,2);
dma=(la/6)*[2 1;1 2];
dkb=[dkb zeros(4,2);zeros(2,4) dka];
dmb=[dmb zeros(4,2);zeros(2,4) dma];
dc=diag(ones(6,1),0);
for i=1:6
if nc(o,i)==-1
dc(i,i)=-1;
end
end
dkb=dc'*dkb*dc;
dmb=dc'*dmb*dc;
dc=diag(ones(6,1),0);
dc(1,1)=cos(t1);
dc(1,5)=-cos(pi/2-t1);
dc(3,3)=cos(t2);
dc(3,6)=-cos(pi/2-t2);
dc(5,1)=cos(pi/2-t1);
dc(5,5)=cos(t1);
dc(6,3)=cos(pi/2-t2);
dc(6,6)=cos(t2);
dkb=dc'*dkb*dc;
dmb=dc'*dmb*dc;
for i=1:6
```

```
for ii=1:6
if ng(o,i)~=0 & ng(o,ii)~=0
dkk(ng(o,i),ng(o,ii))=dkb(i,ii);
dmm(ng(o,i),ng(o,ii))=dmb(i,ii);
end
end
end
dk=dk+dkk;
dm=dm+dmm;
end % *** end of pd(2,o)=jj
end % *** end of o=ne
end % ****************************** end of jj<ne+1
if jj>nne
% ****** **** ****** ****
if jj-nne<bck+1
if bcm(jj-nne,2)~=0
if bcm(jj-nne,4)==0
dk(bcm(jj-nne,1),bcm(jj-nne,1))=1;
end
if bcm(jj-nne,4)>0
dk(bcm(jj-nne,1),bcm(jj-nne,1))=1;
dk(bcm(jj-nne,4),bcm(jj-nne,4))=1;
dk(bcm(jj-nne,1),bcm(jj-nne,4))=-1;
dk(bcm(jj-nne,4),bcm(jj-nne,1))=-1;
end
nnk=nnk+1;
end
if jj-nne>bck
nnk==0;
end
end
if bcm(jj-nne,3)~=0
dm(bcm(jj-nne,1),bcm(jj-nne,1))=1;
nnm=nnm+1;
end
end % ****** ***** **** *******
if nr<dof
for i=1:nr
for ii=1:nr
dk11(i,ii)=dk(nm(i),nm(ii));
dm11(i,ii)=dm(nm(i),nm(ii));
end
end
```

```
for  i=1:nr
for   ii=1:dof-nr
dk12(i,ii)=dk(nm(i),ns(ii));
dm12(i,ii)=dm(nm(i),ns(ii));
end
end
dk21=dk12';
dm21=dm12';
for  i=1:dof-nr
for  ii=1:dof-nr
dk22(i,ii)=dk(ns(i),ns(ii));
dm22(i,ii)=dm(ns(i),ns(ii));
end
end
end
if  nr==dof
dk11=dk;
dk12=zeros(nr,nr);
dk21=dk12;
dk22=dk12;
dm11=dm;
dm12=zeros(nr,nr);
dm21=dm12;
dm22=dm12;
end
return
```

MODULE ngdisc3.m

```
% ngdisc3.m
% jacobian matrices
mre=-dk12*a5*m21+a4*a5*dk22*a5*m21+m12*a5*dk22*a5*a6-m1
2*a5*dk21+dk12*a5*m22*a5*a6-a4*a5*dk22*a5*m22*a5*a6-a4*a
5*m22*a5*dk22*a5*a6+a4*a5*m22*a5*dk21;
mru=dm11+lb(j,a)*(dm12*a5*m21-a4*a5*dm22*a5*m21-m12*a5*d
m22*a5*a6+m12*a5*dm21-dm12*a5*m22*a5*a6+a4*a5*dm22*a5*
m22*a5*a6+a4*a5*m22*a5*dm22*a5*a6-a4*a5*m22*a5*dm21)-a4
*a5*dm21-dm12*a5*a6+a4*a5*dm22*a5*a6;
mrl=m12*a5*m21-a4*a5*m22*a5*m21-m12*a5*m22*a5*a6+m12*a
5*m21-m12*a5*m22*a5*a6+a4*a5*m22*a5*m22*a5*a6+a4*a5*m2
2*a5*m22*a5*a6-a4*a5*m22*a5*m21;
ca=dk11-dk12*a5*a6-a4*a5*dk21+a4*a5*dk22*a5*a6;
cc=-lb(j,a)*(dm11-dm12*a5*a6-a4*a5*dm21+a4*a5*dm22*a5*a6);
kdl=-(m11-m12*a5*a6-a4*a5*m21+a4*a5*m22*a5*a6);
if jj<nne+1
if so==1 % ******* pert of eigvalues **********************
cy(a,b+1)=ua(:,a)'*ca*ua(:,a);
cy(a,b+2)=ua(:,a)'*cc*ua(:,a);
end
if so==2 % ************************** pert of eigvectors
for v=1:nr
l1=lb(j,a);
if j==1 & v==1
js=2;
end
if v==1
dy(:,b+1)=zeros(nr,1);
dy(:,b+2)=zeros(nr,1);
end
if v~=j & v~=js
aa=v;
l2=lx(v,v);
dy(:,b+1)=dy(:,b+1)+ux(:,aa)*ux(:,aa)'*ca*ua(:,a)/(l1-l2)-ux(:,aa)*ux(:,aa
)'*kdl*ua(:,a)*ua(:,a)'*ca*ua(:,a)/(ua(:,a)'*kdl*ua(:,a)*(l1-l2));
dy(:,b+2)=dy(:,b+2)+ux(:,aa)*ux(:,aa)'*cc*ua(:,a)/(l1-l2)-ux(:,aa)*ux(:,aa
)'*kdl*ua(:,a)*ua(:,a)'*cc*ua(:,a)/(ua(:,a)'*kdl*ua(:,a)*  (l1-l2));
end
if v==j
dy(:,b+2)=dy(:,b+2)-0.5*ua(:,a)*ua(:,a)'*mru*ua(:,a)-0.5*ua(:,a)*ua(:,a)'
*mrl*ua(:,a)*ua(:,a)'*cc*ua(:,a);
```

```
dy(:,b+1)=dy(:,b+1)-0.5*ua(:,a)*ua(:,a)'*mre*ua(:,a)-0.5*ua(:,a)*ua(:,a)'
*mrl*ua(:,a)*ua(:,a)'*ca*ua(:,a);
end
js=nr+1;
end % ************ end of next v
end % *************** end of so==2
end % ******************* end of jj<nne+1
if jj>nne % **** *** *** *** *** *** *** *** *** *** *
if so==1 % ******** *******
if nnk>jj-nne-1
cy(a,b)=ua(:,a)'*ca*ua(:,a);
end
if nnk<jj-nne & nnm>0
cy(a,b)=ua(:,a)'*cc*ua(:,a);
end
end % ****** ****** ********
if so==2 % *****************
for v=1:nr
l1=lb(j,a);
if j==1 & v==1
js=2;
end
if v==1
dy(:,b)=zeros(nr,1);
end
if v~=j & v~=js
aa=v;
l2=lx(v,v);
if nnk>jj-nne-1
dy(:,b)=dy(:,b)+ux(:,aa)*ux(:,aa)'*ca*ua(:,a)/(l1-l2)-ux(:,aa)*ux(:,aa)'*kd
l*ua(:,a)*ua(:,a)'*ca*ua(:,a)/(ua(:,a)'*kdl*ua(:,a)*(l1-l  2));
end
if nnk<jj-nne & nnm>0
dy(:,b)=dy(:,b)+ux(:,aa)*ux(:,aa)'*cc*ua(:,a)/(l1-l2)-ux(:,aa)*ux(:,aa)'*kd
l*ua(:,a)*ua(:,a)'*cc*ua(:,a)/(ua(:,a)'*kdl*ua(:,a)*(l1-l  2));
end
end
if v==j
if nnk>jj-nne-1
dy(:,b)=dy(:,b)-0.5*ua(:,a)*ua(:,a)'*mre*ua(:,a)-0.5*ua(:,a)*ua(:,a)'*mrl
*ua(:,a)*ua(:,a)'*ca*ua(:,a);
end
if nnk<jj-nne & nnm>0
```

```
dy(:,b)=dy(:,b)-0.5*ua(:,a)*ua(:,a)'*mru*ua(:,a)-0.5*ua(:,a)*ua(:,a)'*mrl
*ua(:,a)*ua(:,a)'*cc*ua(:,a);
end
end
js=nr+1;
end % ***************** end of next v
end % **************** end of so=2
end % **** ***** **** ***** end of jj>nne
if s==1+p*q & j==r
if jj==nne+bct
if so==1 % ********** ** ** ** ** **
c=cy;
clear cy
if pp1==1 % ***************** ** ** **
c=[c;diag(ones(iii,1),0)];
if ds==1
for i=1:ne
ndy(2*i-1,1)=nd(i,1);
ndy(2*i,1)=nd(i,3);
end
end
if bcn>0
ii=1;
for i=1:bcn
if bcm(i,2)>0
ndy(2*ne+ii,1)=bcm(i,2);
ii=ii+1;
end
end
ii=1;
for i=1:bcn
if bcm(i,3)>0
ndy(2*ne+bck+ii,1)=bcm(i,3);
ii=ii+1;
end
end
end
if ds==1
for ii=1:ne
for i=1:ne
if pd(2,i)==ii
ndu(2*pd(2,i)-1,1)=ndy(2*i-1,1);
ndu(2*pd(2,i),1)=ndy(2*i,1);
```

```
end
end
end
ndu=[ndu;ndy(2*ne+1:2*ne+bct,1)];
end
if ds==0
ndu=ndy;
end
dd=[dd;nduo-ndu];
end % ************** ** ** *** ** **
ao=max(abs(c));
for i=1:iii
c(:,i)=c(:,i)/ao(i);
end
end % *** if so==1 ** ** ** * **
end % ***** end of jj=nne+bct ** ** **
end % ***************************** if s=1+pq
if so==2
if jj==nne+bct
d=dy;
for i=1:iii
d(:,i)=d(:,i)/ao(i);
end
end % ****** jj=nne+bct
end % ******************************** so=2
return
```